The role of Prostaglandin E2 in the pathogenesis of Autosomal Dominant Polycystic Kidney Disease

The Medical School – Department of Infection and Immunity – Academic Nephrology Unit

Supervisors: Professor Albert Ong and Dr Andrew Streets

Fatima Abdela-Ali

Registration Number:

100147430

Lists of contents

Abstract **iii**

Acknowledgements **v**

List of Abbreviations **vi**

List of contents **xi**

List of figures **xviii**

List of tables **xxiii**

Abstract

Rationale & Hypothesis.

Autosomal Dominant Polycystic Kidney Disease (ADPKD) is the most common genetic cause of end stage renal disease (ESRD). Cyst formation in ADPKD requires epithelial cell proliferation and fluid secretion into closed cyst cavities. These effects are mediated mainly by elevated intracellular cAMP levels which induce both cell proliferation and increased fluid secretion. Prostaglandin E2 (PGE2) has been shown to increase intracellular cAMP levels and we and others have shown that its receptor (PTGER2) is increased in renal cyst epithelia possibly leading to increases in cAMP levels in these cells. This study was designed to test the hypothesis that blocking PGE2 activation might have a therapeutic role in reducing cyst growth in ADPKD.

Methodology.

Taqman qPCR, Western blotting, immunohistochemistry and ELISA for cAMP level were used to determine the expression of PTGER2 and PTGER4 in normal and ADPKD samples. Kidney epithelial cells derived from patients with ADPKD, non-ADPKD controls and MDCK cells were tested for their ability to form cysts or tubules in 3D cultures using a variety of extracellular matrices. The effect of selective PTGER2 and PTGER4 antagonists on cystogenesis was determined in 3D cultures. Furthermore, I tested the effect of PGE2, PTGER2 and PTGER4 antagonist on cell proliferation and apoptosis. Levels of intracellular cAMP in cystic human cells, and control cells were measured by commercial ELISA assays.

Results:

PTGER2 mRNA and protein levels were significantly increased in cells and tissue sections derived from patients with ADPKD compared to normal controls and also in inducible kidney

specific *PKD1 knock-out* mouse models compared to wild-type littermates. In human 3D cyst assays, PTGER2 and PTGER4 antagonists inhibited cytogenesis in a dose dependent manner. Furthermore, PTGER2 and PTGER4 antagonists inhibited cystic cell proliferation and increased apoptosis compared to the control cells.

Conclusions:

These results suggest that the use of specific PTGER2 and PTGER4 receptor antagonists could be effective in slowing cyst growth in human ADPKD.

Acknowledgements

First, I would like to thank my God for keeping me strong throughout my research and helping me complete my PhD. Second, I would like to extend my deepest thanks to Dr Andrew Streets, for his unfailing help, support, advice, guidance in teaching me how to conduct and plan my experiments and for closely directing me throughout my thesis writing. Third, special thanks to Professor Albert Ong, for his overall guidance, help and support throughout the whole study. Fourth, I would thank my husband Mohamed for his love and help and for taking care of our children.

Thanks also to our laboratory technician Fiona Wright, for teaching me immunohistochemistry, for delicious cakes every Friday meeting and for social support during my pregnancy and delivery period. I am grateful to the Libyan government for generously funding my research for 4 year PhD. I wish to thank all my friends in the lab who gave me help, support and encouragement.

Finally I wish to dedicate this work to my parents (Mum and Dad), my husband Mohamed and my children (Batool, Mohamed and Yousef) for their great patience and love which kept me strong to finish the project.

Abbreviations

ADPKD	**Autosomal dominant polycystic kidney disease**
AMP	**Adenosine monophosphate**
AKAP	**A kinase- anchoring protein**
ARPKD	**Autosomal receive polycystic kidney disease**
AP-1	**Activator protein -1**
APC	**Adenomatous polyposis coli**
AC	**Adenylate cyclase**
ANOVA	**Analysis of variance**
ACEI	**Angiotensin converting enzyme inhibitor**
ATP	**Adenosine triphosphate**
BrdU	**5-Bromo-2deoxyuridine (BrdU)**
BM	**Basement membrane**
CFTR	**Cystic fibrosis transmembrane regulator**
CREB	**cAMP response element binding protein**
CTT	**C- terminal tail**
cAMP	**3", 5"- Cyclic adenosine monophosphate**
COX	**Cyclooxygenase**
Ct	**Cycle threshold**
CT	**Computed tomography**

Cdk	**Cyclin dependent kinase**
DMEM	**Dulbecco's modified Eagle**
DMSO	**Dimethyl sulfoxide**
3 D	**Three dimensional**
DNA	**Deoxyribonucleic acid**
ERK	**Extracellular regulated kinase**
EHS	**Engelbreth-holm-swarm**
EGR-1	**Early growth response-1**
ESRD	**End stage renal disease**
EP	**E-Prostanoid**
ECM	**Extracellular matrix**
EGF	**Epidermal growth factor**
FBS	**Foetal bovine serum**
FCS	**Foetal calf serum**
GPS	**G- protein proteolytic cleavage site**
GRK	**G-protein receptor kinase**
GTP	**Guanosine triphosphate**
GSK	**Glycogen synthase kinase**
HGF	**Hepatocyte growth factor**
IMCD-3	**Inner medullary collecting duct-3**

IP	**Immunoprecipitation**
IF	**Immunofluorescence**
IGF	**Insulin-like growth factor**
JAK	**Janus kinase**
LRR	**leucine-rich repeats**
LOH	**Loss of heterozygosity**
MAP	**Mitogen activated protein**
MAPK	**Mitogen activated protein kinase**
MEK	**Mitogen extracellular kinase**
MMP	**Matrix metalloproteinase**
mRNA	**Messenger ribonucleic acid**
mTOR	**Mammalian target of rapamycin**
MTS	**3(4,5-Dimethylthiazol-2-yl)-2.5-diphenyltetrazolium**
NF	**Nuclear factor**
NFAT	**Nuclear factor of activated T-cells**
NSAID	**Non-steroidal anti-inflammatory drugs**
PKD	**Polycystic kidney disease**
PLAT	**Polycystin-1, lipoxygenase and alpha toxin**
PC-1	**Polycystin-1**
PC-2	**Polycystin-2**

PI3K	**Phosphatidylinositol 3 kinase**
PCR	**Polymerase chain reaction**
PGE2	**Prostaglandin-E2**
PKA	**Protein kinase –A**
PDE	**Phosphodiesterase**
PLC	**Phospholipid C**
PIP3	**Phosphatidylinositol (3,4,5)-trisphosphate**
PTGER2, 4	**Prostaglandin receptor 2 and 4**
PBS	**Phosphate buffered saline**
PFA	**Paraformaldehyde**
qPCR	**Quantitative PCR**
RNA	**Ribose nucleic acid**
REJ	**Sea urchin egg jelly receptor**
Rpm	**Rotation per minute**
SDS	**Sodium dodecyl sulfate**
SDS-PAGE	**Sodium dodecyl sulfate polyacrylamide gel electrophoresis**
SEM	**Standard error of the mean**
Ser	**Serine**
STAT	**Signal transducers and activators of transcription**
TRP	**Transient receptor potential channel**

TSC1, 2	**Tuberous sclerosis 1 and 2**
TCF	**T-cell factor**
TIMP	**Tissue inhibitor of metalloproteinase**
TGF	**Transforming growth factor**
TXA2	**Thromboxane**
TUNEL	**Terminal deoxynucleotidyl transferase mediated deoxyuridine Triphosphate nick end labelling**
VEGF	**Vascular endothelial growth factor**

Lists of contents

Chapter 1

General introduction

1.1.The Definition of ADPKD **2**

1.2.The PKD genes encode the Polycystin proteins **4**

1.3.Polycystin 1 **6**

1.4.Polycystin 2 **7**

1.5.The role of primary cilia in ADPKD **10**

1.6.Pathophysiology of cystogenesis **12**

1.7.Treatment of ADPKD **13**

1.8.The role of cyclic AMP in a normal kidney **15**

1.9. The role of cyclic AMP in ADPKD **21**

1.10. Targeting the cAMP pathway in ADPKD **22**

1.11. The prostaglandins and their receptor function in normal kidney **24**

1.12. PTGER2 and PTGER4 receptor signaling **29**

1.13. Prostaglandins and their receptors in ADPKD **30**

Hypothesis and objectives of the study **34**

Chapter 2

Material and Methods

2.1. Mammalian cell culture **44**

2.2. Rat tail collagen preparation **45**

2.3.1. Type I collagen gel cyst assay **46**

2.3.2. Cyst assay with Collagen and Matrigel **47**

2.3.3. Matrigel cyst assay **47**

2.3.4. Measurement of average cyst area and statistical analysis **48**

2.4.5. Testing the effect of PTGER2 and PTGER4 receptor antagonists in cyst assays **48**

2.4. Immunofluorescence **49**

2.4.1. Staining the cells in Collagen and Matrigel **49**

2.5.1. Cell Lysate preparation **50**

2.5.2. Protein concentration assay **50**

2.5.3. Western Blotting **51**

2.5.4. SDS-PAGE **52**

2.5.5 Transfer **53**

2.5.6. Detection of antigen on membranes **53**

2.6.1 RNA extraction from human ADPKD cell lines **54**

2.6.2. Agarose gel electrophoresis **55**

2.6.3. Reverse Transcription **55**

2.6.4. TaqMan qPCR gene expression assay **56**

2.7. Immunohistochemistry **58**

2.8.1. Apoptosis assay (TUNEL staining) **59**

2.8.2. Caspase-3 staining **60**

2.9.1. BrdU cell proliferation assay **60**

2.9.2. Cell Titer 96® AQueous One Solution Cell (MTS) Proliferation Assay **61**

2.10. cAMP assay (ELISA) **61**

Chapter 3

Establishment of a 3D culture assay to investigate cyst formation in human ADPKD cell lines

3.1. Introduction **65**

3.2. Aim and objectives **69**

3.3. Results **70**

3.3.1. Mutation analysis of human cell lines derived from patients with ADPKD **70**

3.3.2. MDCKII cells form cysts in Type I collagen gels **75**

3.3.3. Comparison of MDCK cell cystogenesis when cultured in Collagen or Matrigel **76**

3.3.4. Human cells form tubules in Collagen gels **79**

3.3.5. Comparison of human cell cystogenesis, when cultured in Collagen and Matrigel **83**

3.3.6. Comparison of human cell cystogenesis when cultured in Matrigel **87**

3.3.7. Morphology of ADPKD and MDCK cysts **92**

3.3.8. Effect of cAMP and Forskolin on MDCK cystogenesis **95**

3.3.9. Effect of prostaglandin E2 on MDCK cystogenesis **96**

3.3.10. Effect of cAMP and Forskolin on OX161/C1 cystogenesis **103**

3.3.11. Effect of prostaglandin E2 on OX161/C1 cystogenesis **103**

3.4. Discussion **107**

Chapter 4

Prostaglandin receptor expression levels in ADPKD

4.1. Introduction **111**

4.2. Aim and objectives **111**

4.3. Results **112**

4.3.1. PTGER 1, 2, 3 and 4 gene expression in human cell lines **112**

4.3.2. PTGER 1, 2, 3 and 4 gene expression in orthologous

mouse models of ADPKD **112**

4.3.3. Western Blotting with PTGER2 and PTGER4 specific antibodies in Human cell lines **119**

4.3.4. Immunohistochemistry of human kidney tissue sections with PTGER2 and PTGER4 specific antibodies **124**

4.3.5. PTGER2 expression in a tamoxifen-inducible, kidney epithelium-specific Pkd1-deletion mouse model **130**

4.3.6. PTGER4 expression in a tamoxifen-inducible, kidney epithelium-specific Pkd1-deletion mouse model **138**

4.3.7. PTGER2 expression in a orthologous Pkd1(nl,nl) mouse model **142**

4.3.8. PTGER4 expression in a orthologous Pkd1(nl,nl) mouse model **142**

4.4 Discussion **146**

Chapter 5

Effect of PTGER 2 and 4 receptor antagonists in cell culture models of ADPKD

5.1. Introduction **151**

5.2. Aim and objectives **153**

5.3. Results **154**

5.3.1. The effect of PGE2 on the proliferation of ADPKD and control kidney epithelial cell lines **154**

5.3.2. The effect of a PTGER2 antagonist on the proliferation of ADPKD and control kidney epithelial cell lines 158

5.3.3. The effect of a PTGER4 antagonist on the proliferation of ADPKD and control kidney epithelial cell lines 161

5.3.4. The effect of PGE2, PTGER2 and PTGER4 antagonists on the proliferation of MDCK II kidney epithelial cells 164

5.3.5. Effect of pre-incubation with PTGER2 and PTGER4 antagonists on PGE2 stimulation of cell proliferation 166

5.3.6. The effect of PGE2, PTGER2 and PTGER4 antagonists on apoptosis of ADPKD and control kidney epithelial cell lines- 168

5.3.7. The effect of a PTGER2 receptor antagonist on cystogenesis in 3D cyst assays 173

5.3.8. The effect of a PTGER4 receptor antagonist on cystogenesis in 3D cyst assays 173

5.3.9. Effect of pre-incubation with PTGER2 and PTGER4 antagonists on PGE2 stimulation of cystogenesis in 3D cyst assays 178

5.3.10. The effect of PTGER2 and 4 receptor antagonists on cAMP levels in ADPKD and control kidney epithelial cell lines 190

5.4. Discussion 193

Chapter 6

General discussion and conclusions

6.1. General discussion **197**

6.2. Limitations **202**

6.3. Conclusions **202**

6.4. Future work **203**

References **204**

Appendix **232**

List of Figures

Figure 1.1: A polycystic kidney from a patient with ADPKD **2**

Figure 1.2: The structure of polycystin-1 and 2 **5**

Figure 1.3: The role of Polycystin-1 and 2 in pathogenesis of ADPKD **9**

Figure 1.4: Model of how cilia mediate flow sensing and calcium signaling in the kidney **11**

Figure 1.5: The cAMP signalling pathway **18**

Figure 1.6: Signal transduction pathways in normal and polycystic Kidney disease **19**

Figure 1.7: Biosynthesis of prostanoid **27**

Figure 1.8: The signalling pathway for PGE2, and its 4 receptors **28**

Figure 1.9: PTGER2 and PTGER4 different signalling pathways activated by PGE2 **33**

Figure 3.1: Domain structure of polycystin-1 with sites of germline and Somatic mutations **73**

Figure 3.2: Human cell lines cultured in monolayer- **74**

Figure 3.3: MDCKII cells form cysts in type I collagen gels **77**

Figure 3.4: Comparison between MDCKII cultured in 3 types of Extracellular matrix: Collagen, Collagen and Matrigel and Matrigel alone **78**

Figure 3.5: Human cells cultured in collagen gels **82**

Figure 3.6: Human cell lines, cystic and normal cultured in Collagen and Matrigel **86**

Figure 3.7: Human cell lines, cystic and normal cultured in Matrigel **90**

Figure 3.8: Immunofluorescence images of MDCKII staining with Phalloidin and GP-135 **93**

Figure 3.9: Immunofluorescence images of OX161/C1staining with Phalloidin and ZO-1 **94**

Figure 3.10: Inverted microscope images of MDCKII cultured in Collagen I and treated with cAMP 100µM and Forskolin10µM **97**

Figure 3.11: Inverted microscope of MDCKII cultured in Collagen I and treated with 4 different concentration of PGE2 **100**

Figure 3.12: Effect of the smaller dose of PGE2 on MDCKII in 3 D culture media **102**

Figure 3.13: The inverted microscope of OX161/C1 cultured in Matrigel and Treated with cAMP and Forskolin **104**

Figure 3.14: Displayed of the effect of PGE2 on cyst formation in 3 D matrix gel Using human epithelial ADPKD cell line clone OX161/C1 in Matrigel **106**

Figure 4.1: Agilent mRNA microarray expression of PTGER 1, 2, 3 **114**

Figure 4.2: TaqMan qPCR expression of PTGER1, 2, 3 and 4 in

human ADPKD cell lines. 115

Figure 4.3: ADPKD orthologous mouse models used in this study 116

Figure 4.4: TaqMan qPCR expression of PTGER1, 2, 3 and 4 in two mouse models of ADPKD 117

Figure 4.5: TaqMan qPCR expression of PTGER2 in two mouse models of ADPKD. 118

Figure 4.6: Western blotting of PTGER2 in human kidney cell line 120

Figure 4.7: PTGER2 expression is increased following serum stimulation in ADPKD cell lines 121

Figure 4.8: Western blotting of PTGER4 in human kidney cell lines 123

Figure 4.9: Average cyst area in human ADPKD tissue sections compared Controls 126

Figure 4.10: Semi-quantitative analysis of DAB staining intensity using ImmunoRatio ImageJ plugin. 127

Figure 4.11: Immunohistochemistry of human kidney tissue sections with an antibody to PTGER2 128

Figure 4.12: Immunohistochemistry of human kidney tissue sections with an antibody to PTGER4 129

Figure 4.13: Average cyst area in a CreLox mouse ADPKD model 132

Figure 4.14: Expression of PTGER2 in a tamoxifen treated CreLox mouse model of ADPKD 134

Figure 4.15: Quantification of PTGER2 expression in a tamoxifen

treated CreLox mouse model of ADPKD **135**

Figure 4.16: Grading PTGER2 staining intensity of tamoxifen treated CreLox mouse tissue sections **137**

Figure 4.17: Expression of PTGER4 in a tamoxifen treated CreLox mouse model of ADPKD **139**

Figure 4.18: Grading PTGER4 staining intensity of tamoxifen treated CreLox mouse tissue sections **141**

Figure 4.19: Average cyst area in a NeoLox mouse ADPKD model **143**

Figure 4.20: Immunohistochemistry of NeoLox mouse kidney tissue sections with an antibody to PTGER2 **144**

Figure 4.21: Immunohistochemistry of NeoLox mouse kidney tissue sections with an antibody to PTGER4. **145**

Figure 5.1: Effect of PGE2 on ADPKD cell proliferation (MTS assay) **156**

Figure 5.2: Effect of PGE2 on ADPKD cell proliferation (BrdU Elisa) **157**

Figure 5.3: Effect of PTGER2 antagonist on ADPKD cell proliferation (MTS assay) **159**

Figure 5.4: Effect of PTGER2 antagonist on ADPKD cell proliferation (BrdU Elisa assay) **160**

Figure 5.5: Effect of PTGER4 antagonist on ADPKD cell proliferation (MTS assay) **162**

Figure 5.6: Effect of PTGER4 antagonist on ADPKD cell proliferation (BrdU Elisa assay) **163**

Figure 5.7: Effect of PGE2, PTGER2 and PTGER4 antagonists on MDCK II cell proliferation (BrdU Elisa assay) **165**

Figure 5.8: Effect of pre-incubation with PTGER2 and PTGER4 antagonists on PGE2 stimulation of cell proliferation **167**

Figure 5.9: Identification of apoptotic cells by TUNEL and Cleaved caspase-3 staining. **170**

Figure 5.10: Effect of PGE2, PTGER2 and PTGER4 receptor antagonists on apoptosis by TUNEL assay **171**

Figure 5.11: Effect of PGE2, PTGER2 and PTGER4 receptor antagonists on apoptosis by cleaved caspase-3 staining. **172**

Figure 5.12: The effect of PTGER2 antagonist on human cell line OX161/C1 cytogenesis in 3 D culture method. **176**

Figure 5.13: The effect of PTGER2 antagonist on MDCKII cytogenesis in 3 D culture method. **180**

Figure 5.14: The effect of PTGER4 antagonist on human cell line OX161/C1 cytogenesis in 3 D culture method. **182**

Figure 5.15: Shows the effect of PTGER4 antagonist on MDCKII cystogenesis in 3 D culture method. **185**

Figure 5.16: The effect of pre-incubation with PTGER2 and PTGER4 antagonists on PGE2 stimulation MDCK II cystogenesis in 3 D culture. **187**

Figure 5.17: The effect of pre-incubation with PTGER2 and PTGER4 antagonists on PGE2 stimulation OX161/C1 cystogenesis in 3 D culture method. **189**

Figure 5.18: The effect of PGE2 on cAMP levels in cystic and normal cell lines. **191**

List of Tables

2.1: Cell lines and culture conditions **36**

2.1.2: Cell culture material that used in the experiments **37**

2.2: Three-dimensional gel types **39**

2.3: List of primary antibodies used in Western Blotting **40**

2.4: Lists of primary antibodies used in Immunofluorescence and immunohistochemistry **41**

2.5: Lists of kits used in ELISA. **41**

2.6.1: qPCR: Samples **42**

2.6.2:RNA isolation **42**

2.6.3: qPCR primers **43**

2.6.4: Reverse Transcription: high capacity RNA-to-cDNA Kit. **43**

2.6.5: qPCR: TaqMan Gene Expression Assay **43**

2.6.6: Reverse Transcription: TaqMan qPCR **44**

3.1: Identification of germline and somatic PKD1 mutations detected in human cystic cell lines with predicted size of mutant proteins **72**

Chapter 1
General Introduction

1.1. The definition of ADPKD.

Autosomal Dominant Polycystic Kidney Disease (ADPKD) is the most common inherited disorder affecting the kidney. Its cardinal feature is the formation of fluid filled cysts **(Figure 1.1)** in both kidneys (Gabow 1993). It is a common cause of end stage renal disease (ESRD) in both adults and children worldwide and accounts for 10% of all ESRD cases (Grantham 1997). Polycystic kidney disease has two traits: an Autosomal dominant trait with 100% penetration which affects mainly adults and second, the recessive pattern which typically affects neonates (Feehally 2007). The autosomal dominant form occurs worldwide and affects all races with a prevalence between 1:400 to 1:1000 and with a 1.2-1.3 male to female ratio; it is a more progressive disease in men than in women (Torres, Harris et al. 2007).

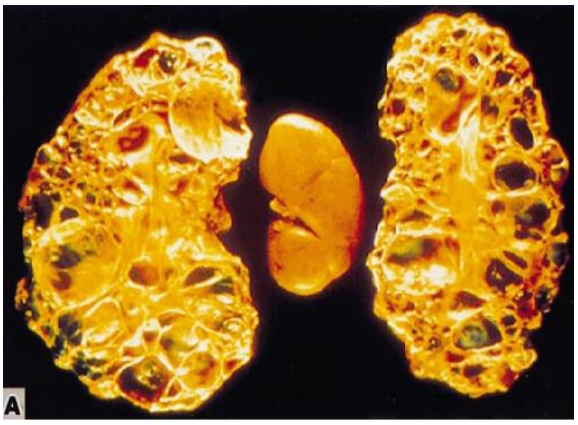

Figure 1.1: **A polycystic kidney from a patient with ADPKD.**

The accumulation of fluid filled cysts leads to enlargement of both kidneys as comparing with normal kidney, and lead to kidney failure (Koptides and Deltas 2000, Wu and Somlo 2000).

Furthermore it is a multi-systemic disorder with bilateral renal cysts as well as the occurrence of cysts in other organs like the liver (75% of patients). Cysts can also be found in the pancreas, seminal vesicle, ovaries and arachnoid membranes. Other extra renal symptoms include: mitral valve prolapse, mitral and tricuspid regurgitation, intracranial and aortic aneurysms, colonic diverticulae and abdominal or inguinal hernias (Torres 1999, Rossetti, Consugar et al. 2007). Hypertension is the most prevalent clinical presentation of polycystic kidney disease affecting 75% of patients. Other common presentations include: abdominal masses, chronic abdominal pain and backache, renal stones, urinary tract infections and hematuria (Boulter, Mulroy et al. 2001). The affected individual usually presents in the 3rd or 4th decade and develops ESRD in the 6th decade of life (Paterson, Magistroni et al. 2005).

The pathophysiological process of the disease involves renal cysts that develop from any segment of the nephron initially as a tubular dilation with increased cellular proliferation, apoptosis, and fluid secretion into cyst lumen, changes in cell polarity and an abnormal extracellular matrix ultra-structure. Eventually when only a few millimeters in diameter, the cyst detaches from the tubule (Grantham, Geiser et al. 1987). The diagnosis of pre-symptomatic ADPKD is usually made by imaging tests such as ultrasound. The diagnostic criteria using ultrasound for an individual's risk (50% risk by positive family history) include the following: two cysts, unilateral or bilateral is diagnostic in a patient younger than 30 years; two cysts in each kidney between 30-59 years; 4 cysts in each kidney for 60 years of age (Nicolau, Torra et al. 1999) (Ravine, Gibson et al. 1994). Other imaging studies such as CT and MRI may also be used as part of donor evaluation. In addition genetic diagnosis by mutation or linkage analysis allows prenatal diagnosis, and can be used for young, living related donors with an inconclusive diagnosis by other imaging studies (Torra, Badenas et al. 1996).

Polycystic kidney disease has a wide differential diagnoses which includes other less common cystic diseases like ARPKD, Von Hipple-Lindau disease, Tuberous Sclerosis, Orofacial Syndrome, Medullary sponge kidney, acquired and simple renal cysts (Fick and Gabow 1994).

One of the most important recent clinical studies in polycystic kidney disease has been the Consortium for Radiologic Imaging Studies of Polycystic Kidney Disease or CRISP study (Chapman, Guay-Woodford et al. 2003). This prospective study has followed a cohort of 240 ADPKD patients with early stage disease over 12 years, monitoring disease progression and renal complications. The investigators found that hypertension and micro-albuminuria are directly related to total kidney volume (TKV) with an average increase of kidney volume by 5.3% a year. Most importantly, a greater baseline TKV was associated with a more rapid decline in renal function (to CKD Stage 3) at 8 years follow-up (Chapman, Guay-Woodford et al. 2003).

1.2. The PKD genes encode the Polycystin proteins.

ADPKD can result in mutations in one of two genes identified. The *PKD1* gene is located on the short arm of chromosome 16p13.3 and accounts for 85% of cases (Hughes, Ward et al. 1995). It is characterized clinically by earlier onset of ESRD (Hateboer, v Dijk et al. 1999). The second gene identified is *PKD2* (4q21-23) which accounts for 15% of cases; patients with usually present later in life. The median age at diagnosis is 65 years for PKD2 versus 42 years for PKD1 (Peters and Sandkuijl 1992, Pei, He et al. 1998). The single gene responsible for ARPKD is *PKHD1* (Bergmann, Senderek et al. 2004).

The *PKD1* gene (45 exons distributed over 52 kb of genomic DNA) can be altered by many different types of mutation in ADPKD. The most common mutation (70%) is a truncating mutation which are strongly associated with early and severe disease with an estimated time to ESRD of 52.5 years. The second most common type of mutation is (NT) non truncating (in frame deletion or insertion (IF) with an estimated time to ESRD of 58.6 years. Finally mis-sense or atypical splice site variants are associated with less severe disease with an estimated time to ESRD of 70.8 years according to Toronto Genetic Epidemiology Study of PKD (TGESP) study (Harris and Torres 2014, Hwang, Conklin et al. 2015). The mutation type and TKV provide valuable prognostic factors for defining disease severity and potentially identifying patients who are candidate for experimental drugs or novel treatment (Hwang, Conklin et al. 2015). In addition, mutations at the 5′ end of the gene have been associated with an earlier onset of ESRD and a higher risk of intracranial aneurysm compared to mutations found in the 3′ end of the gene (Rossetti, Burton et al. 2002).

The *PKD2* gene consists of 15 exons distributed over 68 kb of genomic DNA. PKD2 mutation is associated with mild disease and may not need to treatment until later age. It encodes the

protein PC2 that acts as calcium channel (Pei, He et al. 1998). These two genes have been shown to encode two proteins termed Polycystin 1 and Polycystin 2 respectively **(Figure 1.2)**

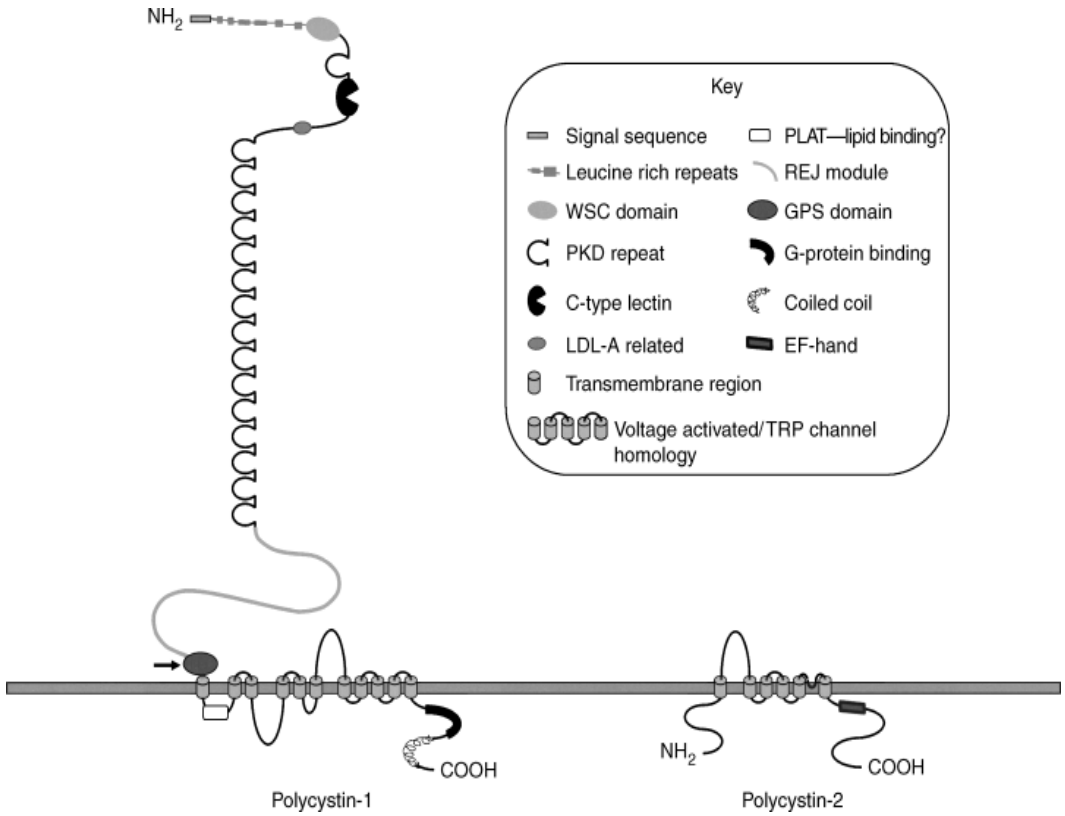

(Ong and Harris 2005) with permission

Figure 1.2: The structure of polycystin-1 and 2

The structure of the Polycystin-1and polycystin 2. Polycystin-1, it contains an extracellular N-terminal domain, 11 transmembrane domains, and a short cytoplasmic C-terminal domain. PC-1 plays an important role in cell-cell and cell-matrix interactions (Sandford, Sgotto et al. 1997). PC-2 is a membrane protein with 6 transmembrane domains, and the intracellular amino and carboxy-terminals. PC-2 is a member of the transient receptor potential channel family of proteins (TRP), acting as a Ca^{2+} channel. Polycystin-1 and-2 interact through domains that are present in their cytoplasmic C-terminal region, known as coiled-coil domains (Tsiokas, Kim et al. 1997).

1.3. Polycystin 1.

The polycystin-1 protein, the product of the PKD1 gene, is a large integral glycoprotein of 4302 amino acid with a molecular mass of 460 KDa (Hughes, Ward et al. 1995). It has a large N-extracellular domain of 3000 amino acids, 11 trans-membrane domains, and a short C-cytoplasmic domain terminal of 200 amino acids, it site for coil-coil protein, and it contains a number of phosphorylation sites and G-protein binding site **(Figure 1.2).** There are a number of short motifs that have been recognized on the N-extracellular terminal domain. Two leucine-rich repeats are flanked by two cysteine–rich domains. The immunoglobulin-like motifs consist of 80-90 amino acids, which are believed to be involved in mediating protein-protein or protein–carbohydrate interactions (Hughes, Ward et al. 1995) (Moy, Mendoza et al. 1996). The C-terminal is the site of the coiled-coil structure through which polycystin-1 interacts with polycystin-2 to form a Polycystin complex that is believed to regulate a number of intracellular signaling pathways (Koptides and Deltas 2000). The C-terminal is also a site of phosphorylation by protein kinase A and a src-like tyrosine kinase (Li, Geng et al. 1999). Polycystin-1 acts as a cell surface receptor protein which undergoes proteolytic cleavage at a proteolytic cleavage site (GPS) which is important for its function (Mengerink, Moy et al. 2002). Polycystin-1 acts as a G- protein coupled receptor which activates the Gα subunit signaling that regulates proliferation, cell polarity and fluid secretion (Grantham 2001, Delmas, Nomura et al. 2002). It is also involved in the activation of other signals like Wnt, STAT/JAK signaling through a carboxyl-terminal domain of polycystin-1(Bhunia, Piontek et al. 2002). PC1 is expressed in many tissues including the kidneys (Yoder, Hou et al. 2002), and other organs like the heart, brain, muscles and bones. Within the cell, it has multiple locations such as in cilia, cytoplasmic vesicle, desmosome, focal adhesion and adherens junctions (Newby, Streets et al. 2002, Yoder, Hou et al. 2002).

1.4. Polycystin 2.

Polycystin-2 is the protein product of the *PKD2* gene. It is composed of 968 amino acids, and six trans-membrane domains (Hanaoka, Qian et al. 2000) with a molecular mass of 110 kDa. Polycystin-2 contains an N-terminal cytoplasmic domain, and a C-terminal cytoplasmic domain. The C-terminal domain contains a calcium binding motif (EF-hand) that has been shown to undergo calcium–induced conformational changes. The C-terminal is also the site of coiled-coil interaction with polycystin-1 (Qian, Germino et al. 1997). Polycystin-2 is localised mainly in the endoplasmic reticulum although it has also been found localised to the basolateral plasma membrane, mitotic spindles and primary cilia (Rundle, Gorbsky et al. 2004) (Newby, Streets et al. 2002, Yoder, Hou et al. 2002). Polycystin-2 shares structural features of voltage activated sodium channels, and calcium channels as well as transient receptor potential (TRP) channels (Tsiokas, Arnould et al. 1999). The structure of polycystin-2 suggests that it may play a role as an ion channel. Polycystin-2 is expressed in the kidneys with the highest levels found in the distal convoluted tubule as well as in other organs including the heart, ovaries, testis and small intestine (Newby, Streets et al. 2002, Yoder, Hou et al. 2002). Polycystin-2 has been shown to act as a Ca^{2+} permeable channel protein regulating calcium releases from intracellular ER stores (Hanaoka, Qian et al. 2000). Both PC-1 and PC-2 interact through the coil-coil domain localized in the C-terminal to form a complex that acts to regulate intracellular calcium levels (Qian, Germino et al. 1997). Extracellular signals are sensed by polycystin-1 passed into polycystin-2 leading to activation of calcium channels and other downstream signaling pathways leading to regulation of cellular function and gene transcription (Tsiokas, Kim et al. 1997) (Hanaoka, Qian et al. 2000). These include G protein, mTOR, STAT and Wnt signaling pathways (**Figure 1.3**)(Chapin and Caplan 2010).

PC1, through inhibition of a mTOR pathway via a TSC1-TSC2 complex, controls the proliferation and growth rate of the cells (Inoki, Li et al. 2002). PC1 also increases the level of

p21 that activates the STAT1-STAT-3 pathways and decreases cell proliferation (Bhunia, Piontek et al. 2002). In addition, PC1 acts as G-protein coupled receptors through C-terminal domains that control the transcriptional factor AP-1 that is important in cell apoptosis, proliferation and differentiation (Le, van der Wal et al. 2005). On other hand, PC2 via NFAT, stimulate the calcineurin and increases the Ca^{2+} level (Puri, Magenheimer et al. 2004). Furthermore, PC1 inhibits the β-catenin pathway and decreases the activity of TCF dependent transcription (Lal, Song et al. 2008). Moreover, PC1 plays a critical role in maintaining planar cell polarity through the non-canonical pathway (Chapin and Caplan 2010) (**Figure 1.3).** The increase in cell proliferation, disturbance of cellular polarity and increase in secretory function results in a transformation of epithelial cells in the kidney from tubular into a cystic phenotype (Torres and Harris 2009).

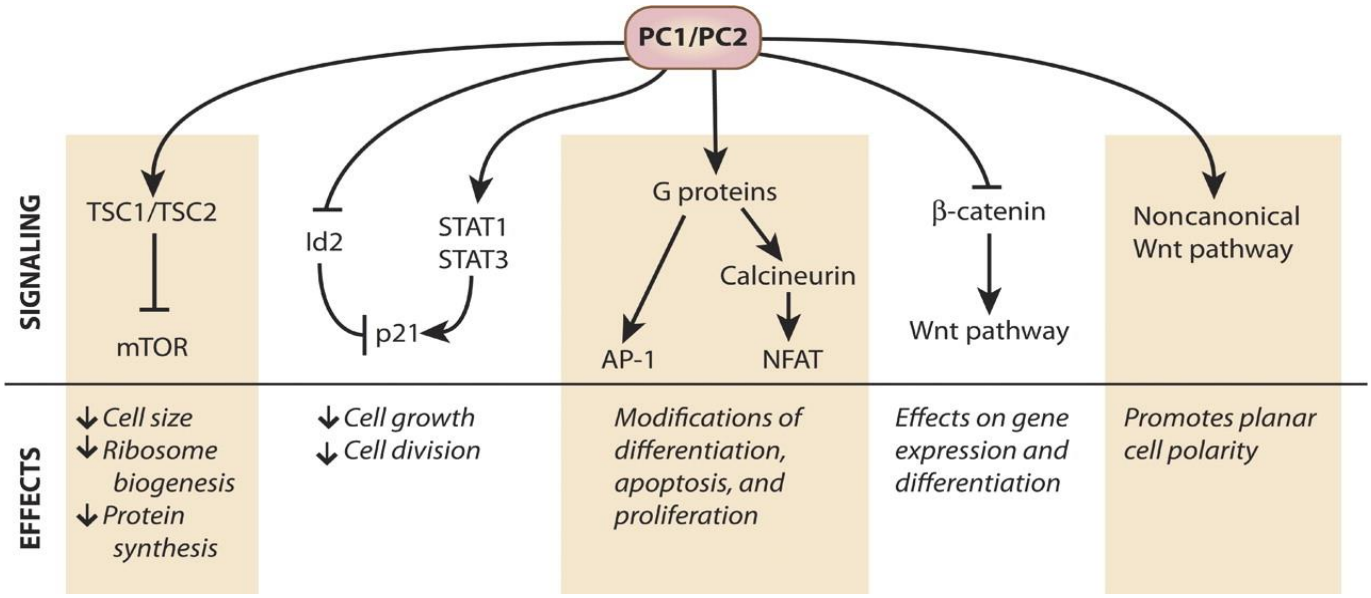

©YEAR AUTHOR et al. Journal of Cell Biology. VOL:PP-PP. doi:10.1083/jcb.######## (Chapin and Caplan 2010) with

Figure 1.3. The role of Polycystin 1 and 2 in the pathogenesis of ADPKD.

A summary of the key roles of Polycystin 1 and 2 in the regulation of signalling pathways are involved in cell proliferation and differentiation (Chapin and Caplan 2010).

1.5. The role of primary cilia in ADPKD.

The primary cilium is a single hair-like organelle which arises from the mother centrosome in non-dividing cells. It is also a major microtubule organizing centre (MTOC) of the cell **(Figure 1.4)**. Primary cilia are expressed by the majority of mammalian cells, including the kidney. They project from the apical surface of tubular cells into the lumen and have a 9+0 microtubules arrangement (non-motile). Primary cilia are thought to play a mechanosensory role through sensing fluid flow. The Polycystin complex in primary cilia is believed to mediate this process by regulating Ca^{2+}influx in response to mechanical stimulation (Yoder, Hou et al. 2002, Nauli, Alenghat et al. 2003). Cilia bending results in Ca^{2+} entry and the further release of intracellular $Ca^{2+}$from intracellular stores (Chebib, Sussman et al. 2015). Mutation of either Polycystin protein leads to a disruption in Ca^{2+} homeostasis with a resultant dysregulation of cAMP signalling and other downstream pathways. This in turn could lead to a cellular switch from inhibition to stimulation of proliferation, increased fluid secretion and interstitial inflammation of ADPKD (Deane and Ricardo 2007, Chebib, Sussman et al. 2015).

Based on this evidence, ADPKD has been classified as a ciliopathy, a group of diseases resulting from mutations in genes encoding proteins that regulate cilia structure or function. Most of these rare syndromic disorders are characterised by renal and hepatic cysts but also other features lacking in ADPKD such as the presence of neural tube defects, polydactyly, brain tumours and retinal abnormalities (Badano, Mitsuma et al. 2006).

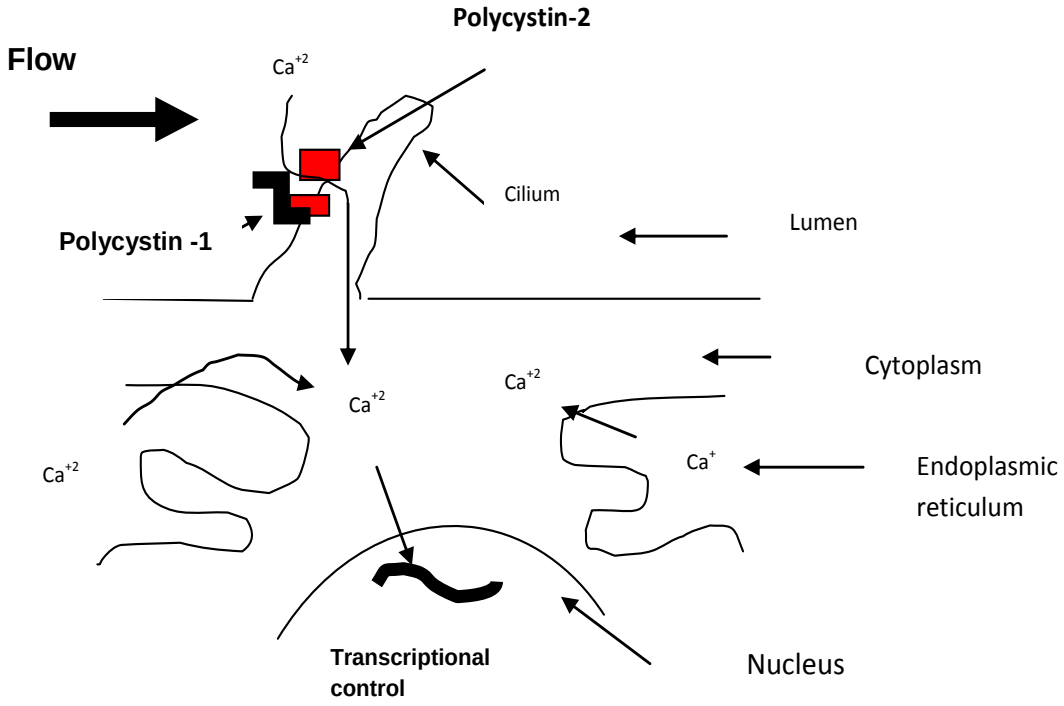

Forman, Qamar et al. 2005.

Figure 1.4: Model of how cilia mediate flow sensing and calcium signaling in the kidney.

The renal cilium is important in the maintenance of renal structure and ability of this organelle to sense fluid flow through collecting ducts and nephrons. Polycystin-1 and 2 are both membrane proteins that co-localize to the renal cilium and both are required for cilium mediated flow sensing in cultured renal epithelial cells (Pazour 2004). Polycystin-1 acts as a mechano-sensor that detects the fluid flow through its extracellular N-terminal domain (Forman, Qamar et al. 2005). The influx of $Ca^{2+}$is augmented by the release of intracellular Ca^{+2} stores. Increased levels of Ca^{+2} into the cell activate a series of events that maintain the epithelial phenotype (Puri, Magenheimer et al. 2004).

1.6. Pathophysiology of cystogenesis.

ADPKD is a disease with a highly variable phenotype, expressed in the interfamilial and intra familial age of onset of ESRD (Qian and Germino 1997, Koptides, Hadjimichael et al. 1999). Cysts develop focally and less than 5% of all nephrons develop cysts, although all cells carry the germline mutation (Koptides, Hadjimichael et al. 1999). A possible explanation for the focal nature of cytogenesis is the somatic mutation 'two hit' model, or haploinsufficiency of PKD1 (Lantinga-van Leeuwen, Dauwerse et al. 2004).

Cysts in ADPKD can originate from all segments of the nephron and therefore are distributed between the cortex and medulla. Increased tubular epithelial proliferation, fluid secretion, loss of differentiation leads to cyst expansion and disconnection from its tubular origin (Mochizuki, Tsuchiya et al. 2013). Tubular epithelial hyperplasia is the most prominent morphological change in human polycystic kidneys. Analysis of cystic kidneys has revealed an increased proliferative index in cysts and non-cystic tubules (Nadasdy, Laszik et al. 1995). Another prominent factor for cyst formation is increased fluid secretion into cyst lumen. The increased fluid secretion is due to presences of chloride channel (CFTR) cystic fibrosis transmembrane conductance regulator (Hanaoka, Devuyst et al. 1996). The increased fluid secretion and cell proliferation is due to inappropriate elevation of cAMP level (Belibi, Reif et al. 2004).

Increases in apoptosis or programmed cell death are seen in kidneys from PKD patients (Savill 1994). High levels of two key genes, *c-myc and bcl-2* suggests dysregulation of both proliferative and apoptosis pathways in ADPKD (Lanoix, D'Agati et al. 1996). Furthermore, over expression of growth factors like TGF-α and EGF in PKD epithelial cells are believed to stimulate cellular proliferation and cyst growth (Lowden, Lindemann et al. 1994).

1.7. Treatment of ADPKD.

Tolvaptan is an orally administered V2 receptor antagonist which was proven to be effective in treatment of hyponatremia in hypervolemia and euvolemia condition like liver cirrhosis, congestive heart failure and SIADHs (syndrome of inappropriate antidiuretic hormone secretion) (Costello-Boerrigter, Boerrigter et al. 2009). OP-31260 the nonpeptide vasopressin antagonist was applied in preclinical trials in four animal models of PKD. Three of which were orthologues to human PKD (Gattone, Wang et al. 2003). In the pcy mouse adolescent nephronophthisis type3, PCK rat (ARPKD), and Pkd2ws25/- mouse ADPKD models treatment with OP-31260 demonstrated a significant decrease in cyst growth, reduced renal cAMP levels, and slower disease progression measured by decreased kidney volume, blood urea nitrogen, and cystic area (Torres 2004, Torres, Wang et al. 2004).

Tolvaptan was proven to be effective in reducing proliferation and chloride secretion of human ADPKD cell *in vitro* culture model (Reif, Yamaguchi et al. 2011). These effects were mainly through inhibition of cAMP and ERK signalling which induce proliferation and fluid secretion (Reif, Yamaguchi et al. 2011).

The result of vasopressin antagonists in PKD cell culture and animal models provided a strong rational for testing V2 antagonists in ADPKD patients which translated into a clinical trial called Tolvaptan efficiency and safety in management of PKD and outcome (TEMPO) clinical trial (Torres, Meijer et al. 2011). The TEMPO phase 2 started in 63 ADPKD patients for three year of Tolvaptan treatment and demonstrated decreased cyst growth by annual increase of total kidney volume 1.7% for Tolvaptan group versus 5.8% for control group $P < 0.001$, and improved the decline of kidney function (annual eGFR decline 0.07 Tolvaptan group versus 2.1 ml/min/1.73m^2 placebo group the $P = 0.01$ (Higashihara, Torres et al. 2011).

Tolvaptan phase 3 (TEMPO 3/4): a three year multicentre randomized double blind trial collected 1445 ADPKD patients treated with 60-120 mg/day twice day versus placebo control.. There was a significant decrease in the rate of TKV increase (2.8% in Tolvaptan group versus 5.5%/year in placebo P > 0.001). While the secondary endpoint of measurement of decreasing kidney function (decreased 2.7 in Tolvaptan group versus 3.7 ml/min/1.37m^2 in placebo group), blood pressure control and renal pain (5 in Tolvaptan group versus 7 event /100 person/year P = 0.007)(Torres, Meijer et al. 2011). The common side effects seen were polyuria, thirst, hyperuricemia, and abnormal liver function lead to 8% of patients being unable to complete the trial (Blair and Keating 2015).

Tolvaptan (Jinarc) has been approved in Europe, Canada and Japan as a potent selective oral V2 antagonist for treatment of ADPKD and to delay the progression of the disease in adults with stage 1-3 of chronic renal failure (Blair and Keating 2015).

Until the development of Tolvaptan the treatment of ADPKD was directed toward managing complications of the disease. Hypertension is a major cause of morbidity and mortality in ADPKD patients. Treatments with ACEI or angiotensin receptor blockers have a renoprotective effect, and reduce both the proteinuria and left ventricular hypertrophy (Osawa, Nakamura et al. 2006). The HALT-PKD study was a prospective trial seeking to determine whether combined therapy with ACEI and an angiotensin II-receptor blocker was superior to ACEI alone in delaying the progression of PKD in patients with stage 1 or 2 of renal failure, or to slow decline of renal function in stage 3. A second aim of this study was to determine whether lower blood pressure (<110/75) control was better than standard blood pressure (130/80) in the group of patients with preserved renal function. The total kidney volume and left ventricular mass index (predictive disease progression of ADPKD) were significantly decreased in low blood pressure control compared to standard blood pressure group (Chapman, Torres et al. 2010, Torres, Chapman et al. 2011, Schrier, Abebe et al. 2014)

Flank pain can be caused by cyst infection, bleeding, kidney stones or renal tumours. This may be avoided by reducing the use of nephrotoxic drugs, and surgical intervention like cyst aspiration under CT guidance may also be helpful in reducing flank pain. Cyst infection and haemorrhage can be treated with bed rest, analgesia, and hydration (Lee and Clayman 2004). Treatment with antibiotics may be difficult due to poor penetration into cysts. ADPKD patients do better on dialysis than other ESRD patients, and this may be due to lower co-morbidity. The treatment of choice of ESRD with ADPKD is transplantation (Abbott and Agodoa 2002).

1.8. The role of cyclic AMP in a normal kidney.

Cyclic AMP was first discovered by Earl Sutherland and a colleague in the 1950's for which they won the Nobel Prize in Physiology and Medicine in 1971. Cyclic AMP is a small cyclized monophosphate that acts as a ubiquitous second messenger, and is involved in the regulation of several biological processes such as cell proliferation, differentiation, transcription, and fluid and electrolyte transport (Dumaz, Hayward et al. 2006).

The cAMP-dependent signal transduction pathway involves different enzymatic reactions. The most important enzymes are the adenylyl cyclases, phosphodiesterases, protein kinase A (PKA) and protein phosphatases. The adenylyl cyclases are comprised of nine isoforms each of which is a product of a distinct gene (Borrelli, Montmayeur et al. 1992). Adenylyl cyclase is dually regulated via G-protein Gs stimulatory activity and Gi inhibitory activity, and can also be stimulated by Forskolin. Certain subclasses are regulated by Ca^{2+}/calmodulin or phosphorylation through various kinases (Taussig and Gilman 1995). Adenylyl cyclase catalyses the conversion of ATP to 3", 5"- cyclic-AMP and pyrophosphate (Taussig and Gilman 1995). Increased cyclic AMP levels lead to activation of specific proteins including protein kinase A (PKA) **(Figure 1.5).** The PKA holoenzyme is a tetrameric complex consisting

of four subunits: two catalytic subunits (C), and two regulatory subunits (R), which bind with two cAMP molecules causing dissociation of holoenzyme and the release of the two active catalytic subunits (Yamaguchi, Pelling et al. 2000). PKA plays an important role in the phosphorylation of membrane receptors (Daniels, Hall et al. 1998) enzymes and transcription factors, leading to changes in gene expression and cell metabolism (Bourne, Tomkins et al. 1973).

Cyclic AMP levels are lowered via phosphodiesterase (PDE) enzymes. The phosphodiesterases are a group of enzymes that degrade the phosphodiesterase bond and hydrolyse cAMP to AMP thus inactivating this second messenger (Conti 2000). Based on their specificity, two of these families (PDE4 and PDE7) have a higher specificity to be activated by cAMP than cGMP. In addition to the activation of existing PDE enzymes, cAMP can stimulate the synthesis of new PDE mRNA (Swinnen, Joseph et al. 1989, Daniels, Hall et al. 1998). The important features of cAMP signalling are the cellular specificity of the response (Houslay and Milligan 1997). Extracellular ligands bind to G protein-coupled receptors that can be either positively stimulated by Gs or negatively stimulated by Gi, both of which can then bind and regulate adenylyl cyclase (ACs). The biological effect of cAMP is mediated mainly by protein kinase A, which is targeted to specific cellular compartments by A kinase-anchoring proteins (AKAPs) (Faux and Scott 1996). The specificity of cAMP signalling is controlled not only through the variety of the enzymes, ACs, PDEs, PKAs and AKAP but also by cell type specific communication with other signalling pathways such as mitogen-activated protein kinase and extracellular regulated kinase (MAPK/ERK) cascades (Lewis, Shapiro et al. 1998). These cascades couple the Ras and growth factor receptors **(Figure 1.5**) which finally lead to cell proliferation (Torres 2004).

In normal renal epithelial cells, cAMP has been found to inhibit proliferation. This effect appears to be mediated by inhibition of the Raf-1/MEK/ERK pathway through PKA. B-Raf,

which is independently stimulated by MEK **(Figure 1.6**), is normally inhibited by Akt (protein kinase B) in the presence of normal intracellular Ca^{2+}levels (Yamaguchi, Hempson et al. 2006). This is dependent on a normal PC1/PC2 complex **(Figure 1.6)** that regulates Ca^{2+} entry and normal intracellular Ca^{2+} levels, which in turn maintain the activity of PI3kinase and Akt pathways **(Figure 1.5)**. Inhibition of B-Raf kinase activity is through the phosphorylation of S365 and T440 residues by Akt (Guan, Figueroa et al. 2000, Wellbrock, Karasarides et al. 2004).

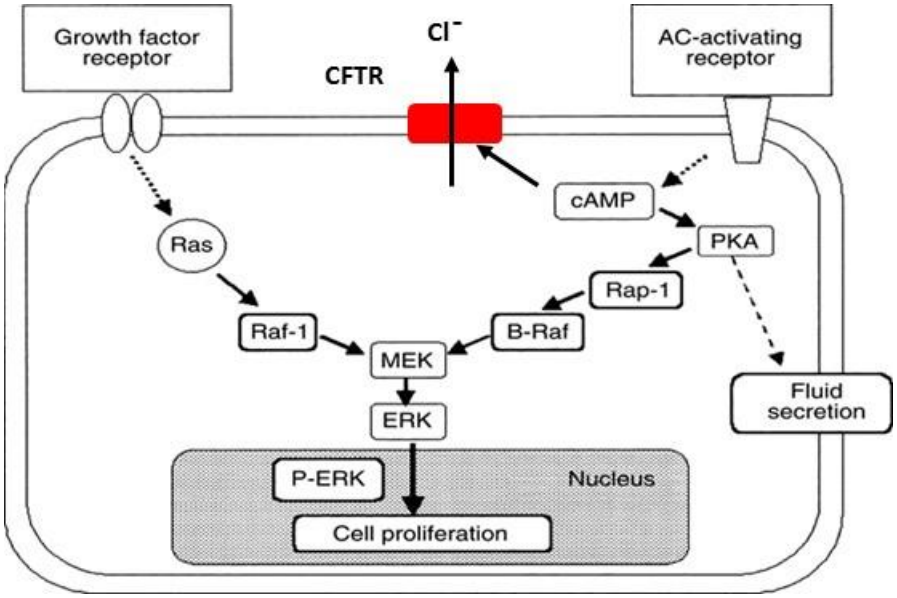

(Nagao, Yamaguchi et al. 2003) with permission.

Figure 1. 5. The cAMP signalling pathway.

cAMP stimulates proliferation through stimulation of a MAP kinase (mitogen activating kinase) pathway at MEK (mitogen extracellular kinase) through intermediate elements. On the other hand growth factors bind with the receptor tyrosine kinase leading to sequential activation of Ras, Raf-1, MEK, and ERK pathways that will stimulate cell proliferation. When a hormone binds with its receptor it blocks the Gi inhibition of adenylyl cyclase (AC) and stimulates Gs proteins that activate AC which catalyzes the conversion of ATP to cAMP, increasing cAMP levels that in turn stimulates PKA. In ADPKD this stimulates cyst formation through cells proliferation via cross talk with ERK (extracellular kinase) pathways. Fluid secretion into cysts occurs through cAMP regulated channels stimulating trans epithelial secretion of Cl^- into the lumen of the cyst mainly through a CFTR (cystic fibrosis transmembrane conductance regulator) chloride channel on an apical membrane of the cells (Yamaguchi, Pelling et al. 2000).

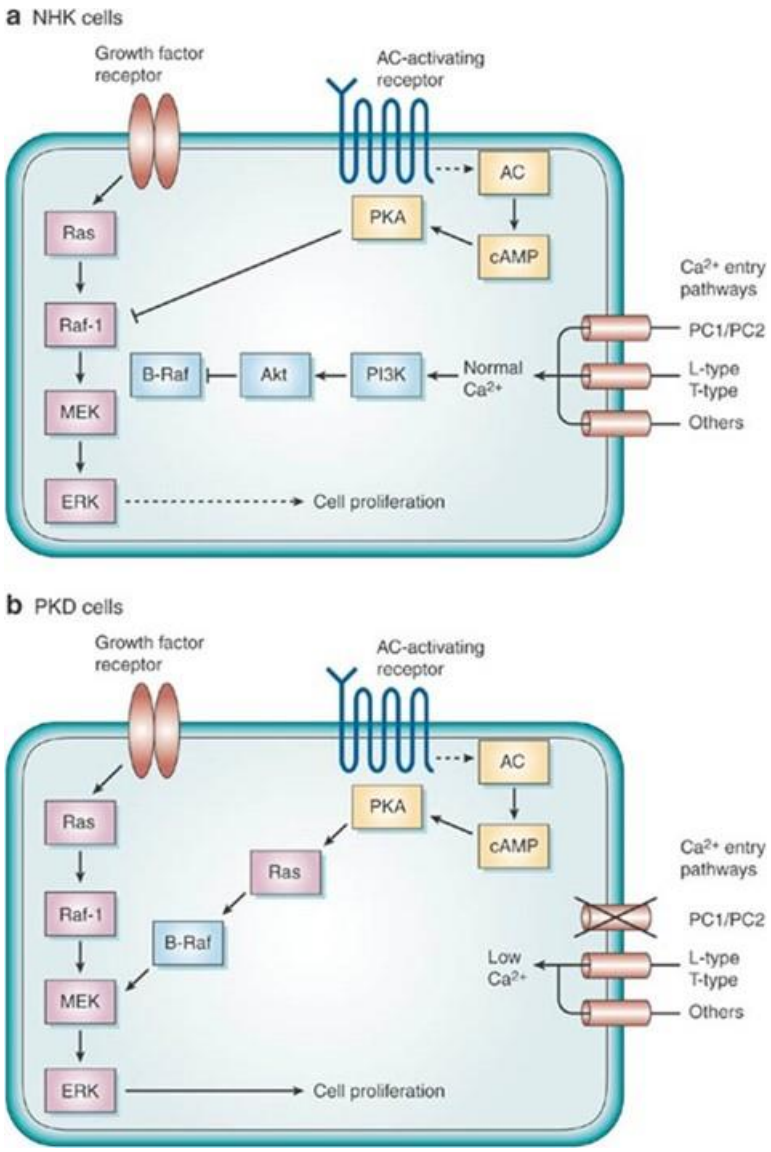

(Cowley 2008) with permission

Figure 1.6: Signal transduction pathways in normal and polycystic kidney disease

(A) Normal kidney cell: adenylyl cyclase is stimulated by extracellular ligands such as vasopressin, prostaglandins, parathyroid hormone; increasing intracellular cAMP leads to activation of protein kinase A; this result in inhibition of Raf-1/MAP kinase Kinase/extracellular signal-regulated kinase (Raf-1/MEK/ERK). B-Raf, which can independently stimulate MEK, is inhibited by Akt with normal intracellular Ca^{2+}levels. Normal intracellular $Ca^{2+}$and activation of tyrosine kinase receptors via EGF lead to activation of phosphatidylinositol -3-kinase to generate PIP3, a ligand for the serine/threonine kinase Akt. This is responsible for inhibition of B-Raf. Inhibitions of Akt by low intracellular Ca^{2+}might

lead to B-Raf dependent ERK activation and hence increase the rate of proliferation and apoptosis in polycystic kidney disease (Yamaguchi, Hempson et al. 2006)

(B) Polycystic kidney cell: when EGF binds to the receptor-tyrosine kinase, it activates Ras which phosphorylates Raf-1, followed by downstream activation of MEK and ERK. Adenylyl cyclase is stimulated by extracellular ligands such as vasopressin, parathyroid hormone and prostaglandins, increasing cAMP results in activation of protein kinase (PKA). Protein kinase activates the B-Raf/MEK/ERK pathway; low Ca^{2+}evels abolish Akt inhibition of B-Raf, with a pro-proliferate effect (Torres and Harris 2006). PC: Polycystin, PI3K: phosphatidylinositol -3-kinase, PKA: protein kinase A, MAP kinase, ERK extracellular signal-regulated kinase, AC Adenylate cyclase (Cowley 2008).

1.9. The role of cyclic AMP in adult polycystic kidney disease.

Cyst formation in ADPKD requires epithelial cell proliferation, and fluid secretion into closed cyst cavities. These effects are mediated mainly by intracellular cAMP through the activation of protein kinase A, MEK and ERK (Nagao, Yamaguchi et al. 2003). When EGF binds to a receptor-tyrosine kinase it activates Ras which phosphorylates Raf-1 and results in activation of MEK and ERK signalling pathways (Erhardt, Troppmair et al. 1995). This in turn induces cell proliferation **(Figure 1.5**).

In ADPKD, there is a phenotypic switch in PKD cells in their response to cAMP such that this stimulates proliferation. In ADPKD cells, there is a decrease in intracellular Ca^{2+} levels, due to a loss of either polycystin-1 or polycystin-2 function (Hanaoka and Guggino 2000). This relieves Akt inhibition of B-Raf leading to B-Raf activation, phosphorylation of MEK, which in turn phosphorylates and activates ERK. Activated ERK then translocated into the nucleus where it upregulates the transcriptional activity of several genes involved in cell proliferation (Chang, Steelman et al. 2003).

In addition to cell proliferation, cAMP has a recognised role in stimulating fluid secretion in ADPKD mediated through a Cl^- dependent mechanism (Hanaoka and Guggino 2000). Fluid secretion in ADPKD cysts is dependent on ion channels and transporters within the basolateral and apical membranes. cAMP-dependent anion secretion is mediated by Cl^- transport through apical CFTR Cl channels (Hanaoka, Devuyst et al. 1996). The Na^+-K^+- ATPase transporter is the important active transporter in the basolateral membrane that pumps sodium out of the cell in exchange with potassium. This is important in maintaining the chemical gradient for Na^+ and K^+ across the membrane (Hanaoka, Devuyst et al. 1996). The second transporter is Na^+-K^+-$2Cl^-$ which utilizes the Na^+ gradient to transport Na^+, K^+, and 2 Cl^- into the cell. This increases the Cl^- concentration above its electrochemical gradient. For example, when

vasopressin binds to the V2 receptor, a G-protein coupled receptor, this leads to an increase in the synthesis of cAMP via adenylyl cyclase. This increase in cAMP activates PKA which in turn activates the cystic fibrosis transmembrane conductance regulator (CFTR) chloride channel on the apical membrane of the cell, leading to Cl^- efflux by cAMP dependent secretion **(Figure 1.5)** (Wallace, Grantham et al. 1996). Subsequently, this activates the KCa3.1 channel which increases basolateral K^+ conductance and both channels create a driving force for paracellular transport of Na^+ and this addition of NaCl to the luminal fluid creates the osmotic movement of fluid into the cyst (Sullivan, Wallace et al. 1998).

1.10. Targeting cAMP pathway in PKD.

Animal models of polycystic kidney disease have helped to provide a significant new understanding of the molecular and cellular pathogenesis of ADPKD. In addition, they have enabled the testing of novel treatments for ADPKD. Furthermore, animal models have been used to identify genes which modify the severity of the disease (Saigusa and Bell 2015). Several trials targeting the cAMP pathway in PKD animal models and ADPKD patients have been completed. One trial used the vasopressin antagonist V2R antagonist **OPC-31260** which was found to be very effective in reducing the disease progression in both ADPKD and ARPKD in animal models pkdws25/- mouse, pck rat respectively, by down regulation of cAMP signalling, cell proliferation and chloride driven fluid secretion (Wang, Gattone et al. 2005).

The second drug was Octreotide, a somatostatin analogue which is being used to antagonise the action of vasopressin in collecting ducts. In one study, octreotide binds with somatostatin G coupled receptors inhibiting AC activity and decreasing cAMP production. It has been shown to decrease kidney and liver cysts in a pck rat model of polycystic kidney disease (Masyuk, Masyuk et al. 2007). A trial was carried out in ADPKD patients using long acting

somatostatin analogue (multicentre randomised controlled trial), on kidney volume and cyst growth in ADPKD patients compared to control group over 3 years There was decrease in total kidney volume in somatostatin group compared to placebo (Caroli, Perico et al. 2013).

Furthermore, the SKI-606, a Src inhibitor, which is intermediate between receptor activation and the Ras/Raf/MEK/ERK pathway, caused a decrease in biliary and renal cysts in pck rat, and bpk mouse models (Sweeney, von Vigier et al. 2008). It was entered into a phase II randomised clinical trial (Riella, Czarnecki et al. 2014). A c-src inhibitor (SKI606) and a tyrosine kinase inhibitor (KD019), both shown to be effective in other cancers e.g. non-small cell lung carcinoma (Pietanza, Gadgeel et al. 2012). Based on promising preclinical data in rodent models (Gile, Cowley et al. 1995), In addition, the inhibition of fluid secretion through the use of CFTR inhibitors was found to decrease cyst expansion in an embryonic pkd1-/- mouse kidney (Yang, Sonawane et al. 2008). BPO-27 is CFTR inhibitor with great efficiency and potency and anti- secretory effects in culture model of PKD. It is potential candidate for further preclinical study (Snyder, Tradtrantip et al. 2011). Other studies have examined a role for the mammalian target of rapamycin (mTOR) pathway in the pathogenesis of ADPKD. In animal models, mTOR inhibition resulted in decreased cyst growth (Tao, Kim et al. 2005, Shillingford, Murcia et al. 2006). Two human trials have studied the effect of sirolimus compared to standard care for 18 months (SUISSE) or everolimus for 24 months in a second trial. However the results have been disappointing with non-significant decreases in kidney volume in the first trial and no improvement in GFR in both studies (Perico, Antiga et al. 2010, Walz, Budde et al. 2010).

Finally, a RCT of pravastatin in paediatric and young adults with ADPKD revealed a positive effect in reducing TKV increase associated with an improvement in oxidative stress markers (Klawitter, McFann et al. 2015).

Many other new treatments for ADPKD have been identified in preclinical studies but have not been formally tested in man. It is likely that the clinical management of ADPKD will change from monitoring to active treatment with a combination of different drugs that targeting different disease pathways (Rathaus 2007).

1.11. The prostaglandins and their receptor function in normal kidney.

Prostaglandins are a group of biologically active lipids originating from the twenty carbon essential fatty acids (Antonucci, Cuzzolin et al. 2007). Prostaglandin production involves three important stages: the first step is the conversion of cell membrane phospholipids by the enzyme phospholipase A2 to arachidonic acid. The second step is catalysis of arachidonic acid by COXs enzymes (COX1-COX2) to an intermediate endoperoxide, prostaglandin H2. The final step consists of a change of PGH2 through enzyme PG synthase to PGs (PGE2, PGI2, PGD2 and PGF2α) and thromboxane (TXA2) (**Figure 1.7**) (Cha, Solnica-Krezel et al. 2006). Prostaglandins have a central ring called the cyclopentane ring, and two side chains called α and ω that are attached to the cyclopentane ring (Narumiya, Sugimoto et al. 1999) (**Figure 1.7**).

PGE2 functions as an autocrine and paracrine factor to maintain local homeostasis (Tsuboi, Sugimoto et al. 2002). The action of prostaglandins is controlled by COX, prostaglandin synthase and its receptors. These prostaglandins have significant roles in body homoeostasis, platelets aggregation, inflammation and control of fever and pain. Furthermore, they play an essential role in renal, respiratory, reproduction and gastrointestinal functions. In addition, they play vital roles in the immune system, sleep control, apoptosis and tumorigenesis (Nasrallah, Clark et al. 2007). The function of PGs is mediated primarily via binding to a family of cell surface membrane proteins called G- protein coupled receptors (GPCRs). These are called EP receptors for PGE2, IP receptors for PGI2, DP receptors for PGD2, FP receptors for PGF2α and TP receptors for thromboxane 2 (Tsuboi, Sugimoto et al. 2002). The GPCRs consist of

seven transmembrane alpha-helices that move in and out of membrane and are involved in cell signalling transmission. PGE2 binds to a G-protein heterotrimer consisting of α, β, and γ subunits, that activates downstream signalling pathways important for regulating cell proliferation, inflammation, tissue repair and remodelling (Dorsam and Gutkind 2007).

Prostaglandin E2 (PGE2) is the major prostanoid in the kidney, followed by PGI2, PGF2α and thromboxane A2 (Nasrallah, Clark et al. 2007). Prostaglandin E2 production occurs primarily in glomeruli and collecting ducts (Breyer and Breyer 2000). It plays a significant role in glomeruli and tubular function. For example, PGE2 maintains the glomeruli filtration rate and regulates renal blood flow through vasoconstrictors and the secretion of renin. In tubules it has an important role in water and electrolyte transport in a different tubular segments and collecting ducts (Breyer and Breyer 2000).

The effect of prostaglandin E2 in the kidney is mediated mainly by four G-protein coupled receptors (PTGER1, PTGER2, PTGER3 and PTGER4) (Nasrallah, Hassouneh et al. 2014). Both receptors PTGER2 and PTGER4 coupled with Gs-activating adenylyl cyclase lead to increased cAMP and protein kinase A activation (Castellone, Teramoto et al. 2005) (**Figure 1.8).**

The PTGER1 and PTGER3 receptors contribute to the renal arterial vasoconstriction through effects on Ca^{2+} levels and the inhibition of cAMP levels respectively (Pena-Silva and Heistad 2010). PTGER1 is located mainly in the connecting segment, cortical collecting ducts, inner and outer medullary collecting ducts. It is coupled to Gq and activates phosphatidylinositol hydrolysis and protein kinase C leading to increases in intracellular Ca^{2+} and a decrease in Na^{+} and water reabsorption in collecting ducts (Morath, Klein et al. 1999) (Breyer and Breyer 2000) (**Figure 1.8**).

PTGER3 is mainly situated in the glomeruli, thick ascending limb, cortical and medullary collecting ducts and arterial endothelial cells. It has multiple splice variants coupled to either Gαi, Gαs, or Gαq and activates multiple signalling pathways. In humans, there are eight PTGER3 splice variants (Hata and Breyer 2004). PTGER3, couples primarily with Gαi and causes vasoconstriction by decreasing cAMP through stimulation of MAPK. It can also couple with Gαs or Gαq depending on the splice variant (Morath, Klein et al. 1999) (Breyer, Davis et al. 1996, Breyer, Jacobson et al. 1996) (**Figure 1.8**).

PTGER2 has the lowest expression in the kidney compared to other PTGER receptors. It is present primarily in interstitial cells, media of arteries and glomerular arterioles and vascular smooth muscle, it has a significant role in salt excretion (Morath, Klein et al. 1999).

PTGER4 is highly expressed in glomeruli, media of arteries and outer medullary collecting ducts. It has an important role in regulating the glomerular filtration and hemodynamic function (Breyer and Breyer 2000). PTGER2 and PTGER4 may cause vasodilatation of renal arteries through their effects on cAMP. They also regulates sodium and electrolytes transport (Poschke, Kern et al. 2012) (Nasrallah, Hassouneh et al. 2014).

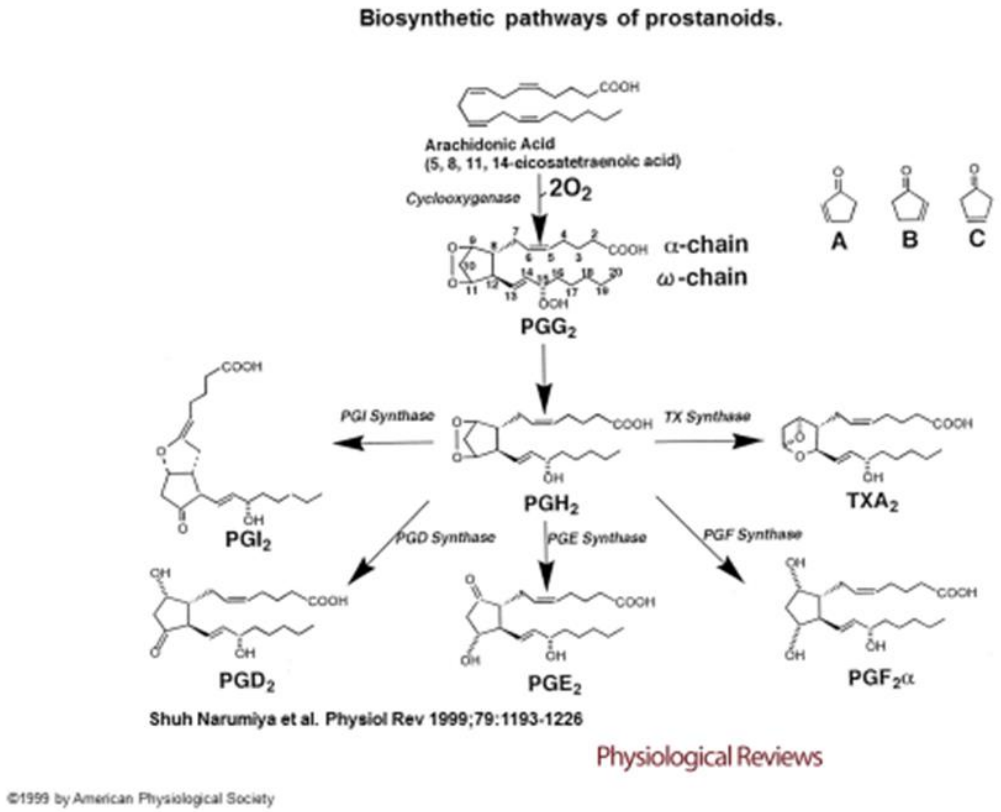

(Narumiya, Sugimoto et al. 1999).

Figure 1.7. Biosynthesis of prostanoid.

The first step is conversion of arachidonic acid to PGG2 and then to PGH2 by cyclooxygenase (COX1-COX2). Step 2 is the change of PGH2 to PGI2, PGD2, PGE2, PGF2α and TXA2 via the enzyme PG synthase (Narumiya, Sugimoto et al. 1999)

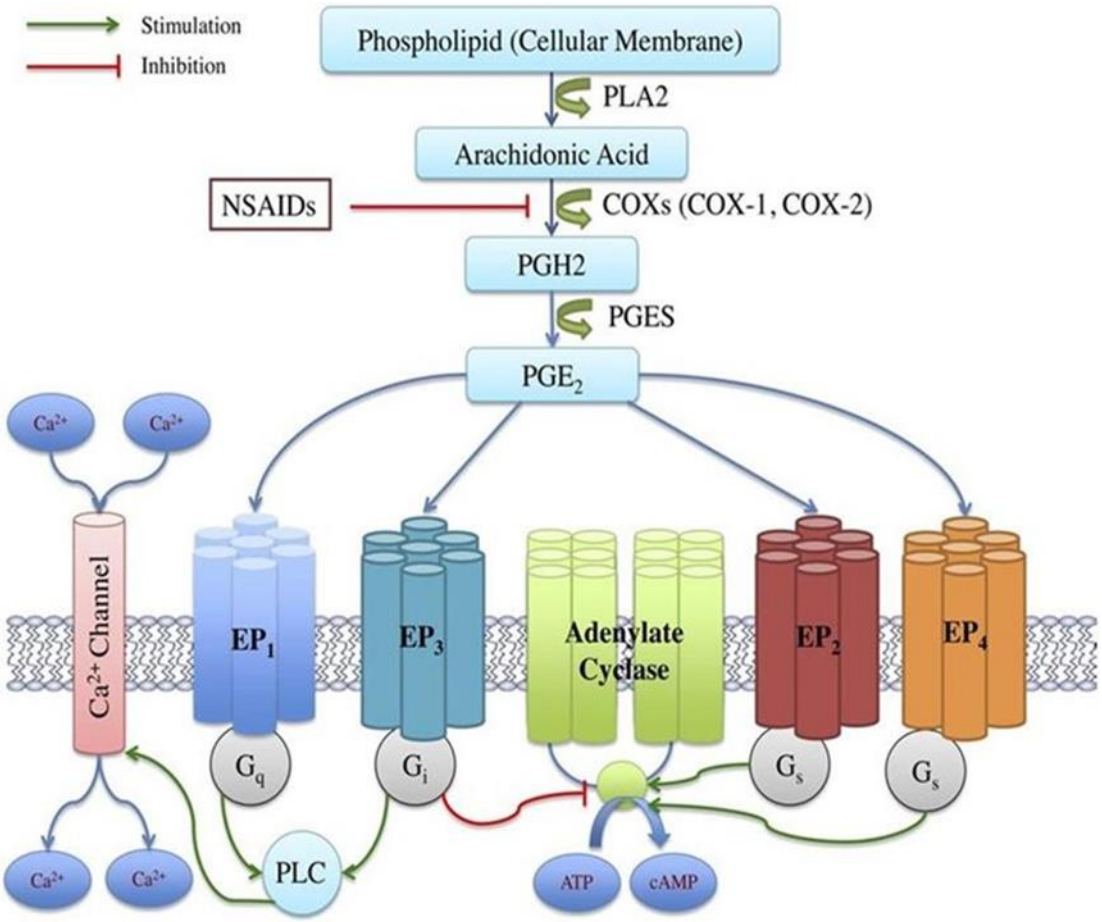

American Journal of Renal Society 2014 (Nasrallah, Hassouneh et al. 2014)

Figure 1.8. The signalling pathway for PGE2, and its 4 receptors.

PGE2 synthesised first from changing of phospholipid by PLA2 to arachidonic acid that changes to PGH2 by cyclooxygenase (COX1/COX2). The PGE2 is produced by changing of PGH2 to PGE2 by enzyme prostaglandin synthase. PGE2 works via its four receptors PTGER1, PTGER2, PTGER3 and PTGER4. The four receptors bind to G protein- coupled receptors; the PTGER1 binds with Gq and increases Ca^{2+} levels by activating PLC. The PTGER2, and PTGER4 couple with G stimulatory protein (Gs) that stimulate AC to increase the cAMP level. PTGER3 acts mainly by coupling with Gi to increase intracellular Ca^{2+}levels through PLC and decreases the cAMP level through AC.

1.12. PTGER2 and PTGER4 receptor signalling.

Although activation of both PTGER2 and PTGER4 receptors lead to increased intracellular cAMP, they differ in both their structure and subcellular localization. Both proteins have only 30% identity in their transmembrane domains (Fujino and Regan 2003). PTGER2 contains 358 amino acids whereas PTGER4 consists of 488 amino acids (Regan 2003). Unlike PTGER2 that has a short tail, PTGER4 has a long carboxyl tail enclosing several phosphorylation sites (Tsuboi, Sugimoto et al. 2002). Furthermore, PTGER4 responds to an agonist by internalisation and desensitisation and no such effect is observed for PTGER2 (Nishigaki, Negishi et al. 1996, Desai, April et al. 2000).

PTGER2 and PTGER4 couple with Gαs proteins to activate adenylate cyclase thus increasing intracellular cAMP levels which activate PKA. The activation of PKA leads to phosphorylation of CREB at Serine-133 (cAMP response element protein) and its nuclear translocation. This is important in promoting cell survival by increasing the gene expression of Bcl-2 which has an anti-apoptotic effect. It can also promote gene expression of COX-2 which leads to increased synthesis of PGE2 and cyclin D1 which is important in regulating cell cycle progression at mid and late G1 phases (Mayr and Montminy 2001). PTGER4 phosphorylates and stimulates CREB (cAMP response element protein) mainly through PI3K/Akt pathway and the PKA pathway (Fujino, Salvi et al. 2005) (**Figure 1.9).**

On other hand, PTGER2 through PKA can also phosphorylate and inactivate glycogen synthase kinase (GSK-3α) which leads to activation of the β-catenin pathway. β-catenin translocate to the nucleus and forms a complex with transcription factor T-cell factor (TCF) (Castellone, Teramoto et al. 2005, Shao, Jung et al. 2005, Elberg, Turman et al. 2012). The TCF complex activates gene expression important in promoting cell growth, decreasing apoptosis, and increasing cell motility (cyclin D1, VEGF or vascular endothelial growth factor, c-myc and

matrilysin) (Shao, Jung et al. 2005) (**Figure 1.9**). The anti-apoptotic effect is mediated through PI3K and phosphorylated Akt that blocks the translocation of BAX from cytoplasm to the mitochondria, this in turn prevents caspase activation and apoptosis (Stenson 2007).

The PTGER4 receptor induces phosphorylation of GSK-3α and subsequent activation of the β-catenin pathway primarily through PI3K pathway rather than through the activation of the cAMP/PKA Pathway (Fujino, West et al. 2002). Additional differences between the two receptors are that PTGER2 principally induces the PKA (protein kinase A) pathway (**Figure 1.9**) which activates the β-catenin pathway and finally stimulates T-cell factor whereas PTGER4, in addition, to stimulating the PKA pathway also activates Gαi protein and downstream signalling through PI3K activating β-catenin and T-cell factor. Furthermore, PTGER4 can increase expression of early growth factor-1 (EGF-1) through the Ras/ MAPK/ERK pathway which is important for the transcription of PGE2 synthase leading to increased production of PGE2. This results in a positive feedback loop that increases cell proliferation **(Figure 1.9**) (Fujino, Xu et al. 2003).

1.13. Prostaglandin and its receptors in ADPKD.

Several previous studies had indicated a role for PGE2 in the pathogenesis of ADPKD, For example, elevated levels of PGE2 were shown to be present in the cystic fluid of human ADPKD patients by radioimmunoassay compared to normal blood levels (Gardner, Burnside et al. 1991). A rodent polycystic kidney model had a higher level of PGE2 compared to control animals (Sankaran, Bankovic-Calic et al. 2007). One study found that an elevated level of PGE2 was present throughout progression of ADPKD (Sorensen, Glud et al. 1990). PGE2 acts to increase cAMP production in cystic epithelial cells of ADPKD, mainly through its

interaction with the receptors PTGER2 and PTGER4. Together they act by coupling the G-stimulatory protein Gs activating adenylyl cyclase to produce cyclic AMP (Sankaran, Bankovic-Calic et al. 2007). Another study was able to demonstrate that cyst formation was increased following stimulation of cystic cells with PGE2. This effect was mediated mainly through increased expression of PTGER2 receptors in these cells (Elberg, Elberg et al. 2007).

Gene analysis to investigate the molecular mechanism of cystogenesis using cDNA microarray analysis of the ADPKD cysts found an upregulation of PTGS2 (8.2 fold) and of PTGER2 (>3-fold) (Song, Di Giovanni et al. 2009). The upregulation of PTGER2 may stimulates adenylyl cyclase and increase cAMP production (Belibi, Reif et al. 2004, Song, Di Giovanni et al. 2009). On the other hand, the PTGER3 receptor is downregulated (-3.5 fold) which decreases the cAMP production in ADPKD.

PGE2 secretion in cyst fluid stimulates PTGER2 receptor mRNA expression by three- to fourfold in cystic epithelial cell (CEC) primary cultures (Elberg, Elberg et al. 2007). The PTGER2 receptor antagonist (AH-6809) has been shown to inhibit PGE2 stimulation of cAMP production in CEC (Elberg, Elberg et al. 2007). Another study highlighted the role of PTGER4 in IMCD-3 cyst expansion (Elberg, Turman et al. 2012). Another study on mouse IMCD-3 cells showed that PGE2 increased proliferation and fluid secretion through a PTGER4 but not PTGER2-dependent pathway (Liu, Rajagopal et al. 2012). Therefore, blocking both PTGER2 and/or PTGER4 receptors using selective antagonists may have a therapeutic role in ADPKD.

These results are consistent with data from studies of PGE2 in cancer. PGE2 is a potent stimulus for the growth of certain tumours such as colorectal carcinoma. PGE2 acting via PTGER4 receptor can enhance the growth and invasiveness of colorectal carcinoma through the Wnt pathway (Sheng, Shao et al. 2001). PTGER4 knockout mice had a decrease in abnormal crypt formation in colon cancer (Regan 2003). While PTGER2 knockout in an APC

mouse model cell decreased the number and size of intestinal polyp in adenomatous polyposis coli (Sonoshita, Takaku et al. 2001).

Although nonsteroidal anti-inflammatory drugs (NSAIDs) have been used for the prevention and treatment of colon cancer through inhibition of cycloxgenase-2 (COX-2), long-term treatment with NSAIDs has been associated however with increased risk of cardiovascular death (Myung and Kim 2008). Similarly, NSAIDs have also been shown to inhibit PKD in rodent models (Aukema, Adolphe et al. 2003). Antagonism of PTGER4 or and PTGER2 receptors could potentially be used for the treatment of ADPKD (Liu, Rajagopal et al. 2012), avoiding cardiovascular side effects (Takahashi, Uehara et al. 2014).

.

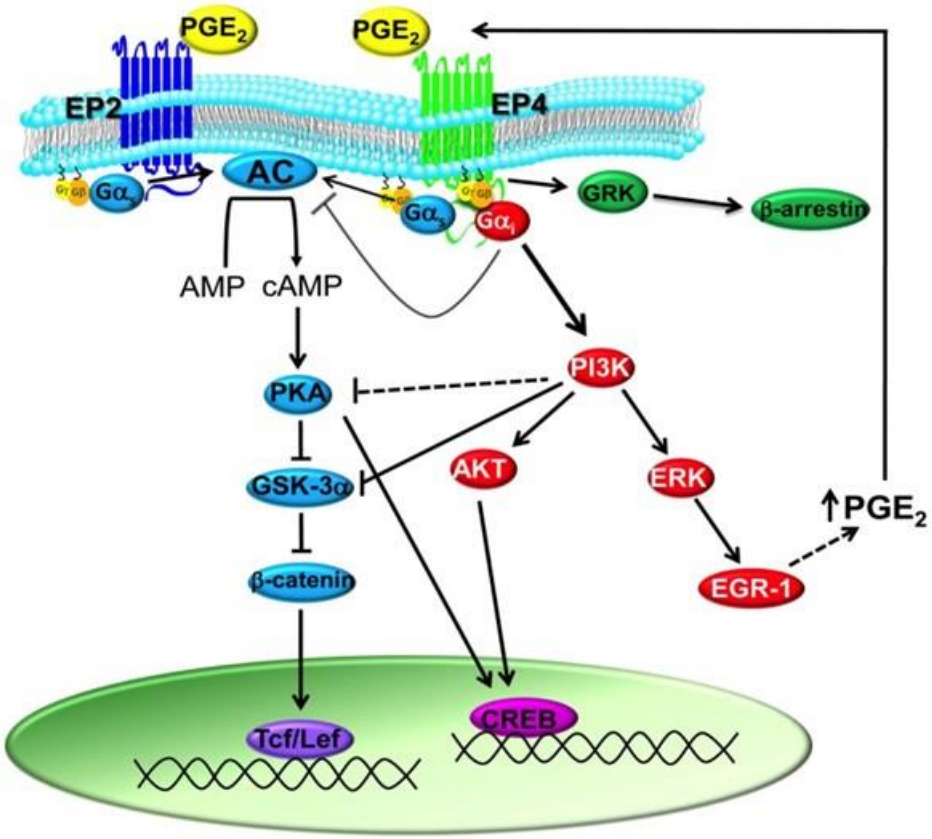

(De Keijzer, Meddens et al. 2013).

Figure 1.9: PTGER2 and PTGER4 regulate different signalling pathways activated by PGE2.

Activation of PKA and PI3K signalling pathways leads to activation of TCF and CREB transcription factors that increase the gene expression which involved in proliferation and cell survival. Activation of PI3K/ERK induce expression of early growth response-1 that increase PGE2 synthase. PI3K and PKA pathway inhibits the GSK-3α leading to stabilization of β-catenin that translocates to the nucleus and regulates TCF dependent genes (De Keijzer, Meddens et al. 2013).

Hypothesis

Increased levels of PTGER2 contribute to the pathogenesis of APDKD. Therefore, blocking PTGER2 using specific receptor antagonists may have a therapeutic role in reducing cyst growth in ADPKD.

Objectives:

1. Optimization of 3D culture method for cell lines derived from patients with ADPKD.
2. Determination of the expression levels of PTGER receptors 2 and 4 by Western blotting, IHC from human ADPKD tissue sections.
3. Determination of expression levels of PTGER receptors 2 and 4 by qPCR and IHC from two independent orthologous mouse models of ADPKD.
4. Test the effect of PGE2, PTGER2, and PTGER4 receptor antagonists on cyst growth, cell proliferation and apoptosis in control and ADPKD kidney epithelial cell lines.
5. Compare cAMP levels in control and ADPKD kidney epithelial cell lines incubated with PTGER2, and PTGER4 receptor antagonists.

Chapter 2

Materials and Methods

2.1. Cell lines and culture conditions:

The primary epithelial cell lines used in this study are tabulated below (**Table 2.1.1**):

Cell Lines	Description	Origin
OX161	Human kidney epithelial cell line originated from ADPKD kidney	Prof. Albert Ong. UK
OX161/C1	Human kidney epithelial cell line originated from ADPKD kidney	Prof. Albert Ong. UK
SKI-001	Human kidney epithelial cell line originated from ADPKD kidney	Prof. Albert Ong. UK
OX938	Human kidney epithelial cell line originated from ADPKD kidney	Prof. Albert Ong. UK
SKI002	Human kidney epithelial cell line originated from ADPKD kidney	Prof. Albert Ong. UK
UCL93	Human kidney epithelial cell line originated from normal adult human kidney	Prof. Albert Ong. UK
RFH	Human kidney epithelial cell line originated from normal paediatric human kidney	Prof. Albert Ong. UK

MDCK II	Canine kidney epithelial cell line originated a cocker spaniel kidney	Prof Nick Simmons, Newcastle

2.1.2. Cell culture material that used in the experiments are tabulated in (Table 2.1.2).

Culture media and reagent in tissue culture	Supplier	Address
Dulbecco's Modified Eagle Medium (DMEM). 500ml	Life technology	3 Fountain Drive Inchinnan Business Park Paisley PA4 9RF, UK Phone: 0141 814 6100 Fax: 0141 814 6260 Email: ukorders@lifetech.com
Dulbecco's Modified Eagle Medium: Nutrient Mixture F-12(DMEM/F-12) 500Ml.	Life technology	
FCS (Foetal Calf Serum)	Bio sera	1 Acorn House, The Broyle, Lewes BN8 5NN +44 1273 814466
NU Serum	Fisher scientific	Fisher Scientific UK Ltd Bishop Meadow Road Loughborough LE11 5RG
Antibiotic-Antimycotic). 100x	Life technology	3 Fountain Drive Inchinnan Business Park

L-Glutamine 1% 200mM	Life technology.	Paisley PA4 9RF, UK Phone: 0141 814 6100 Fax: 0141 814 6260 Email: ukorders@lifetech.com
Phosphate buffer saline (PBS) (1X).	Bio Whittaker.	875 Brockelman Road Lancaster, MA 01523 Phone: (978) 368-3124
.05% trypsin-EDTA (1x)	Life technology.	3 Fountain Drive Inchinnan Business Park Paisley PA4 9RF, UK Phone: 0141 814 6100 Fax: 0141 814 6260 Email: ukorders@lifetech.com
EGF (epidermal growth factor) 10ng/ml 5ul	Sigma	Technical Services PO Box 14508 St. Louis, MO 63178 UNITED STATES
Hydrocortisone 5ug/ml	Sigma	
Prostaglandin E2	Sigma	
100X Insulin-Transferrin-Selenium (ITS -G)	Life technology	3 Fountain Drive Inchinnan Business Park Paisley PA4 9RF, UK Phone: 0141 814 6100
db-cAMP	Calbiochem	165 New Boston Street Woburn, MA 01801

		Phone: +1-781-937-0777
Forskolin	Sigma	Technical Services PO Box 14508 St. Louis, MO 63178 United states
10x MEM	Sigma	
EGF	Sigma	

2.2. Three Dimensional gel cell cultures

Gels	**Amount**
Collagen I Rat tail (Invitrogen)	5mg/ml
Collagen 2009 Rat tail	Prepared in house
Geltrex (Invitrogen cell culture)	5ml
BD Matrigel	BD Biosciences
BD matrigel matrix high concentration	BD Biosciences

2.3. Western Blotting

2.3.1 List of primary antibodies used in Western Blotting and immunohistochemistry.

Raised in	Name	Directed against	Dilutions	Source	Catalogues number
Rabbit	Calnexin	Control	WB1/2000	Sigma	C4731
Mouse	7e12	PC1	WB1/2500	Albert Ong	
Goat	G-20	PC-2	W.B 1/1000	SantaCruz biotechnology	Sc10376
Mouse Rabbit	PTGER2 PTGER2	PGER2 PTGER2	WB 2ug/ml IH 8-25ug/ml WB 100µg 0.6mg/ml	Rand D System Abcam	MAB6656 Ab73191
Rabbit	PP-30	PC-2	WB 1/2000	Albert Ong	
Mouse	IAII	PC2	WB 1/2500	Guangqing Wu, Vanderbilt	
Rabbit	β-actin	β-actin protein	WB 1/2000	Cell signaling	4970P
Rabbit	PTGER4	PTGER4	WB1/1000	Sigma	HPA012756

2.4. Lists of primary antibodies used in Immunofluorescence and immunohistochemistry.

Raised in	**Name**	**Directed against**	**Dilutions**	**Source**	**Catalogues number**
Rabbit	Cleaved-Caspase-3(Asp175) (D3E9)	Caspase-3	1/200	Cell signaling technology	**9579S**
Rat	Zo-1 R26-4C	Zo	1/200	David Goodenough	
Mouse	Gp135	GP135	1/200	George Ojakian	
Mouse	PTGER2	PGER2	IH 8-25ug/ml	R and D Systems	MAB6656
Rabbit	PTGER4	PTGER4	IHC 1/25	Sigma	HPA011226
Alexa	Phalloidin	Actin	IF 1/40	Life technology	A12381

2.5. Lists of kits used in ELISA.

Kit	Supplier	Catalogues number
In Situ Cell Death Detection Fluorescein	Roche	Version 17 11684795910
Cell proliferation Elisa BrdU	Roche	Version 16 11647229001
cAMP Assay	R& D	KGE002B
Cell Titer 96® AQueous One Solution Cell (MTS) Proliferation Assay	Promega	G3582

2.6. mRNA assay (qPCR):

2.6.1 Samples:

N^0	Cell Line	Normal/Cystic
1	CL5	Normal
2	CL8	Normal
3	CL11	Normal
4	RFH	Normal
5	UCL93	Normal
6	OX161	Cystic
7	OX938	Cystic
8	SKI-001	Cystic
9	SKI-002	Cystic

2. 6.2 RNA isolation:

Chloroform (sigma)
Isopropyl alcohol (sigma)
75% ethanol (in DEPC-Treated water) VWR
RNase-free water
Polypropylene micro centrifuge tubes DNA ladder life technology
Water bath (55-60^{0}C)
Ethidium bromide (sigma)
Centrifuge and rotor capable of reaching up to 12,000xg

2.6.3. qPCR primers:

N^0	qPCR	Reference/Experimental	Source
1	GADPH	Human control RNA	A&B applied biosystems
2	PTGER-1	Human Hs00909194 g1	
3	PTGER-2	Human Hs04183523 m1	
4	PTGER-3	Human Hs00168755 m1	
5	PTGER-4	Human Hs00168761 m1	

2.6.4 Reverse Transcription: high capacity RNA-to-cDNA Kit.

Component	Component volume/ Reaction(ul)	
	+ RT reaction	-RT reaction
2X RT Buffer	10.00	10.00
20X Enzyme Mix	1.0	-
RNA Sample	Up to 9ul	up to 9 ul
Nuclease- free H_2O	To final volume 20ul	To final volume 20ul
Total per Reaction	20.0	20.0

2.6.5 qPCR: TaqMan Gene Expression Assay

component	Volume(ul)/20ul Reaction
20X TaqMan Gene Expression Assay	1.0 µl
2X TaqMan Gene Expression Master Mix	10µl
cDNA template(1-100 ng)	x µl
RNase-free Water	Up to 9µl
Total	19ul

2.6.6. Reverse Transcription: TaqMan qPCR

Thermal cycle conditions

Time (Minutes)	Temperature (°C)
60	37
5	95
∞	4

2.1. Mammalian cell culture.

The kidney epithelial cells that were used throughout the project were of two types: non cystic cells (UCL93, RFH), and cystic cells (OX161, OX161/C1, OX938, SKI-001, SK002). All cell lines, other than the MDCK II, were immortalised from primary cultures of tubular cells taken from ADPKD and the normal human kidneys which were removed for clinical proposes. The cells were transduced with replication-defective retroviral vector containing the temperature sensitive LT antigen and the catalytic subunit of human telomerase (hTERT) or sequentially with vectors containing either gene. All clones were generated from pooled cultures of cystic cells at early passage except for OX938 where cells were isolated from three individual cysts (C6-8) and propagated.

The cells were grown in the DMEM-F12 media (Invitrogen) with 1% L-Glutamine 5ml supplement and1% antibiotic/anti-mycotic (penicillin/streptomycin) (Invitrogen) 5ml to prevent bacterial and fungal infections, and 5% (25ml) NuSerum (Becton Dickinson). In preliminary experiments a number of different kidney cell lines were tested for their ability to form cysts in 3D cultures including, IMCD3 (Inner medullary collecting duct), MEK wildtype and null (PC1) cells and PTEC (proximal tubular epithelial) cell. Unfortunately, none of these cells form cystic structures in 3D culture media. That is why I decided to use the MDCKII cell line which forms cysts in 3D culture and has been used in many studies as a model of cystic

cells (Buchholz, Teschemacher et al. 2011, Engelberg, Datta et al. 2011) The MDCKII cell kidney epithelial cells were cultured in Dulbecco's Modified Eagle Medium (DMEM) (life technology) supplemented with 1% L-Glutamine (Invitrogen), 10% FCS and 1% antibiotic/antimycotic solution (Invitrogen).

T75 flasks were used for the cell growth at 33^0C and 5% CO_2. The cells were passaged when they reached 75-95% confluence. The passaging was carried out by applying aseptic technique in hood with gloves; media was aspirated from the flask by suction and the cell monolayer was washed with 10ml sterile PBS. 1X trypsin 2ml (Invitrogen) solution was added to the cell and flask was incubated for 5min in an incubator 33ºC or until the cells were detached from the flask. Trypsin was then neutralised by adding 10ml of the culture media. The cells were by pipetted into a universal tube and centrifuged for 5 minutes. The media was removed and the cell pallet was dissolved in 5ml media; the cell was then seeded into a new flask. The process was followed up by microscope for confluency. The media was usually changed every 2 days.

Cell cryopreservation: after trypsinisation and centrifugation, the cells pellets were resuspended using freeze media containing 10 %(v/v) Nu serum, 10% DMSO. The cell were placed into a cryovial, and frozen in a -80ºC freezer in an isopropanol container for 24 hours, before transferring them into liquid nitrogen reservoir at -190 ºC for long term storage.

2.2. Rat tail collagen preparation.

Rat tail tendons were dissected from 70% ethanol washed rat tails and extensively washed in sterile distilled water. Type I collagen was extracted by incubation in 0.1M acetic acid for 72 hours at 4°C with stirring. The solution was transferred to ultra-centrifuge tubes and insoluble material spun down at 10000g for 30 min. The supernatant was transferred to sterile tubes and stored at 4°C until use.

2.3. Three-dimensional Cyst assays.

2.3.1. Type I collagen gel cyst assay.

Collagen gels were formed by mixing ice-cold type I Collagen gel (3.84 mg/ml 70% vol/vol), 20% NaHCO3 solution (11.76 mg/ml), and 10% 10X MEM (Invitrogen). A mixture (100µl/well) of Collagen and cells at a density of $2x10^4$ cells/well were plated in triplicate into 96 well plates. The gel was allowed to polymerise at 37^0C for 20 minutes prior to adding 100 µl of the growth media on top of the polymerised cell-containing Collagen gel. This was then incubated at 37^0C in a humidified atmosphere of 5% CO2 for 10-15 days. The media was changed every 2 days. The cells were observed and phase-contrast images of cells were taken by inverted microscope (Olympus IX71) from day 2 and observed every two days for eight days. The cAMP and Forskolin experiment first the dibutyryl cAMP 100µM (Calbiochem) and Forskolin (Calbiochem) 10µM were added to MDCK II cells at day 2 in triplicate, and the control cells were added just media in triplicate. The treatment and control were changed every two days as well. The cells were observed, phase contrast image of the cells were taken every two days and measurement of cyst area were taken for treatment and control cells every two days.

To test the effects of prostaglandin E2, different concentrations of PGE2 (Sigma) were first prepared by diluting with the media (12.5nM, 25nM, 50nMand 100nM, 250nM, 500nM, 1µM) and every concentration were adding in triplicate into the seeding MDCK II cells. The control cells were maintained in normal media in triplicate from day 2 and media changed every two days. Cells were observed daily and phase contrast images taken every two days for the measurement of cyst area.

2.3.2. Cyst assay with collagen and Matrigel

Collagen gels were formed as described in section 2.4.1 and mixed with an equal volume of Matrigel. Cell density and cyst growth were as described in section 2.4.1.

2.3.3. Matrigel cyst assay.

To culture cells on top of a Matrigel layer, Matrigel was first thawed on tice for 1-2 hours before 100 µl of Matrigel was added to each well of a 96 well plate. The plate was incubated at 37°C for 30 minutes to promote polymerisation of the Matrigel. Cells were plated directly onto the surface of the gel at a density of $4x10^4$ cells/well in culture media containing 100 µl matrigel/5ml media.

To culture cells embedded inside Matrigel 4 $x10^4$ cells were mixed with 100µl of matrigel and seeded in triplicate into the wells of a 96 well plate. The plate was incubated at 37°C for 30 minutes to promote polymerisation of the Matrigel. Culture media was added to the top of the Matrigel.

This was then incubated at 33^0C (human cells) or 37^0C (MDCK II) in a humidified atmosphere of 5% CO2 for 10-15 days. The media was changed every 2 days. The cells were observed, and phase-contrast images of cells were taken by inverted microscope (Olympus IX71) from day 2. After 48 h, the dibutyryl cAMP 100µM (Calbiochem) and Forskolin (Calbiochem) 10µM were added to OX161/C1cells in triplicate, and the control cells were added just media in triplicate. The cells were observed every two days and measurement of cyst area were taken for treatment and control cells every two days. Next, the prostaglandin experiment was carried out. First different concentrations of PGE2 (Sigma) were prepared by diluting with the media (12.5nM, 25nM, 50nM, 100nMm, 500nM, and 1µM) and every concentration were adding in triplicate into seeding OX161/C1 cells. The control was treating with just media in triplicate

as well at day 2. The cells were observed and phase-contrast images of cells were taken by inverted microscope (Olympus IX71) and measurement of cyst area were taken for treatment and control cells every two days.

2.3.4. Measurement of average cyst area and statistical analysis.

To measure the growth rate cysts from 3 independent wells were counted with at least 8 cysts/ well, 20 cysts for total 3 wells for MDCK II and 15 cysts/ well, 45 cysts / total 3 wells for OX161/C1. Cysts were defined according to the following criteria: transverse diameter of the cysts >100µm and cyst area >50µm^2 (Elberg, Turman et al. 2012). We measured at least 8 randomly selected fields for each well measuring all the observable cysts which met our criteria for a definition of a cysts in each field. For statistical interpretation unpaired t test was used for two groups(two sets of measurement) and ANOVA test for more than two groups (mean± SEM). P value was significant if <0.05 .

The average cyst area was measured using SimplePCI software (x20 magnification) and average cyst area in triplicate wells calculated. Three independent experiments were performed for each condition, and one experiment was chosen to represent the result of the experiment.

The statistical analysis were carried out using Prism software (Graph Pad) with P-values reported as >0.05 (Non-significant) or <0.05 (significant). An unpaired t- test was performed to compare two groups, and one way ANOVA test was carried out to compare three or more groups.

2.3.5. Testing the effect of PTGER2 and PTGER4 receptor antagonists in cyst assays.

MDCK II and OX161/C1 cells were cultured in Collagen or Matrigel cyst assays as described previously. After 48h cells were treated in triplicate with PTGER2 antagonist (**PF-04418948**)

or PTGER4 antagonist (**CJ-042794**) with concentration ranging from 100 nM to 10 µM. Control cells were treated with 0.1% DMSO. In some experiments 50 nM PGE2 was added following pre-incubation for 2 hrs with PTGER2 or PTGER4 or a combination of PTGER2 and PTGER4 receptor antagonists (500 nM or 1µM). Media was changed every 2 days and phase-contrast images of cysts were taken by inverted microscope (Olympus IX71) from day 2.

2.4. Immunofluorescence.

2.4.1. Staining the cells in Collagen and Matrigel.

The cell suspension of MDCK II and OX161/C1 was counted in heamocytometer to desired concentration of $2x10^4$, and then plated in Collagen gel and OX161/C1 in Matrigel in 96well plates. Next day, the media was removed from the gel and replaced by media containing PGE2 with three different concentrations (12.5nM, 25nM, 50nM, and100nM) in triplicate. The cAMP (50µm) and Forskolin (5µm) were prepared and added to gel in triplicate. The cell in the gel was followed in the microscope and media changed every two days for 10 days. On day eleven, the media was removed and washed three times with PBS. First, the cells were fixed with 4% paraformaldehyde for one hour at room temperature. Then, the gel was washed again three times with PBS with shaking for 10minutes. Next, the 4% paraformaldehyde was quenched with 0.15M glycine in PBS for 10min. After the gel had been washed with PBS three times for five minutes the gel permeabilized in 0.1% triton x-100 in PBS followed by washed three time with PBS for 10 min. Next, the cells were blocked with BSA for 30 minutes at room temperature. Subsequently, the cells were incubated with Phalloidin red 1/40 or ZO-1 or gp-135 1/200 overnight at 4^0C. Next day, the gel was washed 1x15 minutes, then twice for 30minutes, and lastly once for 15 min with PBS. For gp-135 and ZO-1 goat anti-mouse and anti-rat Alexa FITC secondary Ab 1/500(Abcam) was added to the cells for 1 hour at room

temperature. Then, the gel scoop out from the plate with spoon and placed in microscopic slides, followed by adding one drop of Vecta Shield mounting media and DAPI. Finally, the slid was sealed with DPX resin. The slides were investigated under fluorescent microscope and image taken for best represented image.

2.5.1. Cell Lysate preparation

Confluent cells in 10cm dishes were washed two times with PBS; then 1ml of PBS was added to the dish and the cells were then detached using a cell scraper. The cells were pipetted into 1.5ml Eppendorf tube and kept on ice 4^0C. They were then centrifuged for 1minute at 4^0C 12. 054g. The supernatant was discarded and the pellets containing the cells was dissolved by gentle pipetting with 100 µl IP Lysis buffer and protease inhibitor (0.5%Nonidet-P40, 1% Triton X-100, 25Mm NaPO4 PH7.0, and150 Mm NaCl) and incubated for 30 minutes on ice at 4^0C. The cell lysates were centrifuged at 17, 000g for 5 minutes at 4^0C. 10µl of the supernatant was used determine protein concentration using a colorimetric Bio-Rad DC protein assay.

2.5.2. Protein concentration assay.

A colorimetric Bio-Rad DC protein assay Kit (Bio-Rad) was used for the measurement of the protein concentration. The cell lysate was diluted 1:2, 1:4 and 1:8 in IP Lysis buffer. BSA was used as a known concentration to obtain a standard curve. The unknown protein samples and the BSA standard dilution (5µl) were pipetted in triplicate into a 96 well plate. 3ml of reagent A mixed with 60ul of reagent S to make a reagent Â. 25ul of reagent Â is added to each sample followed by 200ul of reagent B. It was incubated at room temperature for 15mints; then the absorbance was measured at 750nm.

2.5.3. Western blotting.

10% Separating gel	6.3 ml H_2O 4.0 ml 1.5 M Tris-HCl pH8.8 5.4 ml acrylamide 30% 160ul SDS 10% 160ul APS 10% 16ulTEMED
6% Separating gel	8.5 ml H_2O 4.0 ml 1.5 M Tris pH8.8 3.2 ml acrylamide 30% 160ul SDS 10% 160ul APS 10% 16ulTEMED
4% Stacking gel	3.05 ml H_2O 1.25 ml 0.5M Tris-HCl pH6.8 0.67 ml acrylamide 30% 50 ul SDS 10% 50 ul APS 10% 12 ul TEMED
SDS- PAGE Running Buffer	1.5g Tris 7.2g Glycine 0.5g SDS H_2O to 500ml
SDS-PAGE sample Buffer (2x)	10% 2-mercaptoethanol

	0.1% Bromophenol Blue 4% SDS 100 Mm Tris pH8.8 20% Glycerol
SDS-PAGE Transfer Buffer	3g Tris 14.4g Glycine 200 ml methanol 800 ml H_2O
IP Lysis Buffer	0.5 % Nonidet-P40 1% Triton X-100 25 Mm NaPO4 PH7.0 150 Mm NaCl
TBST	8g NaCl 2 ml Tween 20 10ml Tris 2M pH 7.6 1L H_2O
Blocking Buffer	10% Non-fat milk in 1x TBST

2.5.4. SDS-PAGE.

Start with preparing a separating gel 6% and 10% as described in section 2.6.3. The separating gel was overlaid with 100% ethanol and gel allowed to set incubator at 37^0C. The gel was set, drained and washed with water. After preparing a 4% stacking gel, it was poured above the separating gel and the wells were made using a comb; they were kept in an incubator at 37^0C until they were set. Prepare the protein samples by mixing them with 20µl of 2x sample buffer.

The protein samples were then denatured at 37^0C for 30mins; then centrifuged at 12,054g for 1 min. afterwards, the samples filled the wells alongside a molecular weight marker (standard protein dual colour, Bio-Rad). The gels ran in SDS-PAGE; the running buffer was at 100 V until the dye in the sample buffer had run to the lower part of the gel.

2.5.5. Protein Transfer.

The protein was transferred from the gels to the PVDF membranes in the presence of transfer buffer. The PVDF membranes were cut into a size similar to that of the gel and it was activated with methanol for 2mins; it was then washed with distilled water and kept shaking in distilled water for 30mints. Finally, the PVDF was soaked into the transfer buffer. For each gel, sandwich was prepared in the transfer buffer with two fibre pad, two filter papers, gel, PVDF membrane, one filter paper, and one fibre pad facing the black side of the cassette. The cassettes were inserted into the electrode module with the direction of the black side of the cassette next to the black side of the electrode module. A stirring magnet was placed with an ice cooling unit (-20^0C) in the butter tank. The tank was filled with transfer buffer to the top, the electrodes were attached to the power pack and electrophoresis was carried out at 100 V for 1 hr.

2.5.6. Detection of antigen on membranes.

After the transfer took place, the membranes were blocked in 10% milk- TBST (0.2% Tween 20) at 4^0C for 1-3 hr. While shaking, the membranes were probed with primary antibodies diluted in 5% blocking buffer and kept in overnight at 4^0C. The membranes were washed 4 times for 20mins with TBST at room temperature. The secondary antibodies were diluted in 5% blocking buffer that was added to the membranes and incubated at room temperature for 1 hr. Next, the membranes were washed 4 times for 20 minutes with TBST at room temperature. The membranes were developed by adding BM chemiluminescence blotting substances (Bio-Rad, Clarity^{TM} Western ECL substance). 1.5ml of bottle one was mixed with 1.5 ml of bottle

2 in a universal tube. The membranes were drained from the access of TBST; the membrane was put in the exposure cassette with the protein side facing up. It was then incubated with a substrate for 1-3 minutes. The membrane was then exposed to molecular imager, Bio-Rad Chemi Doc^{TM}XRST. Or to Super RX Fu medical X-ray films.

2.6.1. RNA extraction from human ADPKD cell lines.

The cells were plated into a 10 cm dishes. The aim was to achieve 60-70% confluence. The cells were incubated overnight. Next, the cells were washed with serum free media and they were incubated in the media with no serum for 24hr to synchronise the cells. After this time, the media was replaced with media containing serum; and incubated for a further 24 hrs. This will allow the cells to re-enter the cell cycle. Culture media was removed from the dish and 1 ml of TRIzol (Ambion) was added directly to the cells. The cells were then lysed by pipetting up and down several times. Subsequently, the sample was incubated for 5 minutes at room temperature to permit complete dissociation of the nucleoprotein complex.

In addition, 0.2ml of chloroform per 1 ml of TRIzol Reagent was used for homogenization. The cap was closed securely, and the tube was shaken vigorously for 15 seconds and incubated for 2-3 minutes at room temperature. The samples were then centrifuged at 12,000xg for 15 minutes at 4^{o}C. The upper phase (aqueous phase) was removed into a new tube. Isopropanol was added to the aqueous phase (0.5ml per 1ml of TRIzol reagent used for homogenization). The complex was incubated at room temperature for 10 minutes.

After that, the complex was centrifuged 12,000 x g for 10 minutes at 4^{o}C. The supernatant was removed from the tube, leaving only the RNA pellet. The pellet was washed with 1 ml of 75% ethanol per 1 ml TRIzol reagent used in the initial homogenization process. The sample was vortexed briefly; it was then centrifuged at 7500 x g for 5 minutes at 4^{o}C. The wash was discarded and the RNA pellet was air dried for 5-10 minutes. The RNA pellet was suspended in 50µl RNase-free water by passing the solution up and down several times through the pipette

tip. The dissolved RNA was then incubated in a water bath 60^0C for 15 minutes. The concentration of RNA was read using a Nano drop machine, quality was assessed by confirming the 260/280 ratio was between 1.8 and 2.0 and RNA was normalised to 1 µg/ml. The isolated RNA was stored at -80^0C.

2.6.2. Agarose gel electrophoresis.

A 1% agarose gel was prepared by dissolving 1 g of agarose powder in 100ml 1x TAE buffer (diluted from 50x stock containing 5% (v/v) glacial acetic acid, 2M Tris, 0.05 M EDTA at PH8.0). The dissolved gel was heated in a microwave for and the melted agarose was allowed to cool for few minutes before pouring the solution into the cast tray. Then 2µl ethidium bromide (10mg/ml, Sigma-Aldrich, UK) was added to the gel. The comb was placed in the tray to create wells for loading the samples. After the gel had set, the comb was removed, and the gel covered by TAE buffer. The RNA samples were mixed with 1:1 with loading dye (Promega) before being loaded into wells, and a 1kb DNA ladder was loaded for estimation of molecular weight of RNA fragment. The gel was run at 100V for 1 hour or until the loading dye had run half of length of the gel. The RNA was then visualised on a UV trans-illuminator.

2.6.3. Reverse Transcription.

Before starting the experiment, the work area was cleaned with 70% ethanol and then with RNase Away (Life Technologies, UK). In addition, all equipment was exposed to UV light for 10 min. The RT Master Mix was prepared by allowing the kit component to thaw on ice. A total of 2µg of RNA was used per 20µl reaction (see the Table below).

Reverse Transcription master Mix.

Component	Component volume/ Reaction(µl)	
	+ RT reaction	-RT reaction
2X RT Buffer	10.00	10.00
20X Enzyme Mix	1.0	-
RNA Sample	up to 9µl	up to 9 µl
Nuclease- free H_2O	To final volume 20µl	To final volume 20µl
Total per Reaction	20.0	20.0

The tubes were caped and inverted several times to mix the reaction components. The tubes were then placed on ice until the start of the reverse transcription reaction.

Time (Minutes)	Temperature (^{0}C)
60	37
5	95
∞	4

2.6.4. TaqMan qPCR gene expression assay.

The following Taqman primers were used for human and mouse cDNA samples.

N^0	qPCR primers	Reference	source
1	GADPH	control RNA	

2	PTGER-1	Human Hs00909194 m1	Applied Biosystems/Life Technologies
3	PTGER-2	Human Hs04183523 m1	
4	PTGER-3	Human Hs00168755 m1	
5	PTGER-4	Human Hs00168761 m1	

A master mix was generated according to the kit instructions.

Component	**Volume(ul)/20ul Reaction**
20X TaqMan Gene Expression Assay	1.0 µl
2X TaqMan Gene Expression Master Mix	10µl
cDNA template(1-100 ng)	x µl
RNase-free Water	Up to 9µl
Total	19ul

The Master Mix was vortexed and 18µl was added to each well of the 384-well plate via reverse pipetting. 2ul of the 20 X TaqMan Gene Expression Assay primers was added to the designated wells. The plate was then sealed with the appropriate cover and centrifuged briefly. Later, the plate was loaded into the instrument and ABI7900 thermal cycler conditions were set.

Time	Temperature	Cycle
10 min	95C	0
15 sec	95C	40
60 sec	60C	

qPCR data was displayed as delta Ct (Ct value of PTGER expression minus Ct value of GAPDH control expression for each sample). Fold changes between control and disease groups

was analysed using the delta delta Ct method with Data Assist v3.1 software (Applied Biosystems).

2.7 Immunohistochemistry.

The human tissue sections from normal and ADPKD and tissue sections of two orthologous mice models of ADPKD used in this study were a gift from Dr. Dorien Peters (Leiden University, Netherlands). The first mouse model is a tamoxifen-inducible, kidney-specific *Pkd1* deletion model (Lantinga-van Leeuwen, Leonhard et al. 2006). The second model was developed by decreasing the expression of the *Pkd1* gene transcription (Happe, van der Wal et al. 2013).

First, each slide was dewaxed with xylene twice for 5 minutes, followed by absolute alcohol for twice for 5 minutes, followed by 95% alcohol for 5minutes and then with 3% H_2O_2 for 20 minutes. The slides were then rinsed under running tap water for 2 minutes. Next, the slides were exposed to the heat- induced epitope retrieval using a 0.1 M tri-sodium citrate buffer for 10 minutes. The slides were then exposed to a high heat microwave for 10 minutes and then washed with cold tap water for 5 minutes. Next, the slides were blocked with peroxide reagent for 5-15 minutes and drained. The slides were then treated with a mixture of 10 ml PBS and 3 drops of goat serum for 30 minutes. Subsequently, the primary antibody against PTGER2 in a concentration of 1:100 (anti mouse AB from R& D cat. No. MA6656) or PTGER4 anti rabbit antibody in a concentration of 1:200 (Sigma Cat. No PK6102) was added to the slides. Two slides were used for the purpose of control: one with a negative control that was treated with mouse IgG in a concentration of 1:100. The slides were incubated with primary antibody for 1hr or at 4^{o}C overnight and then washed with PBS and drained. The secondary antibody biotinylated anti-mouse or anti-rabbit IgG secondary antibody (1:200 dilution) (Vector Elite

mouse kit Cat. Number PK6102) was applied to incubate the slides for 30 minutes at room temperature.

After that, each section was washed three times with PBS for 5 minutes and incubated with ABC (Avidin-biotin complex) (Vector Elite mouse kit) for 30 minutes at room temperature.

The polymer HRP secondary detection Ab (MaxVisionbio) 100µl per slide for the mouse, or rabbit primary Ab incubated for 15 minutes were utilised as a secondary Ab to decrease the background from biotin activity. Next, the slides were washed three times with PBS and incubated with the DAB chromogen solution for 5 minutes and counterstained with Gills haematoxylin for 30 seconds to stain the nuclei (blue). Then, the slides were blued with Scott's tap water and then mounted and covered with a coverslip. Finally, the images were taken using F-Cell software by Leica DMI 4000B inverted microscope at a different magnification (20X-60X).

2.8.1. Apoptosis assay (TUNEL staining).

Labelling of DNA strand breaks was done using terminal deoxynucleotidyl transferase TdT labelling, which catalyzes the polymerization of labelled nucleotides to free 3´-OH DNA in a template-independent manner (TUNEL-reaction). Fluorescein labels incorporated in nucleotide polymers are detected and quantified by fluorescence microscopy (Roche).

Cells were plated in triplicate ($2x10^4$ cells/ml; 100µl /well). When the cells had become 70% confluent they were treated with PGE2, PTGER2 and PTGER4 receptor antagonists as described for 72 hrs. As a positive control 100 µm of 3% H2O2 was added to control wells in triplicate and incubated for four hours. The staining assay was carried out according to the manufacturer's instructions. Cells were washed three times with PBS, followed by fixation with 4% paraformaldehyde for 60 min. Next, the cells were washed three times with PBS.

Subsequently, the cells were permeabilized with 0.1% Triton-X-100 in 0.1% sodium citrate solution for two min on ice. Next, a TUNEL reaction mixture was prepared by mixing the total volume (50 µl) of enzyme solution (bottle 1) with 450 µl label solution in (bottle 2) to obtain 500 µl TUNEL reaction mixture. Cells were rinsed twice with PBS to dry the area around the samples. Then, 50 µl of TUNEL reaction mixture was added to the samples. At that point, label solution 50 µl was added in duplicate to the negative control. The slides were incubated in a humidified atmosphere for 60 minutes at 37^0C in the dark. Later, the cells were rinsed three times with PBS. Finally, the samples were analysed under a fluorescence microscope to detect the apoptotic cells.

2.8.2. Caspase-3 staining.

Cells were cultured in 96 well plates until they reached 70% confluence. The cells were fixed with 4% PFA for 20 minutes. Next, the cells were permeabilized with 0.25% TritonX-100 for 15 minutes and blocked with 5% BSA in PBS for one hour at room temperature. Cells were stained with a caspase-3 (Asp175) rabbit monoclonal antibody at a dilution of 1:200(Cell signaling) in 1% BSA in PBS and incubated at room temperature for 1 hour. Next the secondary antibody goat anti rabbit FITC antibody at a dilution of 1:500 was added to the cells for 1 hour at room temperature. A DAPI counterstain was used top stain cell nuclei. Images were captured using Olympus IX71 microscope at 20X magnification.

2.9.1. BrdU cell proliferation assay.

The cells were cultured in flat-bottomed 96-well microplates at a seeding density of $2x10^3$ cells per well. When the cells had become 70% confluent they were treated with PGE2, PTGER2 and PTGER4 receptor antagonists as described for 72 hrs. The assay was carried

out according to the manufacturer's instructions. BrdU labelling solution (10 µl/well) was added and cells incubated for two hours at 37^0C. Culture media was removed and cells were dried. The FixDenat solution was then added to the cells, and incubated for 30 min. An anti-BrdU-POD working solution was added to the cells, and incubated for 90 min. Cells were washed three times with PBS. A substrate solution was added to the cells and incubated for 5 min. The absorbance was measured at 340 nm.

2.9.2. Cell Titer 96® AQueous One Solution Cell (MTS) Proliferation Assay.

The cells were cultured in flat-bottomed 96-well microplates at a seeding density of $2x10^3$ cells per well. When the cells had become 70% confluent they were treated with PGE2, PTGER2 and PTGER4 receptor antagonists as described for 72 hrs. The assay was carried out according to the manufacturer's instructions. Labelling reagent was added into each well of the 96 well plate in 100µl of serum free culture media and incubated at 37°C for 2 hours. The absorbance was measured at 490nm wavelength using a 96-well plate reader (LabSystem Multiskan Ascent).

2.10. cAMP assay.

A cAMP ELISA kit (R&D Systems) was used to measure cAMP levels in the cells. It based on a competitive binding technique, using cAMP specific monoclonal antibody to bind to goat anti-mouse antibody coated onto the microplate. The cAMP was present in the samples, to compete with a fixed amount of (HRP)-labeled cAMP for sites on the monoclonal antibody. This was followed by 3 washes to remove excess conjugate and unbound samples, and a substrate solution was added to the wells to determine the bound enzyme activity. Color development was stopped and absorbance was read at 450nm. The intensity of color was inversely proportional to the concentration of cAMP samples.

The cells were washed three times in cold PBS. Then the cells were re-suspended in cell lysis Buffers 5(1X) to a concentration of 1x 10^7 cells/ml. Next, the cells were frozen at $<20^0$C, then the cells were thawed with gentle mixing. This freeze and thaw cycle was repeated until the cells were completely Lysate. Subsequently, the cells were centrifuged at 600Xg for 10 minutes at 2-8˚C to remove cellular debris. The supernate was assayed immediately, or aliquots of the supernate, and stored at $<-20^0$C.

The reagents and samples should be brought to room temperature before use, and the samples, control and standards should be assayed in duplicate. First, the primary antibody solution was added to all wells plates except the non-specific binding wells; then; the plate was covered with the adhesive strips provided, and incubated for one hour at room temperature on a horizontal micro plate shaker set at 500 rpm±50 rpm. After one hour, the primary antibody solution was aspirated from each well and washed, repeating the process three times for a total of four washes. Washing was done by filling each well with wash buffer (300 µl) using a squirt bottle, and after the last wash, the plate was inverted and blotted against clean paper towels. Next, cAMP conjugate 50µl was added to all wells. Then, the standard, control, and samples (100 µl) were added to appropriate wells within 15 minutes of addition of the cAMP conjugate. The cell lysis buffer 5(1X) was added to NSB and zero standard (B0) wells. They were covered with a new adhesive strip, and incubated for two hours at room temperature on the shaker.

Next, the aspiration and washing cycle was repeated three times with washing buffer. Subsequently, 200µl of the substrate solution was added to each well and incubated for 30 minutes at room temperature on the bench top, protecting it from the light. After that, 100 µl of the stop solution was added to each well, which caused the color in the well to change from blue to yellow. The optical density was determined of each well within 30 minutes, using a microplate reader set at 450 nm. Then, the calculations of the results were done by averaging the duplication for each standard, control, and the sample and then subtracting to obtain the

average NSB optical density. Finally, a standard curve was created using computer software that can generate four parameter logistic (4-PL) curves- fit.

Chapter 3

Establishment of a 3D culture assay to investigate cyst formation in human ADPKD cell lines

3.1. Introduction.

Cells cultured in 3 D environments allow *in vitro* modelling in order to study cell behaviours such as differentiation, apoptosis, cell signalling, and drug metabolism (Benton, George et al. 2009). It has the advantage over traditional monolayer cultures by creating environmental conditions similar to cells growing *in vivo*. Many different types of extracellular matrices have been used to grow cells in 3D cultures. The most commonly used include collagen, proteoglycoproteins, and glycoproteins such as laminin and fibronectin (Kleinman, McGarvey et al. 1986).

3D cultures provide a controlled *in vitro* setting more closely resembling the *in vivo* environment, enabling the effects of drugs and reagents (either inhibitory or stimulatory) to be tested on cell differentiation and growth (Benelli and Albini 1999). However, 3D cultures have the disadvantage that not all cells respond as expected and the response may be partial due to the absence of required growth factors in the matrix. Furthermore, there are several preconditions for optimising the 3D basement membrane, depending on the cell type, passage number, type of growth factors needed for the cells, type and amount of serum, time in 3D culture, and finally, the amount of protein concentration of the basement membrane (Yamada and Cukierman 2007).

The most commonly used extracellular matrix is type I collagen. It has successfully been used as a 3D matrix for culturing bone, hepatocytes, prostate and respiratory cells amongst others (Morath, Klein et al. 1999, Chen, Revoltella et al. 2003, Zhang, Xu et al. 2010). Cells cultured in Type I collagen often exhibit enhanced growth and differentiation compared to other extracellular matrices (Elsdale and Bard 1972). Collagen I, which is abundant in bone, skin, and other connective tissues, is, therefore, the well-characterised gel used in 3D cultures. It is mainly isolated from rat tail tendons (Ehrmann and Gey 1956, Elsdale and Bard 1972). Cells

can typically be grown either on top of, inside or under a preformed collagen gel (Ball, Scoggin et al. 2013) depending on the experimental conditions being tested. The gel induces polarity of the cells generating a three-dimensional situation representative of the *in vivo* environment (Elsdale and Bard 1972). In the 1980s, a second basement membrane began to be used for three-dimensional gel cultures (Kleinman, McGarvey et al. 1986). EHS (Engelbreth-Holm-Swarm) matrix was purified from a mouse sarcoma line that produces a significant amount of basement membrane and extracellular matrix proteins (Benton, George et al. 2009). It is composed mainly of laminin, collagen IV, nidogen, entactin, and heparin sulphate proteoglycan (Kleinman, McGarvey et al. 1986). It also contains TGF-beta, EGF, insulin-like growth factor, fibroblast growth factors, and other growth factors which occur naturally in EHS tumours. These growth factors play important roles in cell differentiation and morphology (Vukicevic, Luyten et al. 1990) and are essential for the growth of cells in 3D cultures.

EHS matrix (or Matrigel) was found to be effective for cell differentiation, morpholgy, and cell attachment of both normal and transformed epithelial cells, including hepatocytes, Sertoli cells, and vascular endothelial cells (Yu, Sidhu et al. 2005, Zhang, Xu et al. 2010, Dal Vechio, Giudice et al. 2011). Matrigel alone as 3 D culture media has been used in a large number of studies, for example breast cancer cells were cultured in Matrigel to study the effect of BMP4 on cells proliferation in 3 D matrix using Matrigel gel and glycol gel {Ampuja, 2013 #377}. Renal carcinoma cells have been successfully cultured in growth factor reduced Matrigel coated filter as 3 D environmental media {Koochekpour, 1999 #380}. To specifically study the PKD orpk mutant cells cultured on top of growth factor reduced Matrigel to study the laminin-332 expression on cell proliferation and cyst growth (Vijayakumar, Dang et al. 2014).

Epithelial cells cultured in 3 D cultures normally respond by ceasing proliferation and start to develop a polarised morphology; for example, breast cells (Becker and Blanchard 2007). The extracellular matrix collagen I and Matrigel induce “capillary-like” structures in endothelial

cells. These are important in growing endothelial cells, which produce capillary-like structures in angiogenesis and vasculogenesis (Kleinman, Philp et al. 2003). Prostate, pancreas and salivary glands cells form acinar structures when cultured in basement membrane matrix {Yonemura, 2014 #385}. On other hand, some cells such as bone cells form interconnecting cell processes in a 3 D matrix (Fridman, Giaccone et al. 1990). Each epithelial cell responds with discrete phenotypes. For example, when Madin-Darby canine kidney (MDCK) cells are seeded in Collagen I gels, they form luminal cystic structures with the apical surface facing the lumen and a basolateral surface that makes contact with adjacent cells and ECM (O'Brien, Jou et al. 2001) However, if MDCK cells are stimulated by hepatocyte growth factor (HGF), they start to develop branching tubular structures (Pollack, Apodaca et al. 2004).

A number of studies have utilised 3 D cyst cultures using patient-derived cells. Renal tubular epithelial cells originating from ADPKD and normal kidneys were cultured in 3D collagen gels to study cadherin eight expression in cystic cells (Kher, Sha et al. 2011). ADPKD and normal cells have been used to investigate the effect of cAMP on cystic cell proliferation and cyst formation in 3 D collagen gels. In this study, the cell treated with 50uM sp-cAMP and Forskolin showed a significant increase in cyst diameter compared to control cells. Furthermore, cysts formation were maintained in presence of growth factors and FCS. cAMP activates cell proliferation, fluid secretion and cysts expansion in ADPKD but not normal cells (Hanaoka and Guggino 2000). Additional studies were performed to study the effect of arginine vasopressin (AVP) and its antagonist Tolvaptan on cyst growth and proliferation. Tolvaptan inhibited the total surface area of cysts stimulated with AVP (Reif, Yamaguchi et al. 2011). Mouse embryonic kidney cells were seeded on mixed Matrigel and Collagen scaffolds matrix and the cells formed cystic structures in cells derived from PKD1 mice and tubular structures in cells from control cells (Subramanian, Rudym et al. 2010). In this study, a mixed

collagen/Matrigel matrix was better than collagen alone for forming cystic structures (Subramanian, Rudym et al. 2010).

In this chapter, a range of 3D culture methods were optimised for the formation of cysts using human kidney epithelial cells as well as the well-established MDCKII model of cystogenesis. Following optimisation of 3D cyst assays the effects of dbcAMP, Forskolin, and PGE2 stimulation on cyst expansion was determined.

3.2. Aim and objectives.

Aims:

1. To establish a 3 D cell culture model system using cells derived from patients with ADPKD, a control renal epithelial cell line and MDCK II.
2. To test the effect of cAMP and PGE2 on cyst growth using these two model systems.

Objectives:

1. Develop a 3D cyst culture model for cell lines derived from patients with ADPKD.
2. Optimisation of cell culture conditions such as growth factors, media, and type of matrix and protein concentration.
3. Test the ability of epithelial cell lines to develop a polarized morphology i.e. to form cysts in cystic cell lines and branching tubules in normal cell lines.
4. Test the effect of cAMP and PGE2 on cyst morphology and growth.

3.3. Results.

3.3.1. Mutation analysis of human cell lines derived from patients with ADPKD.

In this chapter, non-cystic (UCL93, RFH) and cystic (OX161, OX161/C1, OX938, SKI-001, SKI002) epithelial cells were used, These lines had been immortalised from primary cultures of tubular cells isolated from normal and ADPKD human kidneys removed for clinical indications (Parker, Newby et al. 2007). Germline PKD1 mutations were identified in all 4 patients studied. In addition, distinct somatic PKD1 mutations or LOH were detected in different cell lines. This data is summarised with the predicted sizes of all potential truncated proteins (**Table 3.1**) and the likely sites of truncation (**Figure 3.1**).

All OX161 clones carried the germline mutation in exon 15 (E1537X). However, two cell lineages with distinct somatic mutations were found: c.402delG (exon 5) and 12335_12350delCCTTGCGTGGAGAGCT (exon 45). The germline mutation in exon 16 (7000_7001insGCTGGCG) was confirmed in all three OX938 clones. The presence of homozygosity for the germline mutation indicated additional LOH of the normal allele (**Figure 3.1**). In one clone (C7), weak heterozygosity was noted at an earlier passage after transduction with T antigen. However, later passage cells transduced with hTERT were hemizygous for the germline mutation.

For SKI-001, two distinct somatic mutations were found suggestive of at least two different original lineages whereas a single somatic change was detected in SKI-002 (**Figure 3.1**). No PKD2 mutations were detected in any of the cystic lines examined.

The cystic cell lines (OX161, OX161/C1, OX938 (C7), and SKI-001), and two normal control kidney cell lines (RFH, UCL93) were grown in a 75cm^2 flask. The cells were confluent, attached as a single monolayer sheet to the bottom of the plastic flask. The cells appeared healthy, with the characteristic polygonal shape seen in epithelial cell culture with

clear cell- cell contacts. Some elongated shaped cells were seen under an inverted phase contrast microscope. (Figure 3.2 A, B, C, D, E, and F).

Patient	Germline or Somatic	Mutation designation	Consequence at the ORF level	Predicted truncated Protein (aa)
SKI-001	Germline	IVS43-2A>G	Skip-Include ex43	3904-4001aa
SKI-001	Somatic (S1)	3364delG	ORF ends at nt3397 (TGA)	1132aa
SKI-001	Somatic (S2)	6549_6550insT	ORF ends at nt6548 (TGA)	2183aa
SKI-002	Germline	IVS25-3C>G	Skip-Include ex25	2983-3067aa
SKI-002	Somatic (S1)	2312_2324delTGCTTGCAGCCAC	ORF ends at nt2350 (TGA)	783aa
OX161	Germline	4609G>T	E1537X (TAG)	1536aa
OX161/C1	Somatic (S1)	12335_12350delCCTTGCGTGGAGAGCT	ORF ends at nt12589 (TGA)	4197aa
OX938	Germline	7000_7001insGCTGGCG	ORF ends at nt7253 (TGA)	2418aa
OX938 C7	Somatic	LOH	Early heterozygosity	Likely null allele

Table 3.1. Identification of germline and somatic PKD1 mutations detected in human cystic cell lines with predicted size of mutant proteins.

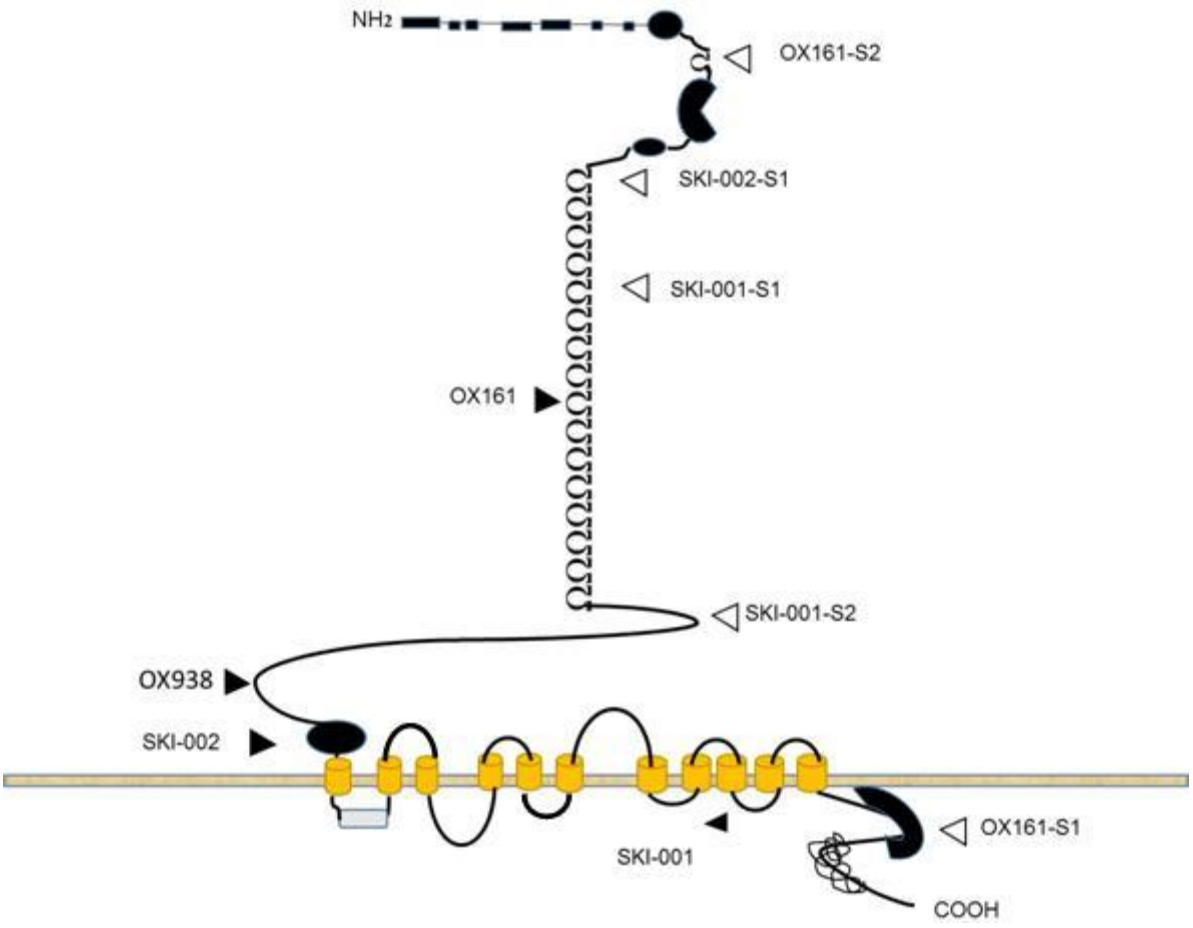

Figure 3.1. Domain structure of polycystin-1 with sites of germline and somatic mutations

DNA was analysed for PKD1 mutations from cystic cell lines derived from four patients (OX161, OX938, SKI-001, and SKI-002). The germline mutations are marked by black arrowheads and somatic mutations by white arrowheads. Refer to Table 3.1 for details of mutations.

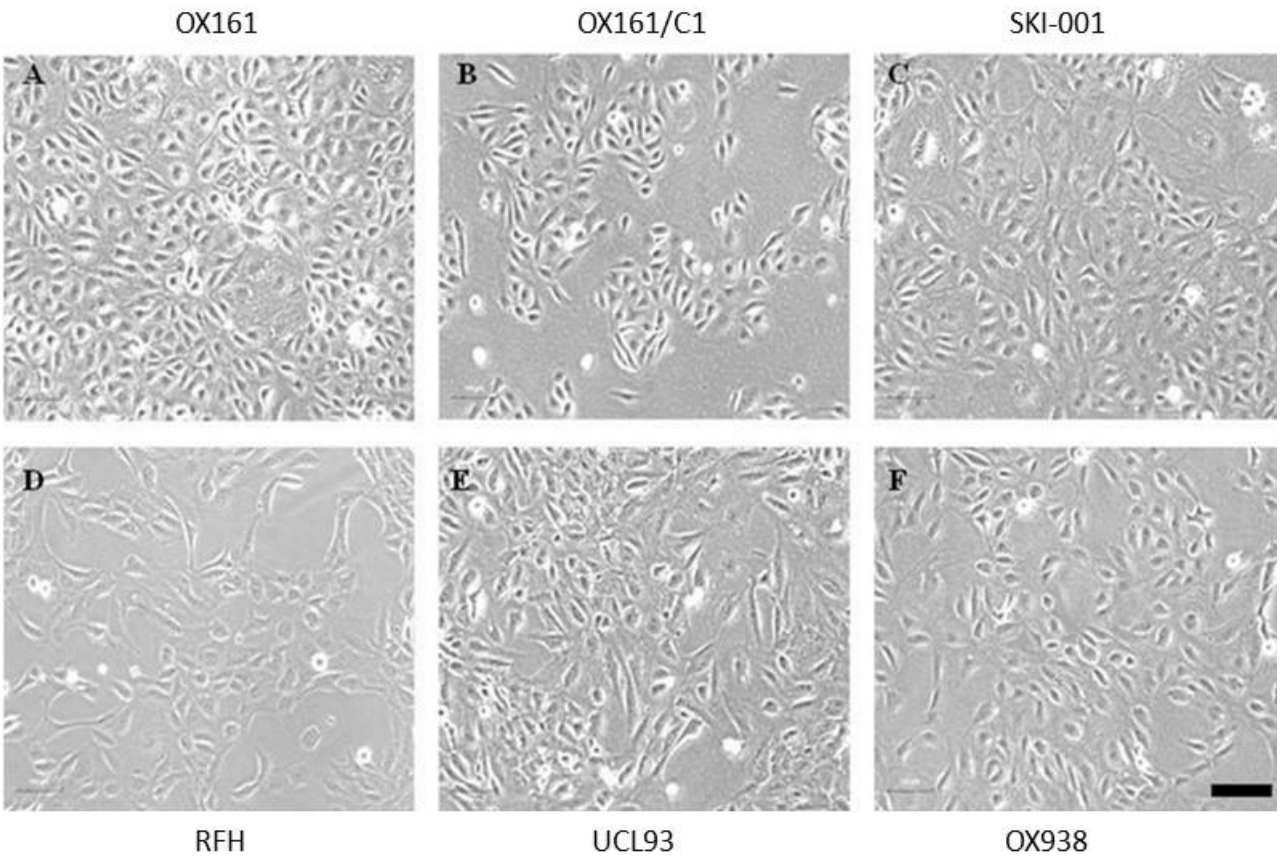

Figure 3.2. Human cell lines cultured in monolayer.

The following cell lines were cultured as a monolayer culture and images captured at x10 magnification (A). OX161, (B). OX161 C1, (C). SKI-001, (D). RFH, (E). UCL93 and (F) OX938 C7. Scale Bar = 100µm.

3.3.2 MDCKII cells form cysts in Type I collagen gels.

The MDCK II cell line is a well-established kidney epithelial model which forms polarised cysts in collagen gels and has been used extensively in 3 D assays. MDCKII cells have previously been used in our lab and others used to study cystogenesis and to evaluate the effects of rosiglitazone and cAMP on cyst growth (Buchholz, Teschemacher et al. 2011, Engelberg, Datta et al. 2011, Mao, Streets et al. 2011).

MDCK II were used to optimise 3D culture techniques prior to using the less well characterised human ADPKD cells. MDCK II cells were cultured in collagen gels composed of two different concentrations (3 or 3.8 mg/ml collagen) and observed over 8 days. The average cyst area was measured every two days for 8 days as described in section 2.4.1 (**Figure 3.3 A, B**). We observed that cells grown in the higher concentration collagen (3.8 mg/ml) formed well polarised cysts with apical lumen which were statistically larger when compared to cells cultured in the lower concentration collagen (3mg/ml) by two way ANOVA test P value 0.0004 (**Figure 3.3 A, B**). Taken together, what was observed under a microscope, and statistical analysis of the cyst area, the high concentration collagen (3.8 mg/ml) was superior to the low concentration collagen (3mg/ml). Therefore, the higher concentration collagen (3.8 mg/ml) was chosen for subsequent experiments in MDCKII.

3.3.3. Comparison of MDCK II cell cystogenesis when cultured in Collagen or Matrigel.

In order to determine the optimal extracellular matrix for culturing MDCK II cells, I tried three types of gels (Collagen I, mixture of Collagen and Matrigel, Matrigel alone). I observed that cells cultured in Collagen exhibited superior growth and well defined formation of cyst lumen at day eight (**Figure 3.4 A**) compared to cells grown in a 1:1 mixture of Collagen and Matrigel or Matrigel alone. Cells grown in 1:1 Collagen and Matrigel exhibited less clear lumen formation and less expansion when compared with cells grown in collagen alone (**Figure 3.4 B**). In the cells cultured in Matrigel alone, MDCKII cells started to cluster together from day 4, and by day 8, the cells had clumped together to form large structures with no clear lumen (**Figure 3.4 C**). From the observation of images of cysts and experimental data, I concluded that MDCK II cells cultured in collagen developed cysts optimally compared to Matrigel or a combination of Collagen and Matrigel.

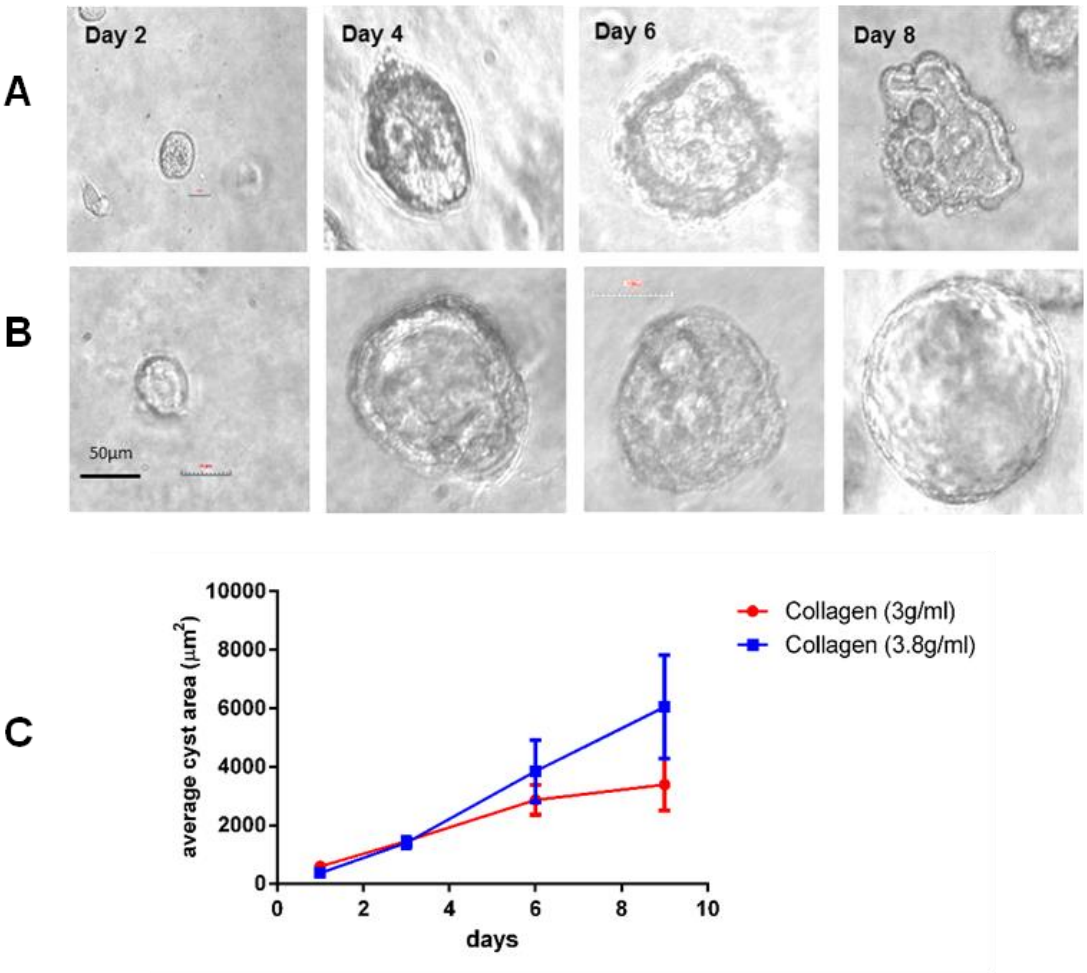

Figure 3.3. MDCKII cells form cysts in type I collagen gels

(A). The inverted light microscope images show MDCK II cultured in Collagen (3 mg/ml) and followed over days 2, 4, 6, and 8. **(B).** MDCKII was grown in Collagen (3.8mg/ml) and developed over days, 2, 4, 6, and 8. The cells grown in Collagen with a higher protein concentration exhibited clearer and well defined lumen and more expansion in cyst size when compared with those grown in Collagen with lower protein concentrations. All scale bars were represented as 50µm. **(C).** The graph illustrates that the average cyst area from 3 wells of MDCK II cells was higher in cells grown in the higher concentration Collagen by two way ANOVA test ***$p<0.0004$.

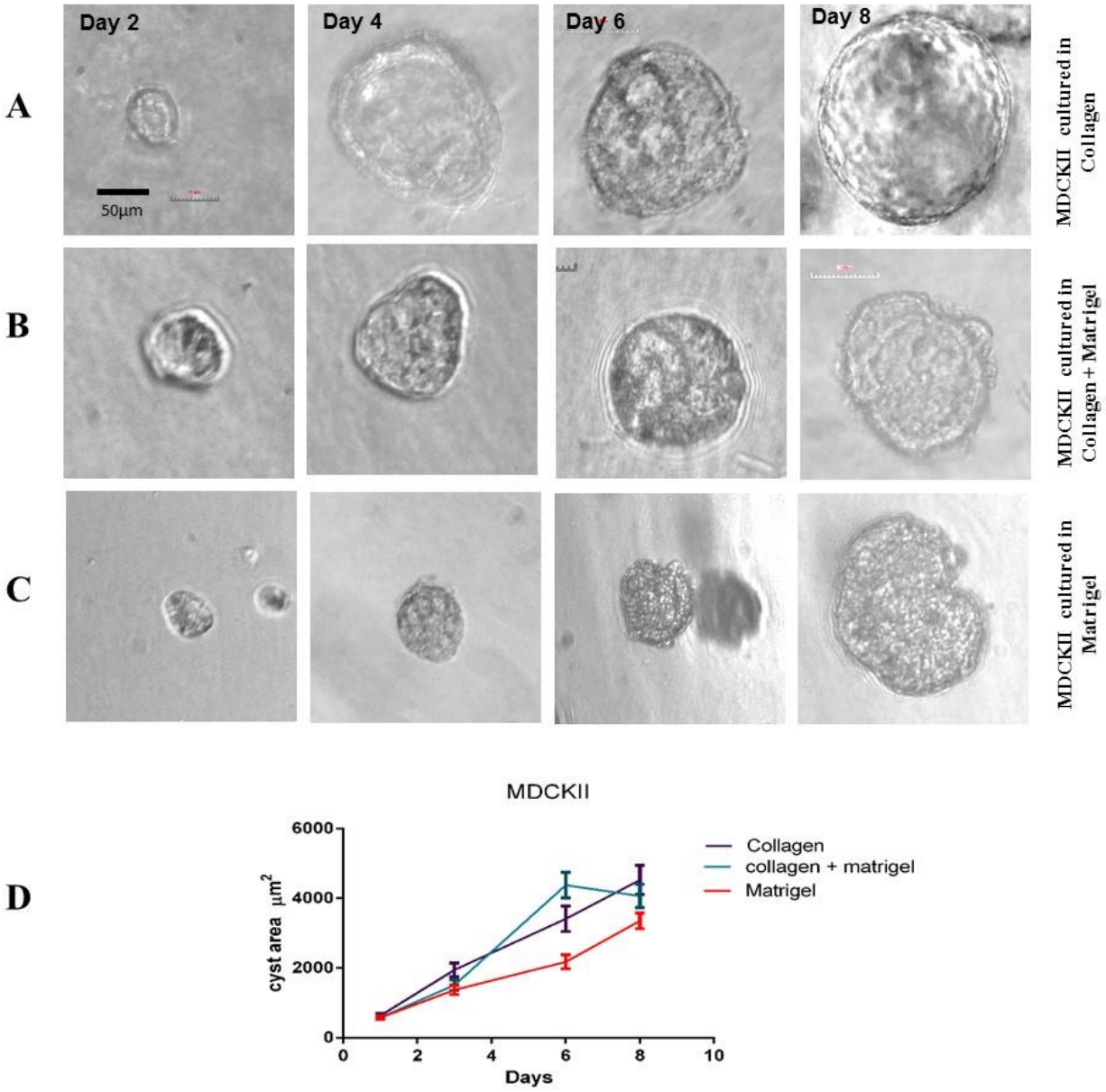

Figure 3.4. Comparison between MDCK II cultured in 3 types of the extracellular matrix: Collagen, Collagen and Matrigel and Matrigel alone.

(A). The inverted light microscope images show MDCKII cultured in Collagen I (3.8 g/ml), followed over days 2, 4, 6, and 8. **(B).** MDCK II cultured in 1:1 Collagen and Matrigel, followed over days, 2, 4, 6, and 8. **(C)** MDCK II colonies inside Matrigel alone. All scale bars were represented as 50µm. **(D).** The graph illustrates that the average cyst area from 3 wells of MDCK II cells was higher in cells grown in Collagen compared to Matrigel ***$p<0.001$ or Matrigel/Collagen to Matrigel ***$p<0.001$. Two way ANOVA test was used. Data represented as mean± SEM.

3.3.4. Human cells form tubules in Collagen gels.

The first aim of this project was to create three- dimension gel conditions suitable for culturing the ADPKD and normal cell lines. Kidney epithelial cells derived from patients with ADPKD (OX161, OX161/C1, SKI-001, and OX938) and normal control cell lines (UCL93, RFH) were cultured in collagen gels for 8 days to determine the ability of these cells to form cysts or tubules in 3D cultures.

The first cystic cell line OX161/C1 formed two distinct structures; the first was a luminal cystic structure in which 20% of the total cells formed developed a well-defined lumen from day 2 to day 4. From day 6, the cells stopped proliferating and by day 8, most of the cystic cells had growth arrested. Around 35% of cells started to develop simple tubules from day 2, which continued to proliferate up to day 8. The remaining 45% of the cell were non-proliferative (non-cystic often single cellular structures which were defined as structures with an area less than 50μm^2 and which do not form a clear lumen) (Figures **3.5 A and B**). The second cystic cell line OX161 formed mainly tubular structures by day 8 (**Figure 3.5 A and B**). In SKI-001 cells, most of the cells formed a definite lumen and cysts by day 2, but from day 4 to day 8, two-thirds of the cells developed simple branching tubules and only 10% of cells had cysts and 15% were dying (**Figure 3.5 A and B**). In OX938, most of the cells started to form branching tubules from day 2 and on day 8, two-thirds of cells formed tubular structures and only 10% formed cystic changes (**Figure 3.5 A and B**). In UCL93, a non-PKD cell line, 85% of cells formed branching complicated tubules with more than two branches by day 8. There were no cystic changes in the normal cell lines (**Figure 3.5 A and B**). The second non-PKD cell line, RFH, formed simple branching tubules from day 2, but two-thirds of cells were starting to die by day 8 (**Figure 3.5 A and B.**). A range of different serum concentrations (0%-2.5%-5%) were tested, but all cells only proliferated in 5% serum conditions.

The graph show the mean of 10 random fields from each cell line in triplicate wells. Each structure within individual fields was assigned as cystic, tubular or non-proliferative and quantified as a percentage of total number of structures. The only cystic cell lines that formed cysts were OX161/C1 and OX161 although these comprised a small percentage of total structures and most had stopped growing by day 8. The other cystic and normal cell lines formed simple tubules or like the normal cell line UCL93, formed complicated tubules with multiple branching structures (**Figure 3.5 A and B**).

In conclusion, our results indicate that the human cystic cells failed to form well-polarised cysts in Collagen gels. Most cystic cells did not proliferate or formed tubular structures in contrast to MDCK II cells that formed well-polarised cysts.

A.

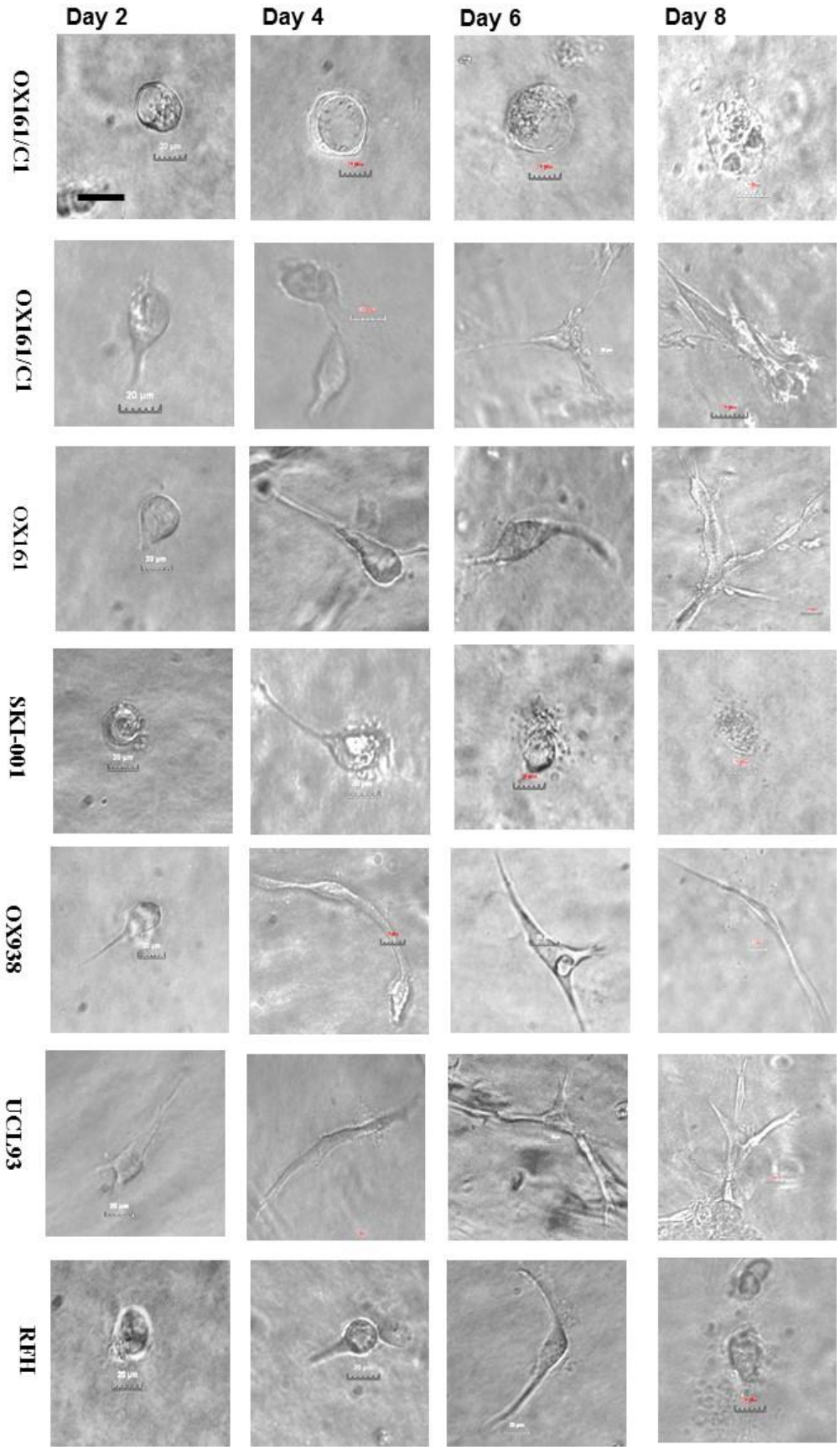
Day 2
Day 4
Day 6
Day 8
OX161/C1
OX161/C1
OX161
SKI-001
OX938
UCL93
RFH

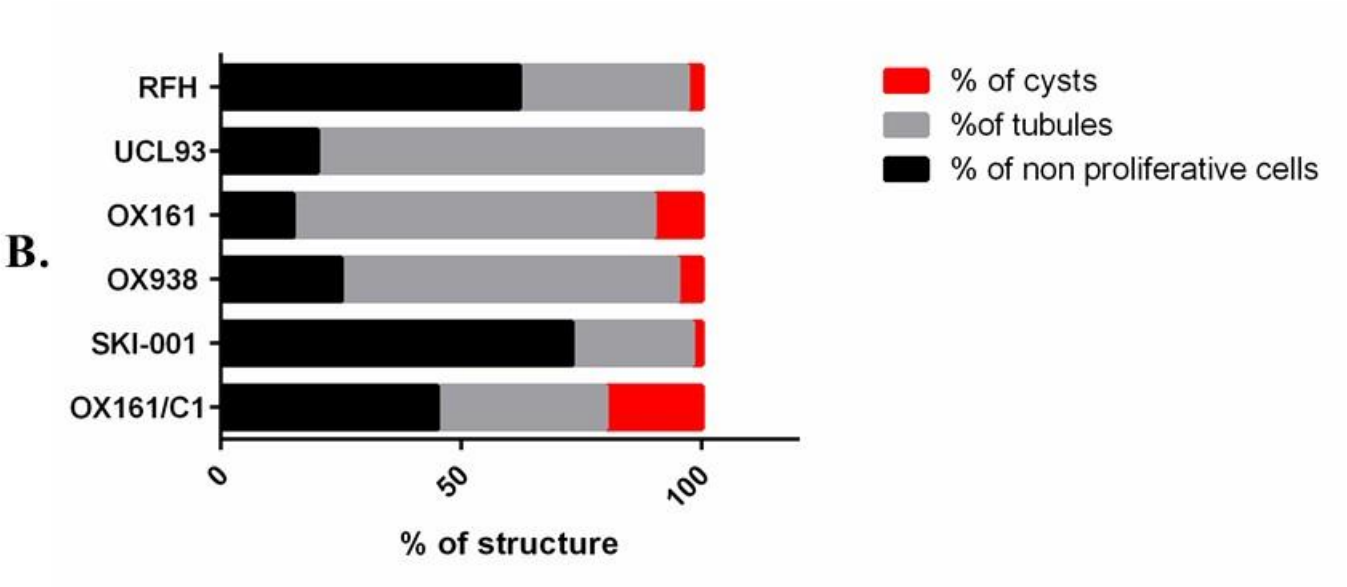

Figure 3.5. Human cells cultured in Collagen gels.

(A). Human cells mainly form tubules when cultured in collagen gels. **(B).** The graph represents the % of structures on day 8; 10 slides were analysed to quantify the percentages of tubules and cysts, and the percentage of cells that were non-proliferative All scale bars represented are 50µm.

3.3.5. Comparison of human cell cystogenesis when cultured in Collagen and Matrigel.

I next cultured cells in a matrix composed of a mixture of 1:1 (vol/vol) Collagen I: Matrigel gels. Previous work had shown that a mixture of Collagen and Matrigel was successfully used in a study of PGE2 on cystogenesis using primary cultures of cystic epithelial cells derived from ADPKD patients compared to normal cells (Elberg, Elberg et al. 2007).

The clone OX161/C1 cultured in 1:1 mixture of Collagen and Matrigel started to form lumen from day 2. However, by day 4, 50% of the cells began to elongate and developed simple tubular structures. On day eight, 30% had definite lumen. The other 20% either died or failed to grow, and remaining cells formed tubular structures **(Figure 3.6. A and B).**

In the parental cell line OX161, simple tubules were observed from day 2. These tubules then became elongated and branching (two branches maximum) in 70% of the cells by day 8. Around 25% of the cells formed lumen with clear cysts, 5% were non-cystic, non-proliferative cysts **(Figure 3.6 A and B).**

SKI-001, the third cystic cell line, developed small notches from the cells from day 2, which elongated and formed simple branching tubules in 60% of cells. 25% showed no proliferation or cystic changes, and only 15% of cells formed cysts with polarized lumen (**Figure 3.6 A and B**).

60% of OX938, the fourth cystic line, formed small tubules from day 2 onward to day 8. Only 10% of cells developed cystic changes. 30% of cells formed non-proliferative cells (**Figure 3.6 A and B**).

90% of the normal cell line UCL93 formed tubular structures from day 2 onward. These tubules developed more than two branching tubules. Only a small percentage (5%) underwent simple cystic change, and 5% of cells formed non-proliferative cells (**Figure 3.6 A and B).**

The second normal cell line, RFH, formed simple tubules from day 2, and these tubules grew to more than two branches by day 8; no cystic changes were followed, and 20% of cells died by day 8 (**Figure 3.6 A and B**).

In summary, our results showed that using a mixture of Collagen and Matrigel did not facilitate the formation of cysts. Most cells derived from patients with ADPKD formed simple tubules or were non-proliferative. The next step was to test the ability of ADPKD cells to form cysts in Matrigel alone.

A.

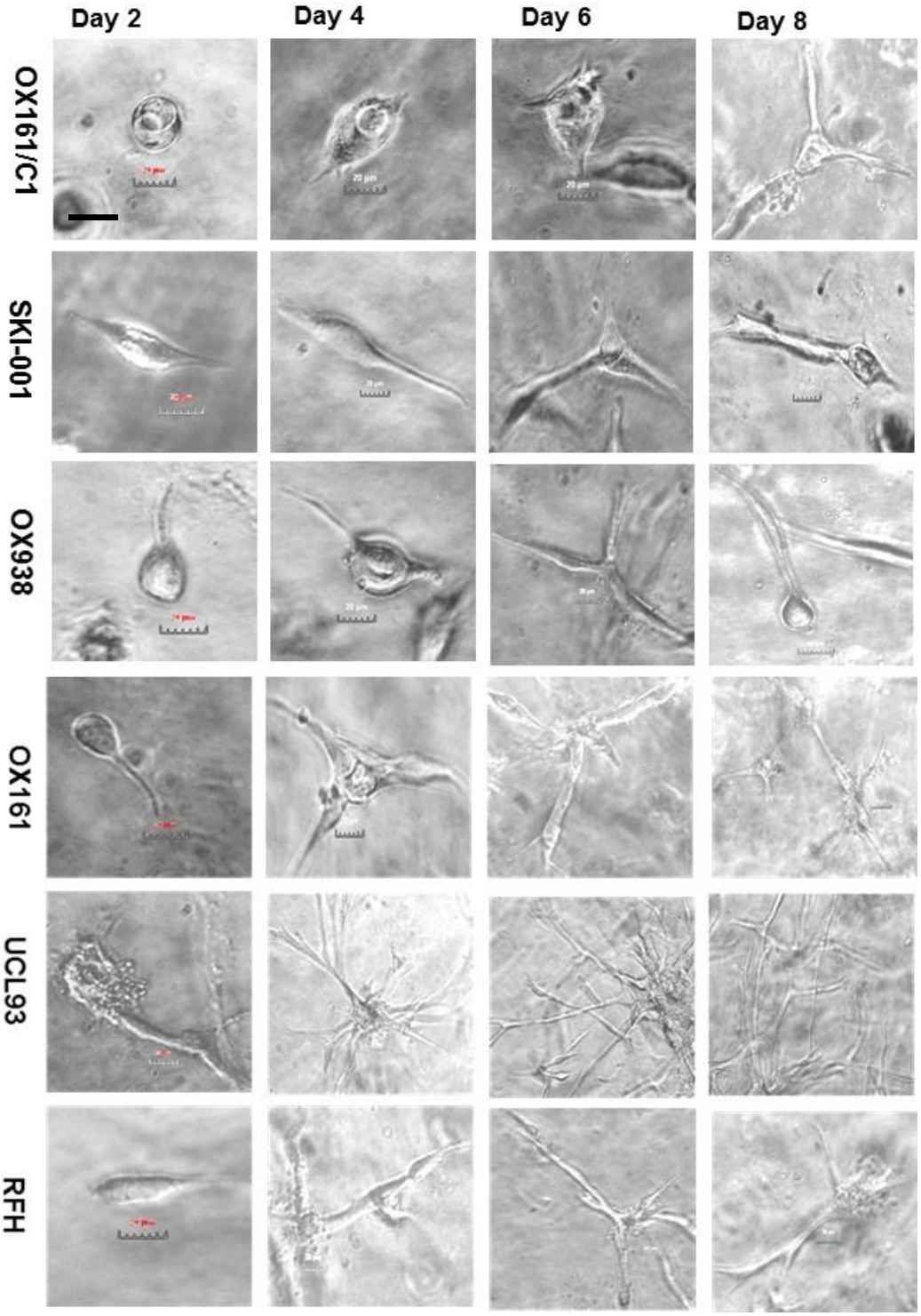

B.

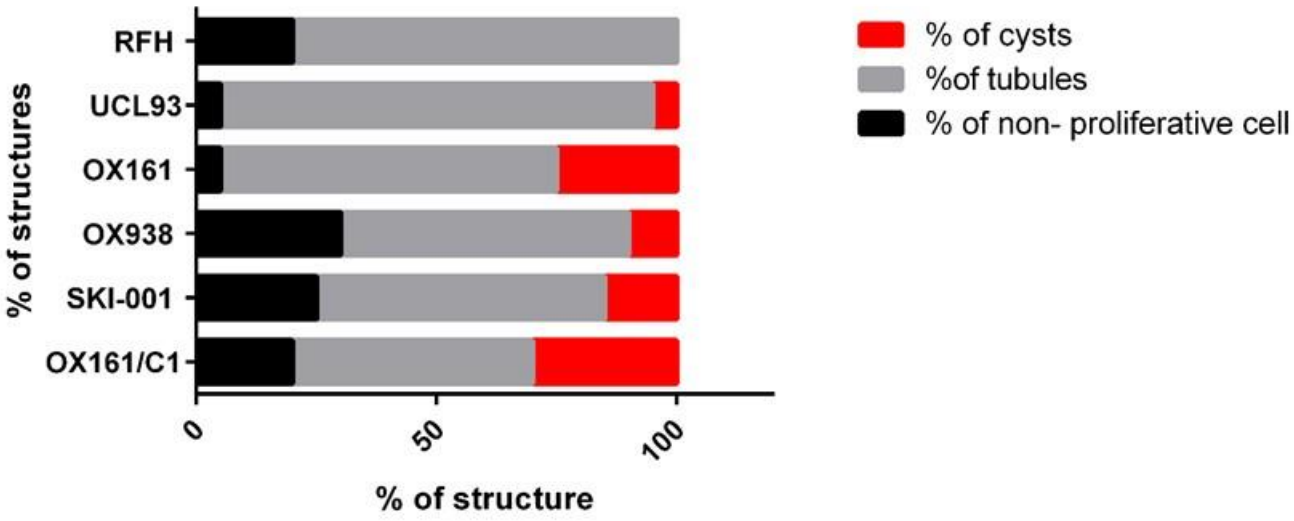

Figure 3.6. Human cell lines, cystic (OX161/C1, SKI-001, OX161, OX938) and normal (UCL93, RFH), cultured in Collagen and Matrigel.

(A). Human cells mainly form tubules at day 8 when cultured in collagen and Matrigel gels. **(B).** The graph represents the % of structures on day 8; 10 slides were analysed to discover the percentages of tubules and cysts, and the percentage of cells that were non-proliferative. All scale bars represented are 50μm.

3.3.6. Comparison of human cell cystogenesis when cultured in Matrigel.

The human ADPKD cell lines (OX161/C1, SKI-001, OX161, and OX938) and normal cells were grown in Matrigel gels for 8 days. When OX161/C1 was cultured inside Matrigel, cells began to create small luminal structures on day 2. This progressively expanded over day 4 such that by day 6, it formed clear cysts with a cell monolayer surrounding a single lumen. By day 8, some cells even developed multiple lumens in a number of cysts. Only a negligible number of cells produced simple tubular structures, and only 5% exhibited non-proliferative non-lumen formation **(Figure 3.7 A and C**). SKI-001, the second cystic cell line, developed small notches from the cells from day 2, which elongated and formed cystic changes in 25% of cells, while 30% of cells formed tubular changes on day 8 (**Figure 3.7 A and C**). However, more than 45% of the cells appeared non-proliferative with no lumen formation.

In OX161, the third cystic line, cultured in Matrigel, cells began to a cluster of cells and developed small lumens on day 2. Then, the cells started to expand and clump together to form larger structures with around 60% developing luminal structures. There were no tubular structures observed (**Figure 3.7 A and B**).

OX938, the fourth cystic cell line, developed small luminal structures. However, most of the cells did not grow well in Matrigel and were non-proliferative by day 8 (**Figure 3.7 A and C**).

The first normal cell line, UCL93, formed clustered structures on day 2, and grew into tubules showing more than two branches on day 4 expanding in size until day 8 (**Figure 3.7 A and C**).

The second normal cell line, RFH, progressed to simple tubular structures from day 2 to day 4 and expanded to form branching tubular structures on day 6 and day 8. However, one- quarter of the cells were non-proliferative by day 8 (**Figure 3.7 A and C)**.

The total cystic area of 20-25 structures per well was measured at day 2, day 4, day 6, and day 8 in triplicate and the mean and SEM values compared between OX161/C1, SKI-001 and

OX161. Significant differences were found between OX161/C1, SKI-001 and OX161 with OX161/C1 forming the largest cysts. (P value <0.0001 for row, column and interaction factors, two-way ANOVA) (**Figure 3.7 B**). From the results of the 3 D culture optimisation experiments, we decided to use the OX161/C1 cell line cultured in Matrigel 3 D gels and MDCK II cells grown in Collagen gels as models of cystogenesis in further experiments.

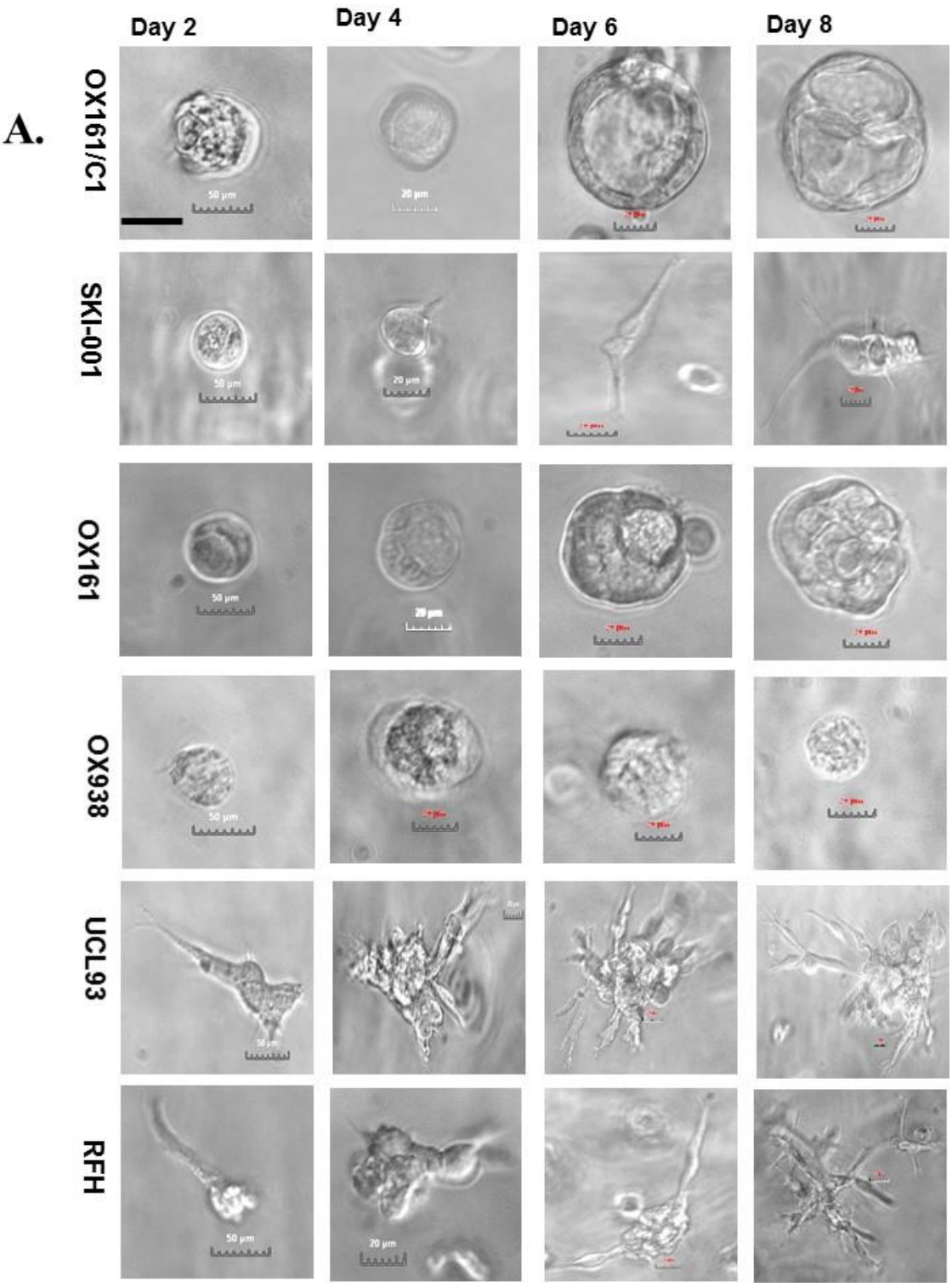
A.
Day 2
Day 4
Day 6
Day 8
OX161/C1
SKI-001
OX161
OX938
UCL93
RFH

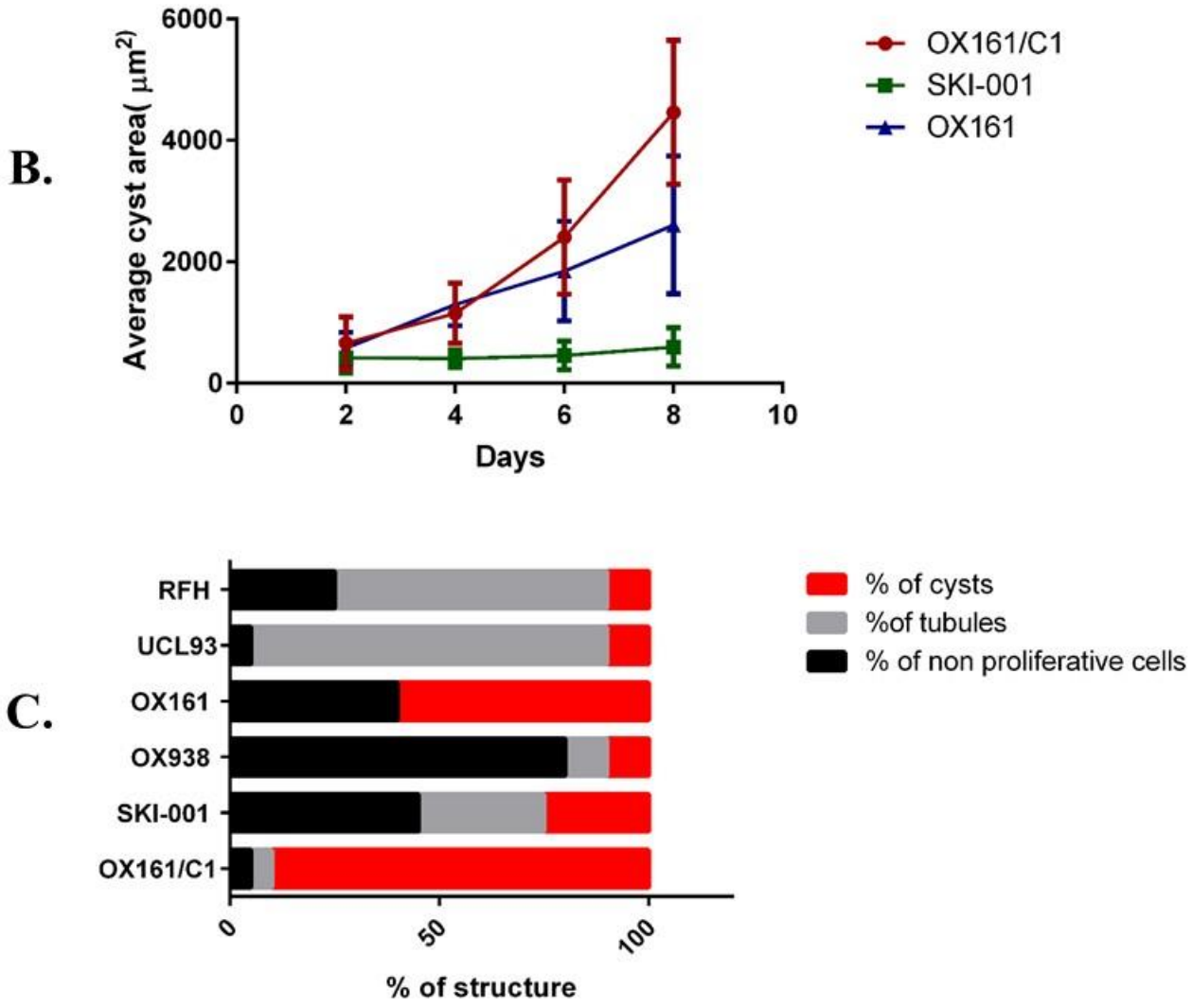

Figure 3.7. Human cell lines, cystic (OX161/C1, SKI-001, OX161, OX938) and normal (UCL93, RFH), cultured in Matrigel for 8 days.

(A). Inverted light microscope images show that the majority of OX161/C1 cells formed a clear polarized lumen at day 6, and even multiple lumens in occasional cells at day 8. For SKI-001, most of the cells formed small cysts but there were some simple branching tubules at day 8. For OX161, most of the cells formed large clumps with few visible lumen but no tubules were observed at day 8. For OX938, most cells were non proliferative and dying at day 8. The normal cell lines, UCL93 and RFH, formed branching complex tubules by day 8. All scale bars were represented as 50µm.

(B). Average cyst area of three cystic cell lines (OX161/C1, OX161, and SKI-001) measured over 8 days. OX161/C1 were the most efficient cells in terms of forming cysts in Matrigel

compared with OX161 and SKI-001. The data are presented as two way ANOVA test with significant differences between OX161/C1 and both OX161 and SKI-001 ****$p<0.0001$.

(C). Graph representing the % of cellular structures present on day 8. Ten slides were analysed to discover the percentages of tubules, cysts, and the percentage of non-proliferative cells. OX161/C1 had the highest percentage of cells forming cysts compared with the other cystic cell lines. While, UCL93 had a higher rate of cell forming tubules compared to RFH.

3.3.7. Morphology of ADPKD and MDCK II cysts.

Immunofluorescence staining was used to confirm the polarity of MDCK II cells cultured in Collagen gels and OX161/C1 cultured in Matrigel. Characteristically epithelial cells grown in 3D extracellular matrix cultures will organise as a single polarised layer of cells containing definite cell-cell attachments and the presence of tight junctions surrounding a fluid filled lumen. Cells will organise themselves with the apical surface facing the lumen and the basolateral surface contacting the extracellular matrix (Ashley, Yeung et al. 2013, Frickmann, Schropfer et al. 2013, Chen, Guo et al. 2014).

MDCK cells formed clear well defined cystic structures, and we were able to delineate a single central lumen clearly by staining the cells with apical protein glycoprotein gp-135/ podocalyxin or by staining F-actin with phalloidin. Cell nuclei were counterstained with DAPI **(Figure 3.8 B, D)**.

OX161/C1 ADPKD cells formed less well defined cystic structures by day 8. However, a lumen was identified following immunofluorescence staining of the core-tight junction protein Zonula-occludes (ZO-1) which stains the border between the apical and baso-lateral membrane (**Figure 3.9 D**). Cells were also stained with phalloidin which stains F-actin and delineates the luminal surface. The nuclei stain blue with DAPI **(Figure 3.9 B**). Taken together these experiments confirmed that both ADPKD and MDCK cells formed polarised cysts with a clearly defined central lumen in Matrigel and Collagen gels respectively.

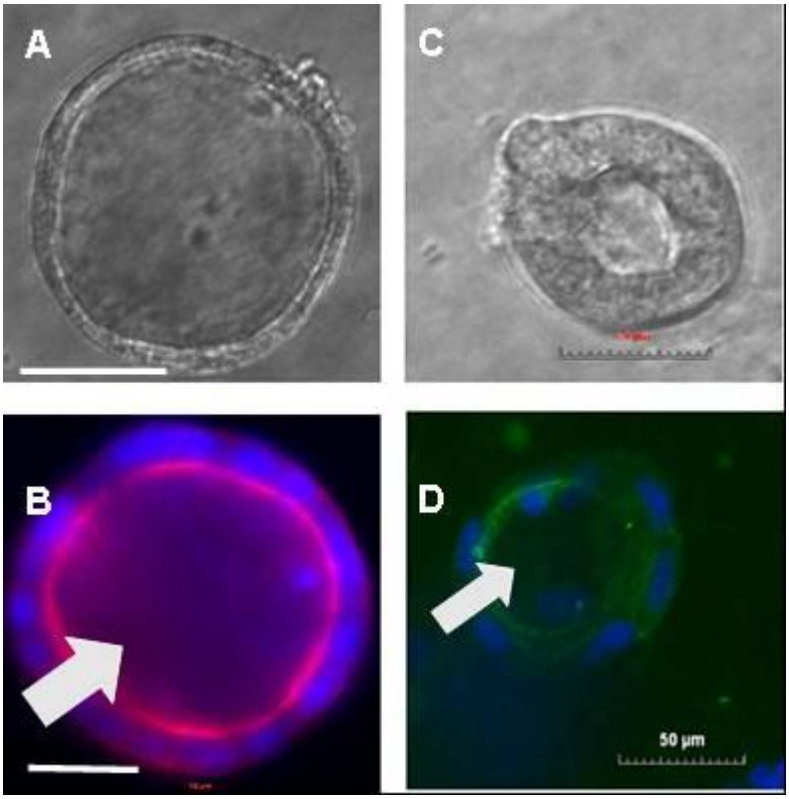

Figure 3.8. Immunofluorescence images of MDCKII staining with phalloidin and GP-135.

(A). The inverted microscope of MDCKII cultured in collagen I at day 8 exhibited clear and well- defined lumen **(B).** MDCKII lumen defined by staining with Alexa fluor® Phalloidin stain F-actin (red), and nuclei were counterstained with DAPI by immunofluorescence. Scale bar was 50µM **(C).** Inverted microscope of MDCKII cultured in collagen I at day 8 exhibited clear and well- defined lumen. **(D)**. Apical staining of gp-135 (green) in MDCKII cells in 3 D cultures, nuclei were counterstained with DAPI Image magnification for immunofluorescence 20X, scale bar was 50µM.

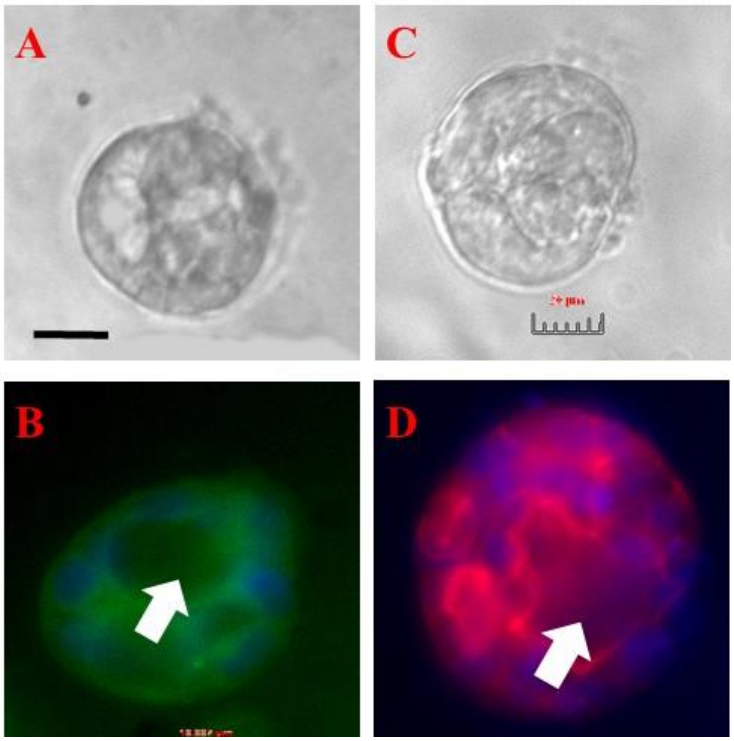

Figure 3.9: Immunofluorescence images of OX161/C1staining with phalloidin and ZO-1.

(A, C). The inverted microscope of OX161/C1 cultured in Matrigel at day 8, exhibited irregular, multi-lumen cell.

(B). OX161/C1stain outlined the lumen with ZO-1 (green) small lumen in the middle (white arrow). Two small lumens in peripheral and nuclei were counterstained with DAPI.

(D). OX161/C1 we delineated the lumen by staining with Alexa fluor® Phalloidin stain F-actin irregular middle lumen (white arrow) (red) and nuclei were counterstained with DAPI. Image magnification for immunofluorescence 20X, scale bar was 50µM.

3.3.8. Effect of cAMP and Forskolin on MDCK cysts.

Levels of the secondary messenger cyclic AMP are elevated in ADPKD cells and tissues. cAMP promotes cell proliferation through the ERK pathway and through phosphorylation of nuclear transcription factor CREB (cAMP response element binding protein) at serine residue 133. The CREB is activating various target genes that is important in cell proliferation and survival like proto-oncogene *c-fos* and cell cycle regulating gene like cyclin D1 and cyclin A1 (Siu and Jin 2007).

cAMP increases chloride secretion into the lumen of the cysts through stimulation of cystic fibrosis transmembrane conductance regulator (CFTR) channel (Belibi, Reif et al. 2004) (Hanaoka and Guggino 2000). Previous studies have shown that cAMP stimulates proliferation of ADPKD cells both in monolayer culture, 3D gel cultures and organ cultures when compared to normal control cells (Hanaoka and Guggino 2000, Belibi, Wallace et al. 2002, Belibi, Reif et al. 2004).

The aim of this experiment was to examine the effect of exogenous dibutyryl-cAMP (dbcAMP) and Forskolin on the growth of MDCK II cysts. Combining dbcAMP and Forskolin as an adenylyl cyclase agonist has been used previously to study the effect of cAMP signalling in kidney cells (Mangoo-Karim, Uchic et al. 1989, Ye, Grant et al. 1992, Yamaguchi, Pelling et al. 2000, Parker, Newby et al. 2007) so this approach was utilised in my experiments. MDCK II cells cultured in collagen gels were stimulated with dbcAMP (100µM) and Forskolin (10µM) for 8 days. The average cyst area was calculated by measuring cysts from at least 10 random fields in triplicate wells. The experiment was repeated 3 times.

MDCK II cells cultured in Collagen gels for 8 days showed a significant increase in average cyst area when stimulated with dbcAMP and Forskolin. Interestingly, cells stimulated with dbcAMP and Forskolin often contained multiple lumen when compared to control cells

indicating an additional effects on cell polarity and apical lumen formation (**Figure 3.10**) (Jaffe, Kaji et al. 2008, Mao, Streets et al. 2011).

3.3.9. Effect of prostaglandin E2 on MDCK II cysts.

Previous studies have shown that prostaglandin E2 (PGE2) signalling is increased in ADPKD. PGE2 has been shown to increase cyst formation, cell proliferation and fluid secretion in mouse and human kidney cells (Elberg, Elberg et al. 2007) (Sauvant, Holzinger et al. 2003) (Elberg, Turman et al. 2012) (Matlhagela and Taub 2006, Buchholz, Teschemacher et al. 2011).

MDCK II cells cultured in Collagen gels for 8 days showed a significant increase in average cyst area when stimulated with PGE2 (**Figure 3.11 and 3.12**). The minimum concentration of PGE2 required to increase average cyst area was 12.5nM and maximum effect was observed at 25nM (**Figure 3.12 A, B)**. No significant effect was seen at the highest dose of 1 µM which may be due to a toxic effect of high dose treatment or saturation of the receptor with PGE2.

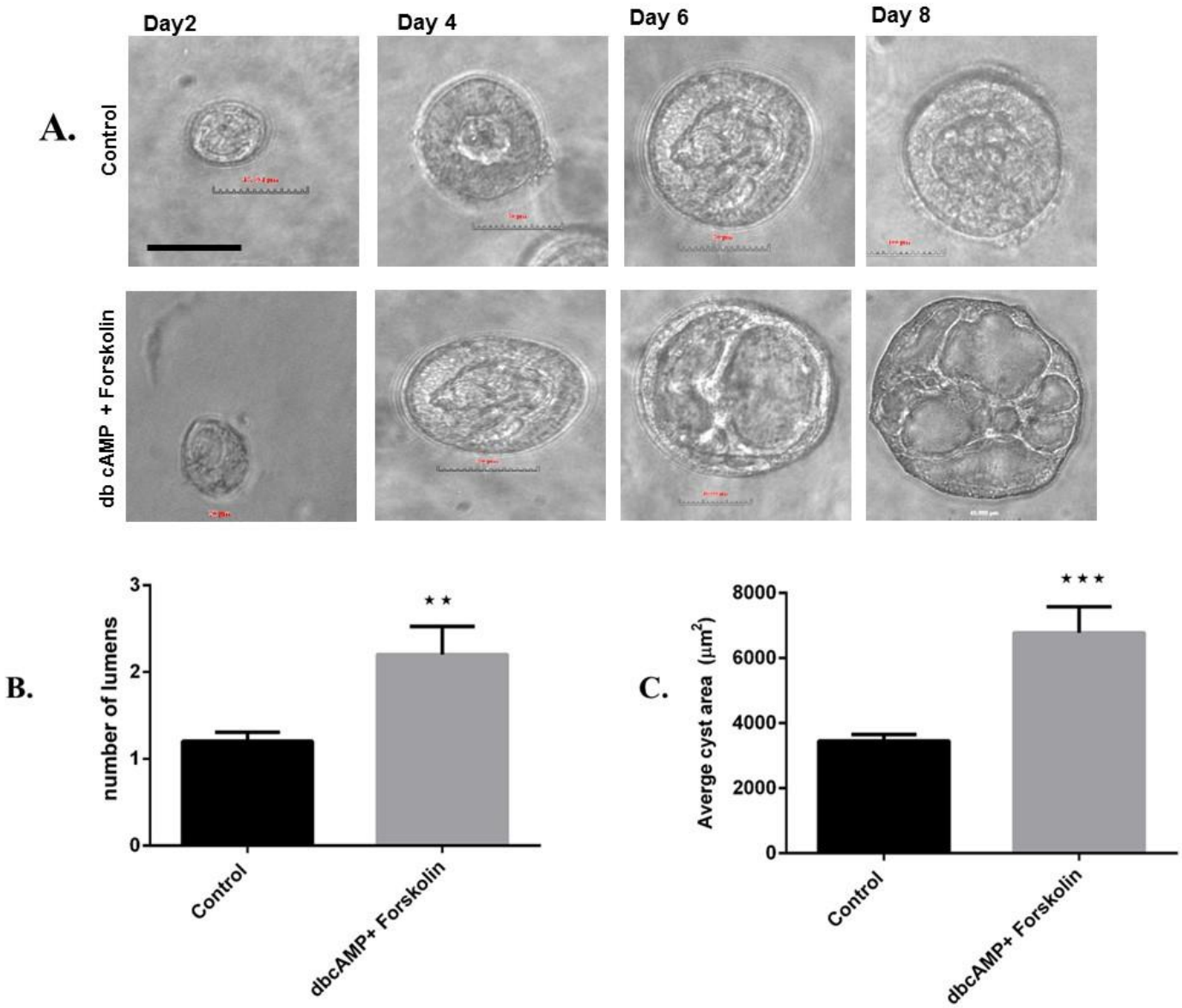

Figure 3.10: MDCKII cells cultured in Collagen I and treated with dbcAMP 100µM and Forskolin10µM.

(A). MDCK II cultured in Collagen I treated with DMEM and 5% FCS alone (control) and MDCK II treated with dbcAMP and Forskolin with media over 8 days. Cyst formation in MDCK II in collagen gel treated with both dbcAMP and Forskolin appeared greater in size and larger in number than the control. All scale bar represent in 50µM. **(B).** Quantification of number of lumen per cyst showed a significant increase of number lumens/ cyst in cells treated with dbcAMP and Forskolin compared to control (Control= 1.200 ± 0.1069, n=15 vs 100µM dbcAMP+10µM Forskolin = 2.200 ± 0.3266, n=15**p value = 0.007. Unpaired t-test was

used. **(C).** MDCK II treated with dbcAMP and Forskolin showed a significant increase in cyst area (Control= 3452 ± 198.9, n=24 vs 100µM dbcAMP+10µM Forskolin = 6773 ± 802.4, n=24)*** P value = 0.0007compared to the control. Unpaired t-test was used. Data represented as mean± SEM.

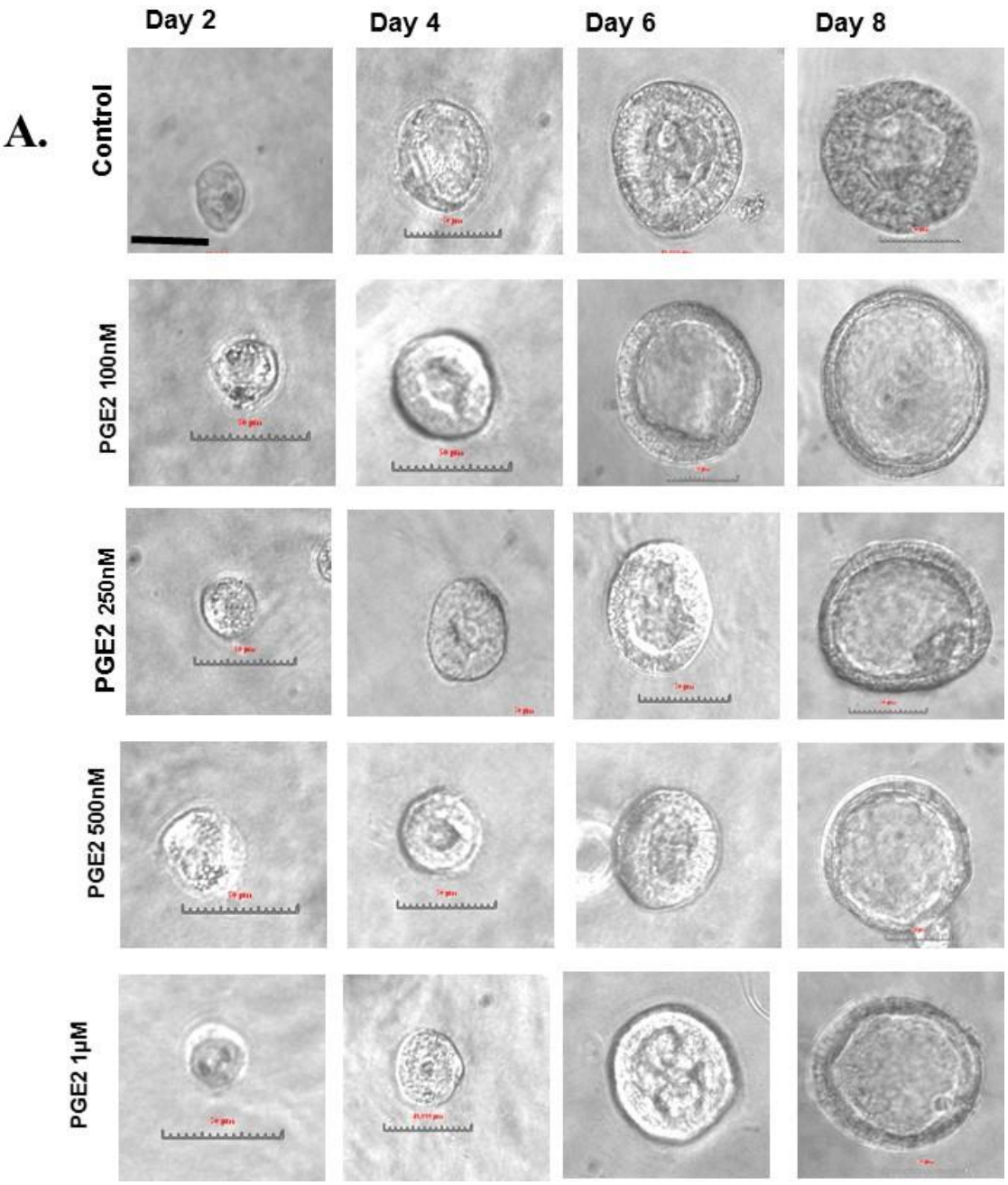
A.
Day 2
Day 4
Day 6
Day 8
Control
PGE2 100nM
PGE2 250nM
PGE2 500nM
PGE2 1µM

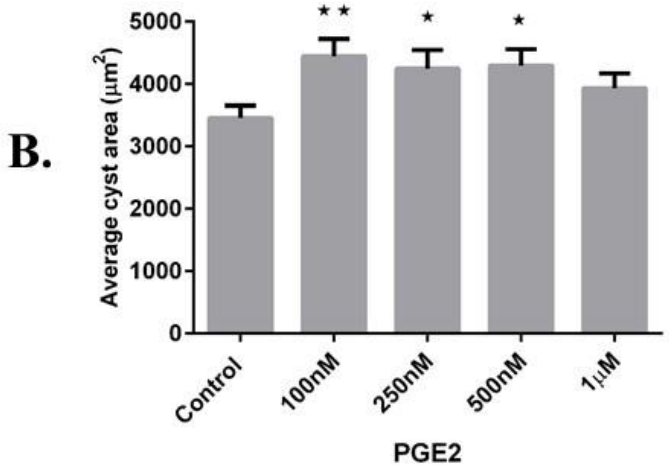
B.
Average cyst area (µm²)
5000
4000
3000
2000
1000
0
★★
★
★
Control
100nM
250nM
500nM
1µM
PGE2

Figure 3.11: MDCK II cells cultured in Collagen I and treated with 4 different concentration of PGE2.

(A). MDCKII cultured in Collagen I treated with DMEM and 5%FCS media alone exhibited an increase in size and lumen formation over 8 days. MDCKII treated with PGE2 100nM, revealed more expansion in the size and apparent lumen formation compared with the control. MDCKII grew in Collagen I treated with 250nM PGE2, developed better growth and lumen formation than the control**.** MDCKII cultured in Collagen I treated with 500nM PGE2, produced superior growth and lumen formation than the control. MDCK II grown in Collagen I treated with 1µM PGE2, produced better lumen formation and clearer cysts than the control. All scale bar represents in 50µM.

(B). Graph represents the average cyst area of MDCKII treated with PGE2 relative to the control on day 8. There was a significant dose-dependent increase in MDCKII treated with 100-500nM PGE2. However there was no significant difference between cells treated with 1µM PGE2 and controls (n=24). One-way ANOVA test was used. Data represented as mean± SEM.

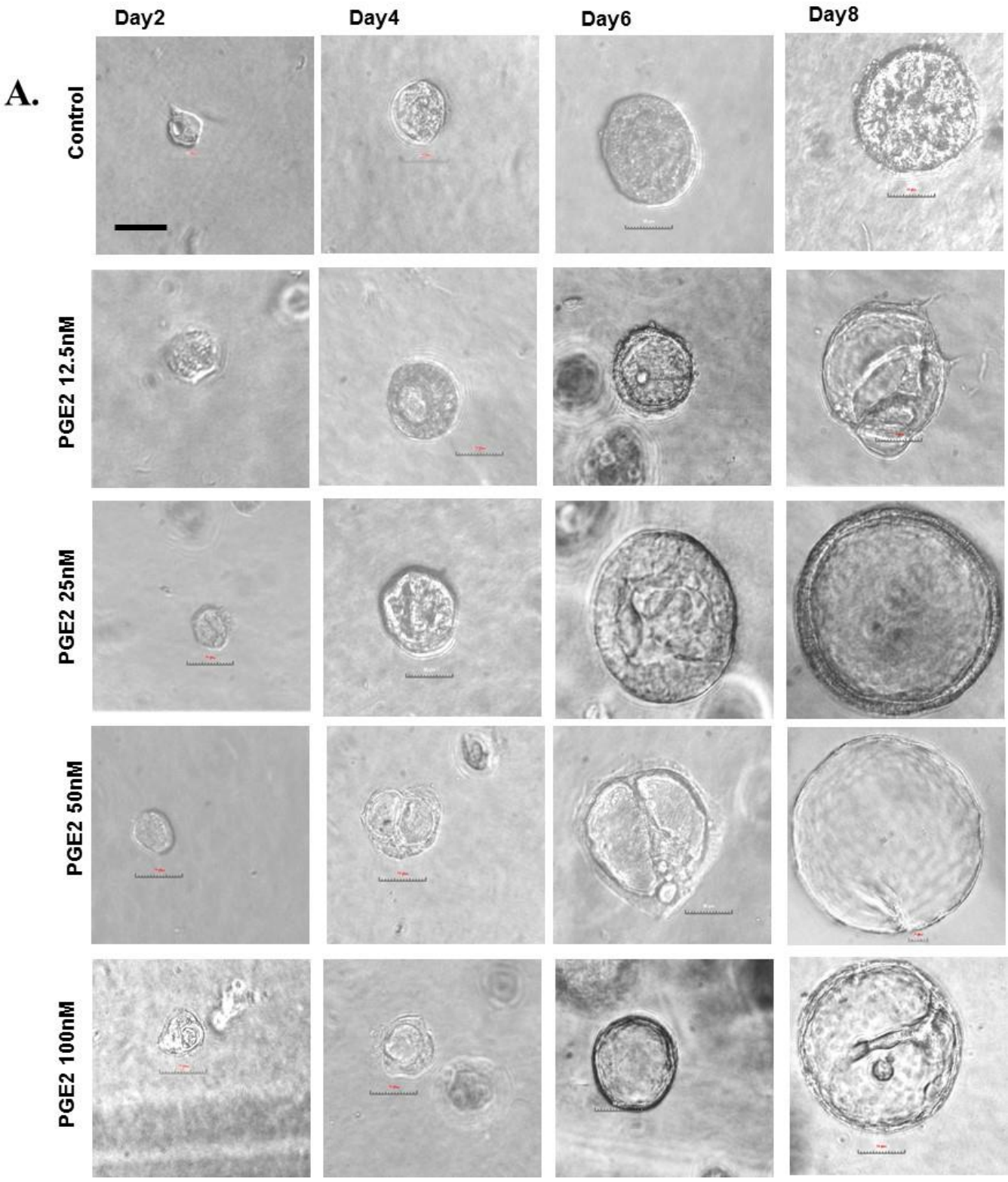
A.
Day2
Day4
Day6
Day8
Control
PGE2 12.5nM
PGE2 25nM
PGE2 50nM
PGE2 100nM

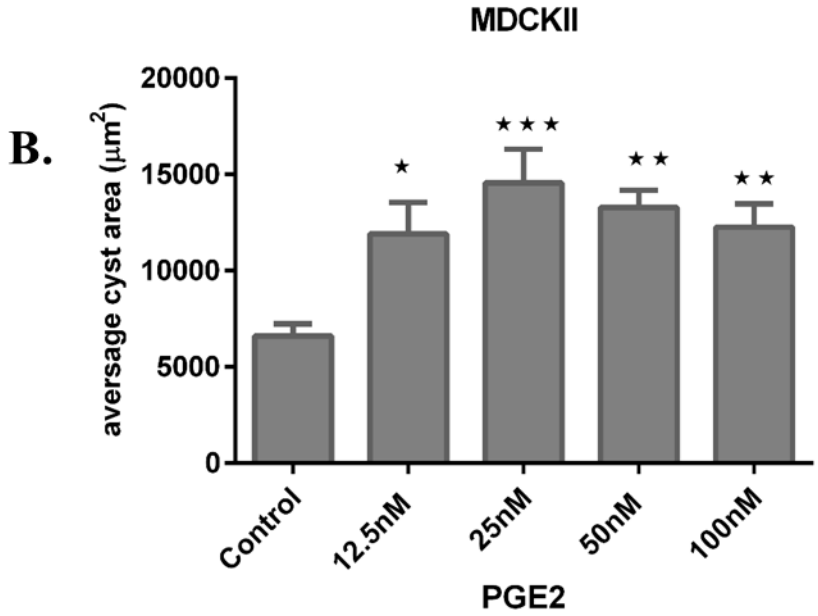

Figure 3.12. Effect of lower doses of PGE2 on MDCKII in 3 D culture media over 8 days.

(A). MDCKII cultured in collagen I treated with DMEM and 5% FCS alone (control) and different concentration of PGE2. The cyst formation in MDCKII in collagen gel treated with the smaller dose of PGE2 appeared more expanded, and the cysts formed by MDCKII were greater in size and larger in number than the control. Scale bar was 50μM.

(B). MDCKII treated with PGE2 (12.5-100nM) showed a significant dose-dependent increase in cyst area compared to controls (n= 20). *p<0.05, **p<0.01, ***p<0.001. One-way ANOVA test was used. Data represented as mean± SEM.

3.3.10. Effect of cAMP and Forskolin on OX161/C1 cystogenesis.

OX161/C1 cells cultured in Matrigel gels were stimulated with dbcAMP (100µM) and Forskolin (10µM) for 8 days. The average cyst area was calculated by measuring cysts from at least 10 random fields in triplicate wells and the experiment repeated 3 times.

OX161/C1 cells cultured in Matrigel gels for 8 days showed a small but significant increase in average cyst area when stimulated with dbcAMP and Forskolin (**Figure 3.13 A-C**). Comparing the two results of dbcAMP effects on MDCK II and OX161/C1. MDCK II showed a larger response to dbcAMP than OX161/C1.

3.3.11. Effect of prostaglandin E2 on OX161/C1 cystogenesis

OX161/C1 cells cultured in Matrigel gels were stimulated with PGE2 at concentrations from 12.5 nM to 1 µM for 8 days. The average cyst area was calculated by measuring cysts from at least 10 random fields in triplicate wells and the experiment repeated 3 times.

OX161/C1 cells cultured in Matrigel gels for 8 days showed a significant increase in average cyst area when stimulated with PGE2 (**Figure 3.14**). The minimum concentration required to increase average cyst area was 25 nM and a maximum response observed at 50nM. Thus, in both MDCK and OX161/C1 cyst assays, cAMP and PGE2 caused a significant increase in average cyst area.

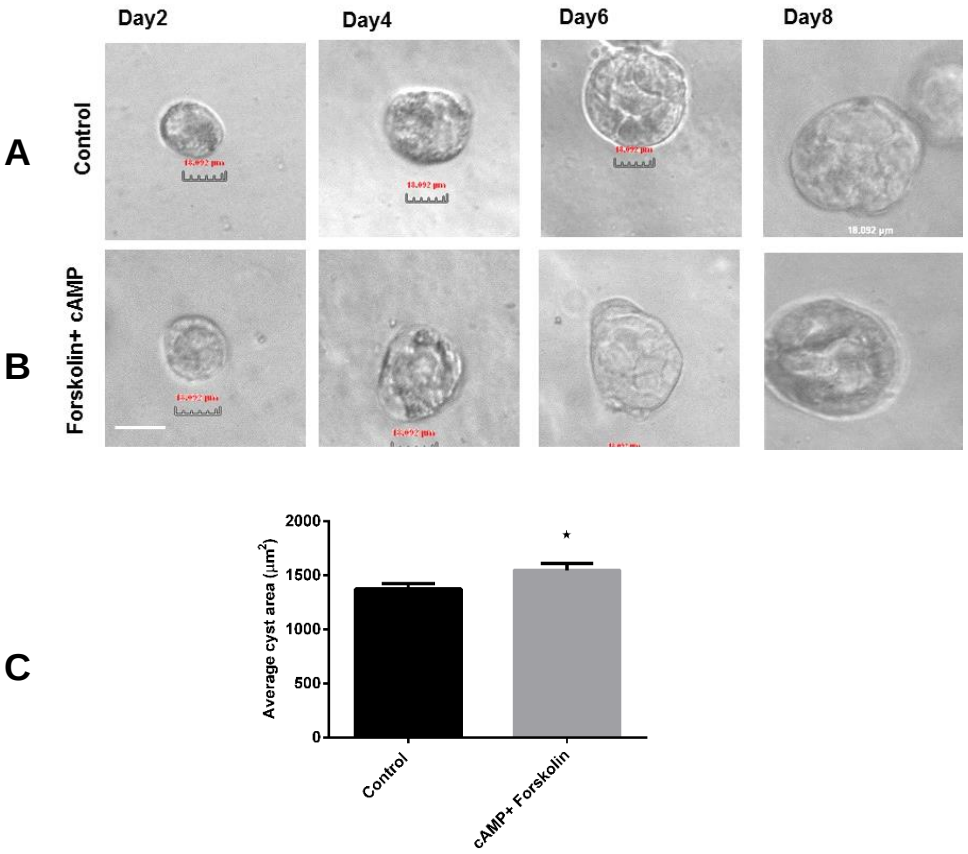

Figure 3.13. OX161/C1 cells cultured in Matrigel and treated with dbcAMP and Forskolin.

(A). Phase contrast microscopy of OX161/C1 cells cultured in Matrigel treated with supplemented media (control) **(B).** OX161/C1 treated with dbcAMP and Forskolin with media over 8 days. Cyst formation in OX161/C1 treated with both dbcAMP 100µM and Forskolin 10µM appeared no different in term of the size and number of cysts compared to the control. **(C).** Average cyst area between the control group and one treated with dbcAMP and Forskolin (Control= 1383 ± 48.86, n=59. vs 100µM dbcAMP +10µM Forskolin = 1545 ± 65.18, n=58) *P value = 0.047compared to the control. The scale bar represents 50µM. Unpaired t-test was used.. Data represented as mean± SEM.

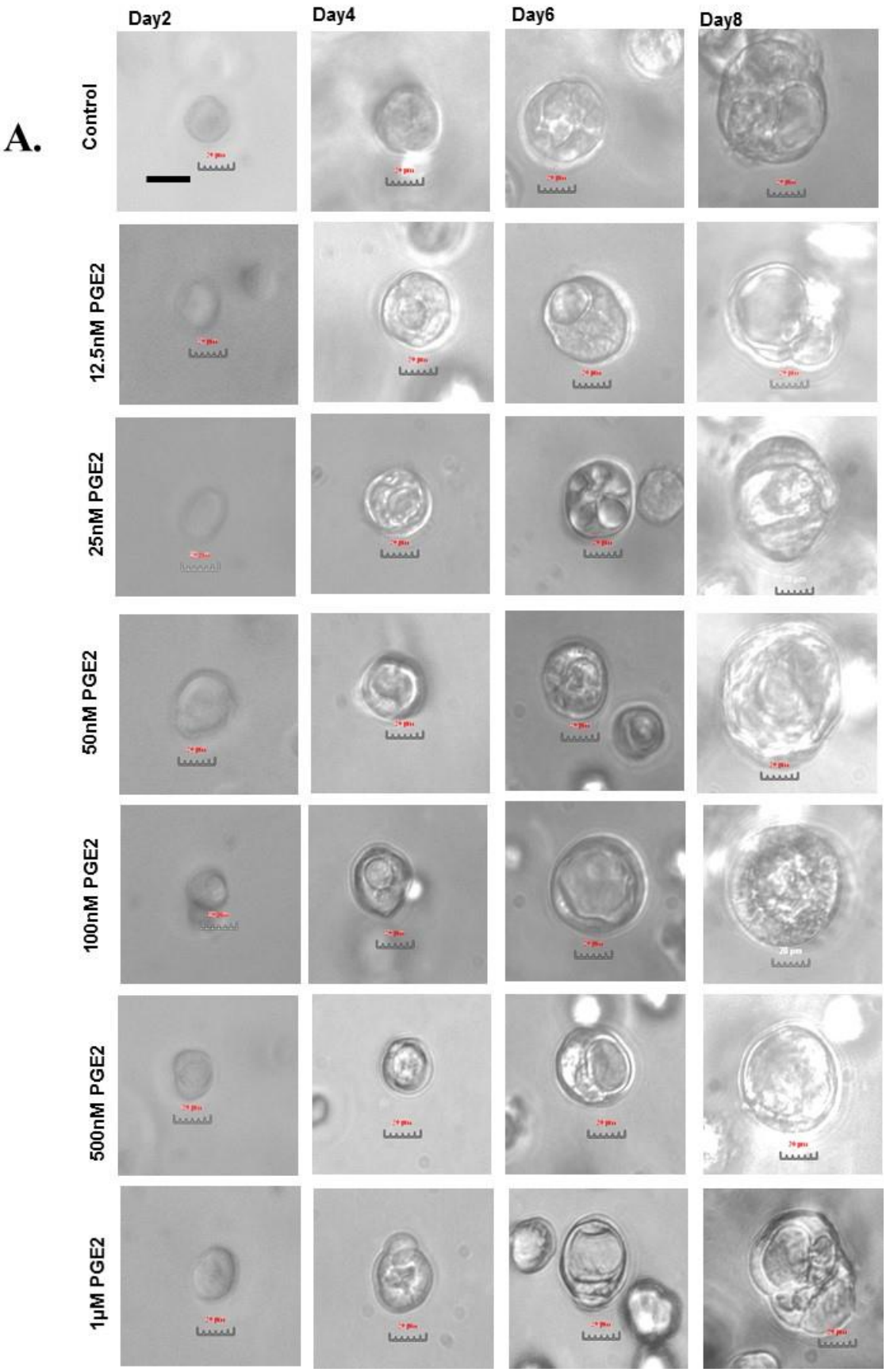
A.
Day2
Day4
Day6
Day8
Control
12.5nM PGE2
25nM PGE2
50nM PGE2
100nM PGE2
500nM PGE2
1μM PGE2

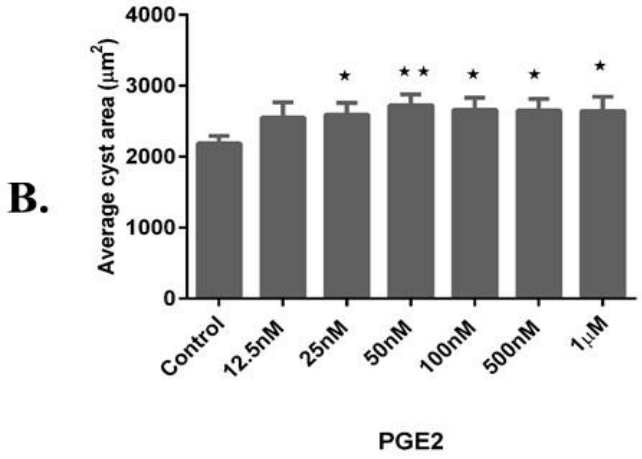

Figure 3.14. The effect of PGE2 on cyst formation in matrigel using human epithelial ADPKD cell line clone OX161/C1.

(A). OX161/C1 treated with supplemented media and 5% Nu serum only (control), and OX161/C1 treated with supplemented media and 5% Nu serum and different concentrations of PGE2. Cysts formed under control conditions but developed well-defined lumen and expanded more in size and the number after treatment with different concentrations of PGE2 (12.5nM, 25nM, 50nM, 100nM, 500nM, 1μM). All scale bars represented 50μM.

(B). There was no significant increase in cyst area when cell treated with 12.5nM PGE2 compared to control (Control= 2186 ± 104.7, n=29 vs 25nM PGE2 = 2548 ± 217.5, n=29, p = 0.13). However, there were significant increases in cyst area at higher concentrations of PGE2 (25nM and above). A maximal increase in cyst area was observed at 50 nM. One-way ANOVA test was used. *$p<0.05$; **$p<0.01$. Data represented as mean± SEM.

3.4. Discussion.

The main aim of this chapter was to optimise the growth of epithelial cell lines derived from patients with ADPKD in 3 D cyst assays. Cells growing in 3D culture are more representative of the *in vivo* situation compared to monolayer cultures and are considered more physiological assays to screen potential compounds prior to testing in animal models. A cellular response to an *in vitro* 3D environment however depends on a number of different factors including cell type, cell density, passage number and protein concentration of the basement membrane (Cukierman, Pankov et al. 2001). Collagen has been used since the 1970s as 3D *in vitro* method for studying cell biology and morphogenesis (Elsdale and Bard 1972, Benton, George et al. 2009). Matrigel is also commonly used in 3 D cultures although it is more expensive and difficult to manipulate compared to collagen (Debnath, Muthuswamy et al. 2003, Yu, Sidhu et al. 2005). Cells will typically polarise in 3 D Collagen or Matrigel cultures to form either cysts or branching tubular structures with an apical side facing the lumen and a basolateral side that is in contact with ECM and adjacent cells (Pampaloni, Reynaud et al. 2007).

In this chapter, the first experiments were designed to develop a suitable 3D culture model that could be utilized to investigate the effects of PGE2 and cAMP on cyst expansion. I first utilised Collagen I as a 3 D matrix. ADPKD cells however failed to differentiate or polarize to form cysts in Collagen I gel despite optimal growth conditions. The reasons for this are unclear. One possible explanation is that the Collagen I is too simple a matrix and lacks growth factors and other essential proteins for promoting differentiation and polarisation. Matrigel has a different composition of basement membrane proteins (laminin, collagen IV and heparin sulphate) and growth factors like EGF that provide natural environmental media for cell differentiation and polarity. However, only OX161/C1 cells reliably formed cysts in matrigel 3 D cultures. SKI-001 and SKI-002 cells formed small cysts and unexpectedly OX938 cells mainly formed

tubules. In addition, these lines did not proliferate well in 3 D cultures compared to OX161/C1 cells.

To complement the OX161/C1 assays, I utilised the well-established MDCK II model of cystogenesis. OX161/C1 and MDCK II cells were cultured in Matrigel and Collagen respectively, and the effect of exogenous cAMP and PGE2 on cyst expansion were tested. Both PGE2 and cAMP have been reported to increase proliferation of ADPKD cells in culture and this was also seen in our 3 D cyst assays. cAMP and PGE2 caused a significant increase in average cyst area after 8 days. The result are consisted with previous studies (Hanaoka and Guggino 2000, Belibi, Reif et al. 2004). The response of OX161/C1 to cAMP was less than that in MDCKII cells. One possible explanation is that the cystic cells could already be maximally stimulated by high levels of cAMP; in this case, a reduction in endogenous cAMP levels could be effective. Elberg et al. (2007) demonstrated that the growth of human ADPKD cysts was increased by PGE2 (Elberg, Elberg et al. 2007) and that these effects were mainly mediated through PTGER2. In contrast, a later study by the same group demonstrated that the effects of PGE2 was primarily through PTGER4 in murine Pkd1 knockdown cells (Elberg, Turman et al. 2012). In contrast to the experiments conducted in this study, Elberg et al used PKD cells with unknown mutations, whereas I used ADPKD cells with a known mutation (PKD1). In addition, Elberg et al used a compound (AH-689) as a PTGER2 antagonist which is both weakly potent and a non-selective PTGER2 antagonist (blocks PTGER2, PTGER2, TP, P3 and DP1) and has agonist activity and was shown to be unsuitable for *in vivo* study (Abramovitz, Adam et al. 2000). This project used a new compound (PF-04418948) which is the first potent and highly selective competitive inhibitor of human PTGER2 showing 2000 fold potency to PTGER2, and is suitable for *in vivo* study (af Forselles, Root et al. 2011).

The aim of the next chapter was to determine the expression of PTGER receptors in our human ADPKD cell lines with the aim of testing the effect of specific PTGER 2 and 4 receptor antagonists on cystogenesis in these two model assays.

Chapter 4

Prostaglandin receptor expression in ADPKD

4.1 Introduction

In this chapter the expression of both PTGER2 and PTGER4 receptors in a variety of ADPKD models was analysed by microarray, qPCR, western blotting and immunohistochemistry (IHC). Human cell lines described in the previous chapter were studied, as well as human ADPKD tissue and two independent orthologous mouse models of ADPKD.

4.2 Aims and objectives:

1. Determination of expression levels of PTGER receptors 1, 2, 3 and 4 by microarray, qPCR and western blotting from human ADPKD cell lines and normal controls.
2. Determination of expression levels of PTGER receptors 2 and 4 by IHC from human ADPKD tissue sections.
3. Determination of expression levels of PTGER receptors 2 and 4 by qPCR and IHC from two independent orthologous mouse models of ADPKD.

4.3 Results

4.3.1. PTGER 1, 2, 3 and 4 gene expression in human cell lines.

A pilot experiment in our lab using an Agilent mRNA expression microarray was performed to identify changes in gene expression levels in the ADPKD cell lines described in chapter 3. This information was used to identify novel genes and pathways which may contribute to the pathogenesis of ADPKD. The expression of 1515 genes was significantly altered by more than 2 fold between control and ADPKD cell lines. Of those, 447 genes were significantly up-regulated and 1068 genes significantly down-regulated in ADPKD cells. Relevant to this project was a significant increase in PTGER2 expression in ADPKD cell lines (6 fold increase), with no significant increase in PTGER 1, 3 or 4 **(Figure 4.1).**

Data generated by microarray was validated in this study. TaqMan qPCR was carried out to determine the mRNA expression levels of PTGER 1, 2, 3 and 4. Expression levels were normalised using GAPDH mRNA expression level as a housekeeping gene. **(Figure 4.2 A, B).** Expression of PTGER2 mRNA was higher in ADPKD cell lines by comparing average ΔCT values (9.18 for ADPKD samples vs 12.745 for controls). The fold change in PTGER2 expression between ADPKD and controls was calculated using the comparative ΔΔCT method of relative quantification. A 6.21 fold increase in PTGER2 was seen in the ADPKD samples compared to normal controls. No significant difference was seen for PTGER1, 3 and 4 mRNA levels validating the results seen in the Agilent microarray.

4.3.2. PTGER 1, 2, 3 and 4 gene expression in orthologous mouse models of ADPKD.

mRNA expression levels of PTGER 1, 2, 3 and 4 was then determined in two orthologous mice models of ADPKD. Samples of cDNA and tissue sections used in this study were a gift from Prof. Dorien Peters (Leiden University, Leiden, Netherlands).

The first mouse model used in this study was the $Pkd^{nl,nl}$ hypomorphic mouse which was developed used a neomycin selection cassette (**Figure 4.3 B**). The second mouse model used in this study was the CreLox model (Lantinga-van Leeuwen, Leonhard et al. 2007). The CreLox model is characterised by a specific deletion of *Pkd1* created using a site-specific recombination mechanism and induced by tamoxifen (Cre-loxP) (Branda and Dymecki 2004). (Lantinga-van Leeuwen, Leonhard et al. 2006) **(Figure 4.3 A)**.

The cystic changes following treatment with tamoxifen were mainly in collecting ducts and distal tubules (Lantinga-van Leeuwen, Leonhard et al. 2007). When tamoxifen was administered to the mice, it induced deletion of the *Pkd1* gene at exons 2 -11 leading to cyst formation. The timing of introduction of tamoxifen to the mice can affect the severity of disease. For example, administration of tamoxifen at one month in adult mice gave few cysts compared to severe cystic disease when tamoxifen was given to new born mice (Lantinga-van Leeuwen, Leonhard et al. 2007). cDNA samples were available from control mice and CreLox mice at 4 months following tamoxifen treatment.

TaqMan qPCR analysis was carried out on cDNA samples from these two independent mice models of ADPKD**.** In both models, a significant increase in PTGER2 mRNA expression was seen when analysed by comparative ΔCT using Data Assist v3.1 software **(Figure 4.5 A, B and C)**. Fold change increases in PTGER2 were 2.68 in the $Pkd1^{nl,nl}$ model and 2.77 in the CreLox model. In contrast to the human ADPKD cells, a significant increase in PTGER4 was also observed in both models. Fold change increases in PTGER4 were 4.61 in the $Pkd1^{nl,nl}$ model and 5.42 in the CreLox model **(Figure 4.4 A , B).** The other two receptors PTGER1 and PTGER3 showed no significant increases by fold change compared to control mice.

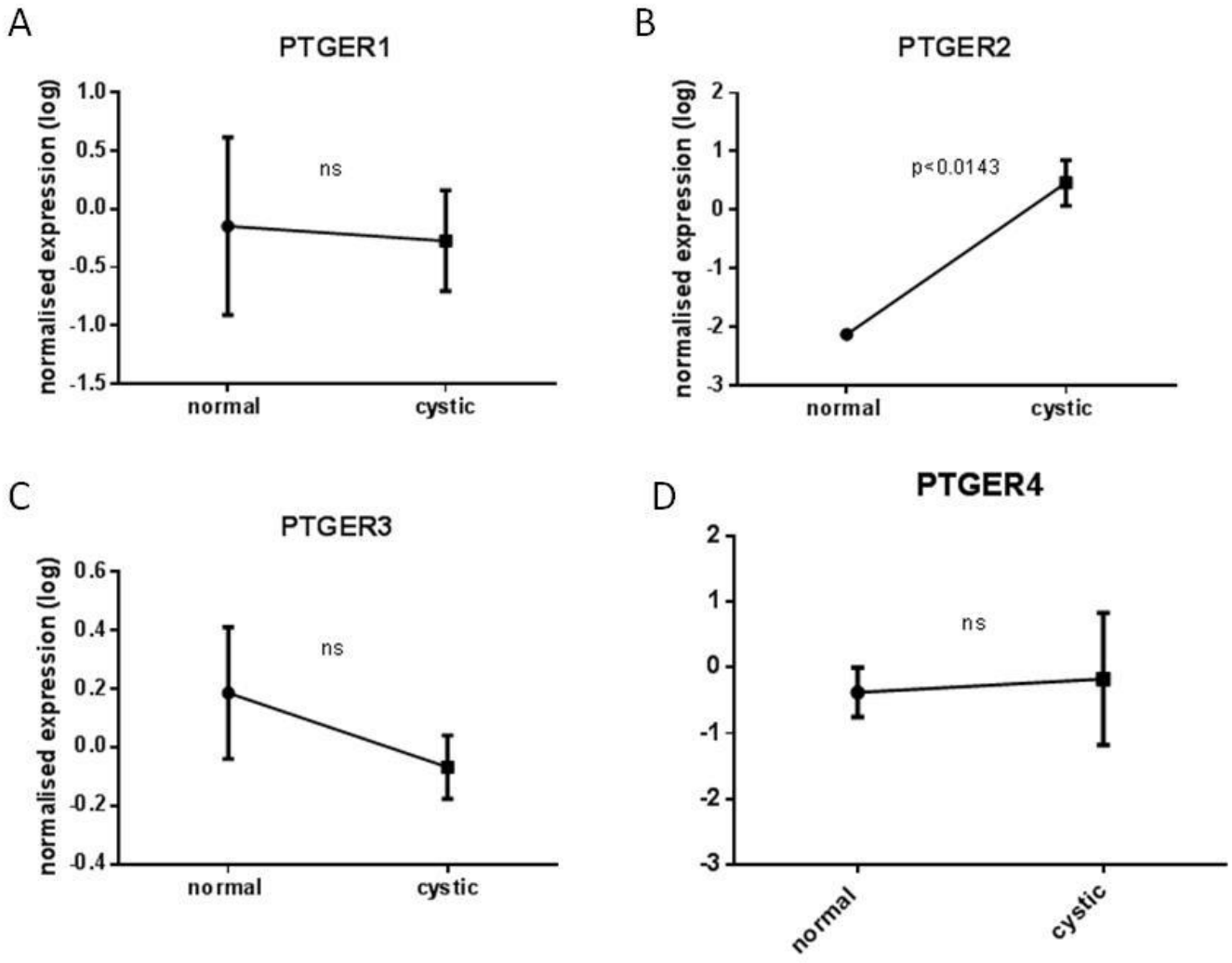

Figure 4.1. Agilent mRNA microarray expression of PTGER 1, 2, 3 and, 4 in human ADPKD cell lines.

mRNA microarray was carried out on 6 cell lines and analysis using Agilent Gene Spring software showed that only PTGER2 mRNA expression levels were significantly increased by 6 fold in the cystic lines (n=4) *P = 0.014 (**B**). No significant increase in PTGER1 (n=4) P= 0.88, PTGER3 (n=2) P= 0.33, or (n=4). P= 0.88 (**A**, **B, D**) was seen.. Unpaired t-test was used. Data represented as mean± SEM.

A

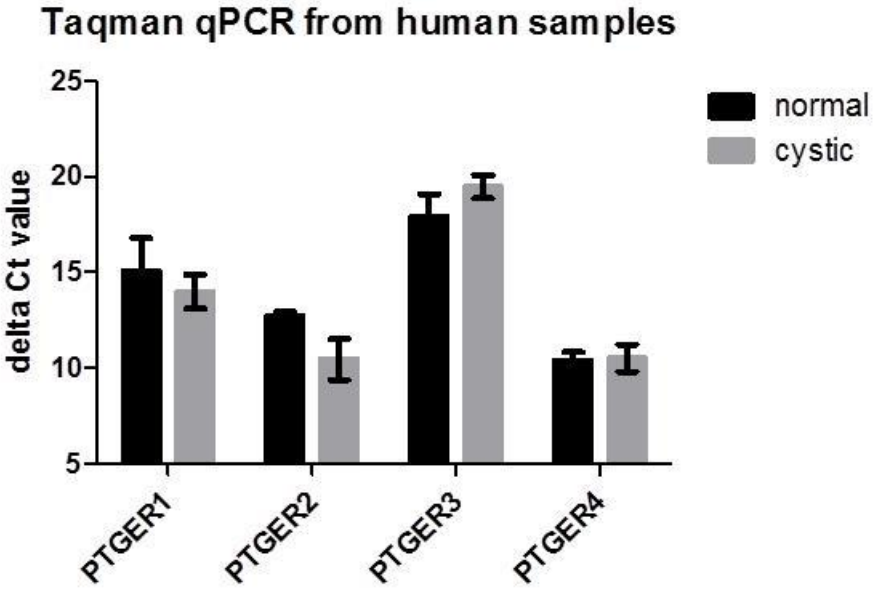

B

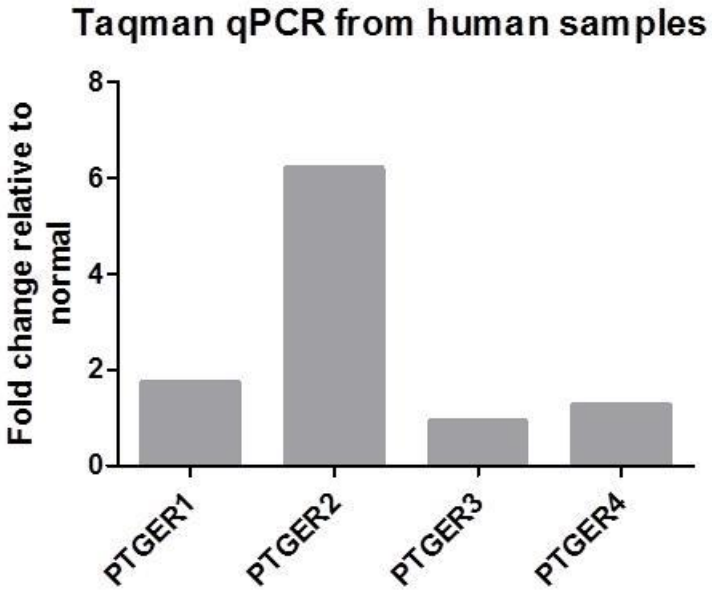

Figure 4.2. TaqMan qPCR expression of PTGER1, 2, 3 and 4 in human ADPKD cell lines.

Taqman qPCR carried out on the same human samples used for microarray. **(A).** an increase in PTGER2 was seen when relative changes in expression were analysed by delta CT values (n=4). P value= 0.09. Unpaired t-test was used. **(B).** Fold changes relative to normal controls (6 fold increase).

A.

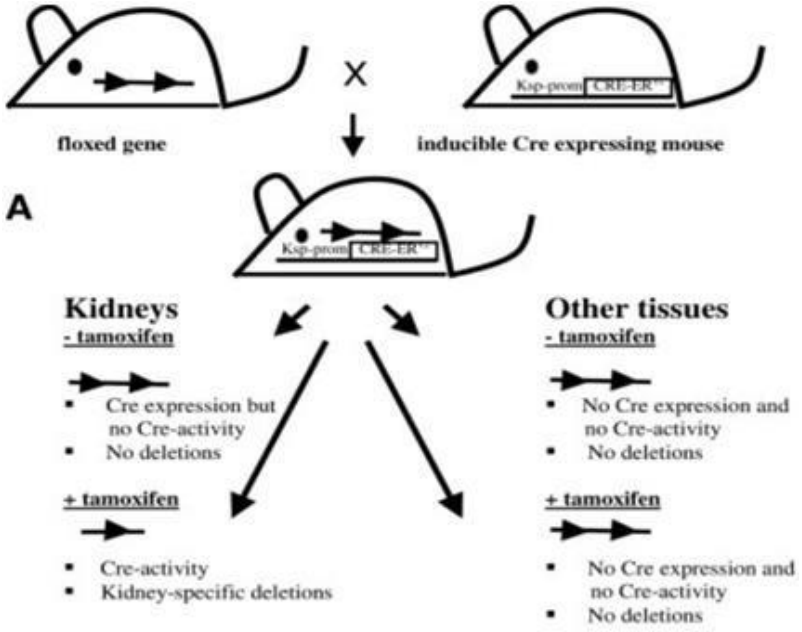

B.

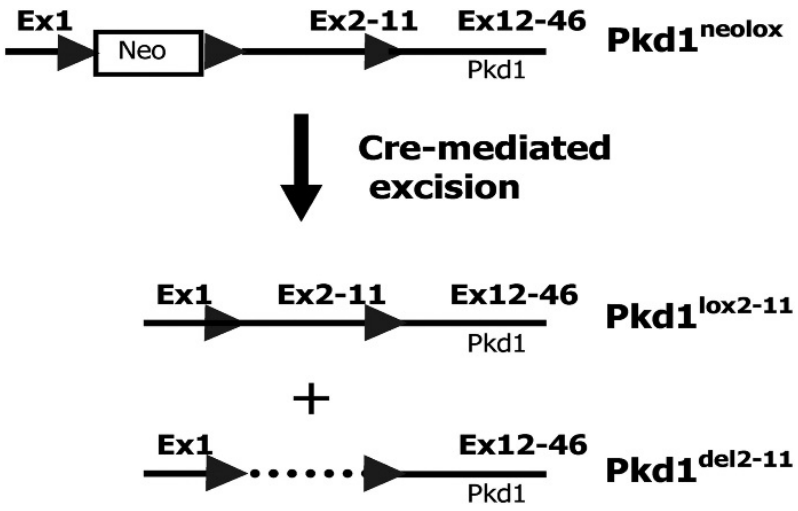

Figure 4.3. ADPKD orthologous mouse models used in this study

A. Transgenic mice containing Cre-recombinase expressed only in the kidneys were crossed with mice containing floxed gene (lox P 2-11). In the presence of tamoxifen the Cre becomes active and deletes the floxed gene resulting in a specific deletion of PKD1 (CreLox model) (Lantinga-van Leeuwen, Leonhard et al. 2007).

B. Transgenic mice with a neomycin cassette flanked in two LoxP position in intron one and third LoxP in intron 11 of the PKD1 gene (Neolox model) (Happe, van der Wal et al. 2013).

A

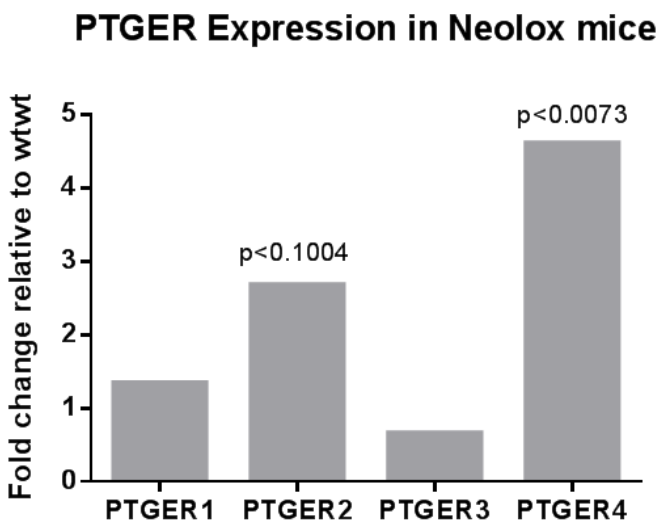

B

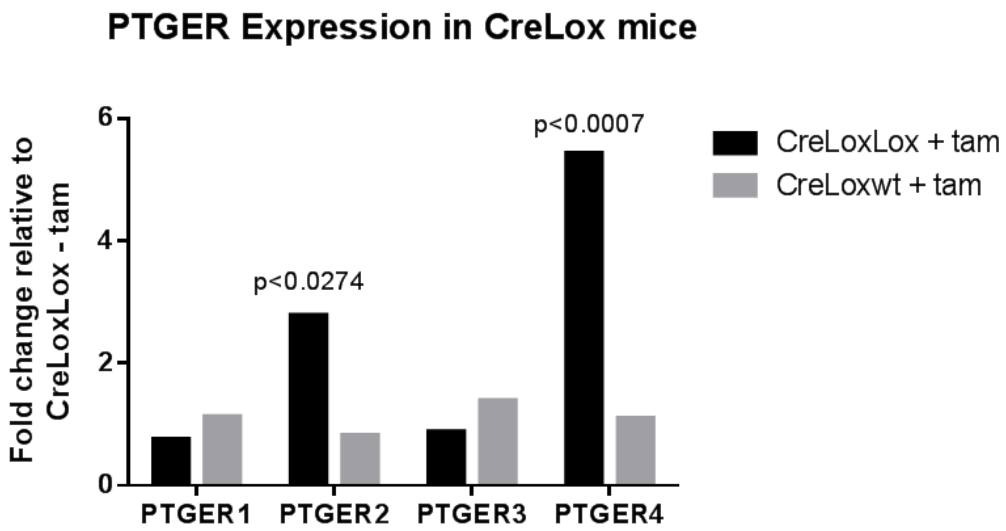

Figure 4.4. TaqMan qPCR expression of PTGER1, 2, 3 and 4 in two mouse models of ADPKD.

A. A significant fold change increase in PTGER4 but not PTGER1, 2 or 3 was seen in the Neolox mouse Pkd1 model.

B. A significant fold change increase in PTGER2 and 4 was seen in the CreLox mouse Pkd1 model (CreLoxLox+tam = 11.66± 0.359, n=5. CrLoxwt+tam=13.45± 0.349, n=5) P<0.0007. (CreLoxLox+tam = 11.33± 0.160, n=3. CrLoxwt+tam=12.87± 0.49, n=3) P<0.03. Unpaired t-test was used

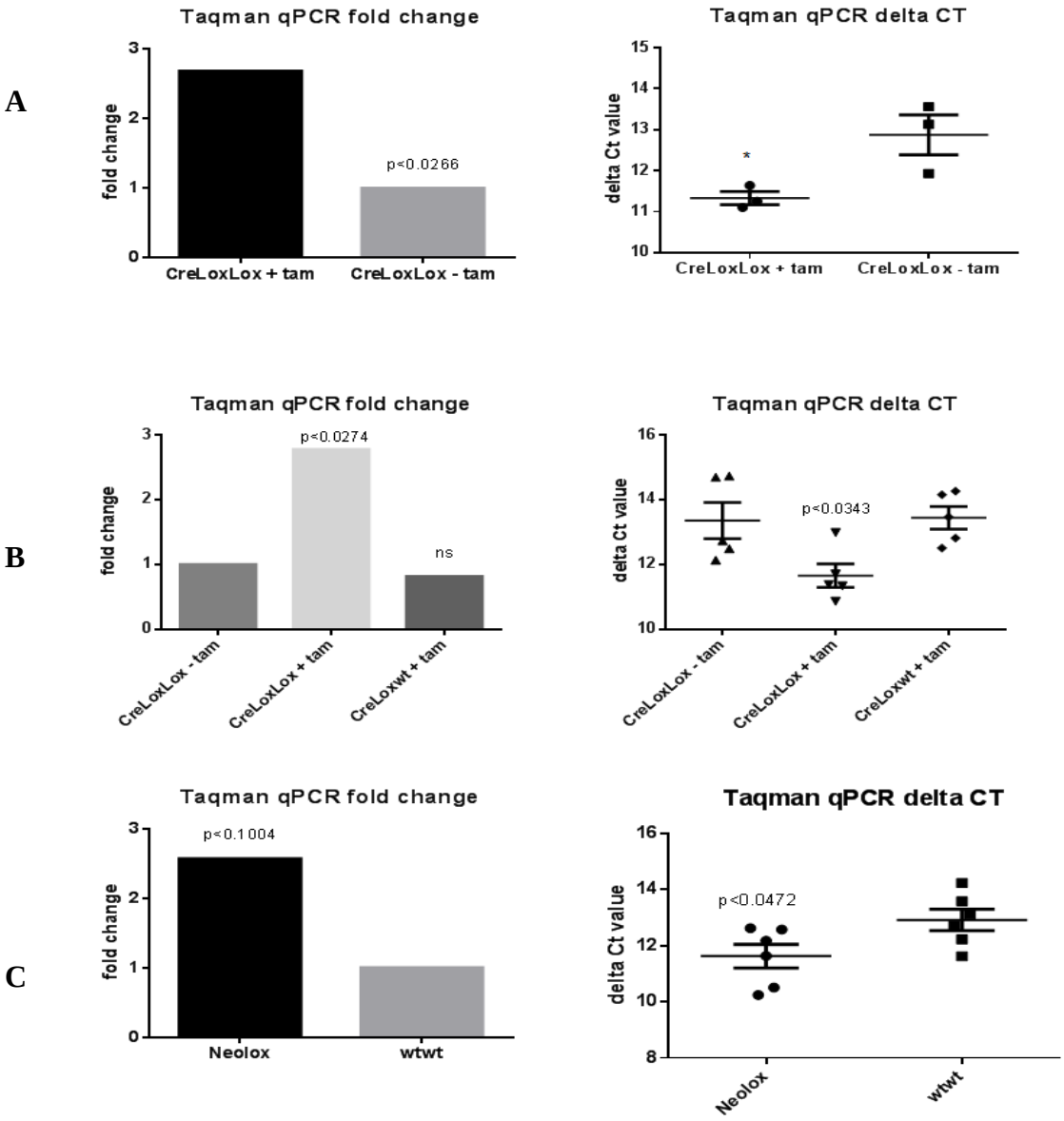

Figure 4.5. TaqMan qPCR expression of PTGER2 in two mouse models of ADPKD.

A. There was a significant increase in PTGER2 as measured by changes in delta CT and fold change in a CreLox Pkd1 model following tamoxifen treatment.

B. There was a significant increase in PTGER2 as measured by changes in delta CT and fold change in a CreLox Pkd1 model following tamoxifen treatment compared to wt mice treated with tamoxifen. One- way ANOVA test was used.

C. There was a significant increase in PTGER2 as measured by changes in delta CT in a Neolox Pkd1 model. Unpaired t-test was used. Data represented as mean± SEM.*$p<0.05$.

4.3.3. Western Blotting with PTGER2 and PTGER4 specific antibodies in human cell lines.

To demonstrate that the increases in PTGER2 and PTGER4 mRNA levels translated into increases in protein receptor expression in human ADPKD cell lines (described in chapter 3), western blotting with specific antibodies was carried out. PTGER2 expression was tested using two separate antibodies. The first experiment used a rabbit polyclonal antibody to PTGER2 (Abcam, UK). This antibody recognised multiple non-specific bands in a preliminary western blot (**Figure 4.6 A**) and was therefore not used in subsequent experiments. A mouse monoclonal antibody to PTGER2 (R+D Systems, UK) recognised a specific protein at the correct MW for PTGER2 (49 kDa). Expression of PTGER2 was significantly increased in 3 ADPKD cell lines and undetectable in two control cell lines confirming the increase in mRNA expression levels seen in the human microarray and qPCR assays (**Figure 4.6 B**).

The expression of PTGER2 in OX161/C1 ADPKD cells was significantly increased in serum-stimulated cells compared to serum-starved cells **(Figure 4.7 B, E).** The increased expression following serum stimulation may be due to the increased proliferation rate in ADPKD cells following serum stimulation. No detectable PTGER2 expression was seen in control UCL93 cells following serum stimulation **(Figure 4.7 B, C and D)**

PTGER4 expression was tested using a rabbit polyclonal antibody to PTGER4 (Sigma, UK). This antibody recognised a specific protein at the correct MW for PTGER4 (50 kDa). Expression of PTGER4 was similar in ADPKD and control cell lines confirming the similar mRNA expression levels seen in the human microarray and qPCR assays **(Figure 4.8 A).**

A.

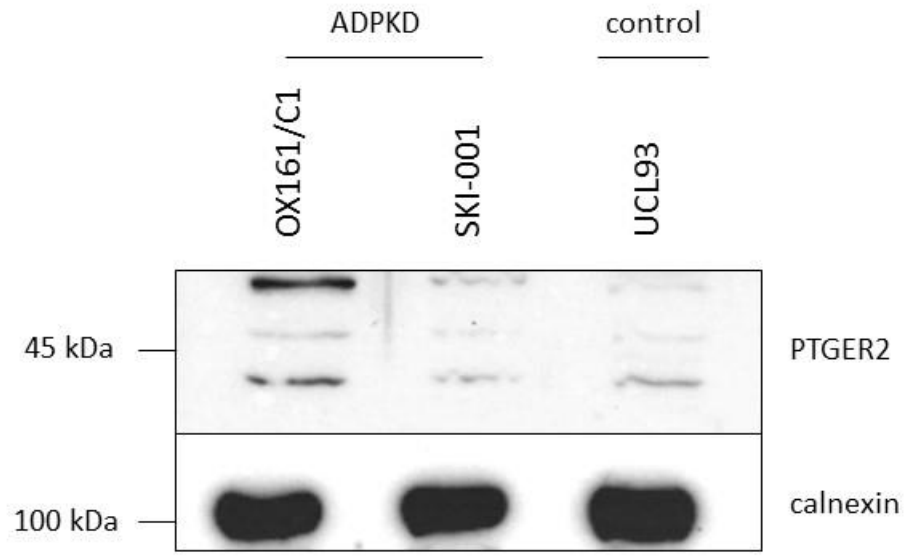

B.

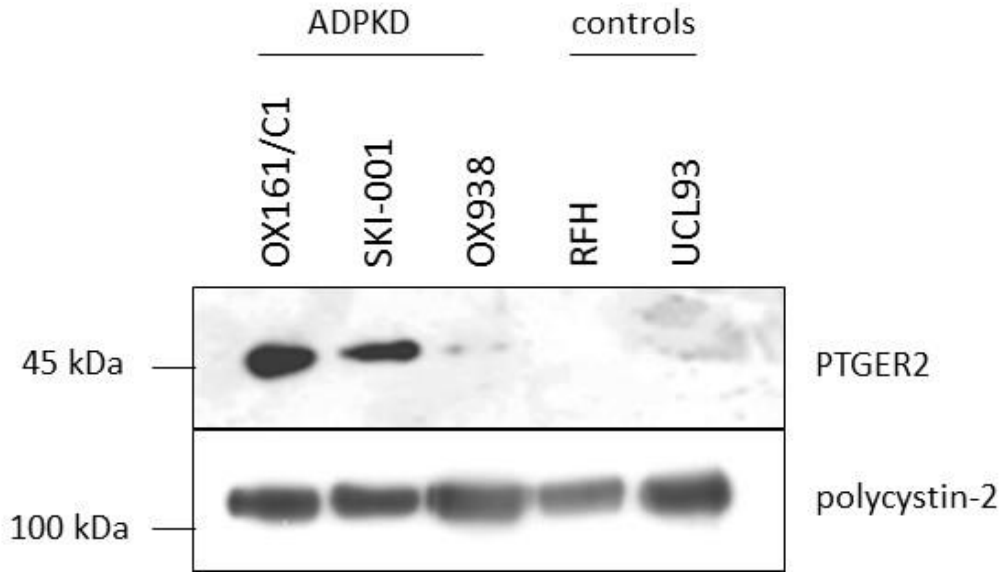

Figure 4.6. Western blotting of PTGER2 in human kidney cell lines

A. Specific detection of PTGER2 was not seen with a rabbit polyclonal antibody against PTGER2. Equal loading was confirmed by probing the same membrane with a specific antibody to Calnexin.

B. Specific detection of PTGER2 was seen with a mouse mAb against PTGER2. Increased expression of PTGER2 was seen in cell lines derived from patients with ADPKD with strongest expression seen in OX161/C1 and SKI-001 cell lines with weaker expression in OX938 cells. No expression was seen in control cell lines. Equal loading was confirmed by probing the membrane with an antibody to polycystin-2.

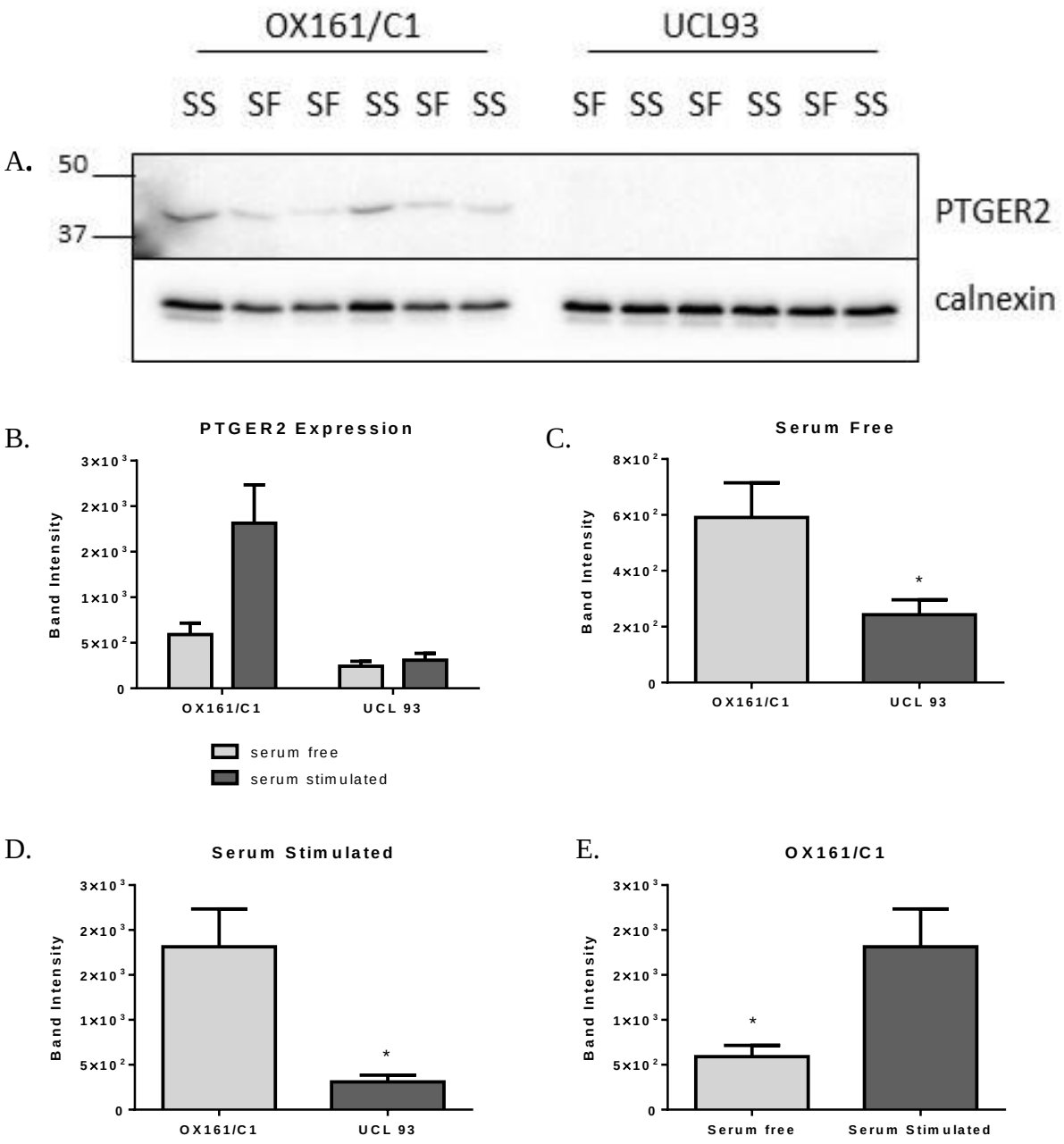

Figure 4.7. PTGER2 expression is increased following serum stimulation in ADPKD cell lines.

A. Increased expression of PTGER2 was seen in the OX161/C1 ADPKD cell line following serum stimulation with no expression detectable in the UCL93 control cell line (n=3) serum free (OXC1= 591±12 n=4, UCL93=243±5, n=4)*P value= 0.04. Serum stimulated (OXC1= 1813±422 n=4, UCL93= 309.5±74) *P value= 0.012. (Serum free=591±1230, n=4, serum stimulated= 1813±422, n=4) *P value=0.03. Equal loading was confirmed by probing the membrane with an antibody to Calnexin. (SF = 24 h serum free, SS = 24 h serum free followed by 24 h serum stimulation). Unpaired t-test was used. Data represented as mean± SEM.

B, C, D, E. Quantification of PTGER2 band intensity relative to calnexin demonstrated a significant increase in PTGER2 expression in OX161/C1 cells following serum stimulation as well as compared to UCL93. Unpaired t-test was used.

A

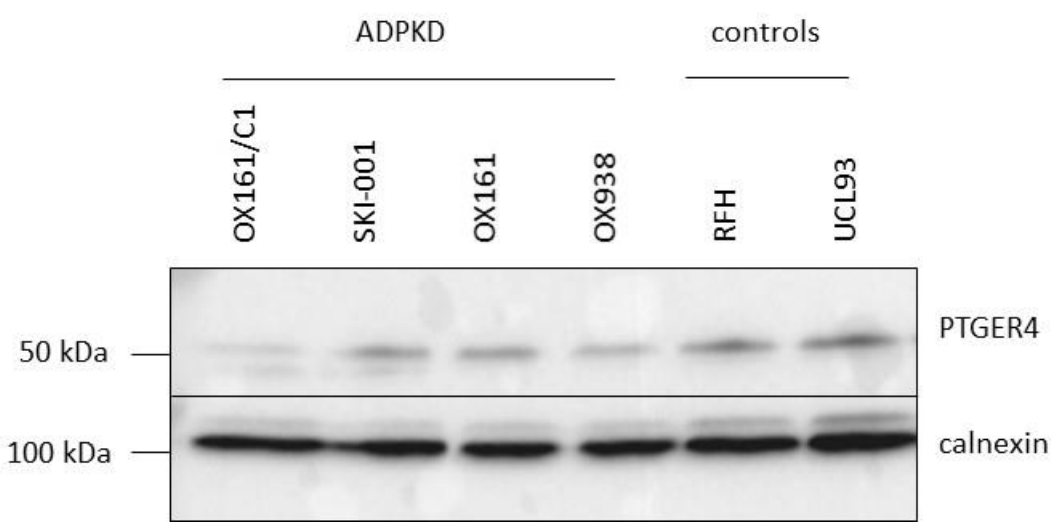

Figure 4.8. Western blotting of PTGER4 in human kidney cell lines

A. No significant change in expression of PTGER4 was seen in cell lines derived from patients with ADPKD compared to control cell lines. Equal loading was confirmed by probing the membrane with an antibody to Calnexin.

4.3.4. Immunohistochemistry of human kidney tissue sections with PTGER2 and PTGER4 specific antibodies.

Next, I studied the expression of PTGER2 and its localisation in human ADPKD kidney tissue sections. Expression was then compared to normal control sections taken from non-ADPKD kidneys removed for clinical indications. In addition, the same tissue samples were used to determine PTGER4 expression.

Firstly, the average cyst area was measured in both the ADPKD and control tissue sections. A cyst was defined a structure with an area greater than five times that of a normal tubule or more than 6000 μm^2 (Chang, Parker et al. 2006). Not surprisingly, there was a significant difference in average cyst area between ADPKD and control tissue sections (**Figure 4.9**).

Immunohistochemistry with a specific antibody revealed weak PTGER2 staining in renal tubules of control tissue sections (**Figure 4.11 A**). In ADPKD tissue sections, prominent tubular cell staining was seen especially in the apical membrane (**Figure 4.11 B**). There was no glomerular staining in control tissues. To analyse the difference in staining intensity, the ImageJ plugin ImmunoRatio which calculates the percentage DAB positive staining relative to total nuclear area to account for cell density was used (**Figure 4.10 B, D**) (Tuominen, Ruotoistenmaki et al. 2010). A total of six ADPKD tissue sections and six normal tissue sections were analysed using ImmunoRatio. There was a significant increase PTGER2 expression in ADPKD tissue compared to control tissue (Control 10.20± 0.948 vs PKD=23.72± 3.705 n=6) **P value= 0.005 (**Figure 4.11 B, D**).

Immunohistochemistry with a specific rabbit PTGER4 antibody in control sections revealed staining primarily in a subset of tubules (**Figure 4.12 A**). In ADPKD tissue, strong PTGER4 staining of non-cystic tissue was mainly localised to tubules and glomeruli (**Figure 4.12 A)**.

There was no significant difference in PTGER4 expression in ADPKD tissue compared to control tissue (Control= 35.69 ± 1.039, n=7 vs PKD=43.89 ± 4.689, n=7. P value 0.11 (**Figure 4.12 C**).

The immunohistochemistry data confirmed the increase in PTGER2 expression in human ADPKD samples seen at the mRNA and protein level in human cell lines, but not of PTGER4.

To confirm these findings in other disease models, the expression of PTGER2 and PTGER4 was next studied by immunohistochemistry in the two orthologous mouse Pkd1 models (Lantinga-van Leeuwen, Leonhard et al. 2006) (Happe, van der Wal et al. 2013).

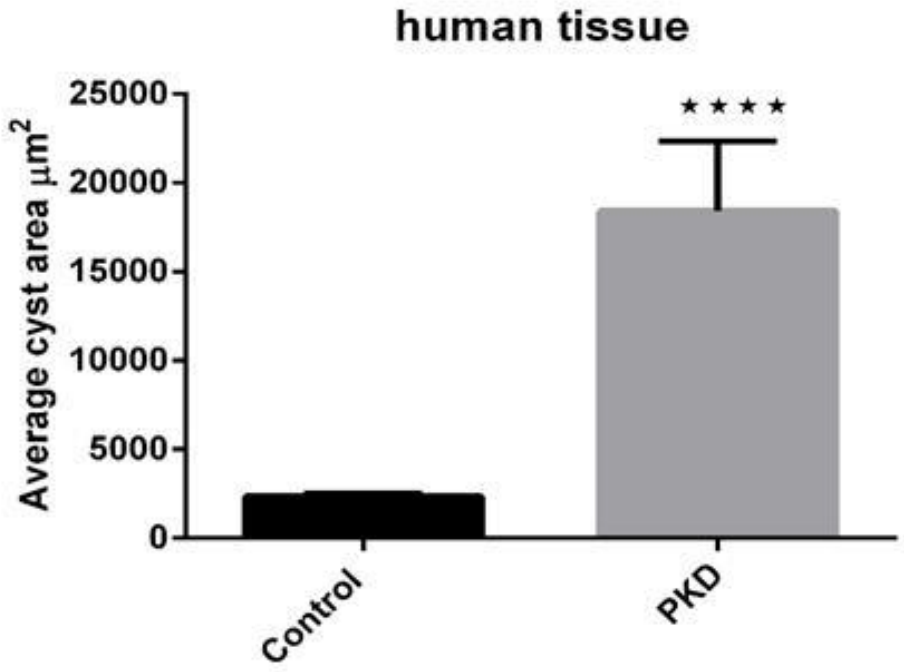

Figure 4.9. Average cyst area in human ADPKD tissue sections compared controls.

A significant increase in average cyst area was observed in human ADPKD tissue sections compared to controls. (Control= 2348 ± 155.8, n=45. PKD= 14462 ± 2570, n=45). Unpaired t-test was used. ****P value <0.0001**.** Data represented as mean± SEM.

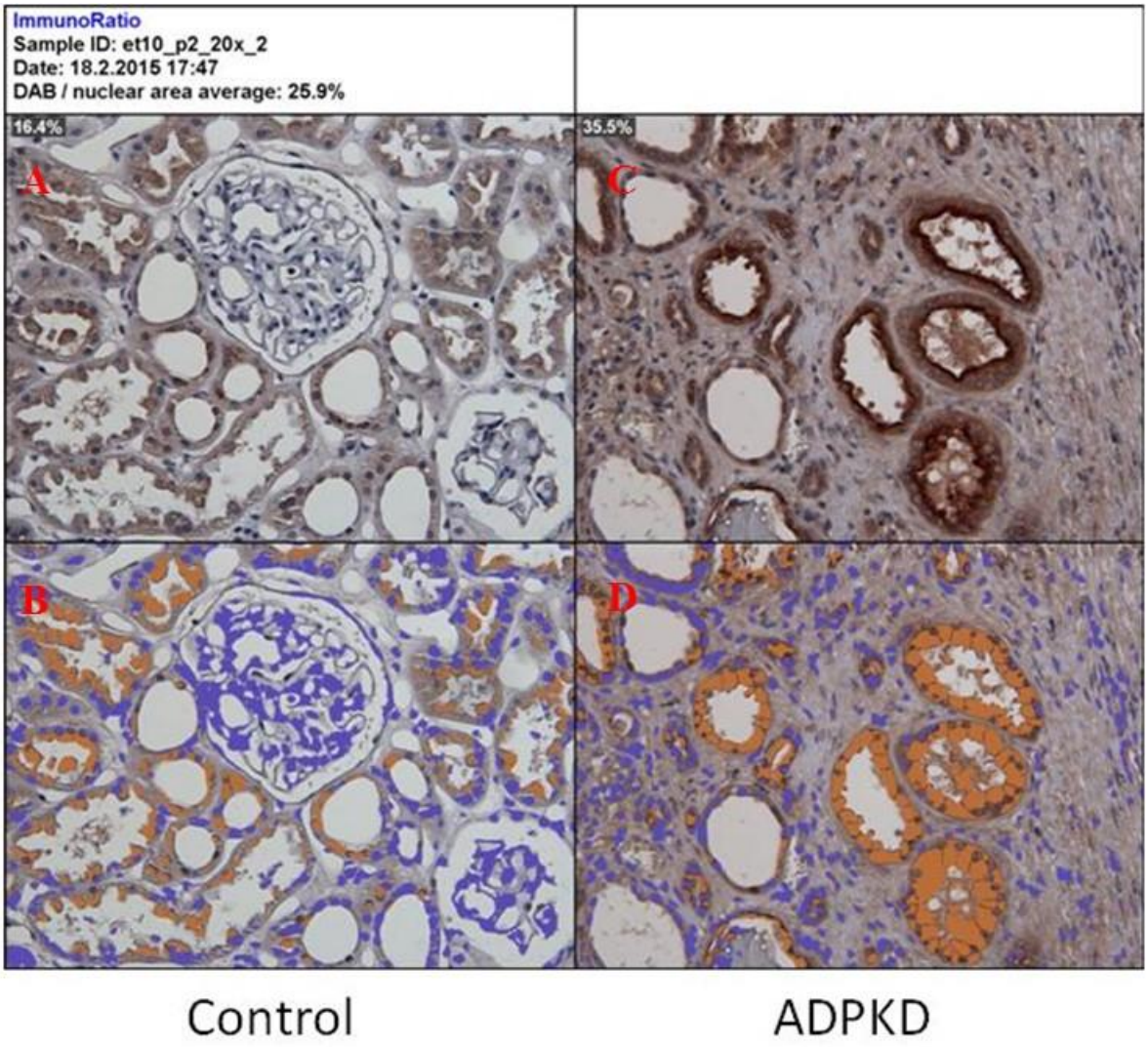

Figure 4.10. Semi-quantitative analysis of DAB staining intensity using ImmunoRatio ImageJ plugin.

A, C. The top panel shows PTGER2 staining of human tissue sections. **B, D**. The bottom panel shows the pseudo coloured image based on threshold DAB staining comapared to a negative control. Nuclear area is coloured blue and DAB staining is coloured orange. The Immunoratio ImageJ plugin uses this to calculate the DAB/nuclear area average % for each image.

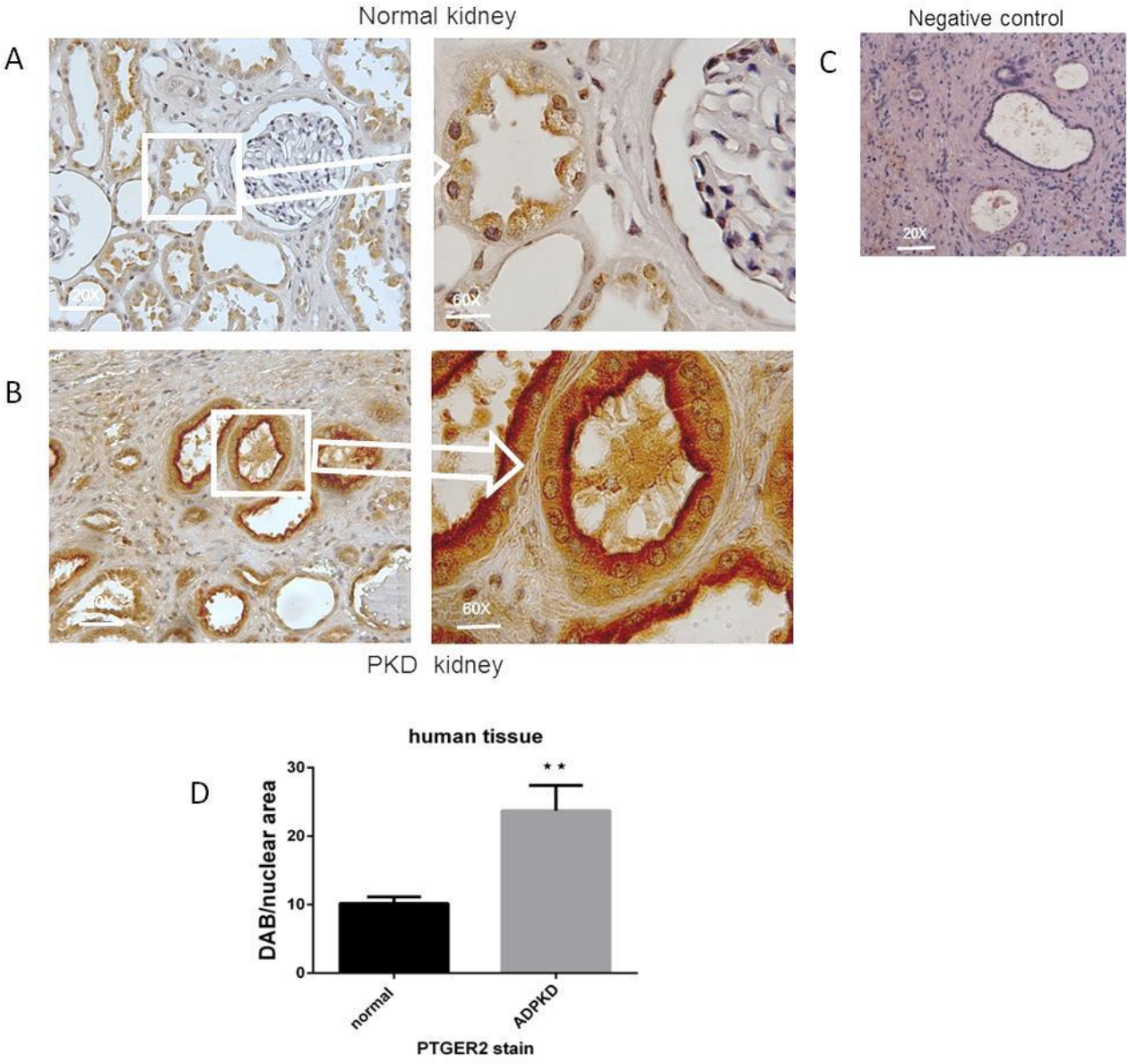

Figure 4.11. Immunohistochemistry of human kidney tissue sections with an antibody to PTGER2.

(A).Control kidney sections showed weak staining at the apical surface in normal tubules

(B).Strong staining for PTGER2 was seen in tubular lining epithelium in human ADPKD tissue sections.

(C). No specific staining was seen in sections incubated with non-immune serum.

(D). ImmunoRatio analysis showed a significant increase in PTGER2 staining in ADPKD sections compared to controls. Unpaired t-test was used. (n= 6)****** P value= 0.0054.

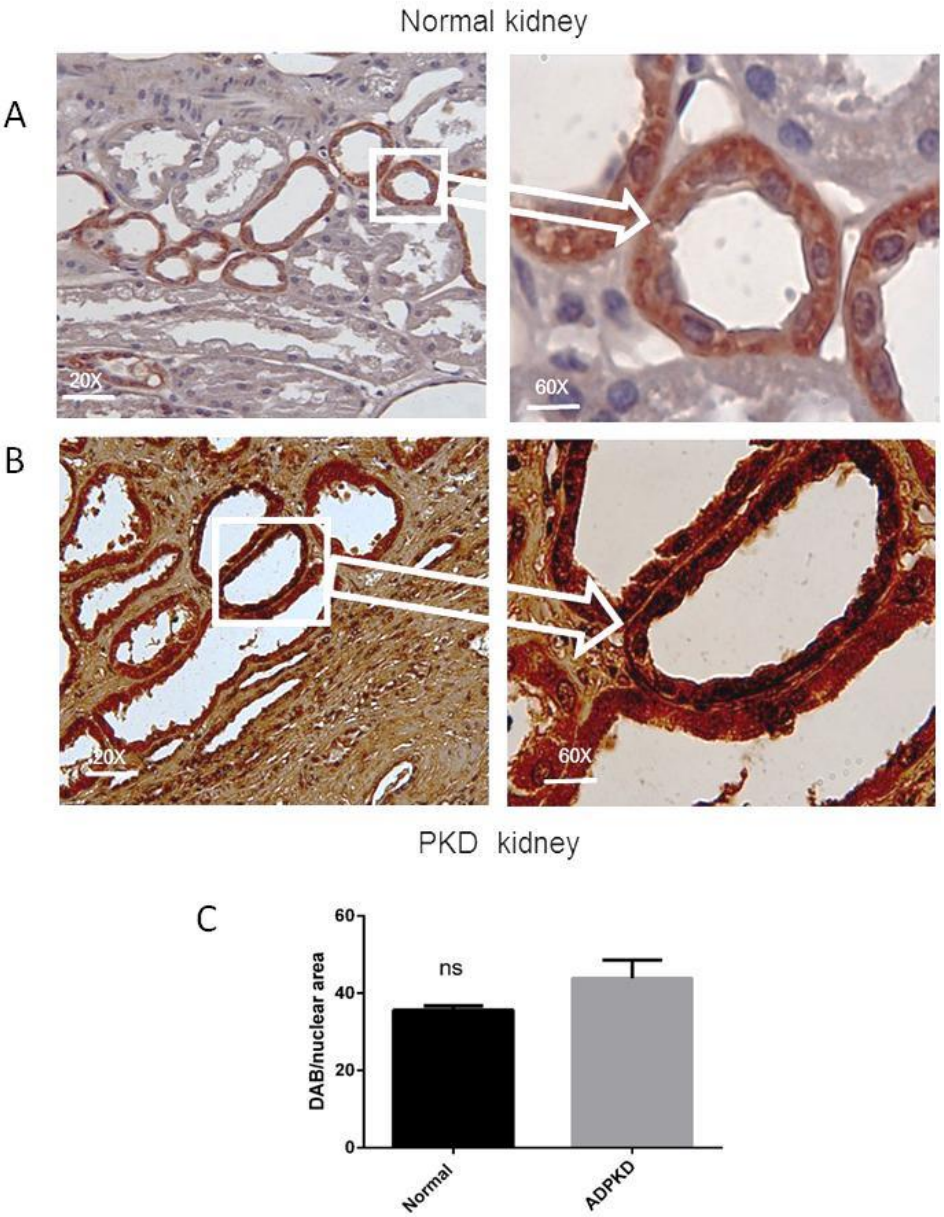

Figure 4.12. Immunohistochemistry of human kidney tissue sections with an antibody to PTGER4.

(A).Control kidney sections showed strong PTGER4 staining at the apical surface and cytoplasm in normal tubules.

(B).Strong staining for PTGER4 was seen in the tubular epithelium in human ADPKD tissue sections.

(C). ImmunoRatio analysis showed no significant increase in PTGER4 staining in ADPKD sections compared to controls. Unpaired t-test was used. (n=7) P value 0.11.

4.3.5. PTGER2 expression in a tamoxifen-inducible, kidney epithelium-specific Pkd1-deletion mouse model.

A significant increase in cyst area was seen after 1 month treatment with tamoxifen and this increase in cyst area become more pronounced following each additional month of treatment (**Figure 4.13 A, B)** . No significant increase in cyst/tubule area was seen in untreated animals highlighting the kidney specific induction of Pkd1 deletion and cystogenesis in this model by tamoxifen. Immunohistochemistry of tamoxifen treated and untreated tissue sections with a specific mouse PTGER2 antibody revelaed staining in all sections localised mainly to the apical surface within tubules with some cytoplasmic but no nuclear staining **(Figure 4.14)**. Quantification of staining by ImageJ immunoRatio plugin showed background staining and no significant difference after 1, 2, 3 or 4 months of non- tamoxifen treatment. While in tomoxifen treatment there is significant difference after 4months of tamoxifen treament **(Figur 4.15 A, B and C).** A significant difference between DAP/nuclear area between between treated and untreated mouse tissue was only observed after 4 months of tamoxifen treatment P value 0.002 (Control= 7.119±.0.381%, PKD=22.03± 0.525 n=12, n=12) **(Figure 4.15 D).**

One problem with quantifying PTGER2 expression by immunohistochemistry was the variable and patchy staining of PTGER2 in tamoxifen- treated mouse tissue. Therefore a grading system was used to classify the intensity of staining of PTGER2 into four classes. These were defined as 0 or no staining; grade 1 or weak staining in apical area; grade 2 or moderate staining and grade 3 or very intense dark staining **(Figure 4.16 A, B, C, and D)**. Analysis was carried out by defining the percentage of positively stained cysts showing each grade of staining per section. Grade 1 was most commonly seen in tamoxifen untreated mouse tissue after one, two, three, and four months. Grade 1 staining was most common in tamoxifen treated mouse tissue after the first, second and less frequently in the third, and fourth month **(Figure 4.16 E, F, G**

and H). Grade 2 staining was seen commonly in three month and in four month treated mouse tissue **(Figure 4.16 G, H)**. Grade 3 staining was present only in four month tamoxifen treated mouse tissue **(Figure 4.16 H)**. In summary, the third and fourth month tamoxifen treated mouse tissue contained more cysts with increased PTGER2 expression (Grade 2, and 3) compared to untreated tamoxifen tissue.

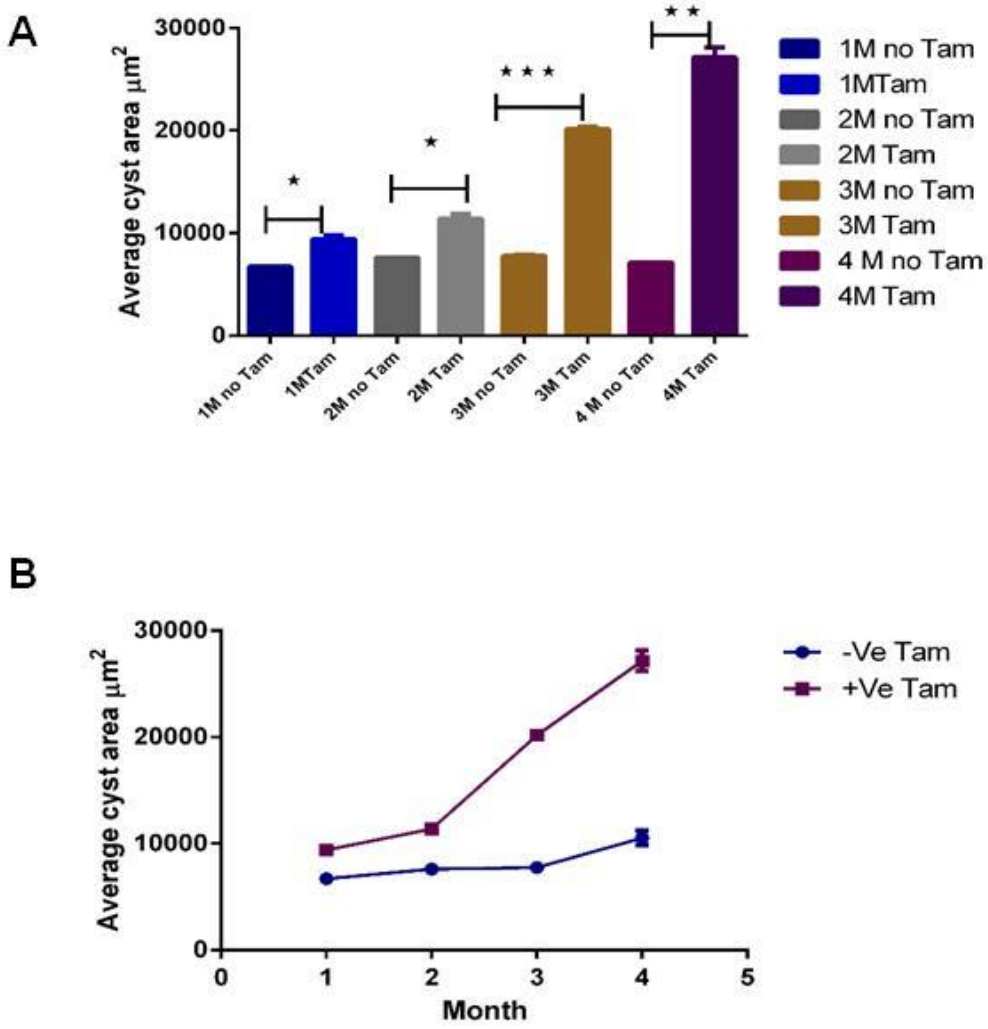

Figure 4.13. Average cyst area in a CreLox mouse ADPKD model

(A). A significant increase in average cyst area was observed in mouse CreLox tissue sections treated with tamoxifen compared to untreated controls at 1, 2, 3 and 4 months after treatment. At 1 month (n=12) *P<0.0203. At 2 months (n=12) *P<0.0145. At 3 months (n=12) ***P<0.0003. At 4 months (n=12) **P<0.003. Unpaired t-test was used. **(B)**. Two-way ANOVA test showed a significant differences between –ve tamoxifen and +ve tamoxifen tissue with ****p value<0.0001.

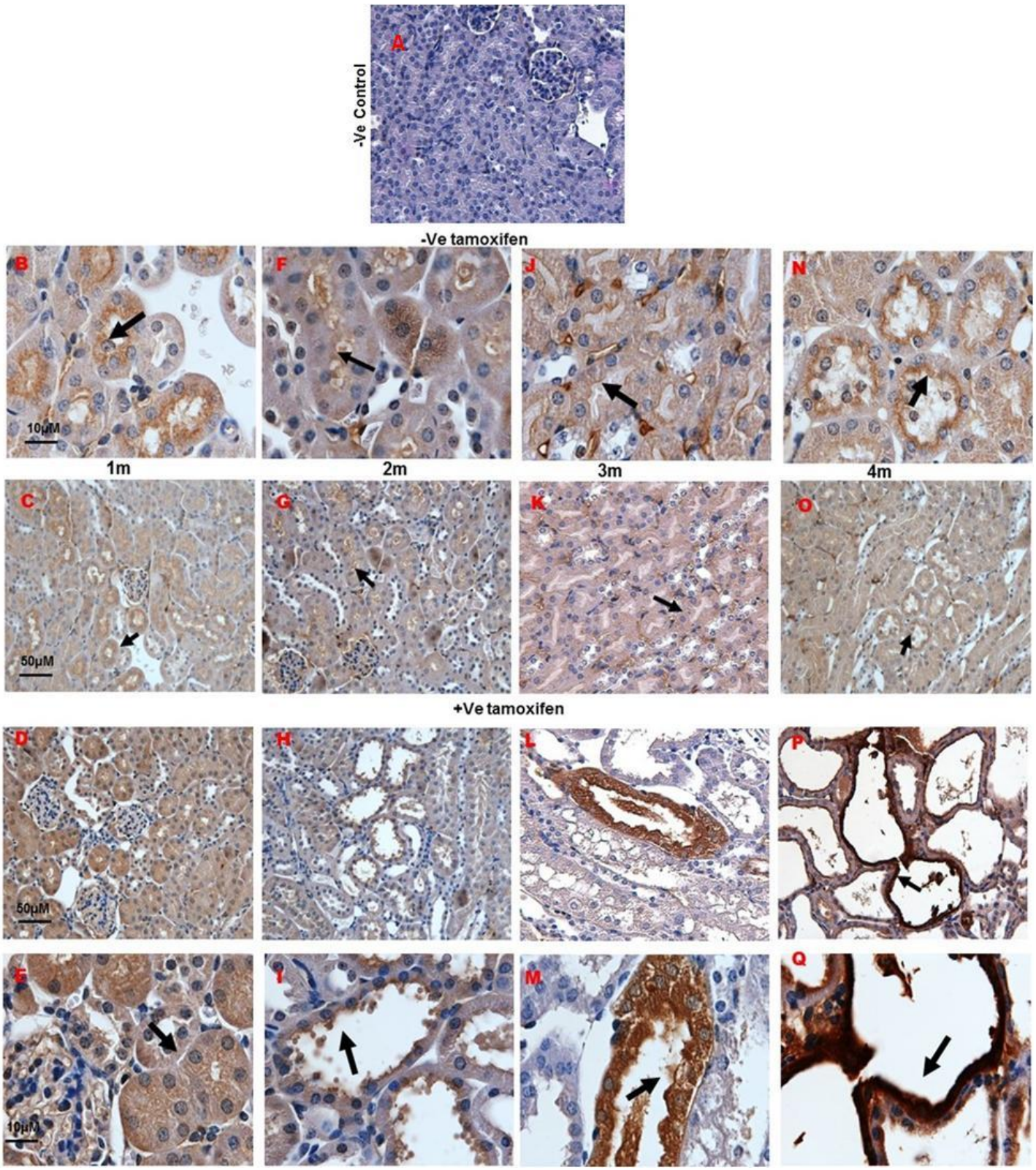
A
-Ve Control
-Ve tamoxifen
B
F
J
N
10μM
1m
2m
3m
4m
C
G
K
O
50μM
+Ve tamoxifen
D
H
L
P
50μM
E
I
M
Q
10μM

Figure 4.14. Expression of PTGER2 in a tamoxifen treated CreLox mouse model of ADPKD

A. No PTGER2 staining was seen in tissue sections incubated with non-immune serum.

B, C, F, G, J, K, N and O. CreLox control mice tissue sections showed weak PTGER2 staining at 1, 2, 3 and 4 months (black arrow).

D, E, H, I, L, M, P and Q CreLox tamoxifen treated mice showed weak PTGER2 staining mainly localised in the tubular epithelial apical surface after 1 month. After 2, 3 and 4 months staining intensity progressively increased at the apical surface of tubular epithelial cells and within the cytoplasm (black arrow).

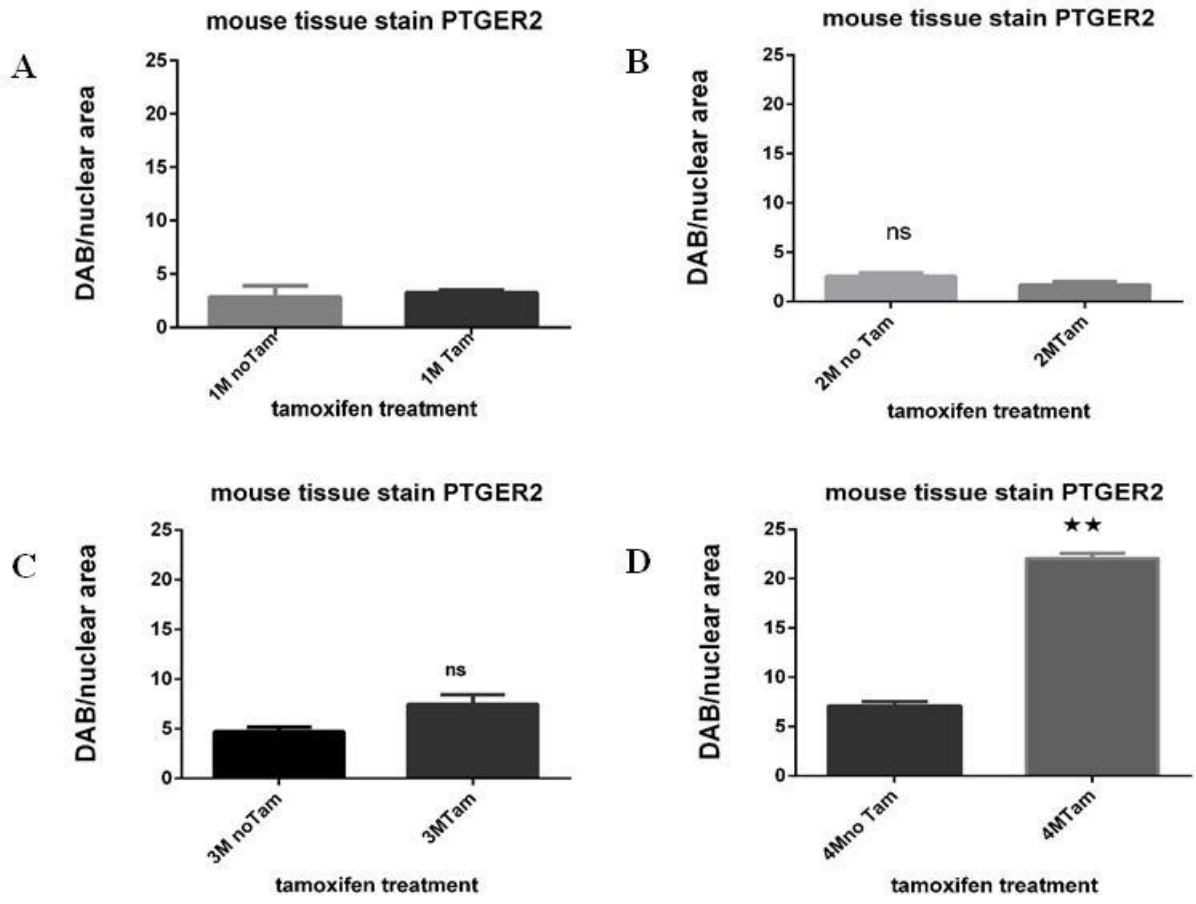

Figure 4.15. Quantification of PTGER2 expression in a tamoxifen treated CreLox mouse model of ADPKD

ImmunoRatio analysis was carried out on tamoxifen treated and untreated CreLox mouse tissue sections.

A. No significant difference in PTGER2 expression was seen after 1 month (n=6). P= 0. 73.

B. No significant difference in PTGER2 expression was seen after 2 month (n=6) P= 0. 219.

C. No significant difference in PTGER2 expression was seen after 3 months (n =6) P= 0. 113.

D. A signifcant increase in PTGER2 expression was seen in tamoxifen treated mice after 4 months(n=6). Unpaired t-test was used. ** P value= 0.002.

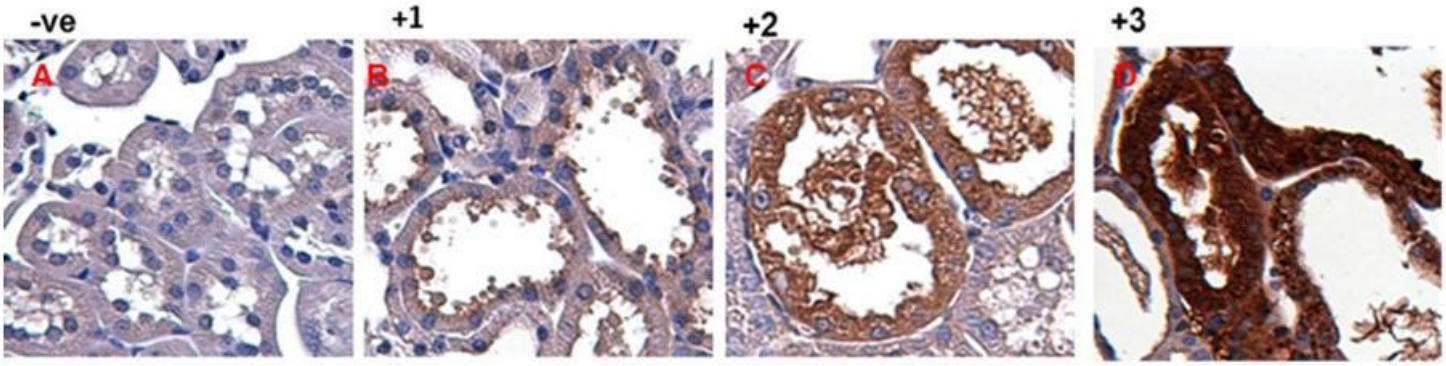
-ve
+1
+2
+3
A
B
C
D

E

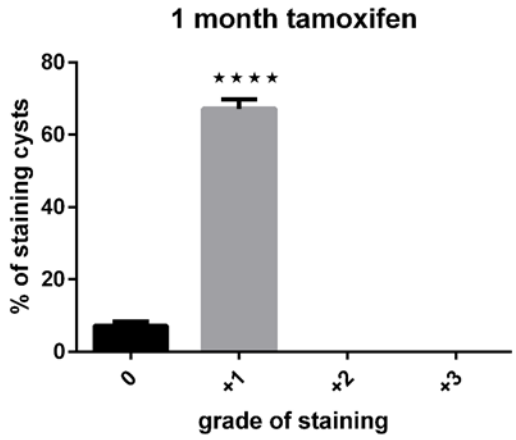
1 month tamoxifen
% of staining cysts
80
60
40
20
0
****
0
×1
×2
×3
grade of staining

F

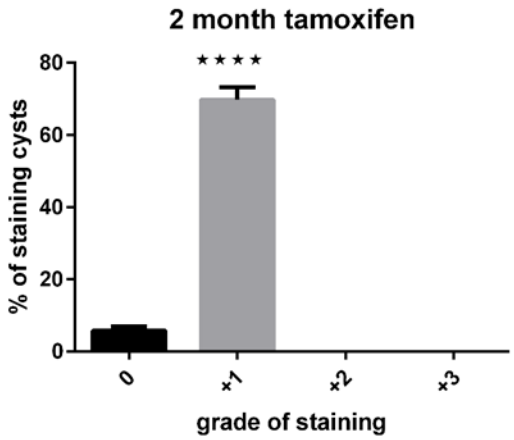
2 month tamoxifen
% of staining cysts
80
60
40
20
0
****
0
×1
×2
×3
grade of staining

G

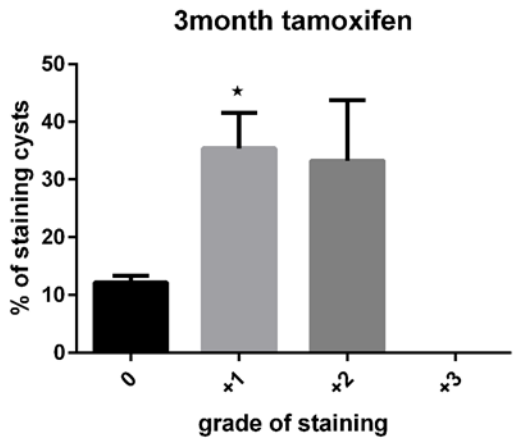
3month tamoxifen
% of staining cysts
50
40
30
20
10
0
*
0
×1
×2
×3
grade of staining

H

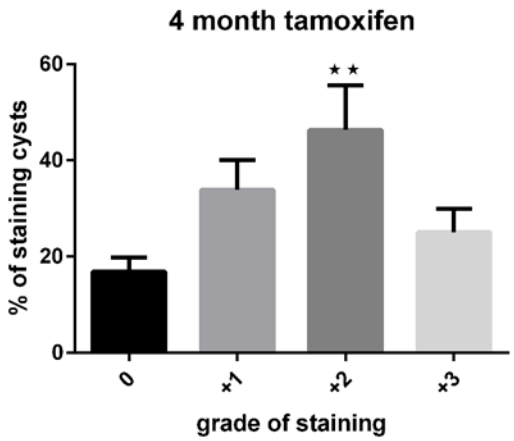
4 month tamoxifen
% of staining cysts
60
40
20
0
**
0
×1
×2
×3
grade of staining

Figure 4.16. Grading PTGER2 staining intensity of tamoxifen treated CreLox mouse tissue sections.

A. PTGER2 staining intensity was graded by intensity level from 0: no staining. **B.** +1: weak staining. **C.** +2: moderate staining **D.** +3: intense staining.

E, F. After 1 and 2 month tamoxifen treatment the majority of positively staining cysts were grades 0 or +1.

G. After 3 months tamoxifen treatment the majority of positively staining cysts were grades +1 or +2.

H. After 4 months tamoxifen treatment the majority of positively staining cysts were grades +1 or +2 with some showing the strongest grade of staining intensity at +3.(n=7). One-way ANOVA test was used. ****$p<0.0001$, **$p<0.01$, *$p<0.05$

4.3.6. PTGER4 expression in a tamoxifen-inducible, kidney epithelium-specific Pkd1-deletion mouse model.

Immunohistochemistry of tamoxifen treated and untreated tissue sections with a specific rabbit PTGER4 antibody staining was carried out. As with PTGER2 expression, PTGER4 staining was localised mainly to the apical surface with weak cytoplasmic and no nuclear staining. PTGER4 staining was similar in both treated and untreated mouse tissue sections at 1, 2, 3 and 4 months **(Figure 4.17).** Staining intensity was graded as previously described due to the variable and patchy staining in tubules and cysts **(Figure 4.18)**. Grade 1 weak apical staining was commonly seen in the treated and untreated mouse tissue at each time point (**Figure 4.18 E, F, G and H)**. Grade 2 staining was seen mainly in third, and fourth months treated mice tissue (**Figure 4.18 G, H)**. Grade 3 staining was seen in the fourth month of both the treated and untreated mice tissue, and less frequently in second, and third month treated mice tissue. (**Figure 4.18 F, G and H).**

In conclusion, PTGER2 staining in a tamoxifen-inducible, kidney epithelium-specific Pkd1-deletion mouse model was significantly increased over treated animals. This was also the case when intensity of PTGER2 staining was considered. The highest intensity (grades 2 and 3) were seen exclusively in treated animals. PTGER4 staining however was seen in both treated and untreated animals and no significant difference was demonstrated.

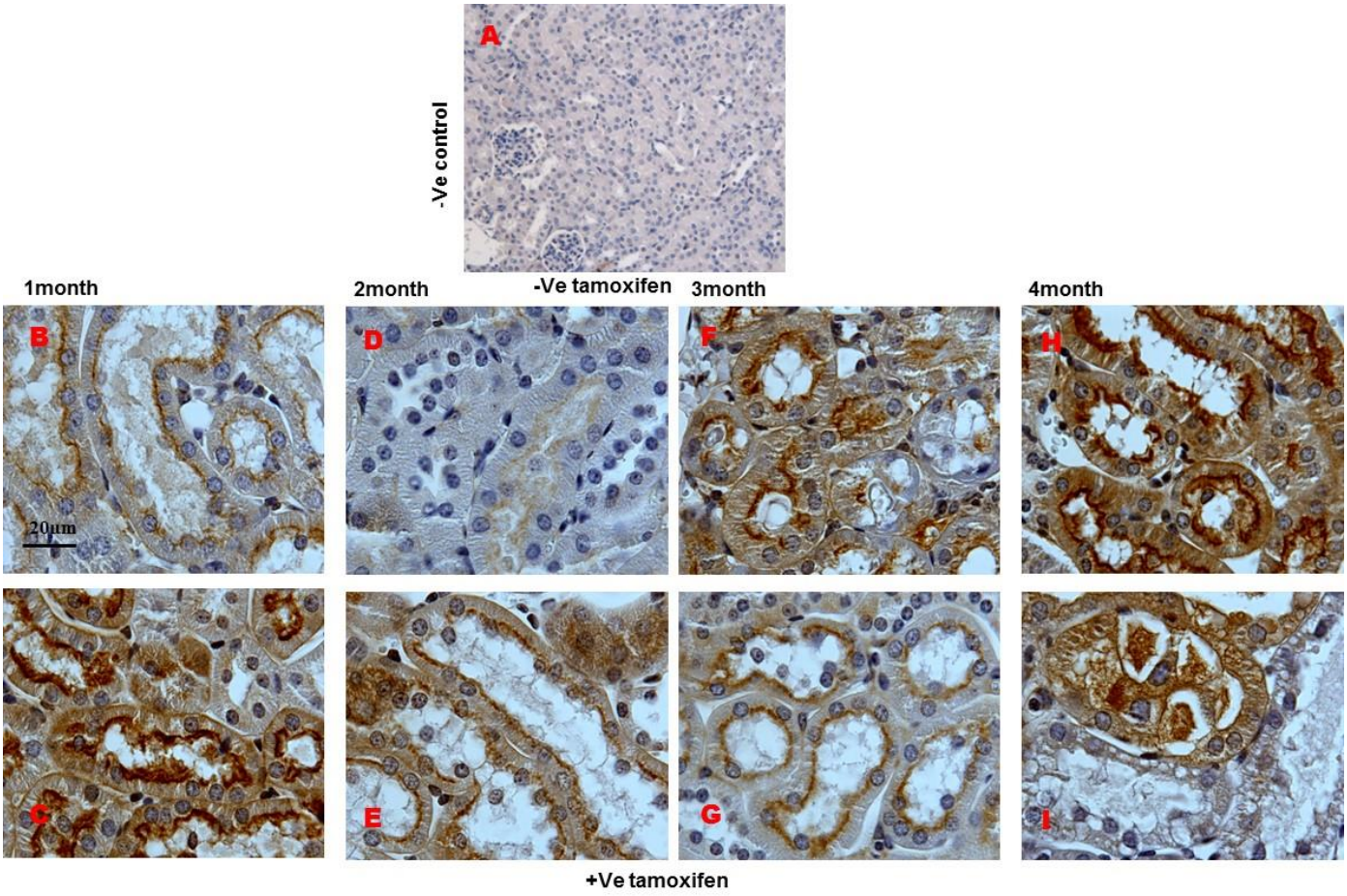

Figure 4.17. Expression of PTGER4 in a tamoxifen treated CreLox mouse model of ADPKD

A. No PTGER4 staining was seen in tissue sections incubated with non-immune serum.

B, D, F and H. CreLox control mice tissue sections showed weak PTGER4 staining at 1 and 2 months which increased in intensity at 3 and 4 months mainly localised to the apical tubular surface with some cytoplasmic staining.

C, E, G and I. CreLox tamoxifen treated mice showed strong PTGER4 staining mainly localised in the tubular epithelial apical surface with some cytoplasmic staining after 1, 2, 3 and 4 months.

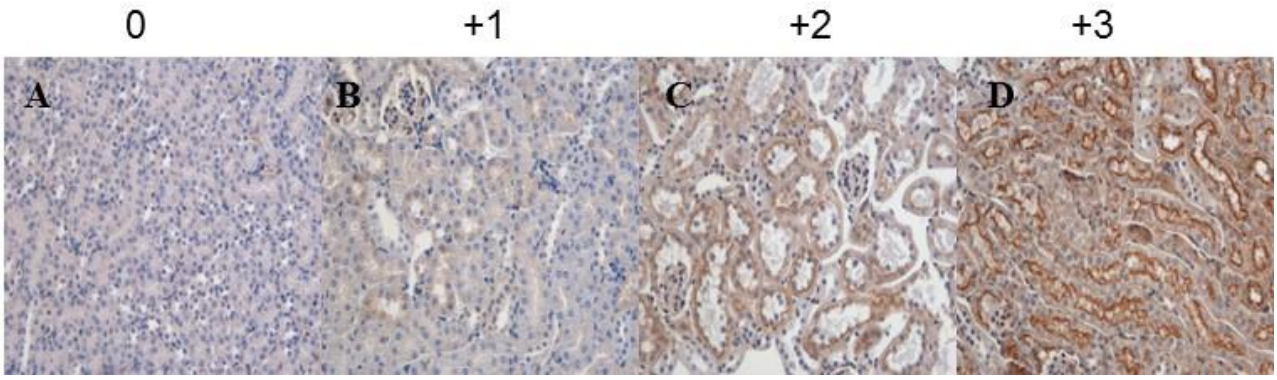
0
+1
+2
+3
A
B
C
D

E

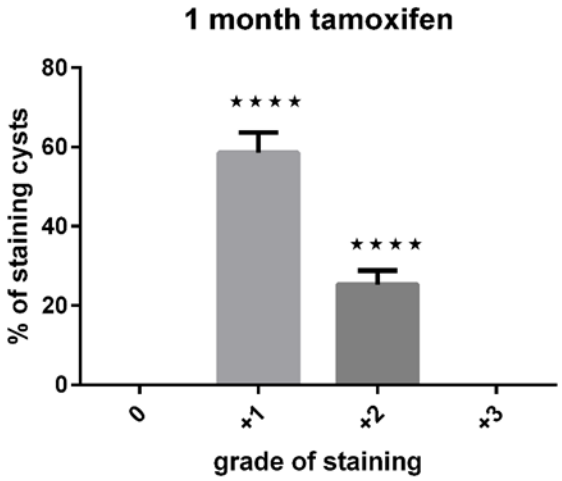
1 month tamoxifen
% of staining cysts
80
60
40
20
0
★★★★
★★★★
0
+1
+2
+3
grade of staining

F

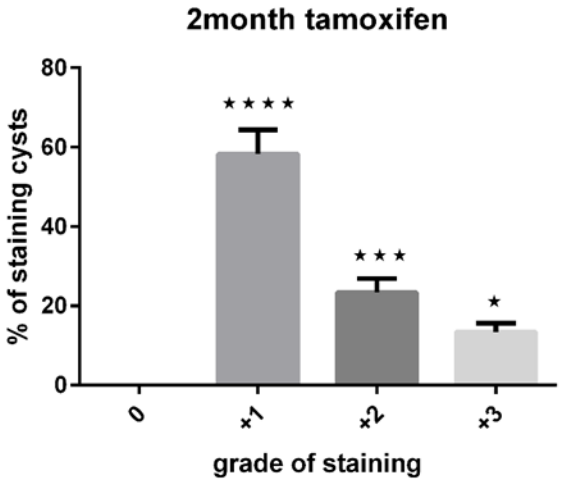
2month tamoxifen
% of staining cysts
80
60
40
20
0
★★★★
★★★
★
0
+1
+2
+3
grade of staining

G

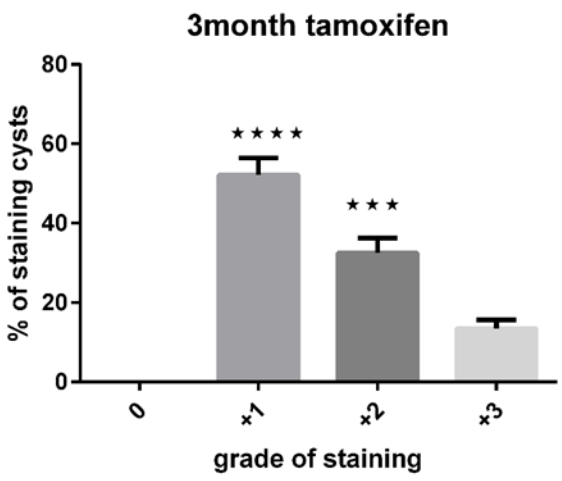
3month tamoxifen
% of staining cysts
80
60
40
20
0
★★★★
★★★
0
+1
+2
+3
grade of staining

H

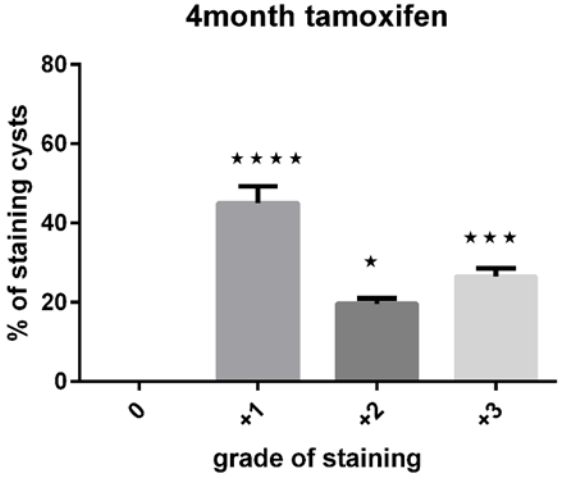
4month tamoxifen
% of staining cysts
80
60
40
20
0
★★★★
★
★★★
0
+1
+2
+3
grade of staining

Figure 4.18. Grading PTGER4 staining intensity of tamoxifen treated CreLox mouse tissue sections.

A. PTGER4 staining intensity was graded by intensity level from 0: no staining. **B.** +1: weak staining. **C.** +2: moderate staining **D.** +3: intense staining.

E, F, G. After 1, 2 and 3 months tamoxifen treatment the majority of positively staining cysts were grade +1 or +2 with a small number of cyst staining grade 3 after 2 and 3 months.(n=7). **H.** After 4 months tamoxifen treatment the majority of positively staining cysts were grade +1 or +2 with a larger proportion at grade +3. One way ANOVA test was used. A significant differences between 0 grade and each grade of staining ****$p<0.0001$. ***$p<0.001$. *$p<0.05$. Data presented as mean± SEM.

4.3.7. PTGER2 expression in a orthologous Pkd1 (nl,nl) mouse model.

There was a significant increase in cyst area in tamoxifen-treated mice compared with untreated animals. The Pkd1 (nl,nl) sections showed a significant increase in cyst area compared to wild-type as represented by average percent of cyst area (wild=4504± 817 vs. PKD=17072±1001%, n=6) ***P<0.0006 **(Figure 4.19).**

Immunohistochemistry of tissue sections with a specific mouse PTGER2 antibody was carried out. Staining with PTGER2 was seen in all sections localised mainly to the apical surface within tubules with some cytoplasmic but no nuclear staining **(Figure 4.20 A, B).** A significant increase in PTGER2 expression was seen in Pkd1 (nl,nl) tissue sections compared to wild type, as represented by the average percentage of DAB/nuclear area (wild=3.730±787, n=10 vs. PKD= 8.525± 2.878%, n=10)*P<0.0263 **(Figure 4.20 C).** In contrast to the tamoxifen-inducible, kidney epithelium-specific Pkd1-deletion mouse model, PTGER2 staining was observed in the majority of cysts and was uniform in intensity.

4.3.8. PTGER4 expression in a orthologous Pkd1(nl,nl) mouse model.

Immunohistochemistry of tissue sections with a specific rabbit PTGER4 antibody was carried out. Staining with PTGER4 was seen in all sections localised mainly to the apical surface within tubules with some cytoplasmic but no nuclear staining. **(Figure 4.21 A, B).** A significant increase in PTGER4 expression was seen in Pkd1(nl,nl) tissue sections compared to wild type, as represented by the average percentage of DAB/nuclear area, as represented by the average percentage of DAB/nuclear area (wild=1.9±0.137, n=10 vs. PKD=30.87±2% n=10)***P<0.0001 (**Figure 4.21 C).** In contrast to the tamoxifen-inducible, kidney epithelium-specific Pkd1-deletion mouse model, PTGER4 staining was observed in the majority of cysts and was uniform in intensity.

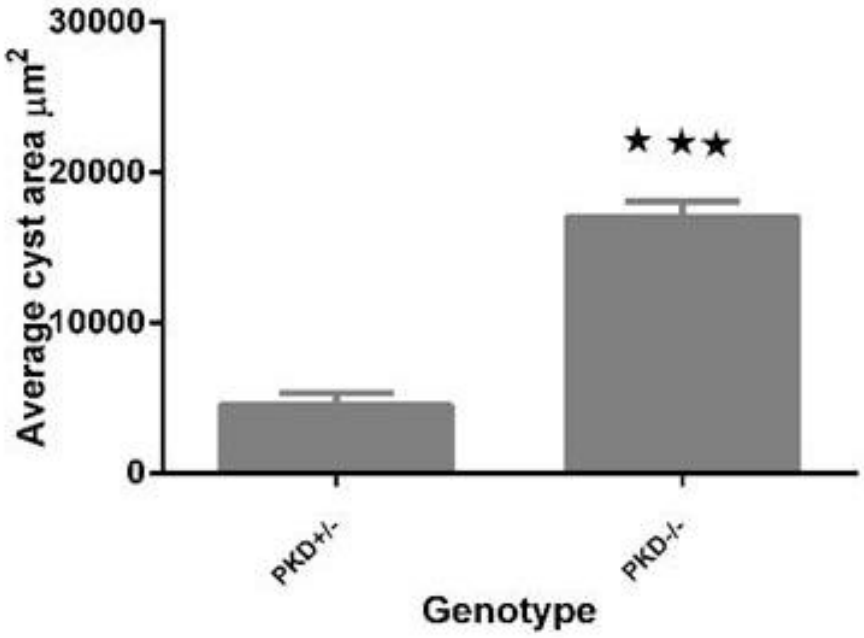

Figure 4.19. Average cyst area in a NeoLox mouse ADPKD model

A significant increase in average cyst area was observed in mouse NeoLox tissue sections compared to controls (n=6). Unpaired t-test was used. Data presented as mean± SEM. ***P<0.0006.

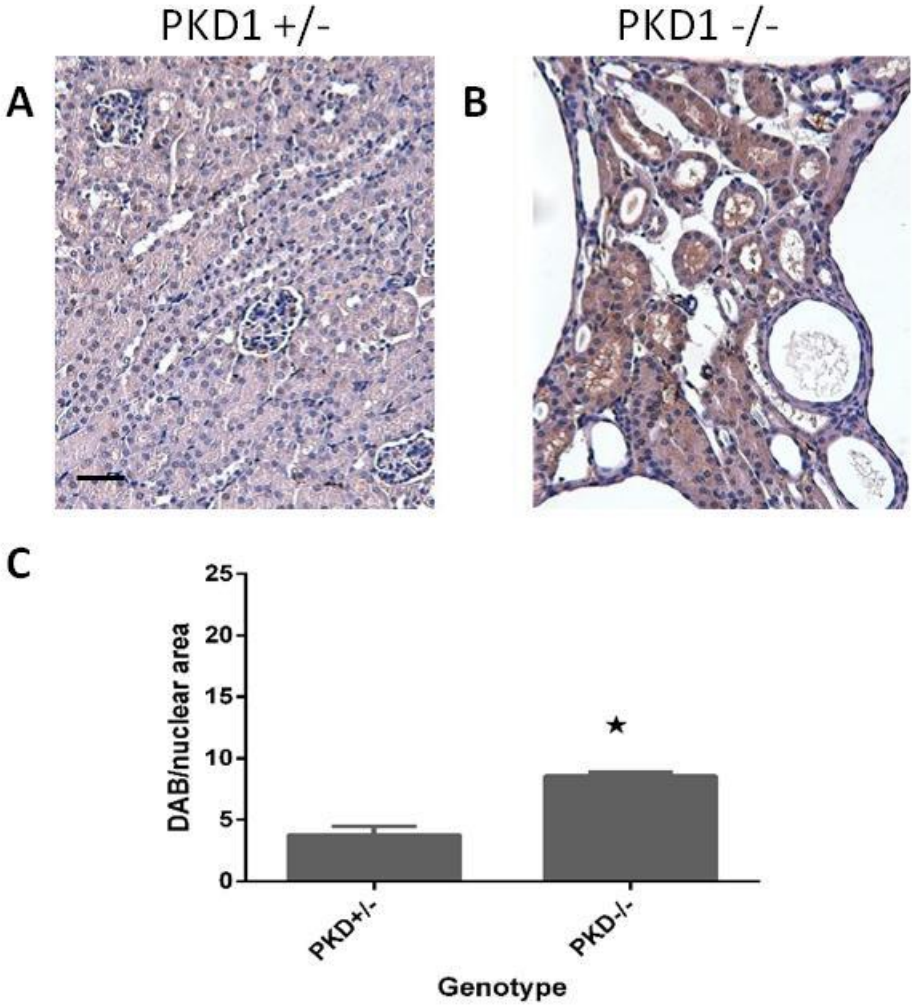

Figure 4.20. Immunohistochemistry of NeoLox mouse kidney tissue sections with an antibody to PTGER2

(A).Control mouse kidney sections showed weak staining at the apical surface in normal tubules.

(B).Strong staining for PTGER2 was seen in the cyst lining epithelium in PKD1 -/- NeoLox mouse tissue sections. Scale bar = 50 µm.

(C). ImmunoRatio analysis showed a significant increase in PTGER2 staining in PKD1 -/- sections (n=10). Unpaired t-test was used. *P<0.0263. Data presented as mean± SEM.

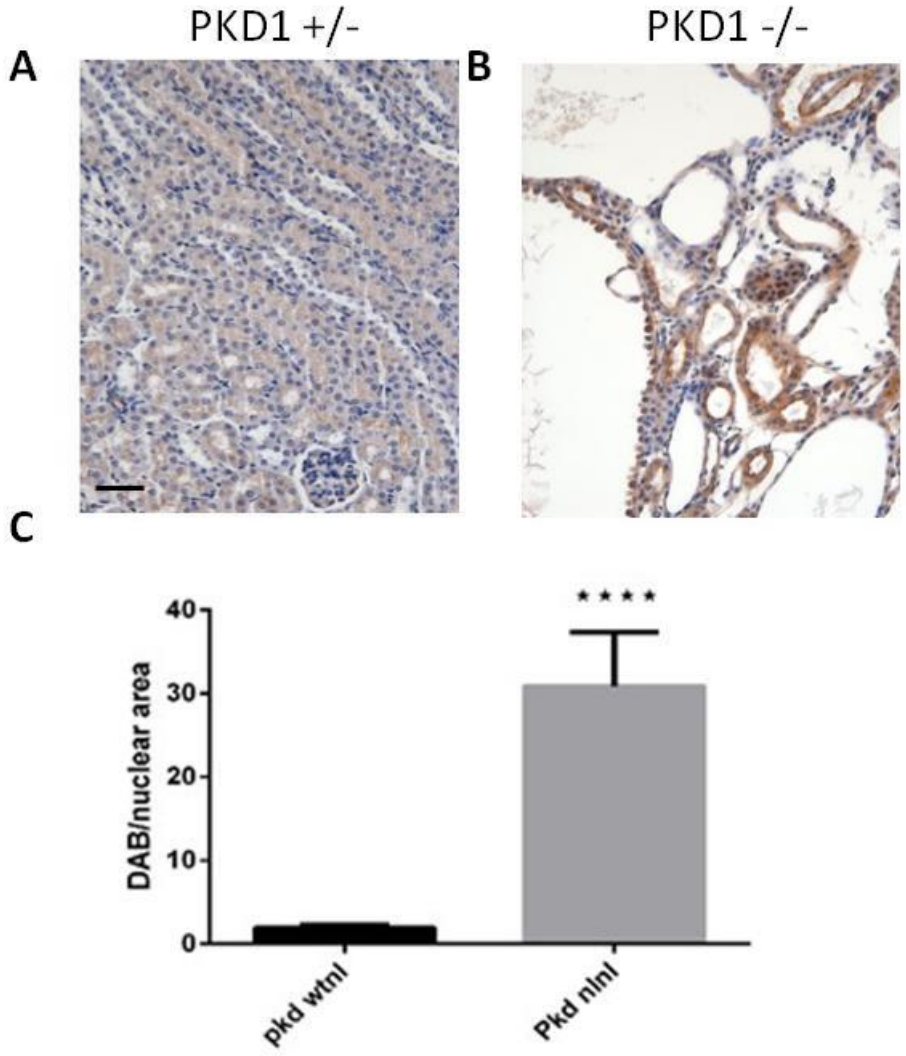

Figure 4.21. Immunohistochemistry of NeoLox mouse kidney tissue sections with an antibody to PTGER4.

(A).Control mouse kidney sections showed weak staining at the apical surface in normal tubules.

(B).Strong staining for PTGER4 was seen in the cyst lining epithelium in PKD1 -/- NeoLox mouse tissue sections. Scale bar = 50 µm

(C). ImmunoRatio analysis showed a significant increase in PTGER4 staining in PKD1 -/- sections compared to controls (n=10). Unpaired t-test was used. $^{**}P<0.001$. Data presented as mean± SEM**.**

4.4. Discussion

The major aim of this chapter was to determine the expression levels of PTGER receptors especially PTGER2 and PTGER4 in human and mouse models of ADPKD. There is evidence in the literature that levels of PTGER receptors as well as the ligand PGE2 may be increased in ADPKD. As such, these receptors may represent a novel therapeutic target.

A study of oxidative stress and endothelial dysfunction in ADPKD showed an increase in prostaglandins including prostaglandin PGF2α, PGD2, and PGE2 in patients with ADPKD patients compared to healthy controls (Klawitter, Reed-Gitomer et al. 2014). Furthermore, there were an increased levels of PGE1, PGE2, vasopressin and cAMP in cystic fluid from ADPKD cells compared to normal kidney cells (Ye, Grant et al. 1992). Adenylyl cyclase agonists such as epinephrine, PGE2, AVP and adenosine increase intracellular cAMP which stimulates proliferation and fluid secretion in ADPKD and ARPKD (Belibi, Reif et al. 2004).

Previous studies have shown that exogenous treatment with PGE2 increased proliferation and fluid secretion in PC1-deficient IMCD3 cells. This effect was mainly through stimulation of PTGER4 receptors which stimulate the β-catenin pathway (Liu, Rajagopal et al. 2012). Other studies have revealed an increased level of PTGER2 and PTGER4 in ADPKD and liver tumour cells (Elberg, Elberg et al. 2007, Elberg, Turman et al. 2012, Xia, Ma et al. 2014). Elberg et al found that PGE2 stimulates cystogenesis in an ADPKD model through the PTGER2 receptor (Elberg, Elberg et al. 2007). Turman and Elberg, discovered that PGE2 stimulates cystogenesis through the PTGER4 receptor in mouse IMCD-3cells (Elberg, Elberg et al. 2007; Elberg, Turman et al. 2012). Increased PTGER4 receptors stimulate tumour growth in hepatocellular carcinoma (Xia, Ma et al. 2014). Another study established that PTGER2 and PTGER4 receptors stimulate tumour growth in colorectal carcinoma (Hawcroft, Ko et al. 2007). PTGER2 receptors have been localised by *in-situ* hybridization in both rabbit and human

kidneys. It was revealed that PTGER2 mRNA expression was localised in glomeruli and medullary collecting ducts of rabbit kidneys (Breyer, Davis et al. 1996, Guan, Stillman et al. 2002). It was also found that PTGER2 mRNA was increased more in the cystic epithelial cells than in normal tubular cells (Elberg, Elberg et al. 2007).

A preliminary study in our laboratory (conducted by Dr Andrew Streets) isolated mRNA from a panel of human cell lines derived from patients with ADPKD and analysed gene expression by microarray. This study identified over 2300 genes which were significantly altered in ADPKD compared to controls. The PTGER2 receptor was shown to be significantly increased in human ADPKD cells **(Figure 4.1)**. I was able to confirm this finding by qPCR on the same cells. In contrast, the other three receptors PTGER1, PTGER3, and PTGER4 were not significantly increased in either the microarray or qPCR assays **(Figure 4.2)**.

Furthermore, I was able to detect the PTGER2 receptors by western blotting using a mouse monoclonal antibody. There was a significant increase in PTGER2 receptors in the cystic cell line (OX161/C1) compared to the normal cells (UCL93). This result was quantified by densitometry **(Figure 4.7 A, B**). These findings confirm the previous finding of increased PTGER2 in cystic epithelial cells (Elberg, Elberg et al. 2007). In contrast to the human data I found that both PTGER2 and PTGER4 mRNA were increased in two orthologous mouse models of ADPKD. Immunohistochemistry of the cystic tissues of human and two mouse models showed a significant increase in PTGER2 receptor expression in cystic tissue compared to control tissue, PTGER2 expression was localised mainly on the apical side of tubules in human and mouse tissue **(Figure. 4.11, 4.14, 4.15 and 4.20)**.

By contrast, expression of PTGER4 was not significantly increased in human ADPKD cell lines as determined by microarray, qPCR or western blotting **(Figure 4.1. 4.2 and 4.8).** Immunohistochemistry also showed no significant difference in PTGER4 expression between

cystic and normal tissue **(Figure 4.12)**. However in both mouse models of ADPKD a significant increase in PTGER4 mRNA was seen by qPCR. Increases in PTGER4 expression in mouse tissue were also clearly seen by immunohistochemistry analysis in contrast to human tissue sections **(Figure 4.4 and 4.21).**

Both PTGER2 and PTGER4 receptors are G-protein coupled receptors that activate the G protein G_S, leading to stimulation of Adenylyl cyclase and increasing the level of intracellular cAMP, and finally it the β-catenin pathway (Liu, Rajagopal et al. 2012). These changes result in increased proliferation and fluid secretion (Fujino, Salvi et al. 2005). However, recent studies have shown functional differences between the PTGER2 and PTGER4 mediated signalling pathways. Firstly, PTGER4 is a larger protein than the PTGER2 (488 versus 358 amino acid). Secondly, PTGER4, but not the PTGER2, can stimulate the expression of early growth response-1 (EGR-1) through activation of the PI3K pathway and ERK signalling (Fujino, Xu et al. 2003). Unlike PTGER2 that acts only on the Gs protein (Fujino and Regan 2006), PTGER4 couples with both Gs and Gi (pertussis toxin-sensitive Gαi) and stimulates the phosphatidylinositol 3 kinase, which inhibits cAMP signalling and stimulates ERK (Fujino and Regan 2006). Thirdly, PTGER4 has a longer intracellular carboxyl terminal than PTGER2 (155 versus 34 amino acid) that can act as phosphorylation sites for PKA and GRK (G-protein receptor kinase) leading to β-arrestin binding (Yokoyama, Iwatsubo et al. 2013). PTGER4 but not PTGER2 undergoes agonist-induced desensitization (Nishigaki, Negishi et al. 1996) and internalization (Desai, April et al. 2000).

The magnitude of PGE2 induced activation of cAMP in PTGER2 expressing cells is greater than (80%) of that observed in PTGER4 expressing cells (Fujino, Xu et al. 2003). Another important point is that the distribution and function of EP receptors are not identical and can be species-dependent (Virgolini, Muller et al. 1988, Larsen, Hansen et al. 2005). A recent study suggested the main receptor of PGE2 that led to an increase in proliferation of mouse cells

(IMCD3) is the PTGER4 receptor, and when antagonised this receptor may have a therapeutic role in murine ADPKD (Elberg, Turman et al. 2012). This indicates that human cells may act differently from animal cells regarding the response to the PTGER2 and PTGER4 receptors. Since PTGER2 and PTGER4 antagonists have highly specific actions and potentially fewer side effects, it is possible that they could be of therapeutic benefit in ADPKD (Zimecki 2012).

Chapter 5

Effect of PTGER 2 and 4 receptor antagonists in cell culture models of ADPKD

5.1. Introduction

The aim of this chapter was twofold. Firstly to investigate the role of cAMP and PGE2 on ADPKD cyst formation and secondly to explore the potential of PTGER2 and 4 antagonists as a novel therapeutic approach in cell models of ADPKD.

Previously, a PTGER2 antagonist (AH-6809) has been used to block PTGER2 receptor function. However this antagonist has poor selectivity and affinity for the PTGER2 receptor (Abramovitz, Adam et al. 2000). Furthermore, it has unknown *in vivo* effects which makes the transition from *in vitro* to *in vivo* model experiments challenging (Abramovitz, Adam et al. 2000).

In this chapter, a new PTGER2 selective antagonist (PF-04418948) developed by Pfizer, was used to inhibit the effect of PGE2 *in vitro*. This compound exhibits a 2000-fold functional selectivity for human PTGER2 over other PTGER receptors (PTGER1, PTGER3 and PTGER4) and prostanoids (CRTH2, DP1, FP, TP and IP) receptors, The IC_{50} value is 16 nM for PTGER2, while for human PTGER1 and PTGER3 the IC_{50} is >10,000Nm The PTGER4 IC_{50} is >33,300 nM. Additionally, it has little activity against a panel of other ion channels and GPCRs even at high concentrations. It acts via competitive inhibition for PGE2 binding (af Forselles, Root et al. 2011, Birrell and Nials 2011). In previous studies PF-04418948 was able to block the effect of PGE2 and the PTGER2 agonist butaprost in an *in vitro* study on human myometrium, animal smooth muscles (dog bronchi, mouse tracheas) and *in vivo* in rats after oral administration (af Forselles, Root et al. 2011).

A second antagonist used in this study was the PTGER4 antagonist, CJ-042794 from Pfizer (Murase, Taniguchi et al. 2008). This compound exhibited a 200-fold functional selectivity for human PTGER4 compared to PTGER1, PTGER2, and PTGER3. Furthermore, it did not show any binding activity against a panel of 65 other proteins including ion channels, transporters

and GPCRs even at high concentration (10μM). CJ-042794 acts mainly through competitive inhibition of PTGER4. It inhibited PGE2 mediated cAMP accumulation with an IC_{50} of 500nM (Murase, Taniguchi et al. 2008). The rodent PTGER4 receptor is highly homologous to the human PTGER4 receptor, therefore, CJ-042794 could serve as useful agent for investigating the physiological role in PTGER4 receptor in the rat (Murase, Taniguchi et al. 2008).

I studied the effect of these two antagonists on cystic and normal human cells and MDCKII cytogenesis in cyst assays. In addition, their effect on proliferation and apoptosis was investigated. Finally, I measured cAMP levels in both cystic and normal human cells, and investigated the effect of PTGER2, and PTGER4 antagonists on cAMP levels.

5.2. Aims and objectives:

1. Test the effect of PGE2, PTGER2, and PTGER4 receptor antagonists on proliferation and apoptosis in control and ADPKD kidney epithelial cell lines.
2. Test the effect of PGE2, PTGER2, and PTGER4 receptor antagonists on cyst growth in control and ADPKD kidney epithelial cell lines.
3. Compare cAMP levels in control and ADPKD kidney epithelial cell lines incubated with PTGER2, and PTGER4 receptor antagonists.

5.3. Results.

5.3.1. The effect of PGE2 on the proliferation of ADPKD and control kidney epithelial cell lines.

Using cell lines derived from ADPKD patients, we aimed to determine whether PGE2 contributed to the hyper-proliferative phenotype of ADPKD renal epithelial cells, a consistent feature of cyst pathogenesis. Four ADPKD cell lines (OX161/C1, OX938, OX161 and SKI-001) and two control cell lines (UCL93, and RFH) were used in these experiments.

The effect of PGE2 on proliferation of ADPKD and control cell lines was determined using two separate assays, an MTS cell viability assay and a BrdU cell proliferation ELISA Assay.

MTS is a widely used assay of cell number and viability. It measures cell metabolic activity by the reduction of yellow tetrazolium MTS (3-(4, 5-dimethylthiazolyl-2)-2, 5-diphenyltetrazolium bromide) salt to purple formazan that can be quantified using a colorimetric method. At the time of the assay, cells looked healthy and viable with no evidence of cell toxicity under the microscope.

The second proliferation test used a BrdU proliferation assay kit. It measures DNA synthesis by detecting 5-bromo-deoxyuridine (BrdU) incorporated into newly synthesised cellular DNA using an anti-BrdU antibody. The BrdU-labeled DNA detected by BrdU mouse Ab does not cross-react with endogenous DNA.

Cells were treated with PGE2 (25, 50, 100 nM) for 72 h prior to each assay. A significant increase in proliferation was seen in three ADPKD cell lines (OX161/C1, OX161 and SKI-001) treated with PGE2 **(Figure 5.1A)**. In contrast, PGE2 had no significant effect or inhibited proliferation in control cell lines and surprisingly, in one ADPKD cell line (OX938).

After 72 hours of incubation with different PGE2 concentrations, ADPKD cells showed a significant increase in proliferation at a concentration of 50nM PGE2 in all four ADPKD cell

lines (OX161/C1, OX161, SKI-001 and OX938) **(Figure 5.2 A).** In control cell lines (UCL93, RFH), PGE2 inhibited proliferation at the same concentrations **(Figure 5.2 B)**. These findings are comparable to those described by Yu Liu, and Yamaguchi *et al* (Yamaguchi, Pelling et al. 2000) (Rajagopal, Thomas et al. 2014).

These results demonstrated that PGE2 selectively increased proliferation of ADPKD cell lines compared to control cell lines presumably as a result of the increased levels of PTGER2 receptors present in ADPKD cells described in chapter 4.

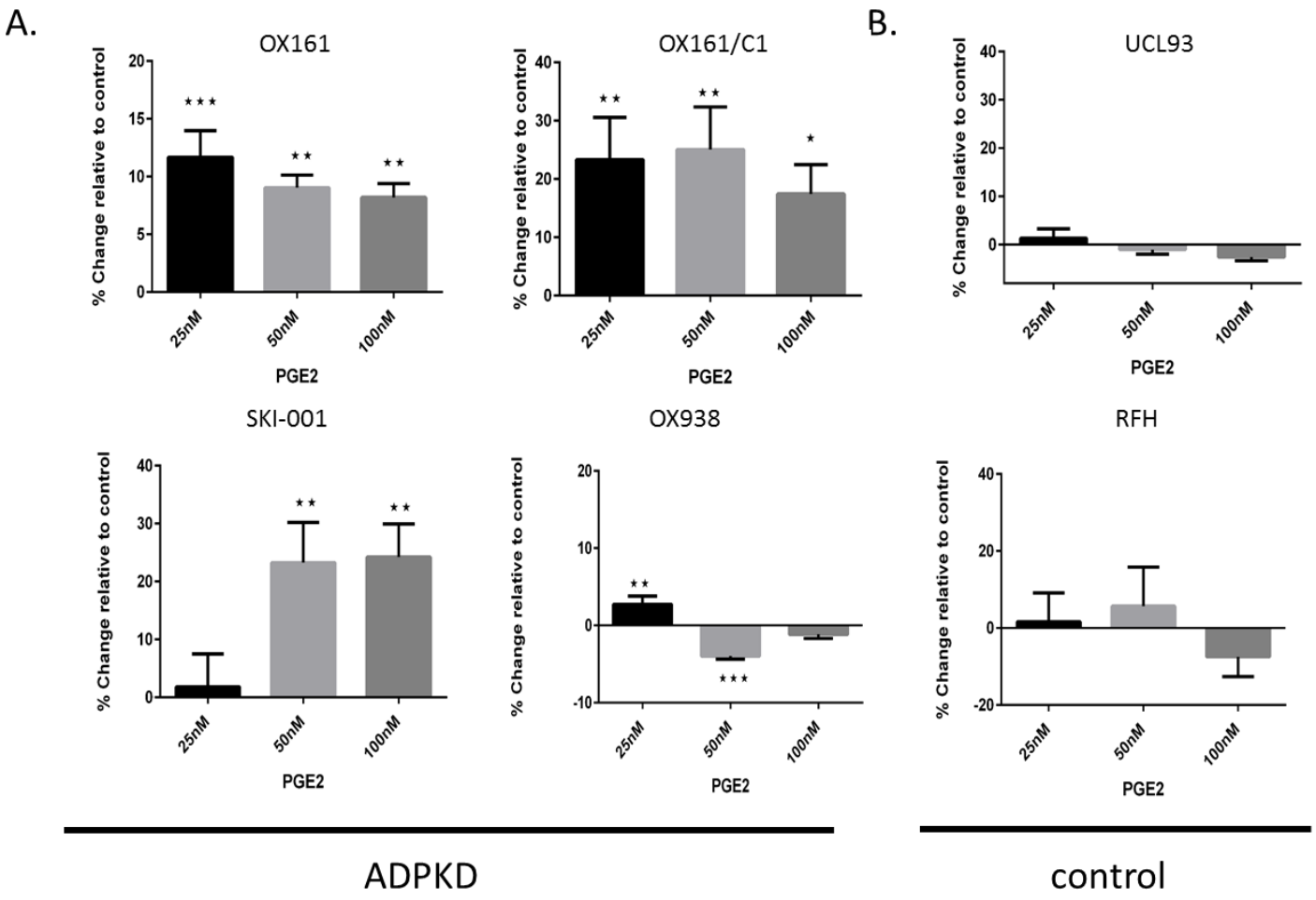

Figure 5.1. Effect of PGE2 on ADPKD cell proliferation (MTS assay)

(A). There was a significant increase in viable cell number as measured by MTS assay after 72 hours in OX161, OX 161/C1 and SKI-001 ADPKD cell lines (n=3) following stimulation with 50 nM PGE2. PGE2 decrease proliferation of OX938 cells at higher doses (50-100nM). One-way ANOVA was used. *$p<0.05$; **$p<0.01$. Data presented as mean± SEM

(B). PGE2 did not cause an increase in viable cell number as measured by MTS assay in control cells. Experiments are representative of 3 separate repeats. Control is DMSO treated cells.

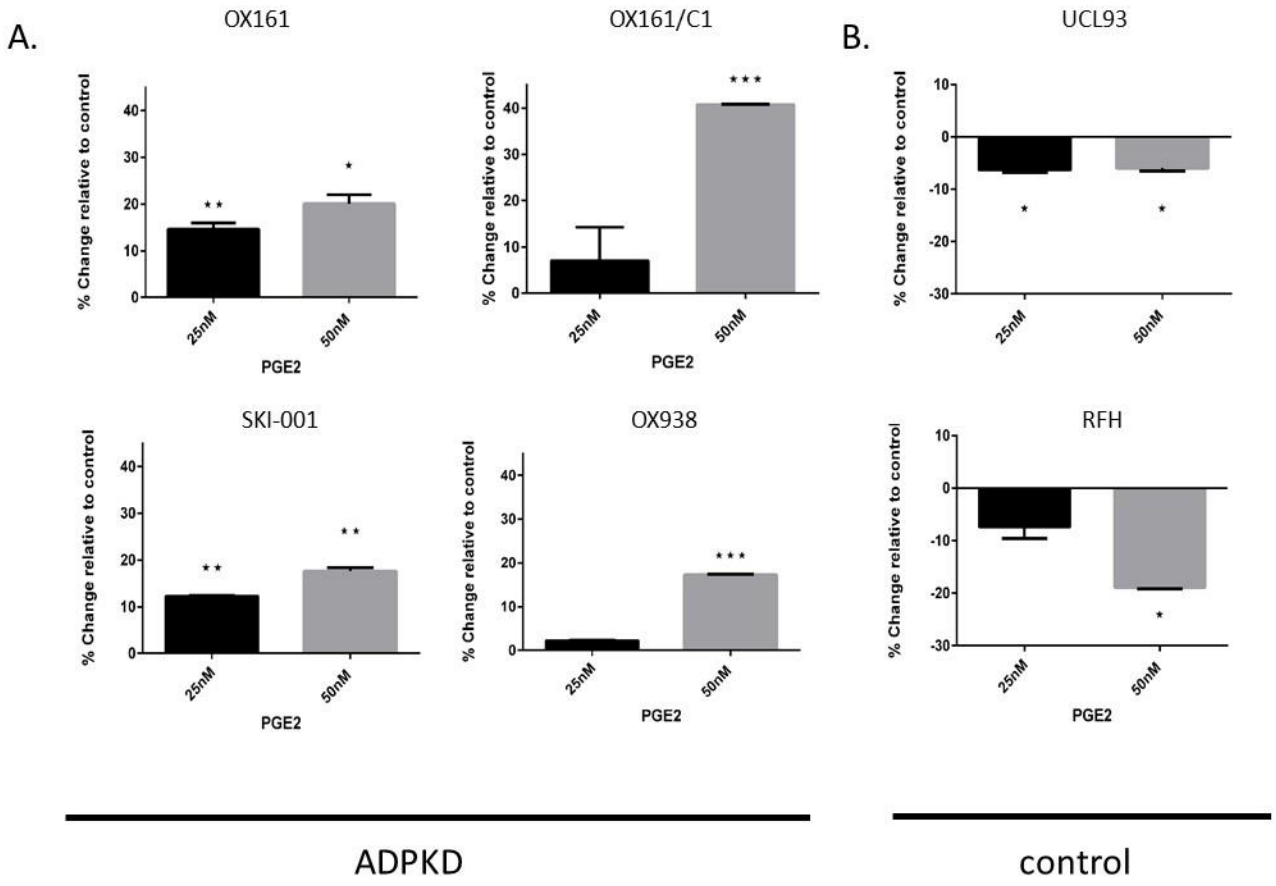

Figure 5.2. Effect of PGE2 on ADPKD cell proliferation (BrdU Elisa).

(A). There was a significant increase in viable cell number as measured by BrdU Elisa assay in OX161, OX161/C1, SKI-001 and OX938 ADPKD cell lines.(n=3), following stimulation with 50 nM PGE2 for 72 hours. Unpaired t-test was used. *p<0.05; **p<0.01, ***p<0.001. Data presented as mean± SEM

(**B**).PGE2 caused a significant decrease in viable cell number as measured by BrdU Elisa assay in control cells. Experiments are representative of 3 separate repeats. Control is DMSO treated cells.

5.3.2. The effect of a PTGER2 antagonist on the proliferation of ADPKD and control kidney epithelial cell lines.

Following the observation that PGE2 selectively stimulates proliferation of ADPKD cell lines, we hypothesised that incubation with a selective PTGER2 receptor antagonist (blocking the action of endogenous PGE2) would have the opposite effect. Cells were treated with three different concentrations of PTGER2 antagonist (100 nM, 500 nM and 1 μM) and were incubated for 72 hours before analysis. PTGER2 antagonist treatment significantly inhibited the proliferation of ADPKD cell lines (OX16/1C1, OX938, OX161 and SKI-001) mainly at concentrations of 500 nM and 1μM **(Figure 5.3 A).** In control cell lines however there was no significant decrease in proliferation when treated with PTGER2 antagonist (500nM- 1μM) **(Figure 5.3 B).**

A second proliferation assay was carried out using a BrdU proliferation ELISA. Incubation with PTGER2 antagonist (500 nM and 1 μM) significantly inhibited proliferation of three ADPKD cell lines (OX161/C1, OX161 and OX938) at a concentration of 500 nM or more **(Figure 5.4 A).** By contrast, in the normal cell lines (UCL93, RFH) there was a small but non-significant decrease in proliferation when cells were treated with the PTGER2 antagonist at the same concentrations **(Figure 5.4 B).** In summary, these results indicate that the PTGER2 antagonist selectively inhibits the proliferation of ADPKD cell lines compared to control cell lines, probably by blocking the action of endogenous PGE2.

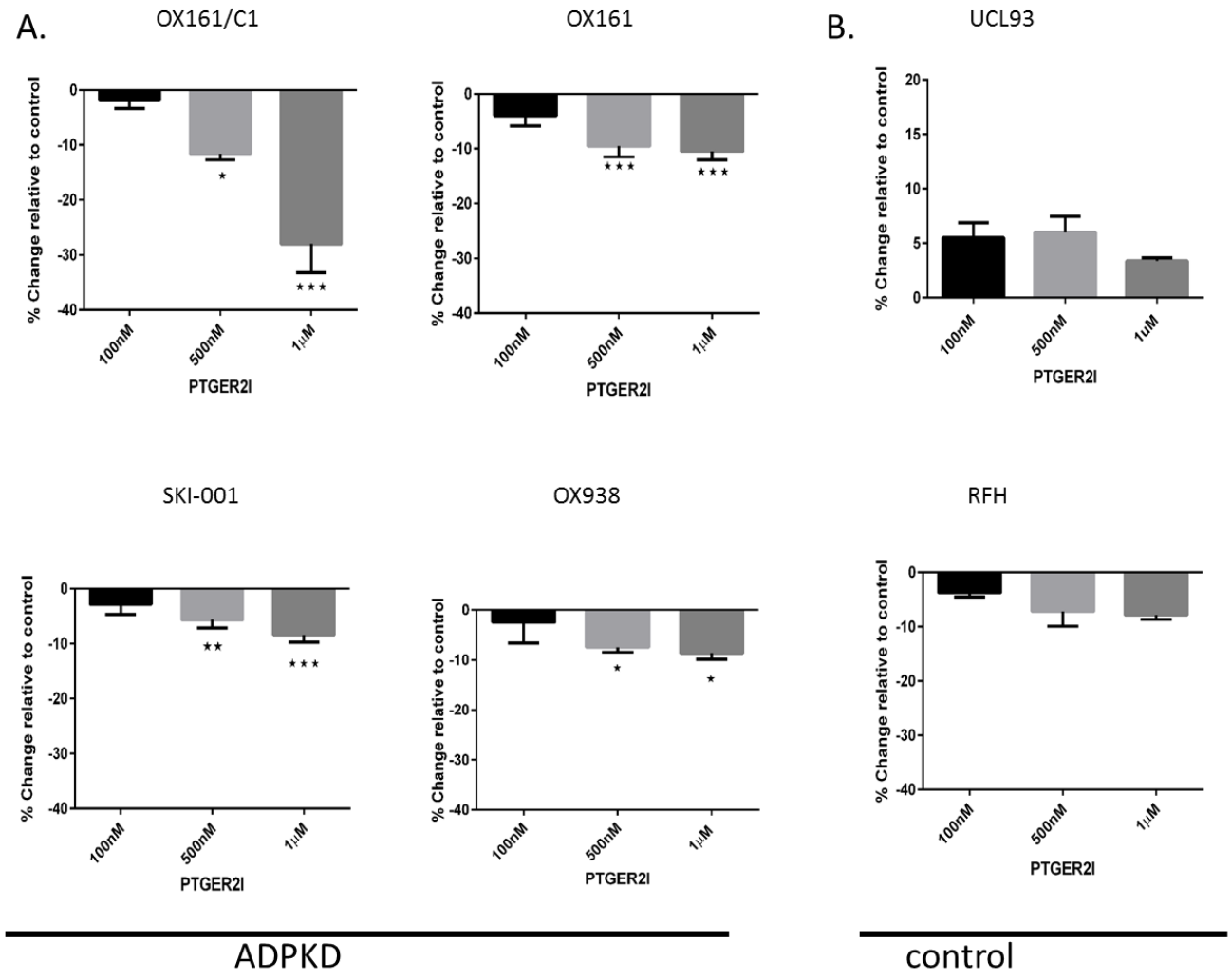

Figure 5.3. Effect of PTGER2 antagonist on ADPKD cell proliferation (MTS assay)

(A). There was a significant decrease in viable cell number as measured by MTS assay in OX161, OX 161/C1, SKI-001 and OX938 ADPKD cell lines(n=3) following incubation (72 hours) with 500 nM -1 μM PTGER2 antagonist compared to control. One-way ANOVA test used. *p<0.05; **p<0.01,***p<0.001. Data presented as mean± SEM.

(B). PTGER2 antagonist did not cause a significant decrease in viable cell number as measured by MTS assay in control cells. Experiments are representative of 3 separate repeats. Control is DMSO treated cells.

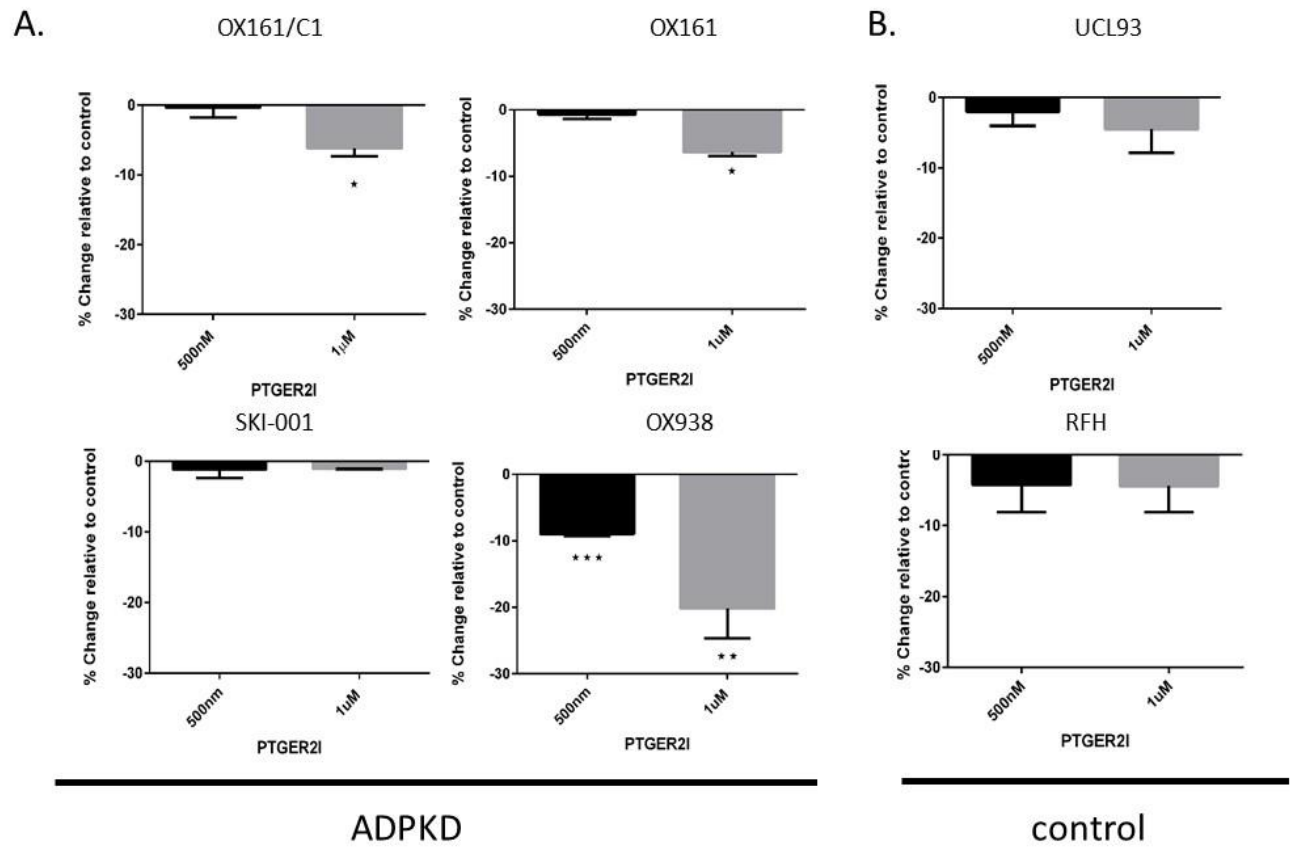

Figure 5.4. Effect of PTGER2 antagonist on ADPKD cell proliferation (BrdU Elisa assay)

(A). There was a significant decrease in DNA synthesis as measured by BrdU Elisa assay in in OX161, OX 161/C1, SKI-001 and OX938 ADPKD cell lines (n=3) following incubation (72 hours) with 500 nM -1 µM PTGER2 antagonist compared to control. Unpaired t-test was used. *p<0.05; **p<0.01*** p<0.001. Data presented as mean± SEM

(B). PTGER2 antagonist did not cause a significant decrease in viable cell number as measured by BrdU Elisa assay in the control cells (UCL93, RFH). Experiments are representative of 3 separate repeats. Control is DMSO treated cells.

5.3.3. The effect of a PTGER4 antagonist on the proliferation of ADPKD and control kidney epithelial cell lines.

The role of PTGER4 was next investigated using a PTGER4 selective antagonist. Cells were treated with three different concentrations of (100 nM, 200 nM and 500 nM) for 72 hours prior to analysis. PTGER4 antagonist treatment significantly inhibited proliferation of ADPKD cell lines (OX161/C1, OX938, OX161 and SKI-001) measured by an MTS assay mainly at concentrations of 200 nM and 500 nM **(Figure 5.5 A).** In both control cell lines there was a significant decrease in proliferation when cells were treated with PTGER4 antagonist at a concentration of 100 nM **(Figure 5.5 B).** Surprisingly, there was a significant increase in proliferation when UCL93 control cells were treated with higher doses (200 nM, 500 nM**)** of the PTGER4 antagonist **(Figure 5.5 B).** This was not observed in RFH cells.

PTGER4 antagonist treatment also significantly reduced BrdU incorporation in three ADPKD cell lines (OX161/C1, OX938, and SKI-001) at concentrations of 200 nM and 500 nM **(Figure 5.6 A).** In the control cell lines, there was no change in proliferation when UCL93 cells were treated with a PTGER4 antagonist **(Figure 5.6 B).** However, unlike the MTS assay, there was a significant increase in BrdU incorporation in RFH cells following incubation with a PTGER4 antagonist. Together, these results suggest that a PTGER4 antagonist inhibits the proliferation of human cystic cells mainly at higher concentrations (500 nM).

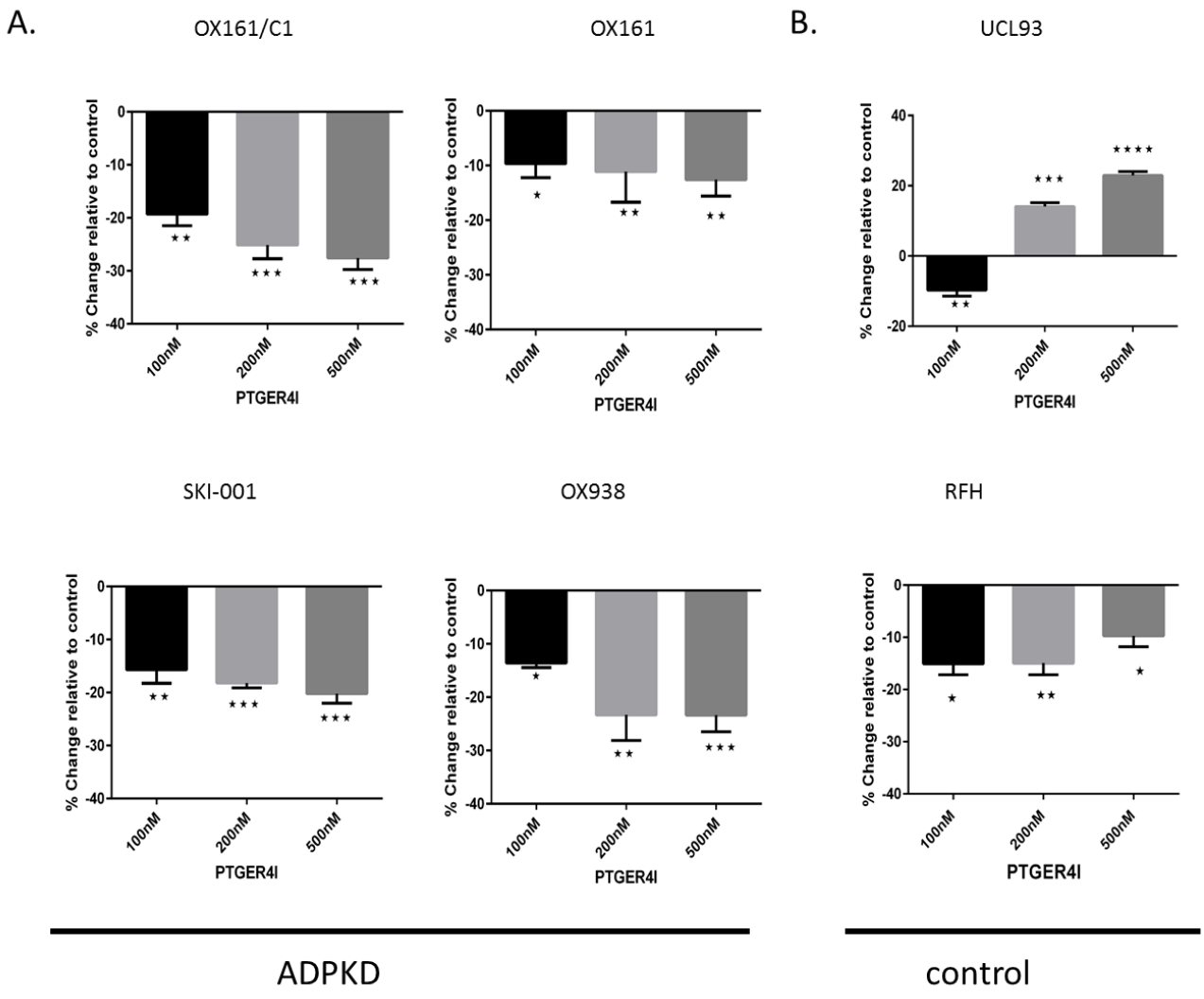

Figure 5.5. Effect of PTGER4 antagonist on ADPKD cell proliferation (MTS assay)

(A). There was a significant decrease in viable cell number as measured by MTS assay in OX161, OX 161/C1, SKI-001 and OX938 ADPKD cell lines (n=3) following incubation (72 hours) with 200 and 500 nM PTGER4 antagonist. One-way ANOVA test was used. *p<0.05; **p<0.01, ***p<0.001, ****p<0.0001 Data presented as mean± SEM.

(B). PTGER4 antagonist caused a significant increase in viable cell number as measured by MTS assay in, UCL93 control cells following incubation with 200 and 500 nM PTGER4 antagonist. (n=3). PTGER4 antagonist caused a significant decrease in viable cell number as measured by MTS assay in RFH control cells at 100, 200 and 500 nM. Experiments are representative of 3 separate repeats. Control is DMSO treated cells.

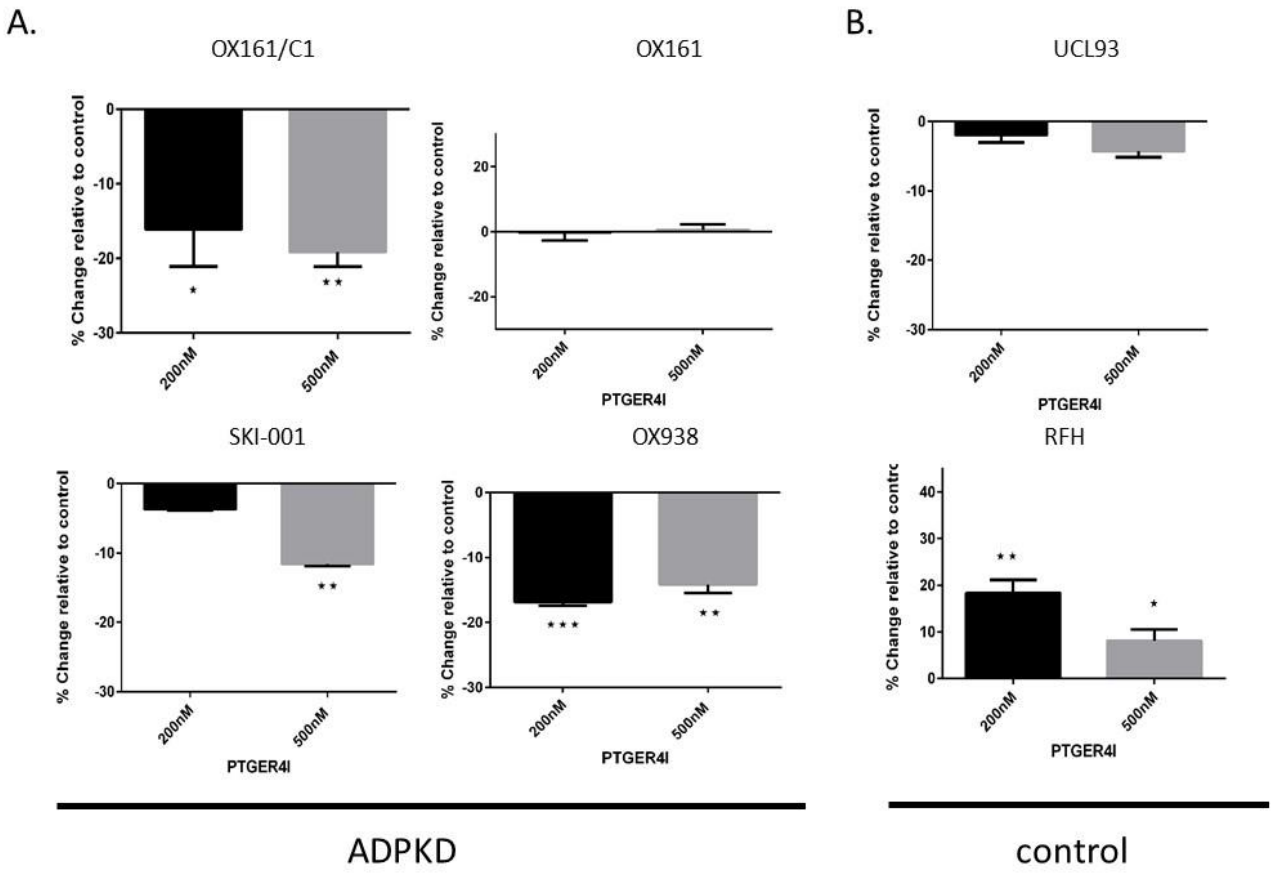

Figure 5.6. Effect of PTGER4 antagonist on ADPKD cell proliferation (BrdU Elisa assay).

(A). There was a significant decrease in DNA synthesis as measured by BrdU Elisa assay in OX161, OX 161/C1, SKI-001 and OX938 ADPKD cell lines (n=3) following incubation (72 hours) with 2 different concentration of PTGRE4I (200nM, 500nM) compared to control. Unpaired t-test was used. *p<0.05; **p<0.01*** p<0.001.

(B). PTGER4 antagonist did not cause a significant decrease in DNA synthesis as measured by BrdU Elisa assay in UCL93 control cells. PTGER4 antagonist caused a significant increase in viable cell number as measured by BrdU Elisa assay in RFH control cells following incubation with 200 and 500 nM PTGER4 antagonist. Data presented as mean± SEM. Experiments are representative of 3 separate repeats. Control is DMSO treated cells.

5.3.4. The effect of PGE2, PTGER2 and PTGER4 antagonists on the proliferation of MDCK II kidney epithelial cells.

In addition to using patient derived cell lines, I used the MDCK II kidney epithelial cell line as a model cell line in 3D cyst assays. Initial experiments were conducted to determine the effect of incubation with PGE2 or PTGER2 and 4 antagonists on proliferation. Incubation with PGE2 had no significant effect on proliferation of MDCK cells at a concentration of 25 and 50 nM; it just failed to reach significance at 25 nM ($p<0.051$) (**Figure 5.7A)**. In contrast, a PTGER2 antagonist significantly decreased MDCK cell proliferation at 500 nM and 1 µM (**Figure 5.7 B)**. Surprisingly, incubation with a PTGER4 antagonist significantly increased proliferation at 200 and 500 nM (**Figure 5.7 C)**.

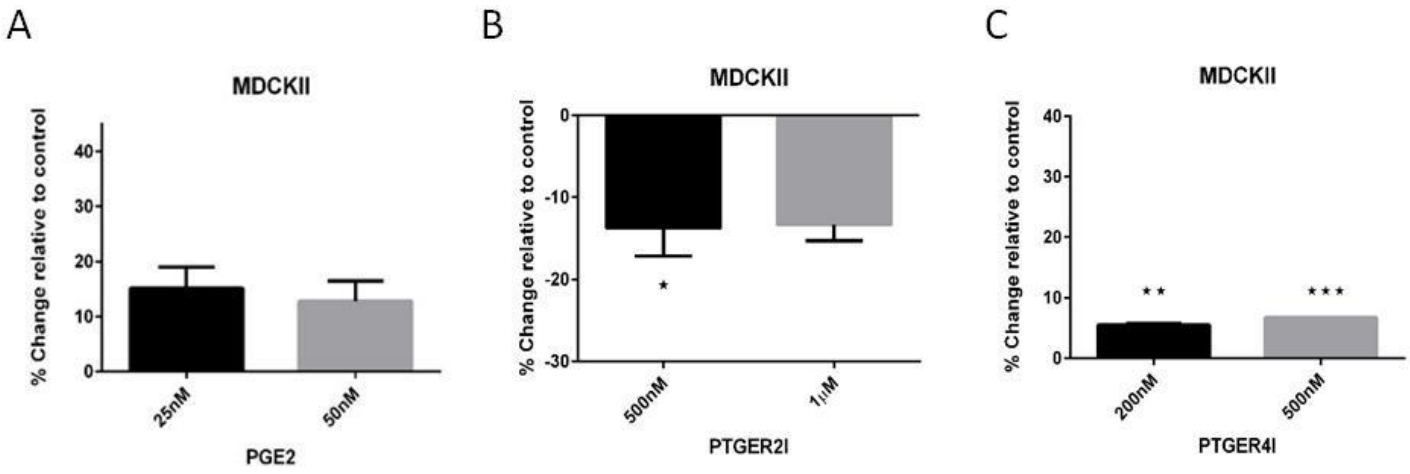

Figure 5.7. Effect of PGE2, PTGER2 and PTGER4 antagonists on MDCK II cell proliferation (BrdU Elisa assay)

(A). There was no significant increase in proliferation of MDCKII cells (n=3) treated with 25 and 50 nM PGE2 by unpaired t-test *p<0.05, **p<0.01, ***p<0.001

(B). There was a significant decrease in proliferation when MDCK II cells were treated with 500 nM PTGER2 antagonist.

(C). There was a significant increase in proliferation when MDCKII cells were incubated with 200 and 500 nM PTGER4 antagonist compared to control. Unpaired t-test was used. Experiments are representative of 3 separate repeats. Control is DMSO treated cells. Data presented as mean± SEM.

5.3.5. Effect of pre-incubation with PTGER2 and PTGER4 antagonists on PGE2 stimulation of cell proliferation.

Since PGE2 was shown to selectively increase proliferation of ADPKD cell lines compared to control cell lines, I sought to confirm the roles of PTGER2 or PTGER4 in mediating this effect in both OX161/C1 and MDCK II cells by pre-incubating cells with antagonists for 2 h prior to adding PGE2. Cell proliferation was then determined using a BrdU ELISA.

BrdU incorporation was significantly increased in OX161/C1 cells following incubation with PGE2 (50 nM). Pre-incubation with either PTGER2 or PTGER4 antagonists completely abolished the effect of PGE2 and further reduced proliferation below untreated controls **(Figure 5.8 A)**. This indicates that PGE2 exerts its effect by binding to PTGER2 and or PTGER4 in OX161/C1 cells.

MDCK II proliferation was also stimulated by PGE2 although the magnitude of change was much smaller. Unlike OX161/C1 cells however, only pre-incubation with the PTGER2 antagonist but not the PTGER4 antagonist blocked PGE2 mediated proliferation in MDCK II cells **(Figure 5.8 B)**. This suggests that in MDCKII cells, PGE2 exerts its effect primarily by binding to the PTGER2 receptor alone.

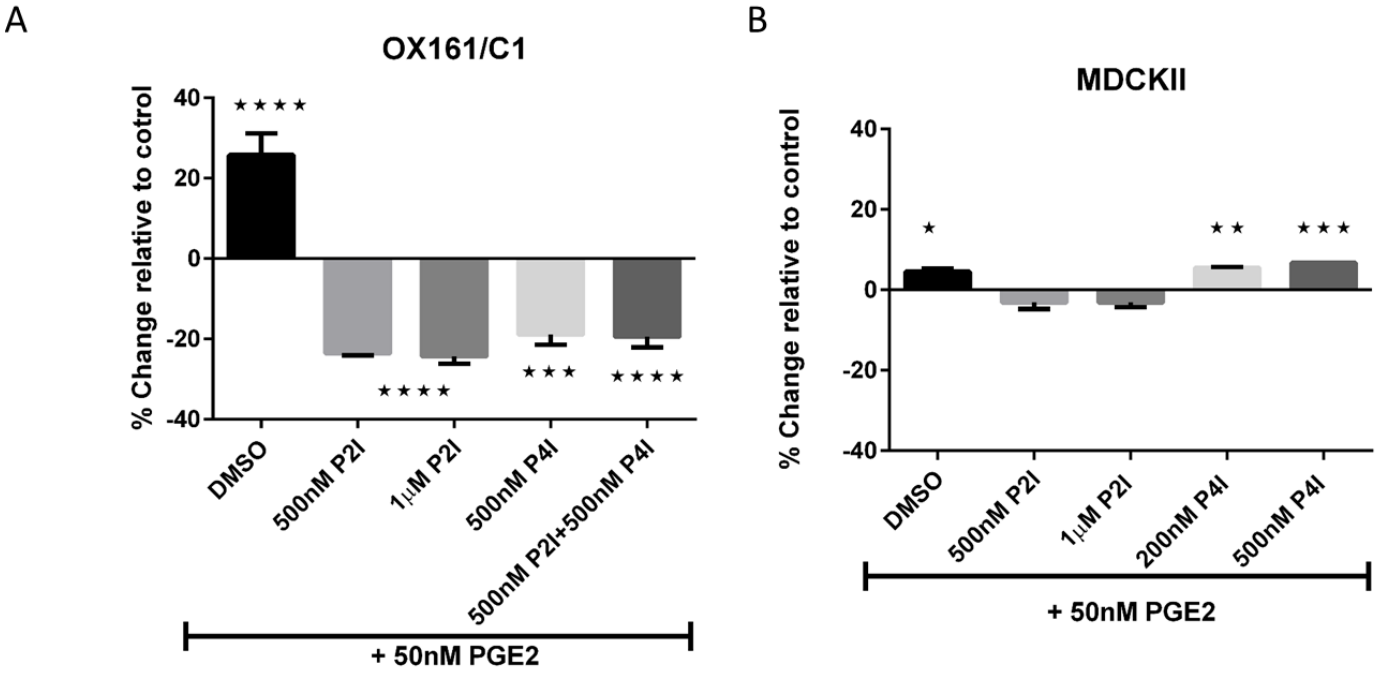

Figure 5.8. Effect of pre-incubation with PTGER2 and PTGER4 antagonists on PGE2 stimulation of cell proliferation

(A). OX161/C1 cells (n=3) showed a significant increase in proliferation when treated with 50 nM PGE2. This was inhibited following pre-incubation with PTGER2 and 4 antagonists. ***p<0.001, ****p<0.0001. One-way ANOVA test was used.

(B). MDCK II cells (n=3) showed a significant increase in proliferation when treated with 50 nM PGE2. This was inhibited following pre-incubation with a PTGER2 antagonist but not by pre-incubation with a PTGER4 antagonist. **p<0.01, ***p<0.001. Experiments are representative of 3 separate repeats. Control is DMSO only treated cells. One-way ANOVA test was used. Data presented as mean± SEM.

5.3.6. The effect of PGE2, PTGER2 and PTGER4 antagonists on apoptosis of ADPKD and control kidney epithelial cell lines.

ADPKD is characterised by increased levels of proliferation as well as apoptosis (Chang, Steelman et al. 2003). The results so far in this chapter have shown that PGE2 selectively stimulates proliferation of ADPKD cell lines compared to control cell lines by binding to both PTGER2 and PTGER4 receptors.

The effect of PGE2 as well as PTGER2 and PTGER4 antagonists on apoptosis was investigated next using two well established methods. Firstly, a TUNEL assay was used to identify DNA strand breaks in apoptotic cells. Secondly, immunofluorescence staining was used to identify activated (cleaved) caspase 3 in apoptotic cells.

For both assays, 100 mM H_2O_2 was used as a positive control to stimulate apoptosis and DMSO alone was used as a negative control. Based on the results of previous experiments, PGE2 was used at a concentration of 50 nM and PTGER2 and PTGER4 antagonists were used at a concentration of 500 nM for 72 h.

Incubation of ADPKD and control cells with 100 mM H_2O_2 resulted in strong TUNEL staining as well as cleaved caspase-3 staining indicating the induction of apoptosis. Incubation with DMSO alone showed very few positively stained cells **(Figure 5.9).** The images shown are representative of the ADPKD and control cell lines used in this study.

Incubation of ADPKD and control cell lines with 50 nM PGE2 had no effect on apoptosis although these cells displayed very low (<5%) levels of apoptosis in the absence of stimuli **(Figure 5.10)**. Interestingly, all three ADPKD cell lines tested showed a significant increase in apoptosis by TUNEL assay following incubation with PTGER2 and PTGER4 receptor antagonists **(Figure 5.10)**. This was not seen as consistently when apoptosis was assayed by staining for cleaved caspase-3 with only the OX161/C1 ADPKD line showing increased

apoptosis with both antagonists in this assay **(Figure 5.11)**. The MDCKII cell line showed a consistent increase in apoptosis when treated with a PTGER2 receptor antagonist in both assays **(Figure 5.10 and 11)**.

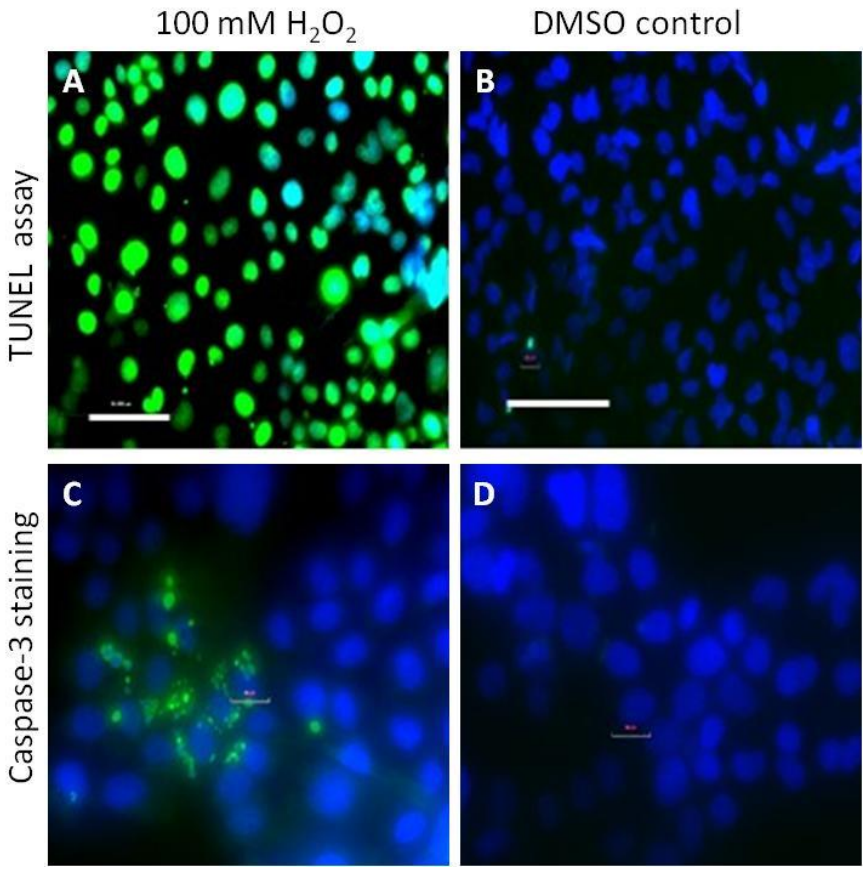

Figure 5.9. Identification of apoptotic cells by TUNEL and cleaved caspase-3 staining.

(A). OX161/C1 cells treated with 100 mM H_2O_2 showed strong TUNEL staining whereas in cells treated with DMSO alone **(B)** staining was mostly absent.

(C). OX161/C1 cells treated with 100 mM H_2O_2 showed strong cleaved caspase-3 staining whereas in cells treated with DMSO alone **(B)** staining was mostly absent. Staining was representative of the results from ADPKD cell lines as well as control cell lines.

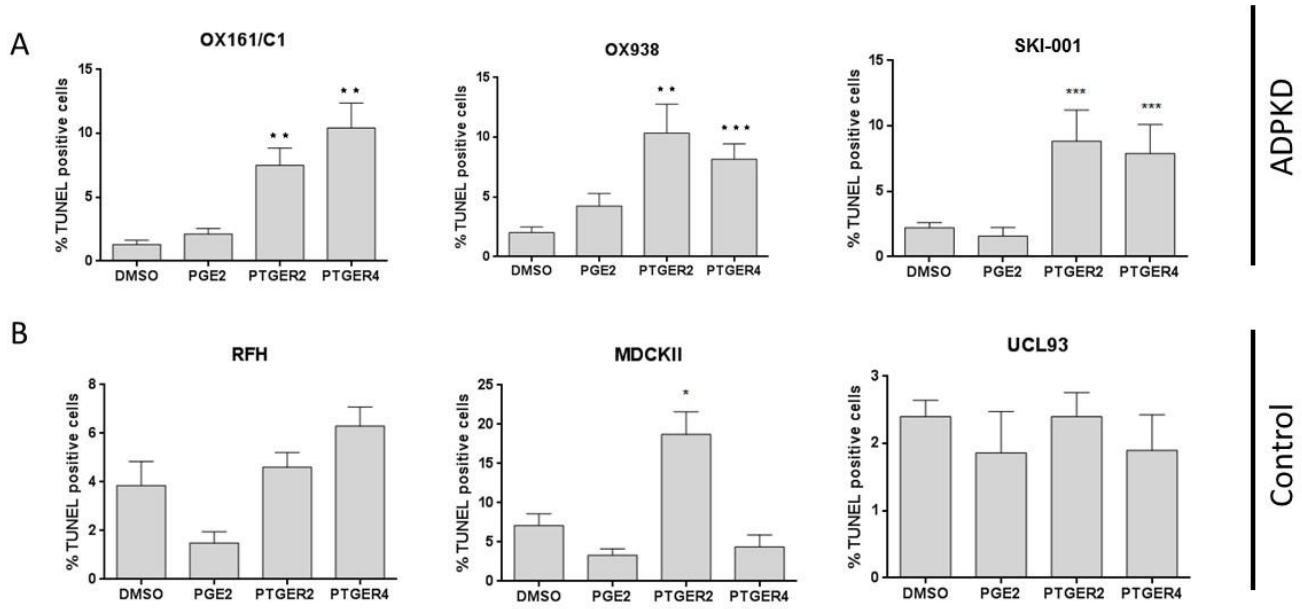

Figure 5.10 Effect of PGE2, PTGER2 and PTGER4 receptor antagonists on apoptosis by TUNEL assay.

(A). ADPKD cells (n=6) showed a significant increase in apoptosis as seen by increased TUNEL staining following incubation with PTGER2 and 4 receptor antagonists. *P<0.05, **p<0.01, ***p<0.001.

(B). Control cells (n=6) showed no significant increases in apoptosis with the exception of MDCKII cells treated with PTGER2 receptor antagonist. Experiments are representative of 3 separate repeats. Control is DMSO only treated cells. One-way ANOVA test was used.

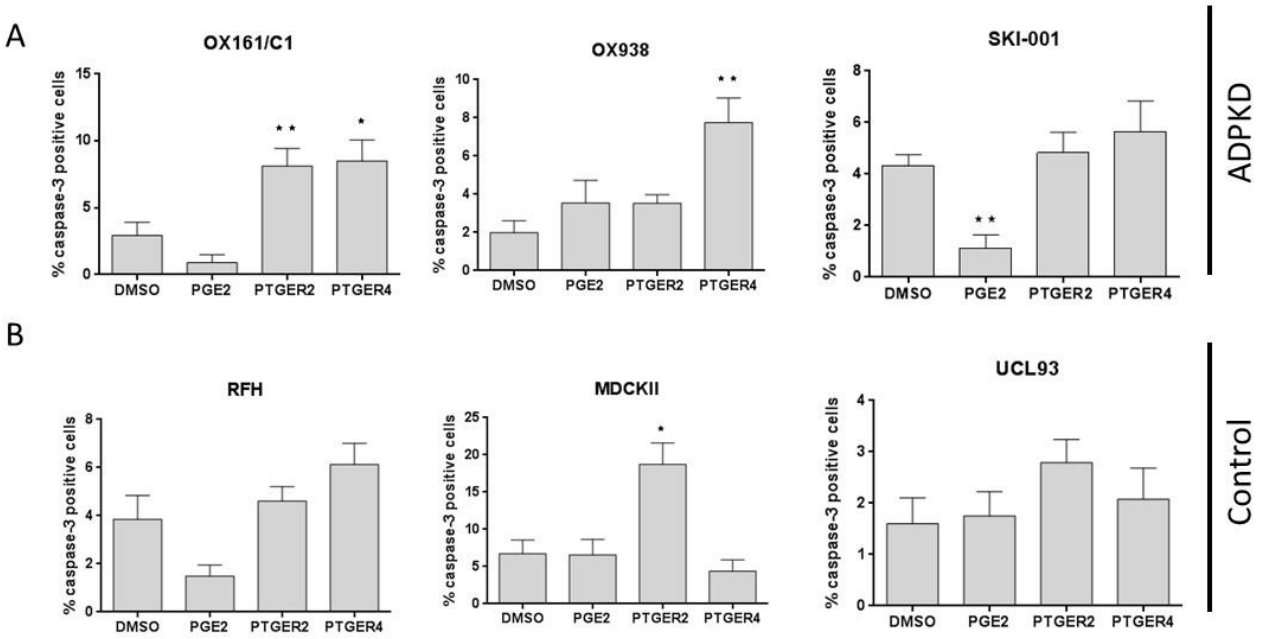

Figure 5.11 Effect of PGE2, PTGER2 and PTGER4 receptor antagonists on apoptosis by cleaved caspase-3 staining.

(A). OX161/C1 ADPKD cells (n=6) showed a significant increase in apoptosis as seen by increased cleaved caspase-3 staining following incubation with PTGER2 and 4 receptor antagonists. OX938 ADPKD cells showed a significant increase in apoptosis as seen by increased cleaved caspase-3 staining following incubation with PTGER4 receptor antagonist. PH1 ADPKD cells showed a significant reduction in apoptosis as seen by decreased cleaved caspase-3 staining following incubation with PGE2.

(B). Control cells showed no significant increases in apoptosis with the exception of MDCKII cells treated with PTGER2 receptor antagonist. Experiments are representative of 3 separate repeats. Control is DMSO only treated cells. Data presented as mean± SEM. One-way Anova test was used.

5.3.7. The effect of a PTGER2 receptor antagonist on cystogenesis in 3D cyst assays.

To assess the effect of a PTGER2 antagonist on cystogenesis, cyst assays were performed on OX161/C1 cells cultured in Matrigel and MDCKII cultured in Collagen gels respectively. The cells were treated in triplicate with different concentration of PTGER2 antagonist (100 nM-10 µM) for 48 h and cells were observed every two days for eight days and average cyst area measured as described in the methods. I found that the PTGER2 receptor antagonist significantly inhibited the growth of cysts in OX161/C1 cells in a concentration dependent manner with a minimum concentration required of 500 nM **(Figure 5.12).** Similar results were observed in MDCKII cells **(Figure 5.13).** The results displayed are representative of 3 separate experiments.

In conclusion, incubation with a PTGER2 antagonist inhibited cyst growth in both cell lines (OX161/C1 and MDCKII) tested. The reduction in average cyst area was seen at a concentration of 500nM and reached a maximum at 1µM.

5.3.8. The effect of a PTGER4 receptor antagonist on cystogenesis in 3D cyst assays.

Next, I assessed the effect of a PTGER4 receptor antagonist on cystogenesis in both OX161/C1 cells and MDCKII cells in 3D culture. Cells were treated in triplicate with different concentrations of the PTGER4 antagonist (100 nM-10 µM) and photographed every two days for ten days.

I found that the PTGER4 receptor antagonist significantly inhibited the growth of OX161/C1 cysts in a concentration dependent manner. The minimum concentration required was 200nM. The maximum effect was seen at concentrations 1 and 10 µM **(Figure 5.14)**.

In contrast to OX161/C1 cells, MDCKII cells showed the unexpected finding that incubation with a PTGER4 receptor antagonist caused a significant increase in average cyst area especially at higher (10μM) concentrations **(Figure 5. 15).** There was no decrease in cyst growth at lower concentrations **(Figure 5. 15).** The mechanism why the PTGER4 antagonist increased average cyst area in MDCK II cells is not clear. At this dose, it may act on other receptors or other pathways in this cell line resulting in stimulation of proliferation. PTGER4 receptors can activate both Gi coupled receptors as well as Gs receptors (Fujino and Regan 2006). Therefore a PTGER4 receptor antagonist may activate alternative pathways which increase cystogenesis rather than inhibit cyst formation.

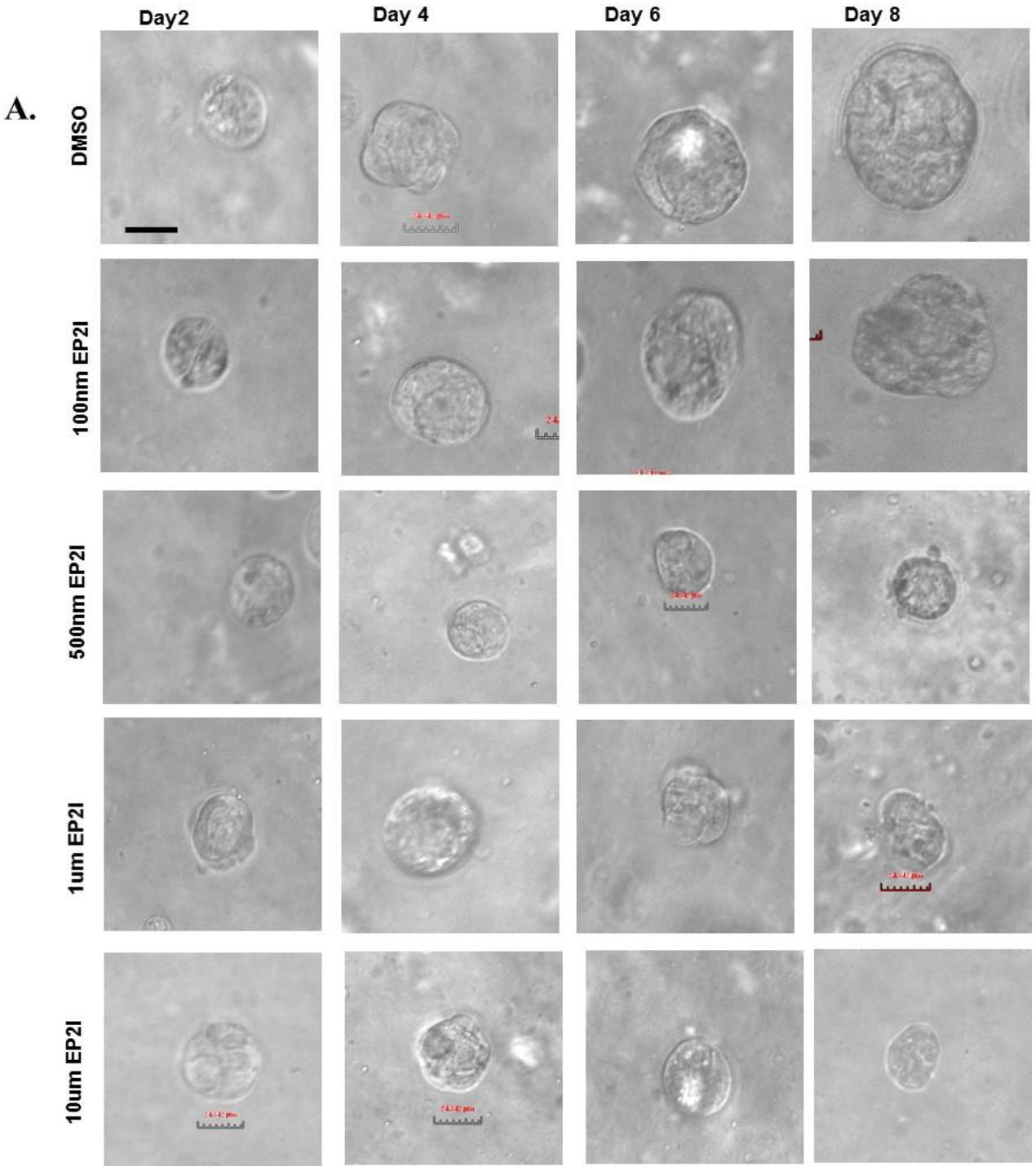
A.
Day2
Day 4
Day 6
Day 8
DMSO
100nm EP2I
500nm EP2I
1um EP2I
10um EP2I

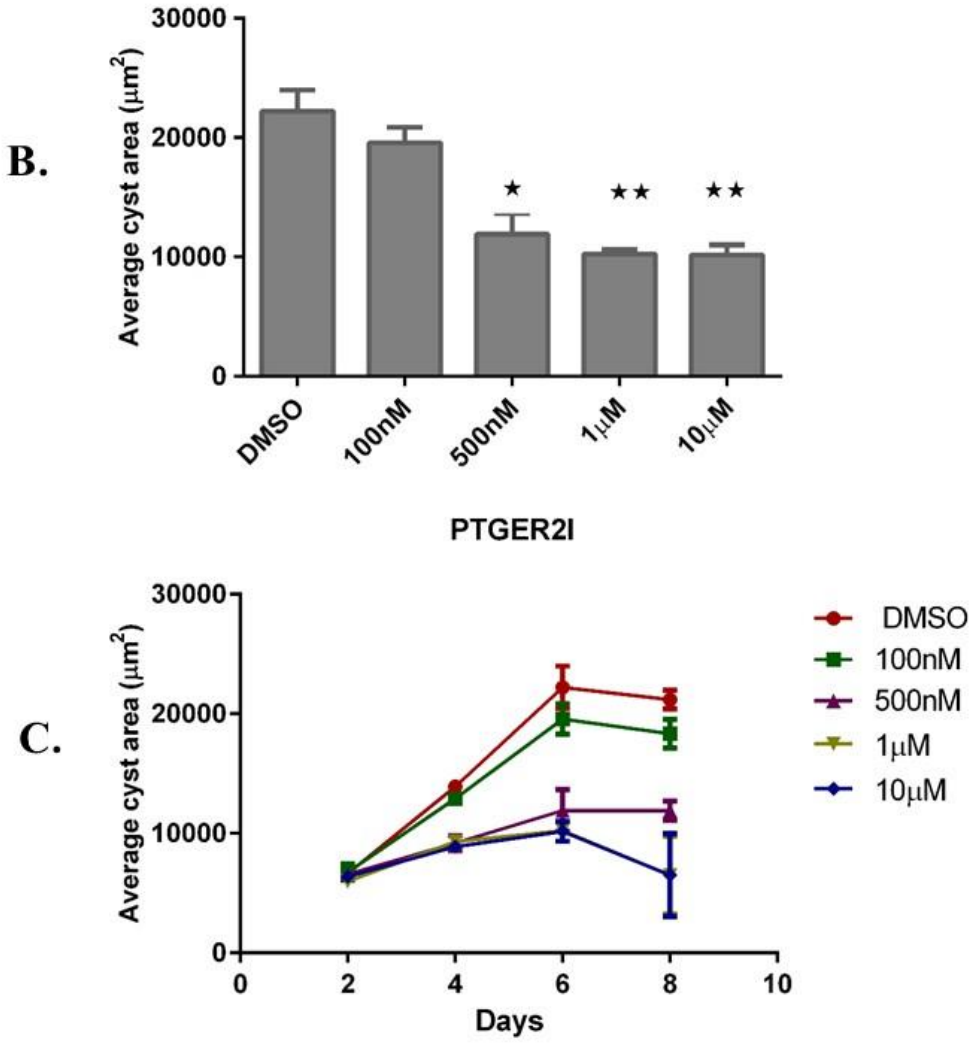

Figure 5.12. The effect of PTGER2 antagonist on OX161/C1 cysts in 3D culture

(A). Photographs of OX16 /C1 cysts cultured in matrigel treated with DMSO (control), or different concentrations of PTGER2 antagonist (100nM-10µM) monitored serially from day 2 to day 8. Cyst formation was visibly reduced especially at concentrations (500nM -10µM) compared to the control. Scale bar 50µM.

(B). Graph showing the change in average cyst area over time of OX161/C1cells treated with PTGER2 antagonist, or DMSO in 3D culture. The average cyst area OX16 /C1 cyst was not significant decreased by PTGER2 antagonist 100nM compared to the control. The values are however, significant suppression of cyst growth was seen by at higher concentrations. One-way ANOVA test was used. *$p<0.05$; **$p<0.01$.

(C). The growth rate of OX16 /C1 cells measured over 8 d. Average cyst area was significantly decreased by the PTGER2 antagonist at concentrations between 500 nM-10 µM . Two way

ANOVA test was used. A total of 20 cysts were measured per well for a total of 3 wells (n=60). ****$p<0.0001$. Experiments are representative of 3 separate repeats. Control is DMSO only treated cells.

5.3.9. Effect of pre-incubation with PTGER2 and PTGER4 antagonists on PGE2 stimulation of cyst formation in 3D cyst assays.

PGE2 was shown to selectively increase proliferation and cystogenesis of ADPKD cell lines. In order to determine whether PGE2 was binding to and mediating its proliferative effect through PTGER2 or PTGER4, OX161/C1 and MDCKII cells were pre-incubated with antagonists for 2 h prior to incubation with PGE2 for 72 h. MDCKII cells treated with 25 nM PGE2 alone showed a significant increase of cyst growth compared to the controls **(Figure 5.16).** Conversely, when MDCKII cells were pre-incubated with a PTGER2 receptor antagonist (100nM -10µM), there was a significant reduction in cyst growth especially at concentrations 1µM and 10µM compared to the control **(Figure 5.16)** indicating that PGE2 was exerting its effects through the PTGER2 receptor in MDCK II cells.

OX161/C1 cells treated with 50nM PGE2 alone showed a significant increase in average cyst area **(Figure 5.17).** Conversely, when cell were pre-incubated with PTGER2, PTGER4 or both together prior to incubation with PGE2 there was a significant reduction in average cyst area **(Figure 5.17).** In summary, cells treated with 50nM PGE2 showed a significant increase in average cyst area. This effect was inhibited by PTGER2 or PTGER4 antagonists singly or in combination. The results displayed are representative of 3 independent experiments.

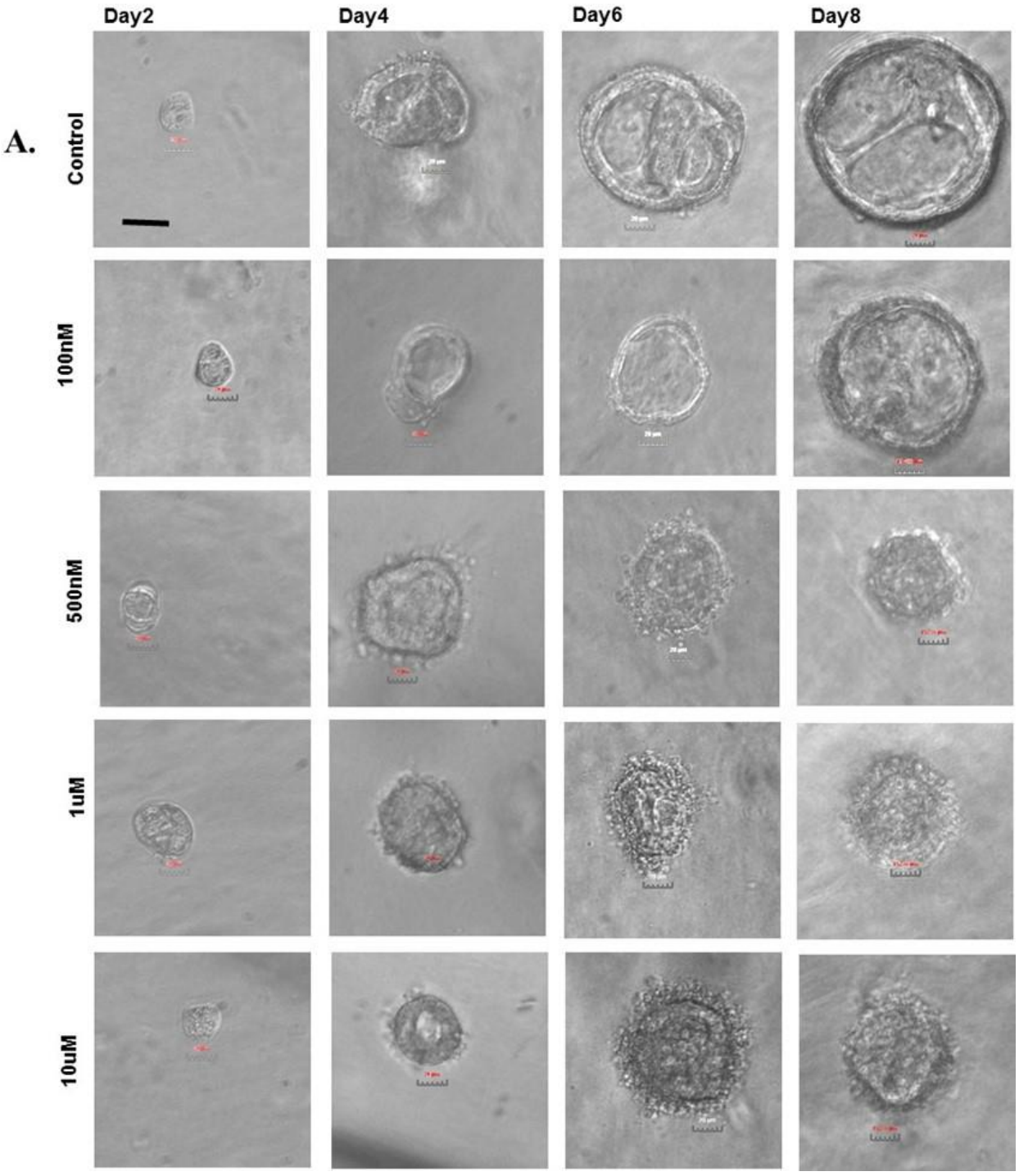
A.
Day2
Day4
Day6
Day8
Control
100nM
500nM
1uM
10uM

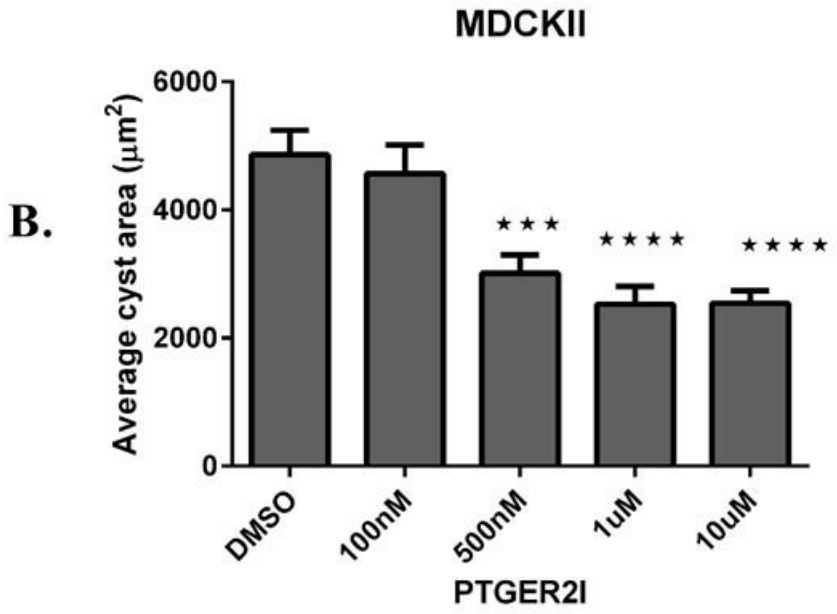

Figure 5.13. The effect of PTGER2 antagonist on MDCKII cysts in 3D culture.

(A). Photographs of MDCKII cyst cultured in Collagen I treated with DMSO (control);or different concentrations of PTGER2 antagonist (100nM-10µM) monitored serially from day 2-day to day 8. Cysts were visibly smaller when treated with 500nM-10µM. All scale bar 50µM.

(B). Graph representing the average cyst area of MDCKII cells treated with PTGER2 antagonist or DMSO on day 8. The total cyst area of MDCKII cysts was not significantly decreased by PTGER2 antagonist 100nM compared to the control. The values are (mean± SEM) (n=20) Average cyst area was significantly reduced by higher concentrations of the antagonist. One-way ANOVA test was used. ***p<0.001; ****p<0.0001.

.

A.

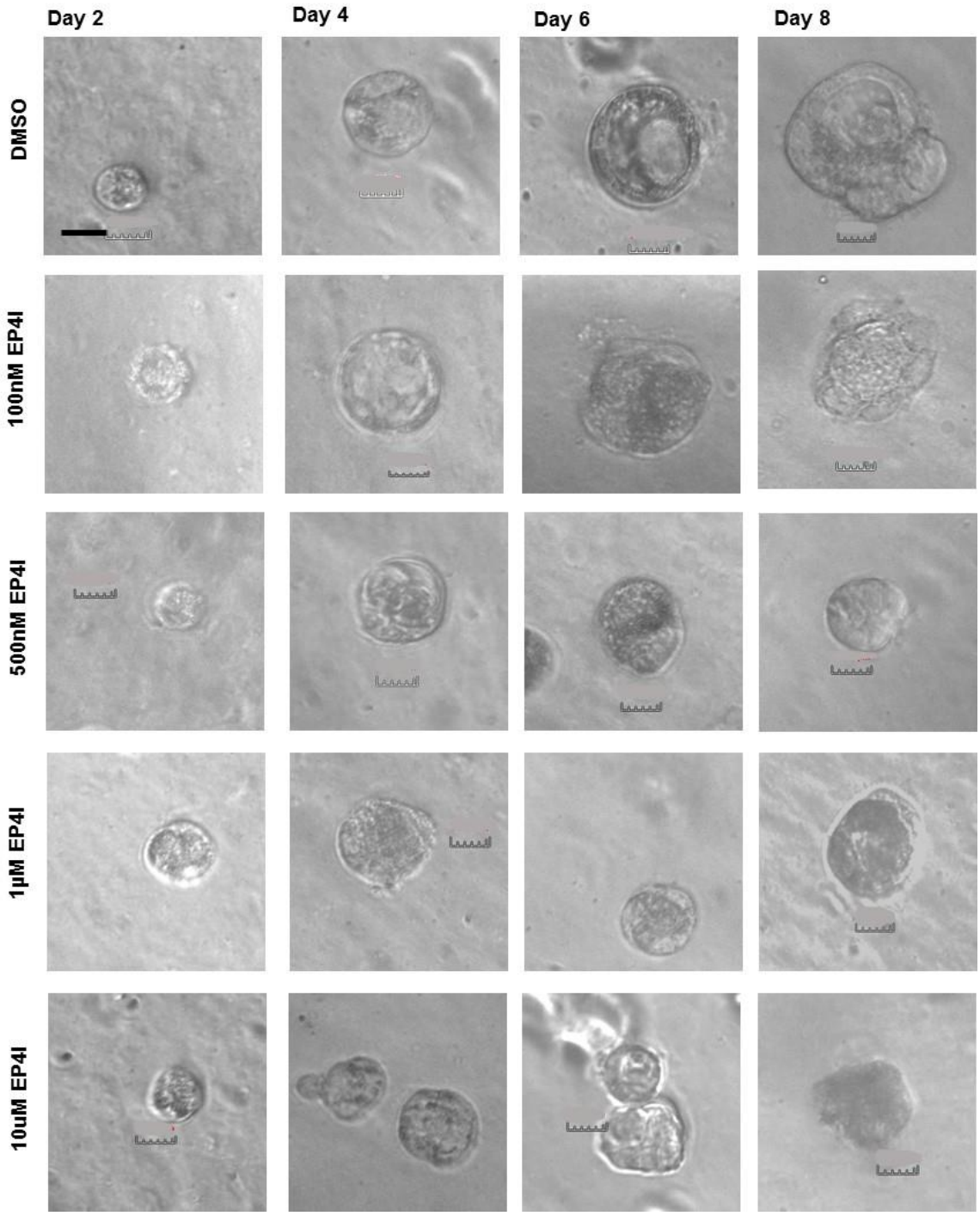
Day 2
Day 4
Day 6
Day 8
DMSO
100nM EP4I
500nM EP4I
1μM EP4I
10uM EP4I

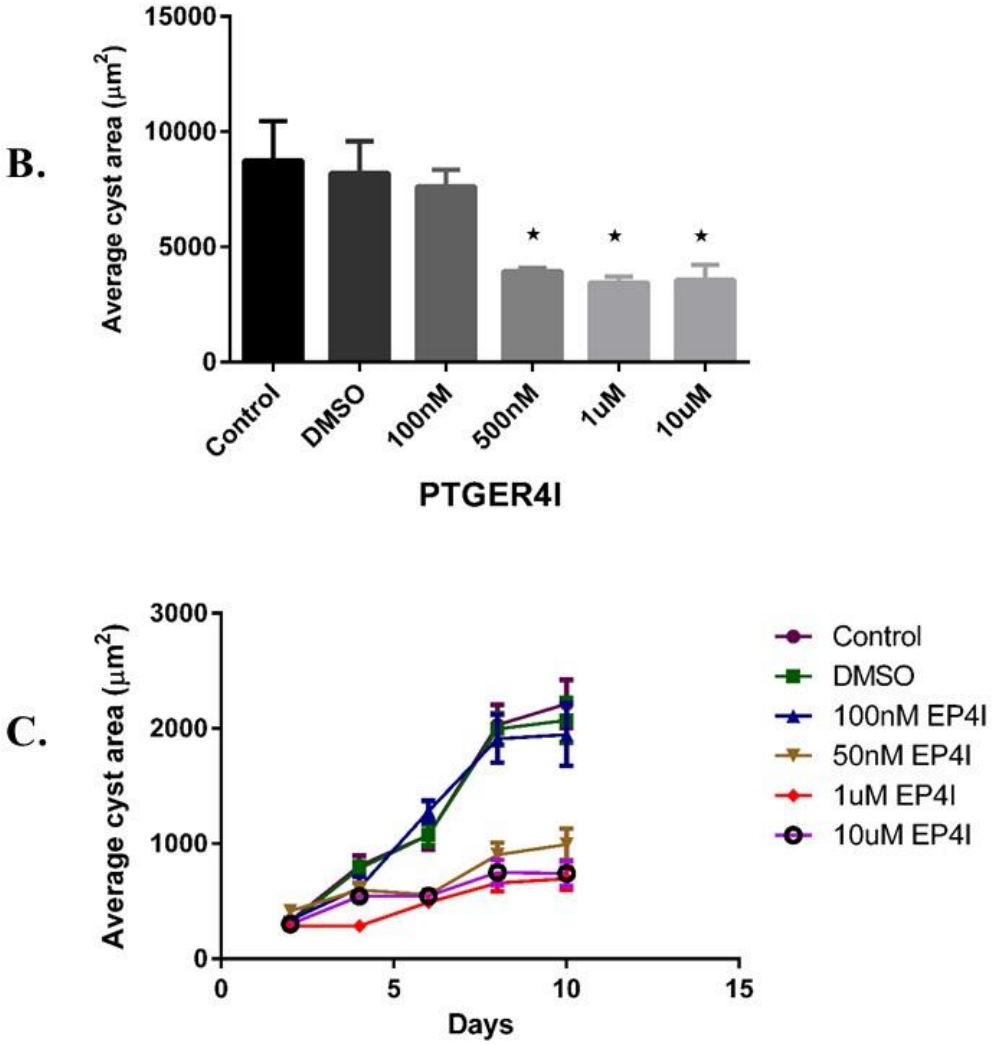

Figure 5.14. The effect of PTGER4 antagonist on OX161/C1 cysts in 3D culture

(A). Photographs of OX161/C1 cyst cultured in Matrigel treated with DMSO (control) or different concentrations of a PTGER4 antagonist (100nM-10µM) monitored serially from day 2 to day 8. There was a clear decrease in size with 500-10µM of the PTGER4 antagonist compared to control. All scale bars - 50µM.

(B). Graph representing the average cyst area of OX161/C1 cells treated with PTGER4 antagonist or DMSO. The average cyst area of OX161/C1 cysts was not significantly decreased by PTGER4 antagonist 100nM compared to the control. The significant value was analysed by one-way ANOVA test. A significant reduction in cyst area was observed at higher concentrations. *$p<0.05$

(C). The growth rate of OX161/C1 cells, treated with DMSO or different concentrations of PTGER4 antagonist over time. Cyst area was decreased by the PTGER4 antagonist at higher concentrations i.e. 500nM-10µM. the significant was analysed by two- way-ANOVA test. A total of 20 cysts were measured per well in 3 wells (60 cysts). ****$p<0.0001$

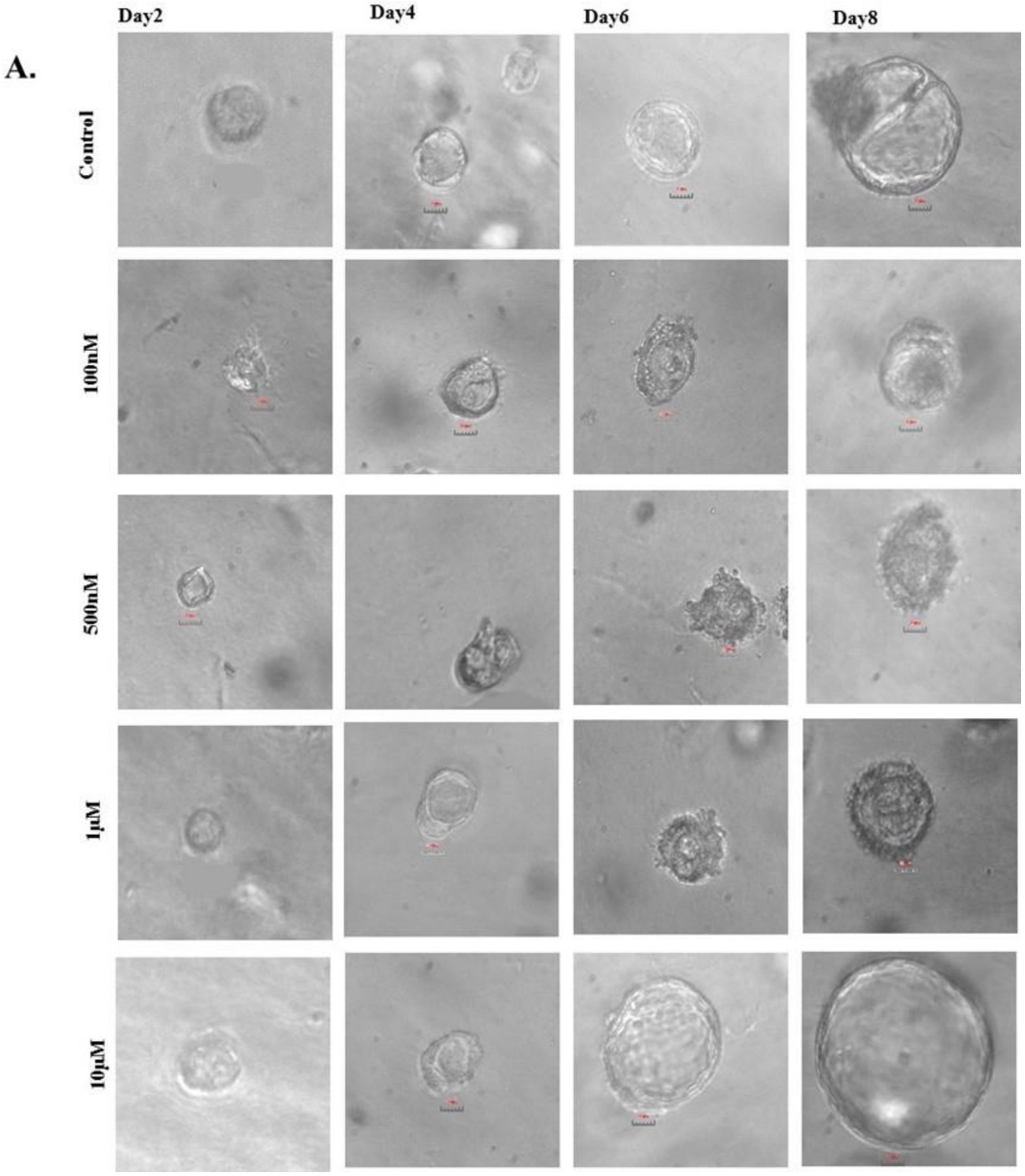
A.
Day2
Day4
Day6
Day8
Control
100nM
500nM
1μM
10μM

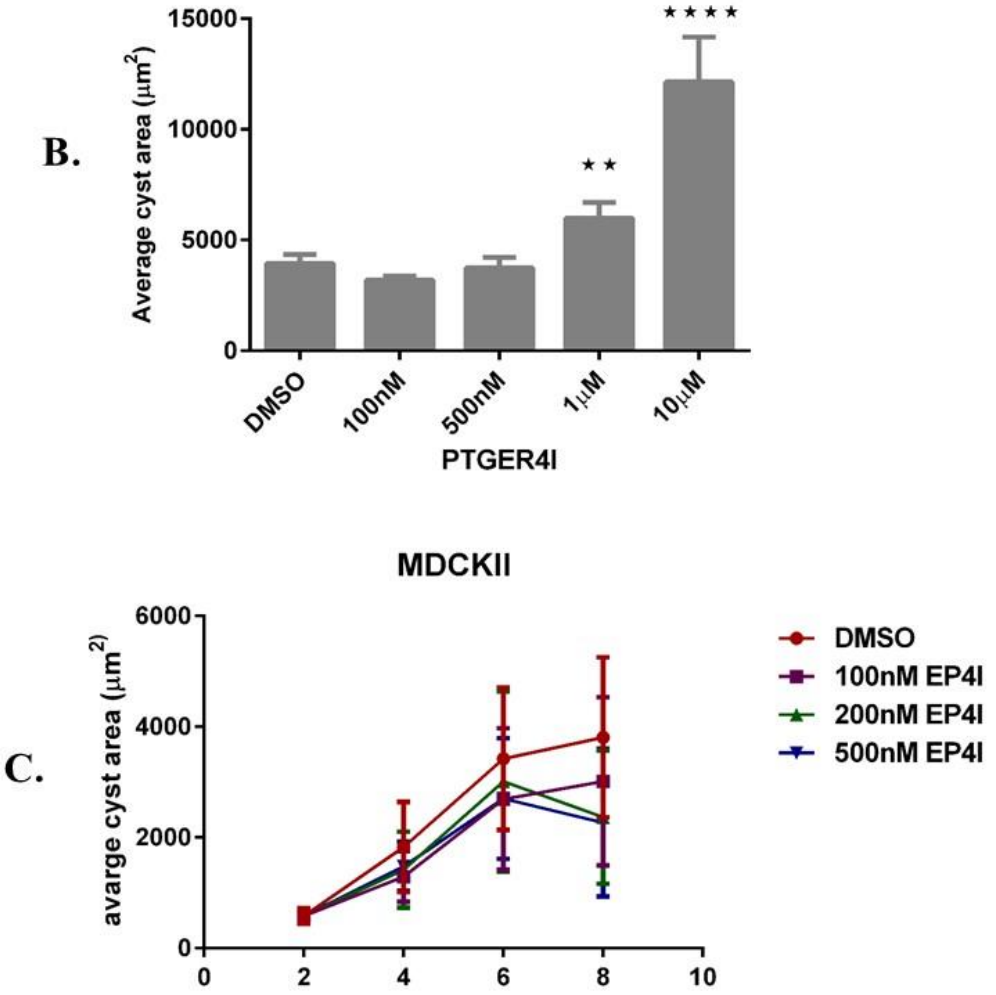

Figure 5.15. Shows the effect of PTGER4 antagonist on MDCKII cysts in 3D culture.

(A). Photographs of MDCKII cyst cultured in Collagen I treated with DMSO (control), and different concentrations of PTGER4 antagonist (100nM-10µM) monitored serially from day 2 to day 8. Cysts increased significantly in size when treated with higher concentrations of PTGER4 antagonist (1µM, 10µM). Scale bar - 50µM.

(B). Graph representing the average cyst area of MDCKII cells treated with different concentrations of PTGER4 antagonist or DMSO. **p<0.01; ****p<0.0001. One-way ANOVA test was used.

(C). The growth rate of MDCKII cells treated with a PTGER4 antagonist (100nM-500nM). There was no significant decrease of the cyst area at these doses 100nM. Significant difference at 200nM* p<0.05 and 500nM**p<0.01 by two-way ANOVA test. A total of 10 cysts were measured per well for a total of 3 wells (n=30) which are monitored every two days for 8 days. Data presented as mean± SEM.

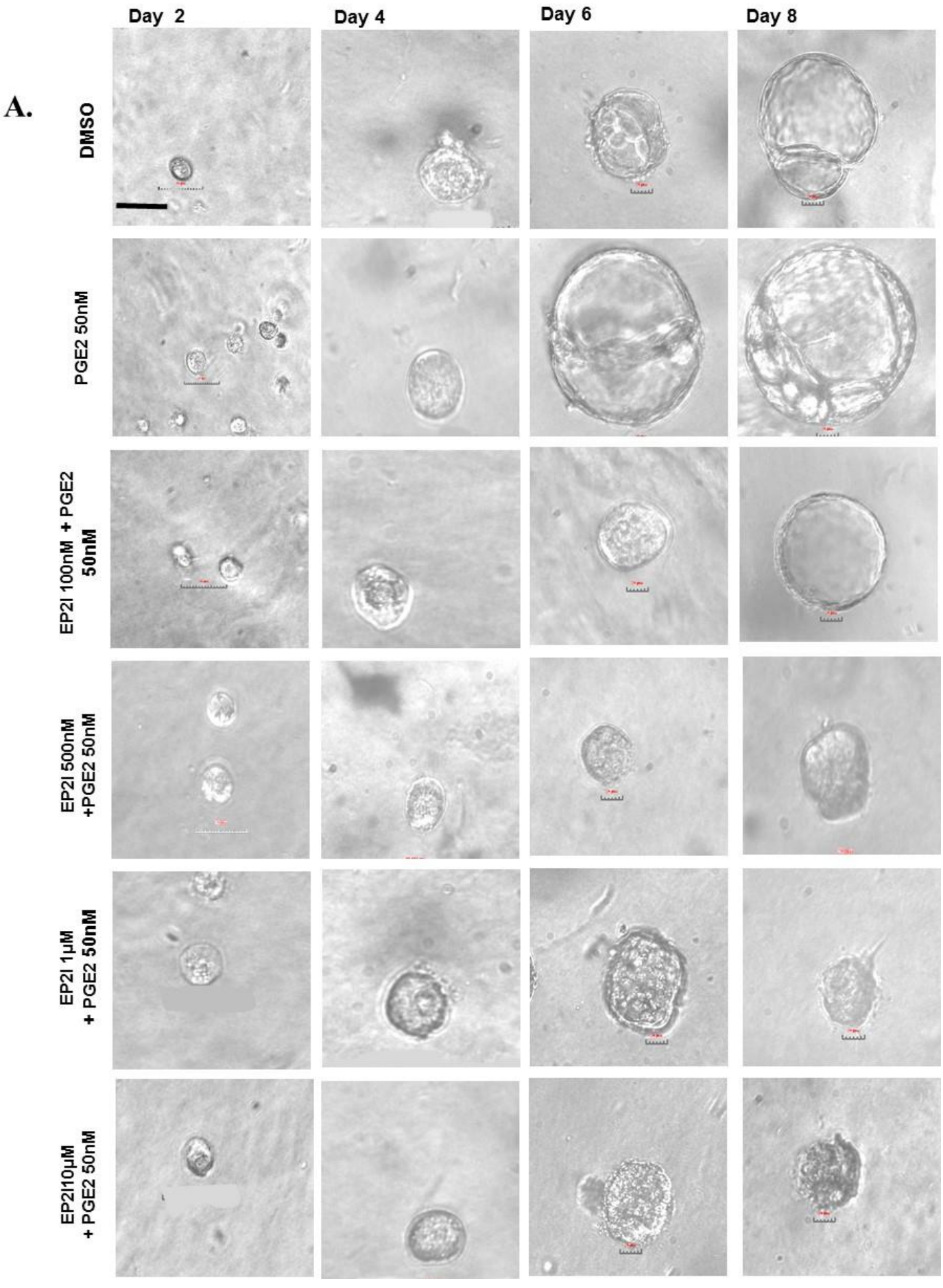
A.
Day 2
Day 4
Day 6
Day 8
DMSO
PGE2 50nM
EP2I 100nM + PGE2 50nM
EP2I 500nM +PGE2 50nM
EP2I 1µM + PGE2 50nM
EP2I10µM + PGE2 50nM

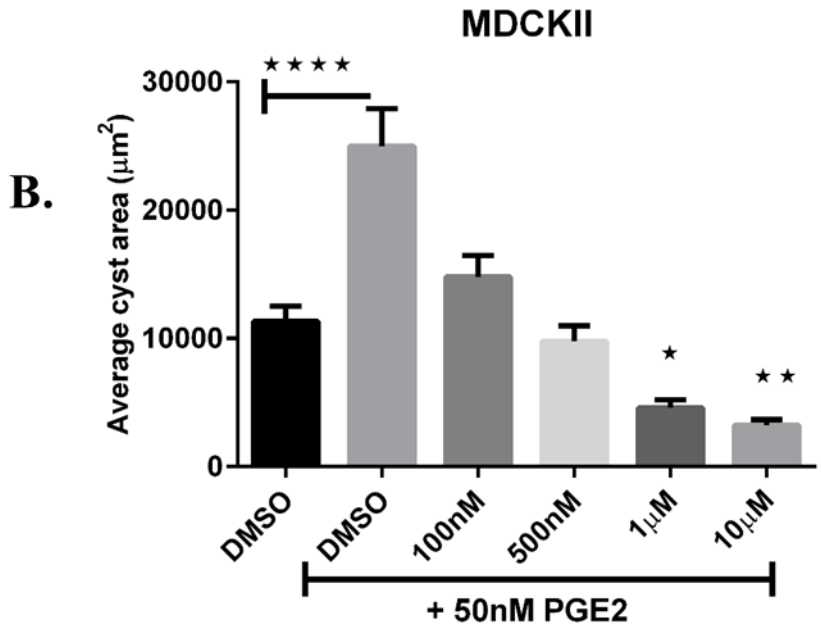

Figure 5.16. The effect of pre-incubation with PTGER2 antagonists on PGE2 stimulated MDCKII cysts.

(A). Photographs of MDCKII cyst cultured in collagen I treated with DMSO (control), 50nM PGE2 and different concentrations of PTGER2 or PTGER4 antagonists monitored serially from day two. Treatment with 50nM PGE2 significantly increased cyst size and number compared to controls. The effect of PGE2 was inhibited by co-incubation with PTGER2 antagonists. All scale bars - 50μM.

(B). Graph representing the average cyst area at day 8 of MDCKII cysts treated with 50nM PGE2 in the presence or absence of a PTGER2 antagonist.

MDCKII treated with PGE2 (50nM), showed a significant increase in cyst area (n=3) **p<0.01, *p<0.05, ****p<0.0001. A significant inhibition of this effect was observed at PTGER2I concentrations of 1 μM and above. Data presented as mean± SEM. One-way ANOVA test was used.

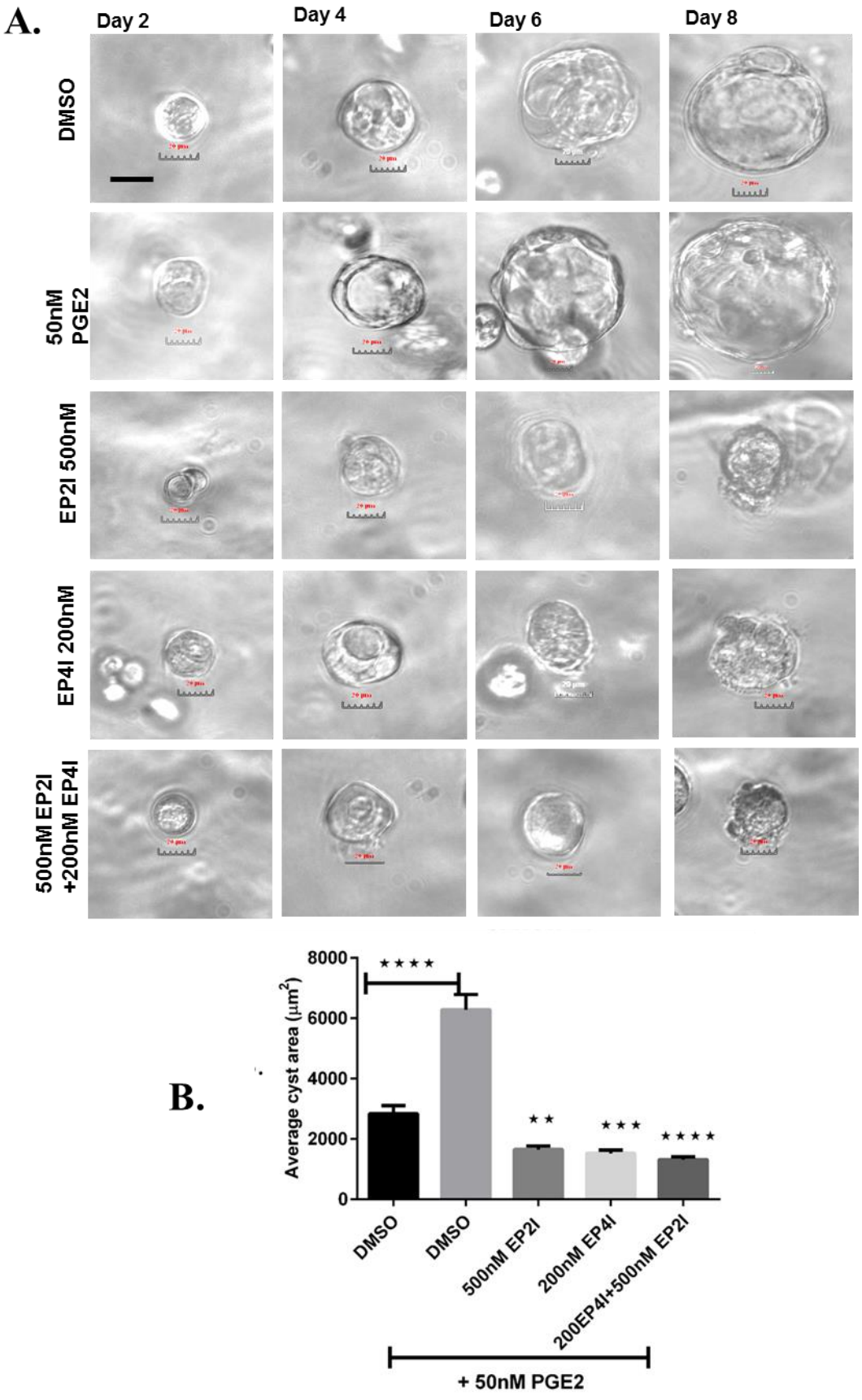
A.
Day 2
Day 4
Day 6
Day 8
DMSO
50nM PGE2
EP2I 500nM
EP4I 200nM
500nM EP2I +200nM EP4I
B.
Average cyst area (μm²)
8000
6000
4000
2000
0
DMSO
DMSO
500nM EP2I
200nM EP4I
200EP4I+500nM EP2I
+ 50nM PGE2

Figure 5.17. The effect of pre-incubation with PTGER2 and PTGER4 antagonists on PGE2 stimulated OX161/C1 cysts.

(A). Photographs of OX161/C1 cysts cultured in Matrigel monitored serially from day 2 to day 8 following treatment with DMSO (control), 50nM PGE2, PTGER2 antagonist 500nM, PTGER4 antagonist 200nM or both. All scale bars - 50 µM.

(B). Average cyst area of OX161/C1 cells treated with PGE2 (50 nM) with PTGER2 and/or PTGER4 antagonists at day 8. ***$p<0.001$; ****$p<0.0001$. (n=3). There is additive effect when both PTGER2I and PTGER4I added to the cell. Data presented as mean± SEM. One-way ANOVA test was used.

5.3.10. The effect of PGE2 on cAMP levels in ADPKD and control kidney epithelial cell lines.

The major effect of PGE2 binding to PTGER2 and PTGER4 receptors is to increase cAMP levels via activation of adenylate cyclase. We utilised a cAMP ELISA assay to determine the effect of PGE2 on baseline cAMP levels in ADPKD and control cell lines. There were significantly higher cAMP levels in OX161/C1 and OX161 ADPKD cells compared to UCL93 control cells (**Fig. 5.18 A**). Levels in another ADPKD line, SKI-001 were raised though not significantly compared to UCL93.

Incubation with PGE2 50nM caused a small but significant increase in cAMP levels in OX161/C1 cells though not in UCL93 cells (**Fig. 5.18 B, C**). Incubation with the PTGER2 antagonist lead to the most striking reduction in cAMP concentrations in OX161/C1 cells, even below that of DMSO controls. No significant effect of either receptor antagonist was seen in normal cell line UCL93. These results suggest that PGE2 exerts its effects mainly through the PTGER2 receptor in human ADPKD cells and this is in agreement with the results seen in chapter 4 which shows that PTGER2 is over-expressed in ADPKD cells and tissue sections.

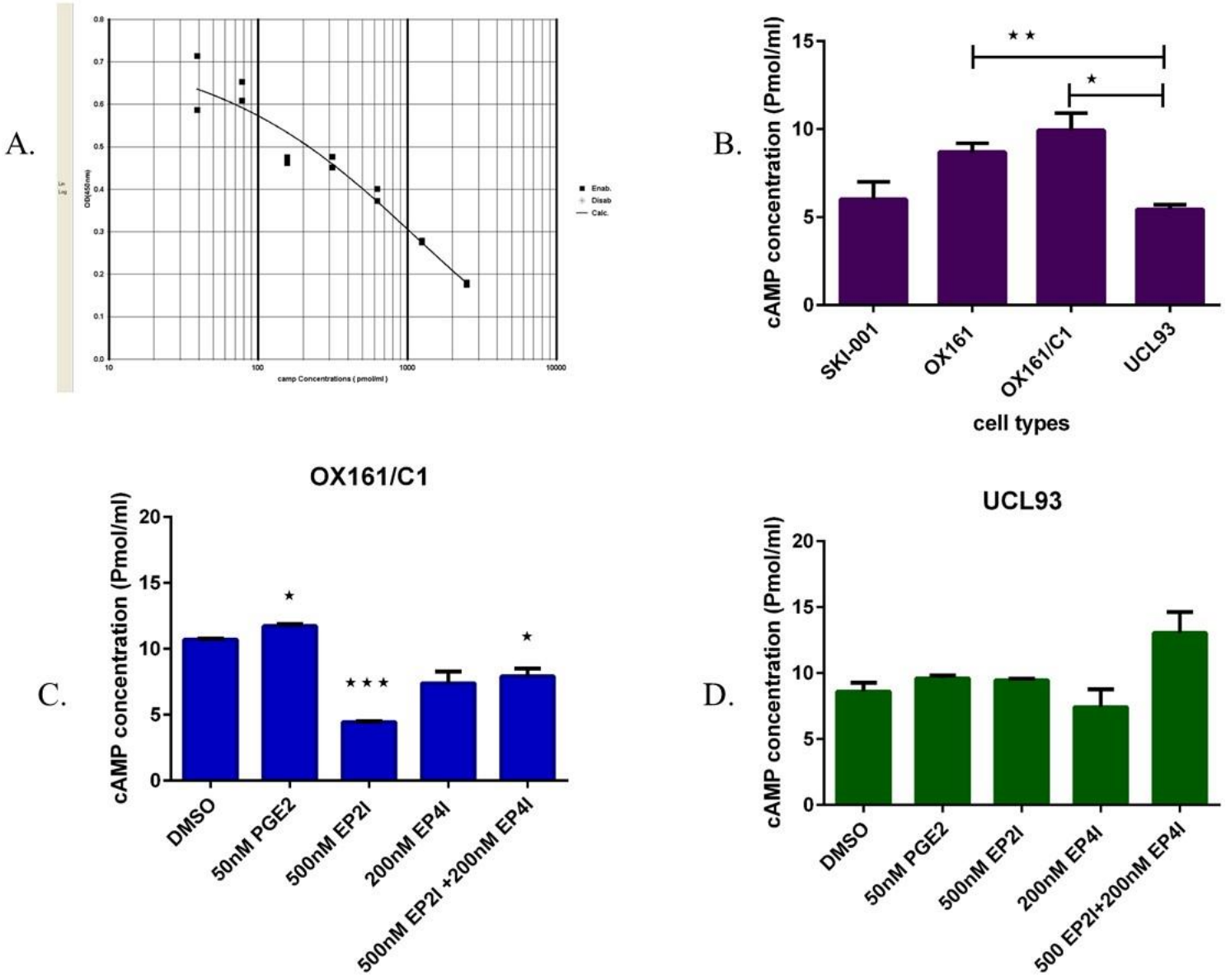

5.18. The effect of PGE2 on cAMP levels in cystic and normal cell lines.

(A). A standard curve of cAMP level created using computer software that generate four parameter logistic (4-PL) curves- fit.

(B). Basal cAMP levels in cystic (OX161/C1, OX161, SKI-001) and control (UCL93) cell lines. *p<0.05; **p<0.01. cAMP levels in SKI-001 were slightly higher than control but not significantly. (n=2). One-way ANOVA test was used. p= 0.22.

(C). PGE2 stimulated cAMP in OX161/C1 cells and this was blocked by the PTGER2 but not the PTGER4 antagonist. *p<0.05; ***p<0.001. (n=3). One-way ANOVA test was used.

(D). PGE2 had no effect on cAMP in UCL93 cells and there were no effects of the PTGER2 and PTGER4 antagonists. (n=3). One-way ANOVA test was used. Data represented as mean± SEM.

5.4. Discussion.

In this chapter, I have studied the possible role of PGE2 in cyst formation using established and unique cellular models. In chapter 3, I had demonstrated that PGE2, like cAMP, increases average cyst area in ADPKD cyst assays **(Figure 3.13 and 3.14).** In this chapter, I showed that PGE2 stimulated cellular proliferation in all ADPKD cell lines tested. PGE2 caused an increase in the proliferation of human renal epithelial cystic cells (OX161/C1, SKI-001, OX938 and OX161) by MTS and BrdU proliferation assays **(Figure 5.1 and 5.2)**. However, normal cell lines (UCL93, and RFH) showed a decrease in proliferation when treated with PGE2, especially at concentrations of 50nM **(Figure 5.1 and 5.2)**. These results are in agreement with those obtained by Liu and Rajagopal 2012 (Liu, Rajagopal et al. 2012) in which PGE2 inhibited the proliferation of wild type renal cells. Using selective receptor antagonists, PTGER2 and PTGER4 were found to inhibit the proliferation and cyst formation in ADPKD cells.

The effects of PGE2 on apoptosis (identified by TUNEL assay and cleaved caspase-3 staining) were more variable. In two human cystic epithelial cells (OX161/C1, and SKI-001) and MDCKII cells, exogenous PGE2 decreased apoptosis or there was a significant increase in apoptosis with PTGER2 or PTGER4 antagonists suggesting an anti-apoptotic effect of endogenous PGE2 **(Figure 5.10 and 5.11)**. These effects were more variable in the other cells.

The anti-apoptotic effect of PGE2 is consistent with a previous report in human cystic cells in which there was a significant decrease of apoptosis by 22% (TUNEL assay) with PGE2 (Elberg, Elberg et al. 2007). Other studies have shown that there is decreased apoptosis in tumour cells treated with PGE2 (Nasrallah, Hassouneh et al. 2014, Xia, Ma et al. 2014). Overall, my results are consistent with primary effects of PGE2 on both proliferation and apoptosis, mediated through both PTGER2 and PTGER4.

I found that PTGER2 and PTGER4 receptor antagonists reduced the average cyst area in 3D gels (**Figure 5.12, 5.13, 5.14, 5.16, and 5.17**). There was a trend towards reduced proliferation when the cells were treated with PTGER2 and PTGER4 antagonists **(Figure 5.3, 5.4 and 5.8).** Although the PTGER4 antagonist inhibited proliferation and cyst formation in cystic cell lines (**Figure 5.5, 5.6, 5.14 and 5.17),** it paradoxically increased cyst formation and increased proliferation of MDCKII and normal cell lines especially in high dose 10µM (**Figures 5.5, 5.6, 5.7, 5.8 and 5.15).** This finding was unexpected and suggests that the PTGER4 antagonist may at very high doses, produce nonspecific effects; or it act in a different manner in non-cystic cells. However, there were also differences between the different ADPKD cell lines in their response to PTGER2 and 4 receptor antagonists. The causes of these differences are unknown but could be due to genetic (mutations, background) or phenotypic (age, tubular origin) variability.

In the study conducted by Elberg *et al* a PTGER2 antagonist (PF-04418948) was applied in a dose range of 0.01 - 10µM and a PTGER4 antagonist (CJ-42794) was applied in a dose range of 10nM - 10µM. These experiments were carried out in 3D cultures using a mouse model cell line (IMCD-3). The effective dose of CJ-42794 that inhibited cystogenesis was 100nM while no effect of a PTGER2 antagonist was seen even at high (10µM) concentrations (Elberg, Turman et al. 2012).

In this study human and dog kidney cell lines were studied in 3D cyst assays. A PTGER2 antagonist was used at a dose range of 100nM - 10µM to ensure high penetration of antagonist to the cells in the gel and media in 3D culture. The most effective dose was 500nM. A PTGER4 antagonist was used at a dose range of 100nM - 10µM and the most effective dose was 200nM. These concentrations are similar to the IC50 values previously reported for these inhibitors.

A recent study of non-steroidal anti-inflammatory drug (NSAID) (celecoxib) in ADPKD has shown that COX2 acts through inhibition of PGE2 and decreases cell proliferation in ADPKD cells by targeting the apoptosis pathway and inducing cell cycle arrest (Xu, Wang et al. 2012). Several reports of NSAIDs have shown that they can decrease the growth of tumour cells. Indomethacin has been shown to have anti-tumour activity in colon cancer cells (Ikawa, Fujino et al. 2012). In addition, diclofenac treatment can lead to increased apoptosis of tumour cells in colon cancer by inhibiting the COX2 and PGE2 pathways (Kaur and Sanyal 2010). However, the long term use of NSAIDs is complicated by increased cardiovascular risks (van den Bemt, Tjwa et al. 2014).

Targeting PTGER2 receptors through the use of highly selective antagonists could result in fewer side effects than NSAIDs (Eriksen, Richelsen et al. 1987). A clinical trial conducted with PTGER4 selective antagonists in colon cancer reported inhibition of PGE2-induced cell proliferation mediated through ERK1/2 and CREB pathways (Cherukuri, Chen et al. 2007).-In hepatic cellular carcinoma, a PTGER2 receptor antagonist was shown to induce apoptosis in tumour cells through the upregulation of caspase-3 (Xia, Ma et al. 2014).

In summary, these results provide the first evidence that specific PTGER2 and PTGER4 antagonists can inhibit cystic cell proliferation and cystogenesis suggesting they could be potential novel treatments for ADPKD through reducing cAMP.

Chapter 6

General discussion and conclusions

6.1. General discussion.

The major aim of this thesis was to investigate the role of prostaglandin E2 in the pathogenesis of ADPKD and to determine the receptor subtypes that could mediate its cellular responses in models of cystogenesis.

One of the most important pathological mechanisms thought to regulate cyst expansion is increased levels of cyclic AMP. Activation of PKA by cAMP is responsible for activating a number of pro-proliferative pathways e.g. PTGER2, Wnt/β-catenin pathways, EGF and IGF-1 (Song, Di Giovanni et al. 2009). The basis for increased cAMP levels in ADPKD is not completely understood but could include changes in calcium-dependent synthesis (adenylate cyclases) and/or breakdown (phosphodiesterase). In addition, the upregulation of certain G-protein coupled receptors such as vasopressin-2 (V2R) in mouse models of ADPKD has been shown to increase ligand-activated cAMP production (Torres, Wang et al. 2004). Treatments that modulate these signalling pathways may therefore be novel therapeutic targets for ADPKD.

A preliminary microarray study in our laboratory was first carried out to investigate differential changes in gene expression between ADPKD and non-ADPKD human kidney cell lines. This demonstrated that PTGER2 expression was upregulated in ADPKD cystic cell lines compared to the normal cell lines (chapter 4). Previous studies have also reported an increase in expression of PTGER2 in ADPKD cell lines (Elberg, Elberg et al. 2007, Song, Di Giovanni et al. 2009). Based on this pilot data, two main objective of this thesis were proposed. Firstly, to investigate the role of PGE2 and expression of its receptors PTGER2 and PTGER4 in ADPKD cell lines. Secondly, to investigate whether specific PTGER2 and 4 receptor antagonists could inhibit cyst formation in *in vitro* using models of cystogenesis.

The first challenge was to optimise an *in-vitro* cyst assay which could be used to mimic cystogenesis of human ADPKD kidney epithelial cells (chapter 3). Different matrices (Collagen, Matrigel and combination of the two) were used to culture human cystic and normal cells in a 3D matrix. Four cystic cell lines (OX161, OX938, OX161/C1 and SKI-001) and one normal cell line (UCL93) were successfully grown in 3D cultures. One cystic line (SKI-002) and one normal cell line (RFH) did not grow in any of the 3D culture conditions used. However, most of the cystic cell lines formed either very small cysts or developed branching tubules similar to the normal cell line. Only the cystic cell line OX161/C1 reliably formed cysts which increased in size over time in a 3D Matrigel environment. This cell line was therefore chosen for further study. A second cellular model of cystogenesis, MDCKII, was used since it is a well-established model.

The effects of PGE2, cAMP and Forskolin on cystogenesis in MDCK cells have been previously reported (Mangoo-Karim, Uchic et al. 1989). I confirmed these results and also showed that cAMP, Forskolin and PGE2 similarly increased cyst expansion in OX161/C1 cells (see in chapter 3).

I initially validated the microarray results on PTGER2 by qPCR. No significant increases in the other PTGER receptors (PTGER1, PTGER3 and PTGER4) were seen in ADPKD cells (chapter 4). Immunoblotting of PTGER2 and PTGER4 receptors in human cystic cells and normal cells revealed increased expression of PTGER2 in the cystic cell lines. In agreement with our microarray data, the PTGER4 receptor was expressed equally in both normal and cystic cell lines (chapter 4).

The renal expression of PTGER receptors by qPCR was then studied in two orthologous Pkd1 mouse models of ADPKD, the Neolox model (Happe, van der Wal et al. 2013) and the CreLox mode l(Lantinga-van Leeuwen, Leonhard et al. 2007) . In contrast to the human cells, both

PTGER2 and PTGER4 receptor expression were found to be significantly higher in cystic kidneys compared to controls.

Immunohistochemistry of human tissues taken from patients with defined mutations in *PKD1* illustrated that the PTGER2 receptor was highly expressed in the apical membrane of dilated tubules compared to control tissue. PTGER4 receptor expression was not significantly different in cystic tissue sections. Immunohistochemistry of the two mouse models of ADPKD revealed similar increased tubular expression of PTGER2 receptors compared to the controls. For PTGER4, staining intensity was significantly different compared to controls only in the NeoLox model.

Differences in the findings between human and mouse tissues could reflect species differences in the expression of PTGER2 and PTGER4. Although PTGER2 has been reported in human epithelial ADPKD cells (Elberg, Elberg et al. 2007), it is absent in mouse IMCD-3 cells where PTGER4 is the functional receptor mediating the effects of PGE2 on proliferation and fluid secretion. Similarly, although all four PTGER receptors are expressed equally in MDCK cells, PTGER2 is the main receptor subtype mediating proliferation and sodium reabsorption (Wegmann and Nusing 2003) (Matlhagela and Taub 2006). Despite the lack of PTGER4 upregulation in human cystic epithelia, my findings suggest that it is functional in mediating proliferation, apoptosis and cyst formation. Of note, the PTGER4 receptor has a higher binding affinity for PGE2 compared to PTGER2 (Fujino and Regan 2006).

In summary, our data generated using microarray, qPCR, immunoblotting and immunostaining provide evidence of an increase expression of PTGER2 in human cystic cells and tissues compared to normal controls and provide a rational for testing the effectiveness of PTGER2 and 4 receptor antagonists on reducing proliferation and inhibiting cyst growth in 3D cyst assays.

In the majority of our ADPKD cell lines, I observed a consistent increase in proliferation in response to PGE2 and a more variable decrease in apoptosis. These results are consistent with previous reports in PC-1 deficient cells (Yamaguchi, Pelling et al. 2000, Liu, Rajagopal et al. 2012). Furthermore, I found a corresponding inhibition of proliferation and increase in apoptosis when these cells were treated with PTGER2 and PTGER4 antagonists. Therefore these responses appear to be mediated by both receptor subtypes.

PTGER2 and PTGER4 antagonists both inhibited PGE2 stimulated cyst formation in OX161/C1 cells. However, the PTGER4 antagonist appeared to stimulate cyst formation in MDCKII cells, unlike the effect of PTGER2 blockade. The reason for this is unclear. Potentially, inhibition of PTGER4 might bypass or shift PGE2 action to an alternative proliferative pathway, similar to the bypass pathway that occurs after selective inhibition of oncogenic signalling in tumours (Niederst and Engelman 2013).

Following the apparent success of these novel PTGER antagonists at inhibiting cystogenesis in *in vitro* cell culture models of ADPKD, the next step would be to test the effectiveness of these compounds in mouse models of ADPKD. However, prostanoid antagonists should be used with caution as PGE2 and PTGER2 and 4 receptor signalling play important roles in the regulation of many different functions in mammals. PTGER2 for example, acts to suppress premature labour and maintaining normal pregnancy. A PTGER2 antagonist was demonstrated to induce premature labour in female monkeys (Peluffo, Stanley et al. 2014). Furthermore, PTGER2 signalling promotes neuroprotection in excitotoxicity, and is important in neural plasticity and long term memory formation (Jiang and Dingledine 2013). PTGER2 and PTGER4 receptor signalling has a bronchodilator effect in asthma in both a human and mouse model (Norel, Walch et al. 1999, Sheller, Mitchell et al. 2000). In addition, both receptors stimulate vasodilation in vascular afferent arterioles smooth muscle which is important in regulating blood pressure and salt water balance in the kidney. Furthermore, PTGER2 and

PTGER4 increase bone formation and protect from osteoporosis in animal study (Li, Okada et al. 2000, Ushikubi, Sugimoto et al. 2000). PTGER4 signalling plays an important role in embryonic development by increasing glomeruli size, PTGER4 knockout mice show a reduction in the size of glomeruli (Aoudjit, Potapov et al. 2006). Outside the kidney, PTGER4 signalling plays an important role in the development of ductus arterioles in embryonic life. PTGER4 signalling also plays an important role in immunomodulation and inflammation by modulating T-cell and macrophage function (Tang, Libby et al. 2012). It also is important in colitis and gastric ulcer healing and acts to decrease inflammation during myocardial infarction (Woodward, Jones et al. 2011, Zimecki 2012).

However therapeutic interventions targeting PTGER have been used successfully with minimal side effects in a number of clinical studies in humans as well as in mouse disease models. PTGER2 antagonist have produced promising results by decreasing the chronic inflammation associated with status epileptics, Alzheimer's and Parkinson's disease in animal model with few side effect (Jiang and Dingledine 2013). Furthermore, genetic ablation of $EP^{-/-}$ reduced skin tumour size in a mouse model by decreasing proliferation, angiogenesis and apoptosis (Sung, He et al. 2006). Interestingly genetically engineered or chemically mutant mice which lack PTGER2 and PTGER4 have been shown to have an obvious decrease in colon cancer incidence (Ushikubi, Sugimoto et al. 2000). From these studies it is clear that Prostanoid antagonist should be studied as a next generation of therapeutic agents in the treatment of cancer and inflammatory conditions rather than COX2 inhibitors which cause side effect in the cardiovascular and gastrointestinal system.

Despite the promising result of the antagonists used in this study there use in human ADPKD must be viewed with caution as side effects could occur in other tissues in response to receptor antagonism. The similarities between receptor function in human and mouse means

investigation must be carried out first in mouse orthologues to human ADPKD and localised drug delivery may be safer to decrease systemic absorption and reduce side effects.

6.2. Limitations.

One of limitations of this study was the difficulty in inducing human cystic epithelial cells to form cysts in 3 D culture. OX161/C1 was the only cell line that form polarised cysts in 3 D culture. In addition, the proliferative and apoptotic responses to PGE2 were variable between different lines. The causes of variability might be due to the fact that cells were obtained from different ADPKD patients with different genetic and environmental backgrounds and types of PC-1 mutation (germline or somatic, complete or partial) or different PTGER receptor expression. In addition, different lines could have originated from different tubular segments or a mixture of cell types.

6.3. Conclusions.

Data presented in this thesis demonstrates that PGE2 and its receptors could play a key role in the pathogenesis of ADPKD. PTGER2 expression was significantly increased in ADPKD cell lines and human tissues and PTGER2 and 4 were significantly increased in orthologous mouse models of ADPKD. Stimulation of human ADPKD cell lines with PGE2 significantly increased proliferation which was blocked by selective PTGER2 and 4 receptor antagonists in monolayer cultures. More importantly in 3D cyst assays, PTGER2 and 4 receptor antagonists were able to significantly inhibit cyst growth of ADPKD cells. These experiments provide a proof of concept for the use of PTGER receptor antagonists as a novel therapy for the treatment of ADPKD.

6.4. Future work.

These results will serve as the basis for future mechanistic studies on PTGER2 and PTGER4 antagonists in ADPKD cells e.g. to examine the changes in cell signalling pathways that occur downstream of PTGER2 and PTGER4 stimulation. In addition, PTGER2 or PTGER4 knockdown experiments by siRNA could be attempted in ADPKD cells.

To further characterise the effect of PTGER2 and PTGER4 on ADPKD progression, we could compare the effect of crossing PTGER2 ($EP2^{-/-}$) or PTGER4 knockout mice ($EP4^{-/-}$) with ADPKD mice models, for example the Neolox or tamoxifen induced model used in this study, as well as ADPKD models already utilised in previous studies of ADPKD such as *pkd1*^{fl} (Shibazaki, Yu et al. 2008), *pkd2*^{fl} (Nishio, Tian et al. 2010), and ksp-cre (Shao, Johnson et al. 2002) with predominant C57B1/6 genetic background (Ma, Tian et al. 2013). If signalling through PTGER receptors contribute to ADPKD progression, then crossing receptor knockouts with ADPKD models should result in slower disease progression. Taking a similar approach, ADPKD researchers have demonstrated that combining conditional inactivation of polycystin genes with knockout of cilia genes supresses cyst growth highlighting the importance of primary cilia signalling in cyst progression (Ma, Tian et al. 2013).Disease progression would be evaluated following measurement of kidney weight to body weight ratio, serum urea, creatinine and percentage of cystic area. Finally, there is a need to validate the effects of PTGER2 and PTGER4 antagonists in animal models of ADPKD prior to clinical trials.

References

Abbott, K. C. and L. Y. Agodoa (2002). "Polycystic kidney disease in patients on the renal transplant waiting list: trends in hematocrit and survival." BMC Nephrol **3**: 7.

Abramovitz, M., M. Adam, Y. Boie, M. Carriere, D. Denis, C. Godbout, S. Lamontagne, C. Rochette, N. Sawyer, N. M. Tremblay, M. Belley, M. Gallant, C. Dufresne, Y. Gareau, R. Ruel, H. Juteau, M. Labelle, N. Ouimet and K. M. Metters (2000). "The utilization of recombinant prostanoid receptors to determine the affinities and selectivities of prostaglandins and related analogs." Biochim Biophys Acta **1483**(2): 285-293.

af Forselles, K. J., J. Root, T. Clarke, D. Davey, K. Aughton, K. Dack and N. Pullen (2011). "In vitro and in vivo characterization of PF-04418948, a novel, potent and selective prostaglandin EP(2) receptor antagonist." Br J Pharmacol **164**(7): 1847-1856.

Antonucci, R., L. Cuzzolin, A. Arceri and V. Fanos (2007). "Urinary prostaglandin E2 in the newborn and infant." Prostaglandins Other Lipid Mediat **84**(1-2): 1-13.

Aoudjit, L., A. Potapov and T. Takano (2006). "Prostaglandin E2 promotes cell survival of glomerular epithelial cells via the EP4 receptor." Am J Physiol Renal Physiol **290**(6): F1534-1542.

Ashley, N., T. M. Yeung and W. F. Bodmer (2013). "Stem cell differentiation and lumen formation in colorectal cancer cell lines and primary tumors." Cancer Res **73**(18): 5798-5809.

Aukema, H. M., J. Adolphe, S. Mishra, J. Jiang, F. P. Cuozzo and M. R. Ogborn (2003). "Alterations in renal cytosolic phospholipase A2 and cyclooxygenases in polycystic kidney disease." Faseb j **17**(2): 298-300.

Badano, J. L., N. Mitsuma, P. L. Beales and N. Katsanis (2006). "The ciliopathies: an emerging class of human genetic disorders." Annu Rev Genomics Hum Genet **7**: 125-148.

Ball, B. A., K. E. Scoggin, M. H. Troedsson and E. L. Squires (2013). "Characterization of prostaglandin E2 receptors (EP2, EP4) in the horse oviduct." Anim Reprod Sci **142**(1-2): 35-41.

Becker, J. L. and D. K. Blanchard (2007). "Characterization of primary breast carcinomas grown in three-dimensional cultures." J Surg Res **142**(2): 256-262.

Belibi, F. A., G. Reif, D. P. Wallace, T. Yamaguchi, L. Olsen, H. Li, G. M. Helmkamp, Jr. and J. J. Grantham (2004). "Cyclic AMP promotes growth and secretion in human polycystic kidney epithelial cells." Kidney Int **66**(3): 964-973.

Belibi, F. A., D. P. Wallace, T. Yamaguchi, M. Christensen, G. Reif and J. J. Grantham (2002). "The effect of caffeine on renal epithelial cells from patients with autosomal dominant polycystic kidney disease." J Am Soc Nephrol **13**(11): 2723-2729.

Benelli, R. and A. Albini (1999). "In vitro models of angiogenesis: the use of Matrigel." Int J Biol Markers **14**(4): 243-246.

Benton, G., J. George, H. K. Kleinman and I. P. Arnaoutova (2009). "Advancing science and technology via 3D culture on basement membrane matrix." J Cell Physiol **221**(1): 18-25.

Bergmann, C., J. Senderek, F. Kupper, F. Schneider, C. Dornia, E. Windelen, T. Eggermann, S. Rudnik-Schoneborn, J. Kirfel, L. Furu, L. F. Onuchic, S. Rossetti, P. C. Harris, S. Somlo, L. Guay-Woodford, G. G. Germino, M. Moser, R. Buttner and K. Zerres (2004). "PKHD1 mutations in autosomal recessive polycystic kidney disease (ARPKD)." Hum Mutat **23**(5): 453-463.

Bhunia, A. K., K. Piontek, A. Boletta, L. Liu, F. Qian, P. N. Xu, F. J. Germino and G. G. Germino (2002). "PKD1 induces p21(waf1) and regulation of the cell cycle via direct activation of the JAK-STAT signaling pathway in a process requiring PKD2." Cell **109**(2): 157-168.

Birrell, M. A. and A. T. Nials (2011). "At last, a truly selective EP2 receptor antagonist." British journal of pharmacology **164**(7): 1845-1846.

Blair, H. A. and G. M. Keating (2015). "Tolvaptan: A Review in Autosomal Dominant Polycystic Kidney Disease." Drugs **75**(15): 1797-1806.

Borrelli, E., J. P. Montmayeur, N. S. Foulkes and P. Sassone-Corsi (1992). "Signal transduction and gene control: the cAMP pathway." Crit Rev Oncog **3**(4): 321-338.

Boulter, C., S. Mulroy, S. Webb, S. Fleming, K. Brindle and R. Sandford (2001). "Cardiovascular, skeletal, and renal defects in mice with a targeted disruption of the Pkd1 gene." Proc Natl Acad Sci U S A **98**(21): 12174-12179.

Bourne, H. R., G. M. Tomkins and S. Dion (1973). "Regulation of phosphodiesterase synthesis: requirement for cyclic adenosine monophosphate-dependent protein kinase." Science **181**(103): 952-954.

Branda, C. S. and S. M. Dymecki (2004). "Talking about a revolution: The impact of site-specific recombinases on genetic analyses in mice." Dev Cell **6**(1): 7-28.

Breyer, M. D. and R. M. Breyer (2000). "Prostaglandin E receptors and the kidney." Am J Physiol Renal Physiol **279**(1): F12-23.

Breyer, M. D., L. Davis, H. R. Jacobson and R. M. Breyer (1996). "Differential localization of prostaglandin E receptor subtypes in human kidney." Am J Physiol **270**(5 Pt 2): F912-918.

Breyer, M. D., H. R. Jacobson and R. M. Breyer (1996). "Functional and molecular aspects of renal prostaglandin receptors." J Am Soc Nephrol **7**(1): 8-17.

Buchholz, B., B. Teschemacher, G. Schley, H. Schillers and K. U. Eckardt (2011). "Formation of cysts by principal-like MDCK cells depends on the synergy of cAMP- and ATP-mediated fluid secretion." J Mol Med (Berl) **89**(3): 251-261.

Caroli, A., N. Perico, A. Perna, L. Antiga, P. Brambilla, A. Pisani, B. Visciano, M. Imbriaco, P. Messa, R. Cerutti, M. Dugo, L. Cancian, E. Buongiorno, A. De Pascalis, F. Gaspari, F. Carrara, N. Rubis, S. Prandini, A. Remuzzi, G. Remuzzi and P. Ruggenenti (2013). "Effect of longacting somatostatin analogue on kidney and cyst growth in autosomal dominant polycystic kidney disease (ALADIN): a randomised, placebo-controlled, multicentre trial." Lancet **382**(9903): 1485-1495.

Castellone, M. D., H. Teramoto, B. O. Williams, K. M. Druey and J. S. Gutkind (2005). "Prostaglandin E2 promotes colon cancer cell growth through a Gs-axin-beta-catenin signaling axis." Science **310**(5753): 1504-1510.

Cha, Y. I., L. Solnica-Krezel and R. N. DuBois (2006). "Fishing for prostanoids: deciphering the developmental functions of cyclooxygenase-derived prostaglandins." Dev Biol **289**(2): 263-272.

Chang, F., L. S. Steelman, J. G. Shelton, J. T. Lee, P. M. Navolanic, W. L. Blalock, R. Franklin and J. A. McCubrey (2003). "Regulation of cell cycle progression and apoptosis by the Ras/Raf/MEK/ERK pathway (Review)." Int J Oncol **22**(3): 469-480.

Chapin, H. C. and M. J. Caplan (2010). "The cell biology of polycystic kidney disease." J Cell Biol **191**(4): 701-710.

Chapman, A. B., L. M. Guay-Woodford, J. J. Grantham, V. E. Torres, K. T. Bae, D. A. Baumgarten, P. J. Kenney, B. F. King, Jr., J. F. Glockner, L. H. Wetzel, M. E. Brummer, W. C. O'Neill, M. L. Robbin, W. M. Bennett, S. Klahr, G. H. Hirschman, P. L. Kimmel, P. A. Thompson and J. P. Miller (2003). "Renal structure in early autosomal-dominant polycystic kidney disease (ADPKD): The Consortium for Radiologic Imaging Studies of Polycystic Kidney Disease (CRISP) cohort." Kidney Int **64**(3): 1035-1045.

Chapman, A. B., V. E. Torres, R. D. Perrone, T. I. Steinman, K. T. Bae, J. P. Miller, D. C. Miskulin, F. Rahbari Oskoui, A. Masoumi, M. C. Hogan, F. T. Winklhofer, W. Braun, P. A. Thompson, C. M. Meyers, C. Kelleher and R. W. Schrier (2010). "The HALT polycystic kidney disease trials: design and implementation." Clin J Am Soc Nephrol **5**(1): 102-109.

Chebib, F. T., C. R. Sussman, X. Wang, P. C. Harris and V. E. Torres (2015). "Vasopressin and disruption of calcium signalling in polycystic kidney disease." Nat Rev Nephrol.

Chen, S. S., R. P. Revoltella, S. Papini, M. Michelini, W. Fitzgerald, J. Zimmerberg and L. Margolis (2003). "Multilineage differentiation of rhesus monkey embryonic stem cells in three-dimensional culture systems." Stem Cells **21**(3): 281-295.

Chen, X., J. Guo, H. Zhang, K. Zuo, Y. Wei, J. Shi, H. Li and G. Xu (2014). "[Expression and regulation of tight junction protein Occludin in nasal polyps]." Zhonghua Er Bi Yan Hou Tou Jing Wai Ke Za Zhi **49**(7): 568-573.

Cherukuri, D. P., X. B. Chen, A. C. Goulet, R. N. Young, Y. Han, R. L. Heimark, J. W. Regan, E. Meuillet and M. A. Nelson (2007). "The EP4 receptor antagonist, L-161,982, blocks prostaglandin E2-induced signal transduction and cell proliferation in HCA-7 colon cancer cells." Exp Cell Res **313**(14): 2969-2979.

Conti, M. (2000). "Phosphodiesterases and cyclic nucleotide signaling in endocrine cells." Mol Endocrinol **14**(9): 1317-1327.

Costello-Boerrigter, L. C., G. Boerrigter and J. C. Burnett, Jr. (2009). "Pharmacology of vasopressin antagonists." Heart Fail Rev **14**(2): 75-82.

Cowley, B. D., Jr. (2008). "Calcium, cyclic AMP, and MAP kinases: dysregulation in polycystic kidney disease." Kidney Int **73**(3): 251-253.

Cukierman, E., R. Pankov, D. R. Stevens and K. M. Yamada (2001). "Taking cell-matrix adhesions to the third dimension." Science **294**(5547): 1708-1712.

Dal Vechio, A. M., F. S. Giudice, F. F. Sperandio, A. Mantesso and S. Pinto Junior Ddos (2011). "Vimentin expression and the influence of Matrigel in cell lines of head and neck squamous cell carcinoma." Braz Oral Res **25**(3): 235-240.

Daniels, R. H., P. S. Hall and G. M. Bokoch (1998). "Membrane targeting of p21-activated kinase 1 (PAK1) induces neurite outgrowth from PC12 cells." EMBO J **17**(3): 754-764.

De Keijzer, S., M. B. Meddens, R. Torensma and A. Cambi (2013). "The multiple faces of prostaglandin E2 G-protein coupled receptor signaling during the dendritic cell life cycle." Int J Mol Sci **14**(4): 6542-6555.

Deane, J. A. and S. D. Ricardo (2007). "Polycystic kidney disease and the renal cilium." Nephrology (Carlton) **12**(6): 559-564.

Debnath, J., S. K. Muthuswamy and J. S. Brugge (2003). "Morphogenesis and oncogenesis of MCF-10A mammary epithelial acini grown in three-dimensional basement membrane cultures." Methods **30**(3): 256-268.

Delmas, P., H. Nomura, X. Li, M. Lakkis, Y. Luo, Y. Segal, J. M. Fernandez-Fernandez, P. Harris, A. M. Frischauf, D. A. Brown and J. Zhou (2002). "Constitutive activation of G-proteins by polycystin-1 is antagonized by polycystin-2." J Biol Chem **277**(13): 11276-11283.

Desai, S., H. April, C. Nwaneshiudu and B. Ashby (2000). "Comparison of agonist-induced internalization of the human EP2 and EP4 prostaglandin receptors: role of the carboxyl terminus in EP4 receptor sequestration." Mol Pharmacol **58**(6): 1279-1286.

Dorsam, R. T. and J. S. Gutkind (2007). "G-protein-coupled receptors and cancer." Nat Rev Cancer **7**(2): 79-94.

Dumaz, N., R. Hayward, J. Martin, L. Ogilvie, D. Hedley, J. A. Curtin, B. C. Bastian, C. Springer and R. Marais (2006). "In melanoma, RAS mutations are accompanied by switching signaling from BRAF to CRAF and disrupted cyclic AMP signaling." Cancer Res **66**(19): 9483-9491.

Ehrmann, R. L. and G. O. Gey (1956). "The growth of cells on a transparent gel of reconstituted rat-tail collagen." J Natl Cancer Inst **16**(6): 1375-1403.

Elberg, D., M. A. Turman, N. Pullen and G. Elberg (2012). "Prostaglandin E2 stimulates cystogenesis through EP4 receptor in IMCD-3 cells." Prostaglandins Other Lipid Mediat **98**(1-2): 11-16.

Elberg, G., D. Elberg, T. V. Lewis, S. Guruswamy, L. Chen, C. J. Logan, M. D. Chan and M. A. Turman (2007). "EP2 receptor mediates PGE2-induced cystogenesis of human renal epithelial cells." Am J Physiol Renal Physiol **293**(5): F1622-1632.

Elsdale, T. and J. Bard (1972). "Collagen substrata for studies on cell behavior." J Cell Biol **54**(3): 626-637.

Engelberg, J. A., A. Datta, K. E. Mostov and C. A. Hunt (2011). "MDCK cystogenesis driven by cell stabilization within computational analogues." PLoS Comput Biol **7**(4): e1002030.

Erhardt, P., J. Troppmair, U. R. Rapp and G. M. Cooper (1995). "Differential regulation of Raf-1 and B-Raf and Ras-dependent activation of mitogen-activated protein kinase by cyclic AMP in PC12 cells." Mol Cell Biol **15**(10): 5524-5530.

Eriksen, E. F., B. Richelsen, B. P. Gesser, N. O. Jacobsen and K. Stengaard-Pedersen (1987). "Prostaglandin-E2 receptors in the rat kidney: biochemical characterization and localization." Kidney Int **32**(2): 181-186.

Faux, M. C. and J. D. Scott (1996). "Molecular glue: kinase anchoring and scaffold proteins." Cell **85**(1): 9-12.

Feehally (2007). comperhansive clinical nephrology.

Fick, G. M. and P. A. Gabow (1994). "Hereditary and acquired cystic disease of the kidney." Kidney Int **46**(4): 951-964.

Forman, J. R., S. Qamar, E. Paci, R. N. Sandford and J. Clarke (2005). "The remarkable mechanical strength of polycystin-1 supports a direct role in mechanotransduction." J Mol Biol **349**(4): 861-871.

Frickmann, H., E. Schropfer and G. Dobler (2013). "Actin assessment in addition to specific immuno-fluorescence staining to demonstrate rickettsial growth in cell culture." Eur J Microbiol Immunol (Bp) **3**(3): 198-203.

Fridman, R., G. Giaccone, T. Kanemoto, G. R. Martin, A. F. Gazdar and J. L. Mulshine (1990). "Reconstituted basement membrane (matrigel) and laminin can enhance the tumorigenicity and

the drug resistance of small cell lung cancer cell lines." Proc Natl Acad Sci U S A **87**(17): 6698-6702.

Fujino, H. and J. W. Regan (2003). "Prostanoid receptors and phosphatidylinositol 3-kinase: a pathway to cancer?" Trends in Pharmacological Sciences **24**(7): 335-340.

Fujino, H. and J. W. Regan (2006). "EP(4) prostanoid receptor coupling to a pertussis toxin-sensitive inhibitory G protein." Mol Pharmacol **69**(1): 5-10.

Fujino, H., S. Salvi and J. W. Regan (2005). "Differential regulation of phosphorylation of the cAMP response element-binding protein after activation of EP2 and EP4 prostanoid receptors by prostaglandin E2." Mol Pharmacol **68**(1): 251-259.

Fujino, H., K. A. West and J. W. Regan (2002). "Phosphorylation of glycogen synthase kinase-3 and stimulation of T-cell factor signaling following activation of EP2 and EP4 prostanoid receptors by prostaglandin E2." J Biol Chem **277**(4): 2614-2619.

Fujino, H., W. Xu and J. W. Regan (2003). "Prostaglandin E2 induced functional expression of early growth response factor-1 by EP4, but not EP2, prostanoid receptors via the phosphatidylinositol 3-kinase and extracellular signal-regulated kinases." J Biol Chem **278**(14): 12151-12156.

Gabow, P. A. (1993). "Autosomal dominant polycystic kidney disease." N Engl J Med **329**(5): 332-342.

Gardner, K. D., Jr., J. S. Burnside, L. W. Elzinga and R. M. Locksley (1991). "Cytokines in fluids from polycystic kidneys." Kidney Int **39**(4): 718-724.

Gattone, V. H., 2nd, X. Wang, P. C. Harris and V. E. Torres (2003). "Inhibition of renal cystic disease development and progression by a vasopressin V2 receptor antagonist." Nat Med **9**(10): 1323-1326.

Gile, R. D., B. D. Cowley, Jr., V. H. Gattone, 2nd, M. P. O'Donnell, S. K. Swan and J. J. Grantham (1995). "Effect of lovastatin on the development of polycystic kidney disease in the Han:SPRD rat." Am J Kidney Dis **26**(3): 501-507.

Grantham, J. J. (1997). "Pathogenesis of autosomal dominant polycystic kidney disease: recent developments." Contrib Nephrol **122**: 1-9.

Grantham, J. J. (2001). "Polycystic kidney disease: from the bedside to the gene and back." Curr Opin Nephrol Hypertens **10**(4): 533-542.

Grantham, J. J., J. L. Geiser and A. P. Evan (1987). "Cyst formation and growth in autosomal dominant polycystic kidney disease." Kidney Int **31**(5): 1145-1152.

Guan, K. L., C. Figueroa, T. R. Brtva, T. Zhu, J. Taylor, T. D. Barber and A. B. Vojtek (2000). "Negative regulation of the serine/threonine kinase B-Raf by Akt." J Biol Chem **275**(35): 27354-27359.

Guan, Y., B. A. Stillman, Y. Zhang, A. Schneider, O. Saito, L. S. Davis, R. Redha, R. M. Breyer and M. D. Breyer (2002). "Cloning and expression of the rabbit prostaglandin EP2 receptor." BMC Pharmacol **2**: 14.

Hanaoka, K., O. Devuyst, E. M. Schwiebert, P. D. Wilson and W. B. Guggino (1996). "A role for CFTR in human autosomal dominant polycystic kidney disease." Am J Physiol **270**(1 Pt 1): C389-399.

Hanaoka, K. and W. B. Guggino (2000). "cAMP regulates cell proliferation and cyst formation in autosomal polycystic kidney disease cells." J Am Soc Nephrol **11**(7): 1179-1187.

Hanaoka, K., F. Qian, A. Boletta, A. K. Bhunia, K. Piontek, L. Tsiokas, V. P. Sukhatme, W. B. Guggino and G. G. Germino (2000). "Co-assembly of polycystin-1 and -2 produces unique cation-permeable currents." Nature **408**(6815): 990-994.

Happe, H., A. M. van der Wal, D. C. Salvatori, W. N. Leonhard, M. H. Breuning, E. de Heer and D. J. Peters (2013). "Cyst expansion and regression in a mouse model of polycystic kidney disease." Kidney Int **83**(6): 1099-1108.

Harris, P. C. and V. E. Torres (2014). "Genetic mechanisms and signaling pathways in autosomal dominant polycystic kidney disease." J Clin Invest **124**(6): 2315-2324.

Hata, A. N. and R. M. Breyer (2004). "Pharmacology and signaling of prostaglandin receptors: multiple roles in inflammation and immune modulation." Pharmacol Ther **103**(2): 147-166.

Hateboer, N., M. A. v Dijk, N. Bogdanova, E. Coto, A. K. Saggar-Malik, J. L. San Millan, R. Torra, M. Breuning and D. Ravine (1999). "Comparison of phenotypes of polycystic kidney disease types 1 and 2. European PKD1-PKD2 Study Group." Lancet **353**(9147): 103-107.

Hawcroft, G., C. W. Ko and M. A. Hull (2007). "Prostaglandin E2-EP4 receptor signalling promotes tumorigenic behaviour of HT-29 human colorectal cancer cells." Oncogene **26**(21): 3006-3019.

Higashihara, E., V. E. Torres, A. B. Chapman, J. J. Grantham, K. Bae, T. J. Watnick, S. Horie, K. Nutahara, J. Ouyang, H. B. Krasa and F. S. Czerwiec (2011). "Tolvaptan in autosomal dominant polycystic kidney disease: three years' experience." Clin J Am Soc Nephrol **6**(10): 2499-2507.

Houslay, M. D. and G. Milligan (1997). "Tailoring cAMP-signalling responses through isoform multiplicity." Trends Biochem Sci **22**(6): 217-224.

Hughes, J., C. J. Ward, B. Peral, R. Aspinwall, K. Clark, J. L. San Millan, V. Gamble and P. C. Harris (1995). "The polycystic kidney disease 1 (PKD1) gene encodes a novel protein with multiple cell recognition domains." Nat Genet **10**(2): 151-160.

Hwang, Y. H., J. Conklin, W. Chan, N. M. Roslin, J. Liu, N. He, K. Wang, J. L. Sundsbak, C. M. Heyer, M. Haider, A. D. Paterson, P. C. Harris and Y. Pei (2015). "Refining Genotype-Phenotype Correlation in Autosomal Dominant Polycystic Kidney Disease." J Am Soc Nephrol.

Ikawa, Y., H. Fujino, S. Otake and T. Murayama (2012). "Indomethacin antagonizes EP(2) prostanoid receptor activation in LS174T human colon cancer cells." Eur J Pharmacol **680**(1-3): 16-21.

Inoki, K., Y. Li, T. Zhu, J. Wu and K. L. Guan (2002). "TSC2 is phosphorylated and inhibited by Akt and suppresses mTOR signalling." Nat Cell Biol **4**(9): 648-657.

Jaffe, A. B., N. Kaji, J. Durgan and A. Hall (2008). "Cdc42 controls spindle orientation to position the apical surface during epithelial morphogenesis." J Cell Biol **183**(4): 625-633.

Jiang, J. and R. Dingledine (2013). "Prostaglandin receptor EP2 in the crosshairs of anti-inflammation, anti-cancer, and neuroprotection." Trends Pharmacol Sci **34**(7): 413-423.

Kaur, J. and S. N. Sanyal (2010). "PI3-kinase/Wnt association mediates COX-2/PGE(2) pathway to inhibit apoptosis in early stages of colon carcinogenesis: chemoprevention by diclofenac." Tumour Biol **31**(6): 623-631.

Kher, R., E. C. Sha, M. R. Escobar, E. M. Andreoli, P. Wang, W. M. Xu, A. Wandinger-Ness and R. L. Bacallao (2011). "Ectopic expression of cadherin 8 is sufficient to cause cyst formation in a novel 3D collagen matrix renal tubule culture." Am J Physiol Cell Physiol **301**(1): C99-C105.

Klawitter, J., K. McFann, A. T. Pennington, W. Wang, J. Klawitter, U. Christians, R. W. Schrier, B. Gitomer and M. A. Cadnapaphornchai (2015). "Pravastatin Therapy and Biomarker Changes in Children and Young Adults with Autosomal Dominant Polycystic Kidney Disease." Clin J Am Soc Nephrol.

Klawitter, J., B. Y. Reed-Gitomer, K. McFann, A. Pennington, J. Klawitter, K. Z. Abebe, J. Klepacki, M. A. Cadnapaphornchai, G. Brosnahan, M. Chonchol, U. Christians and R. W. Schrier (2014). "Endothelial dysfunction and oxidative stress in polycystic kidney disease." Am J Physiol Renal Physiol **307**(11): F1198-1206.

Kleinman, H. K., M. L. McGarvey, J. R. Hassell, V. L. Star, F. B. Cannon, G. W. Laurie and G. R. Martin (1986). "Basement membrane complexes with biological activity." Biochemistry **25**(2): 312-318.

Kleinman, H. K., D. Philp and M. P. Hoffman (2003). "Role of the extracellular matrix in morphogenesis." Curr Opin Biotechnol **14**(5): 526-532.

Koptides, M. and C. C. Deltas (2000). "Autosomal dominant polycystic kidney disease: molecular genetics and molecular pathogenesis." Hum Genet **107**(2): 115-126.

Koptides, M., C. Hadjimichael, P. Koupepidou, A. Pierides and C. Constantinou Deltas (1999). "Germinal and somatic mutations in the PKD2 gene of renal cysts in autosomal dominant polycystic kidney disease." Hum Mol Genet **8**(3): 509-513.

Lal, M., X. Song, J. L. Pluznick, V. Di Giovanni, D. M. Merrick, N. D. Rosenblum, V. Chauvet, C. J. Gottardi, Y. Pei and M. J. Caplan (2008). "Polycystin-1 C-terminal tail associates with beta-catenin and inhibits canonical Wnt signaling." Hum Mol Genet **17**(20): 3105-3117.

Lanoix, J., V. D'Agati, M. Szabolcs and M. Trudel (1996). "Dysregulation of cellular proliferation and apoptosis mediates human autosomal dominant polycystic kidney disease (ADPKD)." Oncogene **13**(6): 1153-1160.

Lantinga-van Leeuwen, I. S., J. G. Dauwerse, H. J. Baelde, W. N. Leonhard, A. van de Wal, C. J. Ward, S. Verbeek, M. C. Deruiter, M. H. Breuning, E. de Heer and D. J. Peters (2004). "Lowering of Pkd1 expression is sufficient to cause polycystic kidney disease." Hum Mol Genet **13**(24): 3069-3077.

Lantinga-van Leeuwen, I. S., W. N. Leonhard, A. van de Wal, M. H. Breuning, S. Verbeek, E. de Heer and D. J. Peters (2006). "Transgenic mice expressing tamoxifen-inducible Cre for somatic gene modification in renal epithelial cells." Genesis **44**(5): 225-232.

Lantinga-van Leeuwen, I. S., W. N. Leonhard, A. van der Wal, M. H. Breuning, E. de Heer and D. J. Peters (2007). "Kidney-specific inactivation of the Pkd1 gene induces rapid cyst formation in developing kidneys and a slow onset of disease in adult mice." Hum Mol Genet **16**(24): 3188-3196.

Larsen, R., M. B. Hansen and N. Bindslev (2005). "Duodenal secretion in humans mediated by the EP4 receptor subtype." Acta Physiol Scand **185**(2): 133-140.

Le, N. H., A. van der Wal, P. van der Bent, I. S. Lantinga-van Leeuwen, M. H. Breuning, H. van Dam, E. de Heer and D. J. Peters (2005). "Increased activity of activator protein-1 transcription factor components ATF2, c-Jun, and c-Fos in human and mouse autosomal dominant polycystic kidney disease." J Am Soc Nephrol **16**(9): 2724-2731.

Lee, D. I. and R. V. Clayman (2004). "Hand-assisted laparoscopic nephrectomy in autosomal dominant polycystic kidney disease." J Endourol **18**(4): 379-382.

Lewis, T. S., P. S. Shapiro and N. G. Ahn (1998). "Signal transduction through MAP kinase cascades." Adv Cancer Res **74**: 49-139.

Li, H. P., L. Geng, C. R. Burrow and P. D. Wilson (1999). "Identification of phosphorylation sites in the PKD1-encoded protein C-terminal domain." Biochem Biophys Res Commun **259**(2): 356-363.

Li, X., Y. Okada, C. C. Pilbeam, J. A. Lorenzo, C. R. Kennedy, R. M. Breyer and L. G. Raisz (2000). "Knockout of the murine prostaglandin EP2 receptor impairs osteoclastogenesis in vitro." Endocrinology **141**(6): 2054-2061.

Liu, Y., M. Rajagopal, K. Lee, L. Battini, D. Flores, G. L. Gusella, A. C. Pao and R. Rohatgi (2012). "Prostaglandin E2 mediates proliferation and chloride secretion in ADPKD cystic renal epithelia." Am J Physiol Renal Physiol.

Liu, Y., M. Rajagopal, K. Lee, L. Battini, D. Flores, G. L. Gusella, A. C. Pao and R. Rohatgi (2012). "Prostaglandin E(2) mediates proliferation and chloride secretion in ADPKD cystic renal epithelia." Am J Physiol Renal Physiol **303**(10): F1425-1434.

Lowden, D. A., G. W. Lindemann, G. Merlino, B. D. Barash, J. P. Calvet and V. H. Gattone, 2nd (1994). "Renal cysts in transgenic mice expressing transforming growth factor-alpha." J Lab Clin Med **124**(3): 386-394.

Ma, M., X. Tian, P. Igarashi, G. J. Pazour and S. Somlo (2013). "Loss of cilia suppresses cyst growth in genetic models of autosomal dominant polycystic kidney disease." Nature genetics **45**(9): 1004-1012.

Mangoo-Karim, R., M. Uchic, C. Lechene and J. J. Grantham (1989). "Renal epithelial cyst formation and enlargement in vitro: dependence on cAMP." Proc Natl Acad Sci U S A **86**(15): 6007-6011.

Mao, Z., A. J. Streets and A. C. Ong (2011). "Thiazolidinediones inhibit MDCK cyst growth through disrupting oriented cell division and apicobasal polarity." Am J Physiol Renal Physiol **300**(6): F1375-1384.

Masyuk, T. V., A. I. Masyuk, V. E. Torres, P. C. Harris and N. F. Larusso (2007). "Octreotide inhibits hepatic cystogenesis in a rodent model of polycystic liver disease by reducing cholangiocyte adenosine 3',5'-cyclic monophosphate." Gastroenterology **132**(3): 1104-1116.

Matlhagela, K. and M. Taub (2006). "Involvement of EP1 and EP2 receptors in the regulation of the Na,K-ATPase by prostaglandins in MDCK cells." Prostaglandins Other Lipid Mediat **79**(1-2): 101-113.

Mayr, B. and M. Montminy (2001). "Transcriptional regulation by the phosphorylation-dependent factor CREB." Nat Rev Mol Cell Biol **2**(8): 599-609.

Mengerink, K. J., G. W. Moy and V. D. Vacquier (2002). "suREJ3, a polycystin-1 protein, is cleaved at the GPS domain and localizes to the acrosomal region of sea urchin sperm." J Biol Chem **277**(2): 943-948.

Mochizuki, T., K. Tsuchiya and K. Nitta (2013). "Autosomal dominant polycystic kidney disease: recent advances in pathogenesis and potential therapies." Clin Exp Nephrol **17**(3): 317-326.

Morath, R., T. Klein, H. W. Seyberth and R. M. Nusing (1999). "Immunolocalization of the four prostaglandin E2 receptor proteins EP1, EP2, EP3, and EP4 in human kidney." J Am Soc Nephrol **10**(9): 1851-1860.

Moy, G. W., L. M. Mendoza, J. R. Schulz, W. J. Swanson, C. G. Glabe and V. D. Vacquier (1996). "The sea urchin sperm receptor for egg jelly is a modular protein with extensive homology to the human polycystic kidney disease protein, PKD1." J Cell Biol **133**(4): 809-817.

Murase, A., Y. Taniguchi, H. Tonai-Kachi, K. Nakao and J. Takada (2008). "In vitro pharmacological characterization of CJ-042794, a novel, potent, and selective prostaglandin EP(4) receptor antagonist." Life Sci **82**(3-4): 226-232.

Myung, S. J. and I. H. Kim (2008). "[Role of prostaglandins in colon cancer]." Korean J Gastroenterol **51**(5): 274-279.

Nadasdy, T., Z. Laszik, G. Lajoie, K. E. Blick, D. E. Wheeler and F. G. Silva (1995). "Proliferative activity of cyst epithelium in human renal cystic diseases." J Am Soc Nephrol **5**(7): 1462-1468.

Nagao, S., T. Yamaguchi, M. Kusaka, R. L. Maser, H. Takahashi, B. D. Cowley and J. J. Grantham (2003). "Renal activation of extracellular signal-regulated kinase in rats with autosomal-dominant polycystic kidney disease." Kidney Int **63**(2): 427-437.

Narumiya, S., Y. Sugimoto and F. Ushikubi (1999). "Prostanoid receptors: structures, properties, and functions." Physiol Rev **79**(4): 1193-1226.

Nasrallah, R., J. Clark and R. L. Hebert (2007). "Prostaglandins in the kidney: developments since Y2K." Clin Sci (Lond) **113**(7): 297-311.

Nasrallah, R., R. Hassouneh and R. L. Hebert (2014). "Chronic kidney disease: targeting prostaglandin E2 receptors." Am J Physiol Renal Physiol **307**(3): F243-F250.

Nauli, S. M., F. J. Alenghat, Y. Luo, E. Williams, P. Vassilev, X. Li, A. E. Elia, W. Lu, E. M. Brown, S. J. Quinn, D. E. Ingber and J. Zhou (2003). "Polycystins 1 and 2 mediate mechanosensation in the primary cilium of kidney cells." Nat Genet **33**(2): 129-137.

Newby, L. J., A. J. Streets, Y. Zhao, P. C. Harris, C. J. Ward and A. C. Ong (2002). "Identification, characterization, and localization of a novel kidney polycystin-1-polycystin-2 complex." J Biol Chem **277**(23): 20763-20773.

Nicolau, C., R. Torra, C. Badenas, R. Vilana, L. Bianchi, R. Gilabert, A. Darnell and C. Bru (1999). "Autosomal dominant polycystic kidney disease types 1 and 2: assessment of US sensitivity for diagnosis." Radiology **213**(1): 273-276.

Niederst, M. J. and J. A. Engelman (2013). "Bypass mechanisms of resistance to receptor tyrosine kinase inhibition in lung cancer." Sci Signal **6**(294): re6.

Nishigaki, N., M. Negishi and A. Ichikawa (1996). "Two Gs-coupled prostaglandin E receptor subtypes, EP2 and EP4, differ in desensitization and sensitivity to the metabolic inactivation of the agonist." Mol Pharmacol **50**(4): 1031-1037.

Nishio, S., X. Tian, A. R. Gallagher, Z. Yu, V. Patel, P. Igarashi and S. Somlo (2010). "Loss of oriented cell division does not initiate cyst formation." J Am Soc Nephrol **21**(2): 295-302.

Norel, X., L. Walch, C. Labat, J.-P. Gascard, E. Dulmet and C. Brink (1999). "Prostanoid receptors involved in the relaxation of human bronchial preparations." British Journal of Pharmacology **126**(4): 867-872.

O'Brien, L. E., T. S. Jou, A. L. Pollack, Q. Zhang, S. H. Hansen, P. Yurchenco and K. E. Mostov (2001). "Rac1 orientates epithelial apical polarity through effects on basolateral laminin assembly." Nat Cell Biol **3**(9): 831-838.

Ong, A. C. and P. C. Harris (2005). "Molecular pathogenesis of ADPKD: the polycystin complex gets complex." Kidney Int **67**(4): 1234-1247.

Osawa, H., N. Nakamura, K. Shirato, M. Nakamura, M. Shimada, R. Kumasaka, R. Murakami, T. Fujita, H. Yamabe and K. Okumura (2006). "Losartan, an angiotensin-II receptor antagonist, retards the progression of advanced renal insufficiency." Tohoku J Exp Med **209**(1): 7-13.

Pampaloni, F., E. G. Reynaud and E. H. Stelzer (2007). "The third dimension bridges the gap between cell culture and live tissue." Nat Rev Mol Cell Biol **8**(10): 839-845.

Parker, E., L. J. Newby, C. C. Sharpe, S. Rossetti, A. J. Streets, P. C. Harris, M. J. O'Hare and A. C. Ong (2007). "Hyperproliferation of PKD1 cystic cells is induced by insulin-like growth factor-1 activation of the Ras/Raf signalling system." Kidney Int **72**(2): 157-165.

Paterson, A. D., R. Magistroni, N. He, K. Wang, A. Johnson, P. R. Fain, E. Dicks, P. Parfrey, P. St George-Hyslop and Y. Pei (2005). "Progressive loss of renal function is an age-dependent heritable trait in type 1 autosomal dominant polycystic kidney disease." J Am Soc Nephrol **16**(3): 755-762.

Pazour, G. J. (2004). "Intraflagellar transport and cilia-dependent renal disease: the ciliary hypothesis of polycystic kidney disease." J Am Soc Nephrol **15**(10): 2528-2536.

Pei, Y., N. He, K. Wang, M. Kasenda, A. D. Paterson, G. Chan, Y. Liang, J. Roscoe, J. Brissenden, D. Hefferton, P. Parfrey, S. Somlo and P. St George-Hyslop (1998). "A spectrum

of mutations in the polycystic kidney disease-2 (PKD2) gene from eight Canadian kindreds." J Am Soc Nephrol **9**(10): 1853-1860.

Peluffo, M. C., J. Stanley, N. Braeuer, A. Rotgeri, K. H. Fritzemeier, U. Fuhrmann, B. Buchmann, T. Adevai, M. J. Murphy, M. B. Zelinski, B. Lindenthal, J. D. Hennebold and R. L. Stouffer (2014). "A prostaglandin E2 receptor antagonist prevents pregnancies during a preclinical contraceptive trial with female macaques." Human Reproduction (Oxford, England) **29**(7): 1400-1412.

Pena-Silva, R. A. and D. D. Heistad (2010). "EP1c times for angiotensin: EP1 receptors facilitate angiotensin II-induced vascular dysfunction." Hypertension **55**(4): 846-848.

Perico, N., L. Antiga, A. Caroli, P. Ruggenenti, G. Fasolini, M. Cafaro, P. Ondei, N. Rubis, O. Diadei, G. Gherardi, S. Prandini, A. Panozo, R. F. Bravo, S. Carminati, F. R. De Leon, F. Gaspari, M. Cortinovis, N. Motterlini, B. Ene-Iordache, A. Remuzzi and G. Remuzzi (2010). "Sirolimus therapy to halt the progression of ADPKD." J Am Soc Nephrol **21**(6): 1031-1040.

Peters, D. J. and L. A. Sandkuijl (1992). "Genetic heterogeneity of polycystic kidney disease in Europe." Contrib Nephrol **97**: 128-139.

Pietanza, M. C., S. M. Gadgeel, A. Dowlati, T. J. Lynch, R. Salgia, K. M. Rowland, Jr., M. S. Wertheim, K. A. Price, G. J. Riely, C. G. Azzoli, V. A. Miller, L. M. Krug, M. G. Kris, J. H. Beumer, M. Tonda, B. Mitchell and N. A. Rizvi (2012). "Phase II study of the multitargeted tyrosine kinase inhibitor XL647 in patients with non-small-cell lung cancer." J Thorac Oncol **7**(5): 856-865.

Pollack, A. L., G. Apodaca and K. E. Mostov (2004). "Hepatocyte growth factor induces MDCK cell morphogenesis without causing loss of tight junction functional integrity." Am J Physiol Cell Physiol **286**(3): C482-494.

Poschke, A., N. Kern, T. Maruyama, H. Pavenstadt, S. Narumiya, B. L. Jensen and R. M. Nusing (2012). "The PGE(2)-EP4 receptor is necessary for stimulation of the renin-angiotensin-aldosterone system in response to low dietary salt intake in vivo." Am J Physiol Renal Physiol **303**(10): F1435-1442.

Puri, S., B. S. Magenheimer, R. L. Maser, E. M. Ryan, C. A. Zien, D. D. Walker, D. P. Wallace, S. J. Hempson and J. P. Calvet (2004). "Polycystin-1 activates the calcineurin/NFAT (nuclear factor of activated T-cells) signaling pathway." J Biol Chem **279**(53): 55455-55464.

Qian, F., F. J. Germino, Y. Cai, X. Zhang, S. Somlo and G. G. Germino (1997). "PKD1 interacts with PKD2 through a probable coiled-coil domain." Nat Genet **16**(2): 179-183.

Qian, F. and G. G. Germino (1997). ""Mistakes happen": somatic mutation and disease." Am J Hum Genet **61**(5): 1000-1005.

Rajagopal, M., S. V. Thomas, P. P. Kathpalia, Y. Chen and A. C. Pao (2014). "Prostaglandin E2 induces chloride secretion through crosstalk between cAMP and calcium signaling in mouse inner medullary collecting duct cells." Am J Physiol Cell Physiol **306**(3): C263-278.

Rathaus, M. (2007). "[New therapies for ADPKD]." G Ital Nefrol **24**(6): 526-534.

Ravine, D., R. N. Gibson, R. G. Walker, L. J. Sheffield, P. Kincaid-Smith and D. M. Danks (1994). "Evaluation of ultrasonographic diagnostic criteria for autosomal dominant polycystic kidney disease 1." Lancet **343**(8901): 824-827.

Regan, J. W. (2003). "EP2 and EP4 prostanoid receptor signaling." Life Sci **74**(2-3): 143-153.

Reif, G. A., T. Yamaguchi, E. Nivens, H. Fujiki, C. S. Pinto and D. P. Wallace (2011). "Tolvaptan inhibits ERK-dependent cell proliferation, Cl(-) secretion, and in vitro cyst growth

of human ADPKD cells stimulated by vasopressin." Am J Physiol Renal Physiol **301**(5): F1005-1013.

Riella, C., P. G. Czarnecki and T. I. Steinman (2014). "Therapeutic advances in the treatment of polycystic kidney disease." Nephron Clin Pract **128**(3-4): 297-302.

Rossetti, S., S. Burton, L. Strmecki, G. R. Pond, J. L. San Millan, K. Zerres, T. M. Barratt, S. Ozen, V. E. Torres, E. J. Bergstralh, C. G. Winearls and P. C. Harris (2002). "The position of the polycystic kidney disease 1 (PKD1) gene mutation correlates with the severity of renal disease." J Am Soc Nephrol **13**(5): 1230-1237.

Rossetti, S., M. B. Consugar, A. B. Chapman, V. E. Torres, L. M. Guay-Woodford, J. J. Grantham, W. M. Bennett, C. M. Meyers, D. L. Walker, K. Bae, Q. J. Zhang, P. A. Thompson, J. P. Miller and P. C. Harris (2007). "Comprehensive molecular diagnostics in autosomal dominant polycystic kidney disease." J Am Soc Nephrol **18**(7): 2143-2160.

Rundle, D. R., G. Gorbsky and L. Tsiokas (2004). "PKD2 interacts and co-localizes with mDia1 to mitotic spindles of dividing cells: role of mDia1 IN PKD2 localization to mitotic spindles." J Biol Chem **279**(28): 29728-29739.

Saigusa, T. and P. D. Bell (2015). "Molecular Pathways and Therapies in Autosomal-Dominant Polycystic Kidney Disease." Physiology (Bethesda) **30**(3): 195-207.

Sandford, R., B. Sgotto, S. Aparicio, S. Brenner, M. Vaudin, R. K. Wilson, S. Chissoe, K. Pepin, A. Bateman, C. Chothia, J. Hughes and P. Harris (1997). "Comparative analysis of the polycystic kidney disease 1 (PKD1) gene reveals an integral membrane glycoprotein with multiple evolutionary conserved domains." Hum Mol Genet **6**(9): 1483-1489.

Sankaran, D., N. Bankovic-Calic, M. R. Ogborn, G. Crow and H. M. Aukema (2007). "Selective COX-2 inhibition markedly slows disease progression and attenuates altered prostanoid production in Han:SPRD-cy rats with inherited kidney disease." Am J Physiol Renal Physiol **293**(3): F821-830.

Sauvant, C., H. Holzinger and M. Gekle (2003). "Short-term regulation of basolateral organic anion uptake in proximal tubular opossum kidney cells: prostaglandin E2 acts via receptor-mediated activation of protein kinase A." J Am Soc Nephrol **14**(12): 3017-3026.

Savill, J. (1994). "Apoptosis and the kidney." J Am Soc Nephrol **5**(1): 12-21.

Schrier, R. W., K. Z. Abebe, R. D. Perrone, V. E. Torres, W. E. Braun, T. I. Steinman, F. T. Winklhofer, G. Brosnahan, P. G. Czarnecki, M. C. Hogan, D. C. Miskulin, F. F. Rahbari-Oskoui, J. J. Grantham, P. C. Harris, M. F. Flessner, K. T. Bae, C. G. Moore and A. B. Chapman (2014). "Blood pressure in early autosomal dominant polycystic kidney disease." N Engl J Med **371**(24): 2255-2266.

Shao, J., C. Jung, C. Liu and H. Sheng (2005). "Prostaglandin E2 Stimulates the beta-catenin/T cell factor-dependent transcription in colon cancer." J Biol Chem **280**(28): 26565-26572.

Shao, X., J. E. Johnson, J. A. Richardson, T. Hiesberger and P. Igarashi (2002). "A minimal Ksp-cadherin promoter linked to a green fluorescent protein reporter gene exhibits tissue-specific expression in the developing kidney and genitourinary tract." J Am Soc Nephrol **13**(7): 1824-1836.

Sheller, J. R., D. Mitchell, B. Meyrick, J. Oates and R. Breyer (2000). "EP2 receptor mediates bronchodilation by PGE2 in mice." Journal of Applied Physiology **88**(6): 2214-2218.

Sheng, H., J. Shao, M. K. Washington and R. N. DuBois (2001). "Prostaglandin E2 increases growth and motility of colorectal carcinoma cells." J Biol Chem **276**(21): 18075-18081.

Shibazaki, S., Z. Yu, S. Nishio, X. Tian, R. B. Thomson, M. Mitobe, A. Louvi, H. Velazquez, S. Ishibe, L. G. Cantley, P. Igarashi and S. Somlo (2008). "Cyst formation and activation of the extracellular regulated kinase pathway after kidney specific inactivation of Pkd1." Hum Mol Genet **17**(11): 1505-1516.

Shillingford, J. M., N. S. Murcia, C. H. Larson, S. H. Low, R. Hedgepeth, N. Brown, C. A. Flask, A. C. Novick, D. A. Goldfarb, A. Kramer-Zucker, G. Walz, K. B. Piontek, G. G. Germino and T. Weimbs (2006). "The mTOR pathway is regulated by polycystin-1, and its inhibition reverses renal cystogenesis in polycystic kidney disease." Proc Natl Acad Sci U S A **103**(14): 5466-5471.

Siu, Y. T. and D. Y. Jin (2007). "CREB--a real culprit in oncogenesis." Febs j **274**(13): 3224-3232.

Snyder, D. S., L. Tradtrantip, C. Yao, M. J. Kurth and A. S. Verkman (2011). "Potent, metabolically stable benzopyrimido-pyrrolo-oxazine-dione (BPO) CFTR inhibitors for polycystic kidney disease." J Med Chem **54**(15): 5468-5477.

Song, X., V. Di Giovanni, N. He, K. Wang, A. Ingram, N. D. Rosenblum and Y. Pei (2009). "Systems biology of autosomal dominant polycystic kidney disease (ADPKD): computational identification of gene expression pathways and integrated regulatory networks." Hum Mol Genet **18**(13): 2328-2343.

Sonoshita, M., K. Takaku, N. Sasaki, Y. Sugimoto, F. Ushikubi, S. Narumiya, M. Oshima and M. M. Taketo (2001). "Acceleration of intestinal polyposis through prostaglandin receptor EP2 in Apc(Delta 716) knockout mice." Nat Med **7**(9): 1048-1051.

Sorensen, S. S., T. K. Glud, P. J. Sorensen, A. Amdisen and E. B. Pedersen (1990). "Change in renal tubular sodium and water handling during progression of polycystic kidney disease: relationship to atrial natriuretic peptide." Nephrol Dial Transplant **5**(4): 247-257.

Stenson, W. F. (2007). "Prostaglandins and epithelial response to injury." Curr Opin Gastroenterol **23**(2): 107-110.

Subramanian, B., D. Rudym, C. Cannizzaro, R. Perrone, J. Zhou and D. L. Kaplan (2010). "Tissue-engineered three-dimensional in vitro models for normal and diseased kidney." Tissue Eng Part A **16**(9): 2821-2831.

Sullivan, L. P., D. P. Wallace and J. J. Grantham (1998). "Chloride and fluid secretion in polycystic kidney disease." J Am Soc Nephrol **9**(5): 903-916.

Sung, Y. M., G. He, D. H. Hwang and S. M. Fischer (2006). "Overexpression of the prostaglandin E2 receptor EP2 results in enhanced skin tumor development." Oncogene **25**(40): 5507-5516.

Sweeney, W. E., Jr., R. O. von Vigier, P. Frost and E. D. Avner (2008). "Src inhibition ameliorates polycystic kidney disease." J Am Soc Nephrol **19**(7): 1331-1341.

Swinnen, J. V., D. R. Joseph and M. Conti (1989). "The mRNA encoding a high-affinity cAMP phosphodiesterase is regulated by hormones and cAMP." Proc Natl Acad Sci U S A **86**(21): 8197-8201.

Takahashi, T., H. Uehara, H. Ogawa, H. Umemoto, Y. Bando and K. Izumi (2014). "Inhibition of EP2/EP4 signaling abrogates IGF-1R-mediated cancer cell growth: Involvement of protein kinase C-theta activation." Oncotarget.

Tang, E. H. C., P. Libby, P. M. Vanhoutte and A. Xu (2012). "Anti-inflammation therapy by activation of prostaglandin EP4 receptor in cardiovascular and other inflammatory diseases." Journal of Cardiovascular Pharmacology **59**(2): 116-123.

Tao, Y., J. Kim, R. W. Schrier and C. L. Edelstein (2005). "Rapamycin markedly slows disease progression in a rat model of polycystic kidney disease." J Am Soc Nephrol **16**(1): 46-51.

Taussig, R. and A. G. Gilman (1995). "Mammalian membrane-bound adenylyl cyclases." J Biol Chem **270**(1): 1-4.

Torra, R., C. Badenas, A. Darnell, C. Nicolau, V. Volpini, L. Revert and X. Estivill (1996). "Linkage, clinical features, and prognosis of autosomal dominant polycystic kidney disease types 1 and 2." J Am Soc Nephrol **7**(10): 2142-2151.

Torres, V. E. (1999). "Extrarenal manifestations of autosomal dominant polycystic kidney disease." Am J Kidney Dis **34**(6): xlv-xlviii.

Torres, V. E. (2004). "Therapies to slow polycystic kidney disease." Nephron Exp Nephrol **98**(1): e1-7.

Torres, V. E., A. B. Chapman, R. D. Perrone, K. T. Bae, K. Z. Abebe, J. E. Bost, D. C. Miskulin, T. I. Steinman, W. E. Braun, F. T. Winklhofer, M. C. Hogan, F. R. Oskoui, C. Kelleher, A. Masoumi, J. Glockner, N. J. Halin, D. R. Martin, E. Remer, N. Patel, I. Pedrosa, L. H. Wetzel, P. A. Thompson, J. P. Miller, C. M. Meyers and R. W. Schrier (2011). "Analysis of baseline parameters in the HALT polycystic kidney disease trials." Kidney Int.

Torres, V. E. and P. C. Harris (2006). "Mechanisms of Disease: autosomal dominant and recessive polycystic kidney diseases." Nat Clin Pract Nephrol **2**(1): 40-55; quiz 55.

Torres, V. E. and P. C. Harris (2009). "Autosomal dominant polycystic kidney disease: the last 3 years." Kidney Int **76**(2): 149-168.

Torres, V. E., P. C. Harris and Y. Pirson (2007). "Autosomal dominant polycystic kidney disease." Lancet **369**(9569): 1287-1301.

Torres, V. E., E. Meijer, K. T. Bae, A. B. Chapman, O. Devuyst, R. T. Gansevoort, J. J. Grantham, E. Higashihara, R. D. Perrone, H. B. Krasa, J. J. Ouyang and F. S. Czerwiec (2011). "Rationale and design of the TEMPO (Tolvaptan Efficacy and Safety in Management of Autosomal Dominant Polycystic Kidney Disease and its Outcomes) 3-4 Study." Am J Kidney Dis **57**(5): 692-699.

Torres, V. E., X. Wang, Q. Qian, S. Somlo, P. C. Harris and V. H. Gattone, 2nd (2004). "Effective treatment of an orthologous model of autosomal dominant polycystic kidney disease." Nat Med **10**(4): 363-364.

Tsiokas, L., T. Arnould, C. Zhu, E. Kim, G. Walz and V. P. Sukhatme (1999). "Specific association of the gene product of PKD2 with the TRPC1 channel." Proc Natl Acad Sci U S A **96**(7): 3934-3939.

Tsiokas, L., E. Kim, T. Arnould, V. P. Sukhatme and G. Walz (1997). "Homo- and heterodimeric interactions between the gene products of PKD1 and PKD2." Proc Natl Acad Sci U S A **94**(13): 6965-6970.

Tsuboi, K., Y. Sugimoto and A. Ichikawa (2002). "Prostanoid receptor subtypes." Prostaglandins & Other Lipid Mediators **68–69**(0): 535-556.

Ushikubi, F., Y. Sugimoto, A. Ichikawa and S. Narumiya (2000). "Roles of prostanoids revealed from studies using mice lacking specific prostanoid receptors." Jpn J Pharmacol **83**(4): 279-285.

van den Bemt, P., E. T. Tjwa and M. G. van Oijen (2014). "[Cardiovascular and gastrointestinal safety of NSAIDs]." Ned Tijdschr Geneeskd **158**: A7311.

Vijayakumar, S., S. Dang, M. P. Marinkovich, Z. Lazarova, B. Yoder, V. E. Torres and D. P. Wallace (2014). "Aberrant expression of laminin-332 promotes cell proliferation and cyst growth in ARPKD." Am J Physiol Renal Physiol **306**(6): F640-654.

Virgolini, I., C. Muller, M. Hermann, W. Schutz and H. Sinzinger (1988). "Evaluation of prostaglandin-receptors in human and rat liver: interspecies differences at the prostaglandin receptor-level." Prostaglandins **36**(6): 807-818.

Vukicevic, S., F. P. Luyten, H. K. Kleinman and A. H. Reddi (1990). "Differentiation of canalicular cell processes in bone cells by basement membrane matrix components: regulation by discrete domains of laminin." Cell **63**(2): 437-445.

Wallace, D. P., J. J. Grantham and L. P. Sullivan (1996). "Chloride and fluid secretion by cultured human polycystic kidney cells." Kidney Int **50**(4): 1327-1336.

Walz, G., K. Budde, M. Mannaa, J. Nurnberger, C. Wanner, C. Sommerer, U. Kunzendorf, B. Banas, W. H. Horl, N. Obermuller, W. Arns, H. Pavenstadt, J. Gaedeke, M. Buchert, C. May, H. Gschaidmeier, S. Kramer and K. U. Eckardt (2010). "Everolimus in patients with autosomal dominant polycystic kidney disease." N Engl J Med **363**(9): 830-840.

Wang, X., V. Gattone, 2nd, P. C. Harris and V. E. Torres (2005). "Effectiveness of vasopressin V2 receptor antagonists OPC-31260 and OPC-41061 on polycystic kidney disease development in the PCK rat." J Am Soc Nephrol **16**(4): 846-851.

Wegmann, M. and R. M. Nusing (2003). "Prostaglandin E2 stimulates sodium reabsorption in MDCK C7 cells, a renal collecting duct principal cell model." Prostaglandins Leukot Essent Fatty Acids **69**(5): 315-322.

Wellbrock, C., M. Karasarides and R. Marais (2004). "The RAF proteins take centre stage." Nat Rev Mol Cell Biol **5**(11): 875-885.

Woodward, D. F., R. L. Jones and S. Narumiya (2011). "International Union of Basic and Clinical Pharmacology. LXXXIII: classification of prostanoid receptors, updating 15 years of progress." Pharmacol Rev **63**(3): 471-538.

Wu, G. and S. Somlo (2000). "Molecular genetics and mechanism of autosomal dominant polycystic kidney disease." Mol Genet Metab **69**(1): 1-15.

Xia, S., J. Ma, X. Bai, H. Zhang, S. Cheng, M. Zhang, L. Zhang, M. Du, Y. Wang, H. Li, R. Rong, F. Shi, Q. Yang and J. Leng (2014). "Prostaglandin E2 promotes the cell growth and invasive ability of hepatocellular carcinoma cells by upregulating c-Myc expression via EP4 receptor and the PKA signaling pathway." Oncol Rep.

Xu, T., N. S. Wang, L. L. Fu, C. Y. Ye, S. Q. Yu and C. L. Mei (2012). "Celecoxib inhibits growth of human autosomal dominant polycystic kidney cyst-lining epithelial cells through the VEGF/Raf/MAPK/ERK signaling pathway." Mol Biol Rep **39**(7): 7743-7753.

Yamada, K. M. and E. Cukierman (2007). "Modeling tissue morphogenesis and cancer in 3D." Cell **130**(4): 601-610.

Yamaguchi, T., S. J. Hempson, G. A. Reif, A. M. Hedge and D. P. Wallace (2006). "Calcium restores a normal proliferation phenotype in human polycystic kidney disease epithelial cells." J Am Soc Nephrol **17**(1): 178-187.

Yamaguchi, T., J. C. Pelling, N. T. Ramaswamy, J. W. Eppler, D. P. Wallace, S. Nagao, L. A. Rome, L. P. Sullivan and J. J. Grantham (2000). "cAMP stimulates the in vitro proliferation of renal cyst epithelial cells by activating the extracellular signal-regulated kinase pathway." Kidney Int **57**(4): 1460-1471.

Yang, B., N. D. Sonawane, D. Zhao, S. Somlo and A. S. Verkman (2008). "Small-molecule CFTR inhibitors slow cyst growth in polycystic kidney disease." J Am Soc Nephrol **19**(7): 1300-1310.

Ye, M., M. Grant, M. Sharma, L. Elzinga, S. Swan, V. E. Torres and J. J. Grantham (1992). "Cyst fluid from human autosomal dominant polycystic kidneys promotes cyst formation and expansion by renal epithelial cells in vitro." J Am Soc Nephrol **3**(4): 984-994.

Yoder, B. K., X. Hou and L. M. Guay-Woodford (2002). "The polycystic kidney disease proteins, polycystin-1, polycystin-2, polaris, and cystin, are co-localized in renal cilia." J Am Soc Nephrol **13**(10): 2508-2516.

Yokoyama, U., K. Iwatsubo, M. Umemura, T. Fujita and Y. Ishikawa (2013). "The prostanoid EP4 receptor and its signaling pathway." Pharmacol Rev **65**(3): 1010-1052.

Yu, X., J. S. Sidhu, S. Hong and E. M. Faustman (2005). "Essential role of extracellular matrix (ECM) overlay in establishing the functional integrity of primary neonatal rat Sertoli cell/gonocyte co-cultures: an improved in vitro model for assessment of male reproductive toxicity." Toxicol Sci **84**(2): 378-393.

Zhang, F., R. Xu and M. J. Zhao (2010). "QSG-7701 human hepatocytes form polarized acini in three-dimensional culture." J Cell Biochem **110**(5): 1175-1186.

Zimecki, M. (2012). "Potential therapeutic interventions via EP2/EP4 prostaglandin receptors." Postepy Hig Med Dosw (Online) **66**: 287-294.

Appendix:

Copyright permission of thesis Figures:

1. Chapter 1 (Figure 1.1):

ELSEVIER LICENSE:

This is a License Agreement between Fatima Abdelaali ("You") and Elsevier ("Elsevier") provided by Copyright Clearance Center ("CCC"). The license consists of your order details, the terms and conditions provided by Elsevier, and the payment terms and conditions.

All payments must be made in full to CCC. For payment instructions, please see information listed at the bottom of this form.

Supplier:	Elsevier Limited
The Boulevard,Langford Lane	
Kidlington,Oxford,OX5 1GB,UK	
Registered Company Number:	1982084
Customer name:	Fatima Abdelaali
Customer address:	10 dorset street
	sheffield, s10 2fx
License number:	3512970676642
License date:	Nov 20, 2014
Licensed content publisher:	Elsevier
Licensed content publication:	Molecular Genetics and Metabolism
Licensed content title:	Molecular Genetics and Mechanism of Autosomal Dominant Polycystic Kidney Disease
Licensed content author:	Guanqing Wu,Stefan Somlo
Licensed content date:	January 2000
Licensed content volume number:	69
Licensed content issue number:	1
Number of pages:	15
Start Page:	1

End Page:	15
Type of Use:	reuse in a thesis/dissertation
Intended publisher of new work	other
Portion:	Figures/tables/illustrations
Number of figures/tables/illustrations:	1
Format	both print and electronic
Are you the author of this Elsevier article?	No
Will you be translating?	No
Title of your thesis/dissertation	the role of PTGER2 in ADPKD
Expected completion date:	May 2015
Estimated size (number of pages):	200
Elsevier VAT number:	GB 494 6272 12
Permissions price:	0.00 USD
VAT/Local Sales Tax:	0.00 USD / 0.00 GBP.

2. Chapter 1 (Figure 1.2):

NATURE PUBLISHING GROUP LICENSE:

This is a License Agreement between Fatima Abdelaali ("You") and Nature Publishing Group ("Nature Publishing Group") provided by Copyright Clearance Center ("CCC"). The license consists of your order details, the terms and conditions provided by Nature Publishing Group, and the payment terms and conditions.

All payments must be made in full to CCC. For payment instructions, please see information listed at the bottom of this form.

License Number:	3596611174571
License date:	Mar 26, 2015
Licensed content publisher:	Nature Publishing Group
Licensed content publication:	Kidney International
Licensed content title:	Molecular pathogenesis of ADPKD: The polycystin complex gets complex
Licensed content author:	ALBERT C M ONG and PETER C HARRIS
Licensed content date :	Apr 1, 2005

Volume number:	67
Issue number:	4
Type of Use:	reuse in a dissertation / thesis
Requestor type:	academic/educational
Format:	print and electronic
Portion:	figures/tables/illustrations
Number:	of figures/tables/illustrations 1
High-res required:	no
Figures:	figure 1
Author of this NPG article:	no
Your reference number:	None
Title of your thesis / dissertation:	the role of PTGER2 in ADPKD
Expected completion date :	May 2015
Estimated size (number of pages):	200
Total:	0.0 USD

3. Chapter1 (Figure 1.3):

Fatima Abdela Ali <mdr10fa@sheffield.ac.uk> 20 November 2014 at 10:29

To: permissions@rockefeller.edu

hi

I am PHD student in sheffield university andi need permission to reuse one figure for my thesis (figure 2. PC1 and PC2 affect multiple signaling pathways.) from your articles if possible

The cell biology of polycystic kidney disease 2010

1. Hannah C. Chapin and
2. Michael J. Caplan

RUP Permissions Dept. <permiss@mail.rockefeller.edu> 24 November 2014 at 04:25

To: Fatima Abdela Ali <mdr10fa@sheffield.ac.uk>

Fatima,

Thank you for letting us know. You may reuse the images as long as you cite the original articles as follows:

©YEAR AUTHOR et al. Journal of Cell Biology. VOL:PP-PP. doi:10.1083/jcb.########

Best wishes,

Suzanne O'Donnell

RUP Permissions Department

4. Chapter 1(Figure 1.5):

NATURE PUBLISHING GROUP LICENSE:

This is a License Agreement between Fatima Abdelaali ("You") and Nature Publishing Group ("Nature Publishing Group") provided by Copyright Clearance Center ("CCC"). The license consists of your order details, the terms and conditions provided by Nature Publishing Group, and the payment terms and conditions.

All payments must be made in full to CCC. For payment instructions, please see information listed at the bottom of this form.

License Number:	3596620827932
License date:	Mar 26, 2015
Licensed content publisher:	Nature Publishing Group
Licensed content publication:	Kidney International
Licensed content title:	Renal activation of extracellular signal-regulated kinase in rats with autosomal-dominant polycystic kidney disease
Licensed content author:	Shizuko Nagao, Tamio Yamaguchi, Masatomo Kusaka, Robin L Maser, Hisahide Takahashi et al.
Licensed content date:	Feb 1, 2003
Volume number:	63
Issue number:	2
Type of Use:	reuse in a dissertation / thesis
Requestor type:	academic/educational
Format:	print and electronic
Portion:	figures/tables/illustrations
Number of figures/tables/illustrations:	1
High-res required:	no
Figures:	FIGURE 7
Author of this NPG article:	no
Your reference number:	None

Title of your thesis / dissertation:	the role of PTGER2 in ADPKD
Expected completion date:	May 2015
Estimated size (number of pages):	200
Total:	0.0USD.

5. Chapter 1 (Figure 1.6):

NATURE PUBLISHING GROUP LICENSE:

This is a License Agreement between Fatima Abdelaali ("You") and Nature Publishing Group ("Nature Publishing Group") provided by Copyright Clearance Center ("CCC"). The license consists of your order details, the terms and conditions provided by Nature Publishing Group, and the payment terms and conditions.

All payments must be made in full to CCC. For payment instructions, please see information listed at the bottom of this form.

License Number:	3596620391892
License date:	Mar 26, 2015
Licensed content publisher:	Nature Publishing Group
Licensed content publication:	Kidney International
Licensed content title:	Cyclic AMP activates B-Raf and ERK in cyst epithelial cells from autosomal-dominant polycystic kidneys
Licensed content author:	Tamio Yamaguchi, Shizuko Nagao, Darren P Wallace, Franck A Belibi, Benjamin D Cowley et al.
Licensed content date:	Jun 1, 2003
Volume number:	63
Issue number:	6
Type of Use:	reuse in a dissertation / thesis
Requestor type:	academic/educational
Format:	print and electronic
Portion:	figures/tables/illustrations
Number of figures/tables/illustrations:	1
High-res required:	no
Figures:	FIGURE 10

Author of this NPG article: no

Your reference number: None

Title of your thesis / dissertation: the role of PTGER2 in ADPKD

Expected completion date: May 2015

Estimated size (number of pages):200

Total: 0.00 USD.

6. Chapter 1 (Figure 1.7 and Figure 1.8)

Prostanoid Receptors: Structures, Properties, and Functions

Author: Shuh Narumiya,Yukihiko Sugimoto,Fumitaka Ushikubi

Publication: Physiological Reviews

Publisher: The American Physiological Society

Date: Jan 10, 1999

Copyright © 1999, The American Physiological Society

Logged in as: Fatima Abdelaali

Account #: 3000853994

Permission Not Required

Permission is not required for this type of use.

Title: Chronic kidney disease: targeting prostaglandin E2 receptors

Author: Rania Nasrallah,Ramzi Hassouneh,Richard L. Hébert

Publication: Am J Physiol-Renal Physiology

Publisher: The American Physiological Society

Date: Aug 1, 2014

Copyright © 2014 , The American Physiological Society

Logged in as: Fatima Abdelaali

Account #: 300085399

Permission Not Required

Permission is not required for this type of use**.**

7. Chapter 1 (Figure 1.9) :

8. Chapter 3 (Figure 3.1):

NATURE PUBLISHING GROUP LICENSE:

License Number:	3512971215378
License date:	Nov 20, 2014
Licensed content publisher:	Nature Publishing Group
Licensed content publication:	Kidney International
Licensed content title:	Hyperproliferation of PKD1 cystic cells is induced by insulin-like growth factor-1 activation of the Ras//Raf signalling system
Licensed content author:	E Parker, L J Newby, C C Sharpe, S Rossetti, A J Streets et al.
Licensed content date:	Mar 28, 2007
Volume number:	72
Issue number:	2
Type of Use:	reuse in a dissertation / thesis
Requestor type:	academic/educational
Format:	print and electronic
Portion:	figures/tables/illustrations
Number of figures/tables/illustrations:	1
High-res required:	no
Figures:	figure 1
Author of this NPG article:	no

Your reference number: None

Title of your thesis / dissertation: the role of PTGER2 in ADPKD

Expected completion date: May 2015

Estimated size (number of pages): 200

Total: 0.00 USD

9. Chapter 4(Figure 4.4 A):

JOHN WILEY AND SONS LICENSE:

This Agreement between Fatima Abdelaali ("You") and John Wiley and Sons ("John Wiley and Sons") consists of your license details and the terms and conditions provided by John Wiley and Sons and Copyright Clearance Center.

License Number: 3565991066822

License date: Feb 11, 2015

Licensed Content Publisher: John Wiley and Sons

Licensed Content Publication : genesis

Licensed Content Title: Transgenic mice expressing tamoxifen-inducible Cre for somatic gene modification in renal epithelial cells

Licensed Content Author: Irma S. Lantinga-van Leeuwen,Wouter N. Leonhard,Annemieke van de Wal,Martijn H. Breuning,Sjef Verbeek,Emile de Heer,Dorien J.M. Peters

Licensed Content Date: May 1, 2006

Pages: 8

Type of use: Dissertation/Thesis

Requestor type: University/Academic

Format: Print and electronic

Portion: Figure/table

Number of figures/tables: 1

Original Wiley figure/table number(s): Figure 1

Will you be translating? No

Title of your thesis / dissertation: the role of PTGER2 in ADPKD

Expected completion date: May 2015

Expected size (number of pages):	200
Requestor Location:	Fatima Abdelaali
10 dorset street	
sheffield, United Kingdom s10 2fx	
Attn:	Fatima Abdelaali
Billing Type:	Invoice
Billing Address:	Fatima Abdelaali
10 dorset street	
sheffield, United Kingdom s10 2fx	
Attn:	Fatima Abdelaali
Total:	0.00 USD.

10. Chapter 4 (Figure 4.4 B):

OXFORD UNIVERSITY PRESS LICENSE:

This is a License Agreement between Fatima Abdelaali ("You") and Oxford University Press ("Oxford University Press") provided by Copyright Clearance Center ("CCC"). The license consists of your order details, the terms and conditions provided by Oxford University Press, and the payment terms and conditions.

All payments must be made in full to CCC. For payment instructions, please see information listed at the bottom of this form.

License Number:	3565991157275
License date:	Feb 11, 2015
Licensed content publisher:	Oxford University Press.
Licensed content publication:	Human Molecular Genetics
Licensed content title:	Kidney-specific inactivation of the Pkd1 gene induces rapid cyst formation in developing kidneys and a slow onset of disease in adult mice:
Licensed content author:	Irma S. Lantinga-van Leeuwen, Wouter N. Leonhard, Annemieke van der Wal, Martijn H. Breuning, Emile de Heer, Dorien J.M. Peters
Licensed content date:	12/15/2007
Type of Use:	Thesis/Dissertation

Institution name:	None
Title of your work:	the role of PTGER2 in ADPKD
Publisher of your work:	n/a
Expected publication date:	May 2015
Permissions cost:	0.00 USD
Value added tax:	0.00 USD
Total	0.00 USD